Determination of Primary Structure and Affinity Characterization of Naturally Occurring β-Amyloid Autoantibodies

Dissertation
zur Erlangung des akademischen Grades
eines Doktors der Naturwissenschaften
an der Universität Konstanz,

vorgelegt von
Claudia Cozma

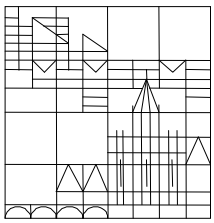

Konstanz, 2014

Tag der mündlichen Prüfung: 25. September 2014
1. Referent: Prof. Dr. Dr. h. c. Michael Przybylski
2. Referent: Prof. Dr. Jörg Hartig
Vorsitzender der prüfungskomission: Prof. Dr. Gerhard Müller

"How far you go in life depends on your being tender with the young, compassionate with the aged, sympathetic with the striving and tolerant of the weak and strong. Because someday in your life you will have been all of these."

George Washington Carver

I dedicate this work to my sister Talida Zaraza, to my parents Zamfira and Octav, to my grandparents Voica and Radu, and to my loving husband, Marius.

The present work has been performed in the time from March 2008 to April 2011 in the Laboratory of Analytical Chemistry and Biopolymer Structure Analysis, Department of Chemistry of the University of Konstanz, under the supervision of Prof. Dr. Dr. h. c. Michael Przybylski.

I would like to express my special gratitude and appreciation to:

Prof. Dr. Dr. h. c. Michael Przybylski for giving me the encouragement to work in this field, for the interesting research topic and discussions concerning my work and for his entire support; furthermore, I am thankful to him for giving me the opportunity to pursue the scientific goals of my work in the research groups of Prof. Dr. Alina Zamfir and Prof. Michael Gross, experiences which added to my scientific development;

Prof. Dr. Hartig, Jörg (University of Konstanz, Germany), for writing the second evaluation of my thesis;

Dr. Marilena Manea, Dr. Irina Perdivara, MSc. Adrian Moise for their continuous collaboration on the Aβ-autoantibodies project;

Prof. Thomas Exner (University of Konstanz, Germany), for providing the computational model of the 3D structure of Aβ-autoantibodies;

Prof. Dr. Alina Zamfir (Aurel Vlaicu University, Arad, Romania), for a wonderful collaboration, in particular for sharing her valuable expertise mass spectrometry field;

Prof. Dr. Michael Gross and Dr. Henry Rohrs (Washington University, Saint Louis), for their hospitality in Saint Louis, for supporting my research projects, and for the great scientific discussions;

Dr. Marilena Manea and Dr. Raluca Stefanescu for guiding my first steps in the laboratory, for their friendship and continuing support both of my work and of my private life;

Dr. Irina Perdivara for her friendship and her unique perspective on life in general and on science in particular;

Ursula Dreher for being an inspiration and the one pillar that I always can count on in my good or bad moments;

All former and present members of the group for the wonderful atmosphere, scientific discussions and advices during my work;

Last but not least I wish to thank my family and all my friends for their patience, love and support.

This dissertation has been published in part, and presented at the following conferences:

Publications

1. Iuraşcu M.I., **Cozma C.**, Tomczyk N., Langridge, J.; Tomczyk, N., Desor M. and Przybylski M.; “Structural Characterization of ß-Amyloid Oligomer-Aggregates by Ion Mobility Mass Spectrometry “, *Ion Mobility Spectrometry Mass Spectrometry*,Ed. by Charles L . Wilkins and Sarah Trimpin. - CRC Press; 1 edition (Dec 14 2010), pp. 313-325.

2. Iuraşcu M.I., **Cozma C.**, Tomczyk N., Rontree J., Desor M., Drescher M. and Przybylski M; “Structural characterization of beta-amyloid oligomer- aggregates by ion mobility mass spectrometry and electron spin resonance spectroscopy.”, *Anal Bioanal Chem.,* 2009; 395:2509-19

3. Perdivara I., Deterding L., **Cozma C.**, Tomer K.B., Przybylski M.; “Glycosylation profiles of epitope-specific anti-β-amyloid antibodies revealed by liquid chromatography – mass spectrometry”, *Glycobiology* 2009,;19:958-70.

4. **Cozma C.**; Dragusanu M.; Przybylski M., " Interaction Studies between Aβ-autoantibodies and Aβ peptides by Immunoaffinity – Mass Spectrometry" , *ASMS proceedings, 2010, Salt Lake City, USA*

5. Iurascu M.I.; **Cozma C.**; Desor M.; Drescher M.; Przybylski M.; "Structure, reaction intermediates and topographical characterization of ß-amyloid oligomerisation revealed by ion mobility mass spectrometry and electron paramagnetic resonance spectroscopy", *ASMS proceedings, 2010, Salt Lake City, USA*

6. **Cozma C.**; Perdivara I.; Moise A.; Przybylski M., ”Sequence determination of β-amyloid autoantibodies using combined liquid

chromatography and tandem mass spectrometry”*, ASMS proceedings***,** *2009*, *Philadelphia, USA*

Conference presentations

1. **Cozma C.**, Manea M., Moise A., Stefanescu R., Przybylski M.**,** "Structural and Affinity Characterisation of human Serum Aβ-autoantibdies*", DGMS, Berlin 2013 - poster presentation*

2. **Cozma C.,** Przybylski M.**, ”**Interaction studies between Aβ-autoantibodies and Aβ-peptides ”, *Affinity MS workshop, DGMS, Halle, 2010 – oral presentation*

3. **Cozma C.**; Perdivara I.; Moise A.; Zhao L.; Przybylski M.; “β-amyloid autoantibodies sequence elucidation using combined liquid chromatography techniques and tandem mass spectrometry ”, *IMSC, Bremen ,2009 - poster presentation*

4. **Cozma C.**; Perdivara I.; Moise A.; Przybylski M., ”Sequence determination of β-amyloid autoantibodies using combined liquid chromatography and tandem mass spectrometry”, *ASMS*, *Philadelphia, 2009 - poster presentation*

5. **Cozma C.,** Manea M., Perdivara I., Moise A., Przybylski M., ”Primary structure determination of Aβ – autoantibodies isolated from human immunoglobulin fraction using high resolution mass spectrometry”, *DGMS, Giessen, 2008 - poster presentation*

TABLE OF CONTENTS

1. INTRODUCTION

1.1. Development of mass spectrometric methods in protein structure determination

From 1910, when J.J.Thomson's parabola mass spectrometer registered the first mass spectrum in history, to present mass spectrometry has developed as a science of its own. During this evolution, from a hand full of mass spectrometry instruments worldwide in the early 1920s to a multi-billion dollar industry in 2012 [1.], four Nobel Prices were awarded for mass spectrometry in physics and chemistry: Joseph John Thomson in 1906, Francis William Aston in 1922, Wolfgang Paul in 1989 and John Bennett Fenn & Koichi Tanaka in 2002. Today, mass spectrometry has applications in all areas of science, e. g. biology and biophysics, chemistry and biochemistry, forensic sciences and medicine [2, 3.]. Mass spectrometry has initially been applied only to small molecules, with molecular weights up to ca. 600 Da. However, the successful development of “soft”- ionization techniques, in particular electrospray (ESI) ionization and matrix assisted laser desorption (MALDI) ionization since the late 1980s, has provided the possibility to analyze macromolecules such as proteins, glycans and nucleic acids, up to several hundred kDa today. Using soft ionization methods, molecules with different molecular weights can be ionized with little or no fragmentation. ESI and MALDI are currently applied in various "-omics" research areas for the study of proteomes, glycomes, metabolomes and lipidomes. [4.].

Different approaches such as "bottom up" (the analysis starts with fragments of the macromolecule) and "top down" (the MS analysis starts with the intact macromolecule, which is subjected to a sequence of fragmentations) are employed on a case to case basis to obtain structural information. Mass spectrometry is used as a stand - alone technique or in combination with other methods (e.g. liquid chromatography, gas chromatography, ion mobility, affinity chromatography etc.) depending on the purpose of the analysis (structural, functional, relational, topography, etc.) [5., 6.].

MALDI-MS is a preferred technique for the analysis of biological samples and complex mixtures, due to its high sensitivity and tolerance of many buffers used in biological studies. The sample is co-crystallized with the matrix molecules on the target and desorbed by laser ionization. The desorbed ions are moved in an electric field and ion optics to reach the analyzer (e.g. ToF, FT-ICR).

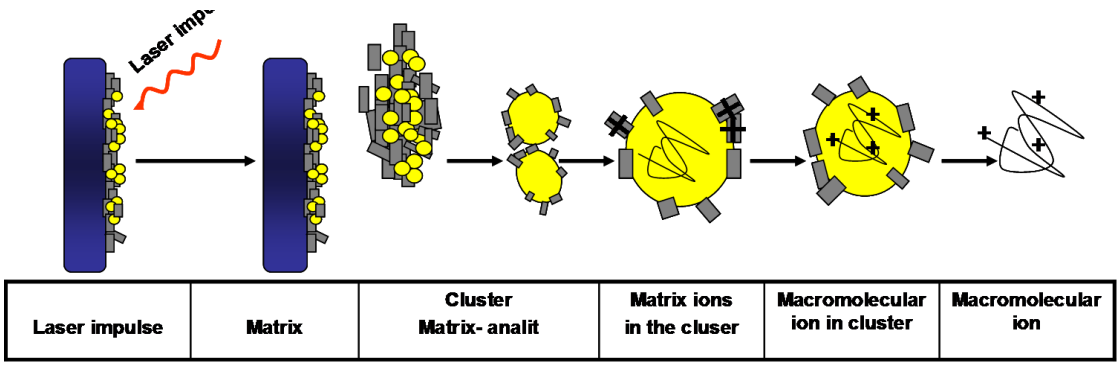

Figure 1. Schematic representation of matrix assisted laser desorption/ ionization mass spectrometry (MALDI MS). The analyte is mixed with a saturated matrix solution on a target and let to dry. Clusters of analyte mixed with matrix are dislocated and ionized with a laser under vacuum. A proton transfer is assumed to take place from the matrix to the analyte a priori reaching the detector by passing through an electrical field.

Electrospray ionization (ESI) is a soft ionization technique in which the ions from solution are transferred into the gas phase. It is extremely useful for the analysis of large, non-volatile, chargeable molecules such as proteins and nucleic acid polymers. For the development of ESI mass spectrometry of biomolecules, John B. Fenn was awarded the Nobel Prize 2002 in Chemistry[7.]. The gaseous ions are formed by creating a fine spray of charged droplets in an electric field. The repulsion between the charges on the surface causes intact ions to leave the droplet by a process of evaporation and to form a spray with a specific shape known as a “Taylor cone”. This ionization method has the advantage to be compatible with liquid separation techniques [8., 9.].

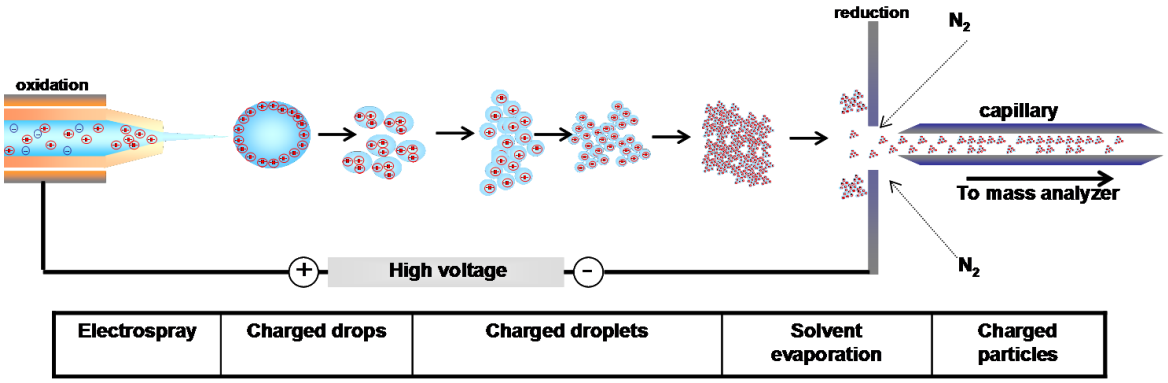

Figure 2. Schematic representation of electrospray ionization mass spectrometry (ESI MS). The analyte dissolved in a proton donor buffer passes through a capillary under high voltage. The spray charged drops, under a flux of inert gas produce smaller droplets; by reaching the optical part of the mass spectrometer the solvent evaporates and transfers the charge to the analyte in the gas phase

Electrospray ionization generally leads to the formation of multiply charged ions. This is an important feature, since by mass spectrometry, m/z values are determined, thus providing the possibility to analyze large molecules with an instrument of a relatively small mass range; this is the main difference compared to MALDI ionization, where mainly singly charged ions are produced[9.].

For the majority of the proteins, the structural characteristics are corroborated with the genetic information, the gene sequencing being performed in parallel with mass spectrometry (or search against the data base of the genome of the analyzed organism). A typical proteomics experiment involves the following steps: (i.) sample preparation for the isolation of the target protein, (ii.) digestion with an endo-protease or in source fragmentation of the whole molecule depending on the method, (iii.) peptide mapping of the proteolytic mixture or fragment identification, (iv.) database search using a suitable search engine (mathematic algorithm) for the identification of the protein. As a precondition, a limited number of variations in the sequence and a genomic mapping of the gene encoding the protein is preferred [5., 10., 11.]. There are classes of proteins, such as antibodies and receptors, that are only partially genetically encoded, the functional part of the molecule being free to adapt to the environmental challenges in processes as somatic recombination. In such cases, for a detailed analysis by mass spectrometry a low number of protein isoforms is usually required. For example, reports on the structural

characterization of a monoclonal antibody have been published since 2008 [12.].

A major goal of this dissertation was to determine the primary structures of a polyclonal antibody against β-amyloid peptide, isolated from a large pool of human serum. By combining several analytical methods, in particular separation and mass spectrometric approaches, the difficulties related to the polyclonality and high variability of the antibody could be overcome. In this case, the use of databases was useful only to map the conserved regions of the antibody by providing homology with other antibodies for such regions. For the unique domains of the antibody, namely the variable and hyper variable regions, mass spectrometry and especially fragmentation techniques were essential in the determination of primary structure. Furthermore, using mass spectrometry and other related techniques, the functionality and affinity of the antibodies towards the antigen were characterized.

1.2. Biochemical basis of antigen-antibody interactions

The immune system is a network of cells, tissues, and organs that work together towards defending the body against attacks by “foreign” organisms (e.g. bacteria, fungi, viruses) or molecules with whom it gets in contact. The basis of the immune system viability is its capacity to detect a multitude of "non-self" agents from its own "self" healthy cells and tissues. The pathogens are a perpetual evolving group, and for this reason the immune system has a series of defense mechanisms in place to overcome a possible liability. In the adaptive immunity, the human body has the ability to adapt over time to recognize specific pathogens that create the antigen specific immunological memory after the first contact. This specificity allows the generation of a specific immune response, which is stored by certain types of cells for a faster elimination of a pathogen in the case of other encounters [13.].

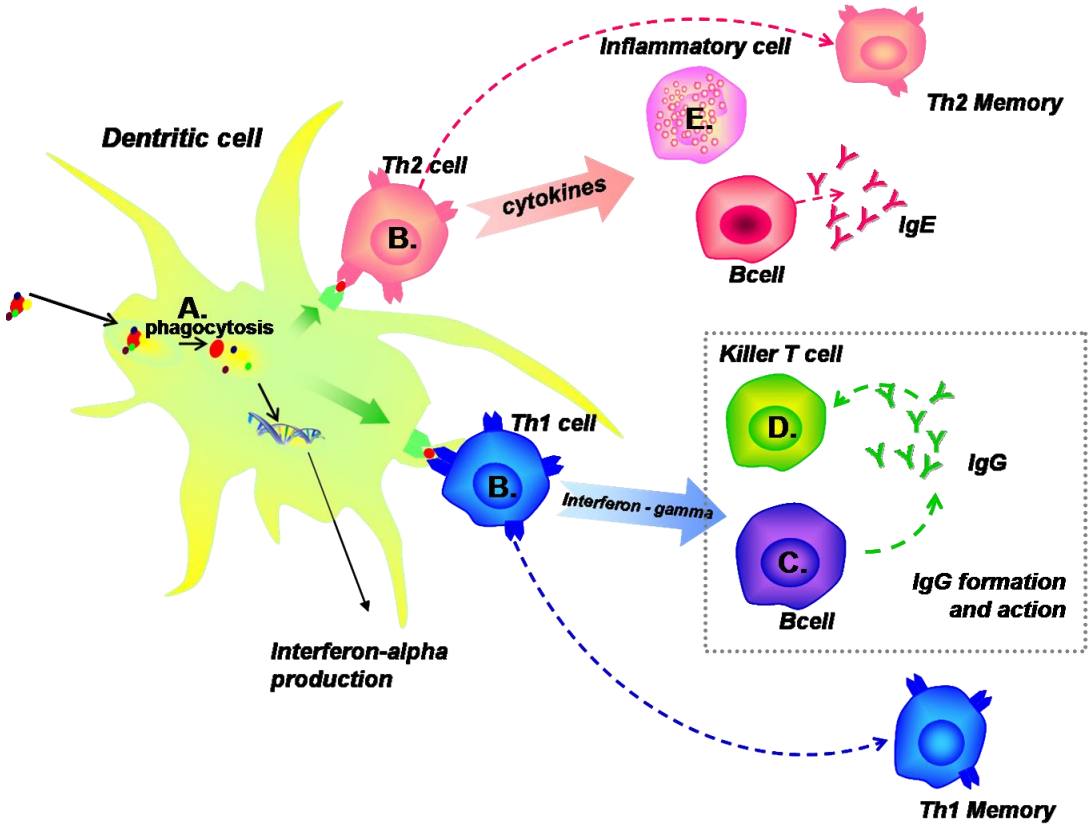

Figure 3. IgG formation during the immune response. A. - antigen phagocytosed by a dendritic cell; B. - parts of the antigen processed to form an MHC receptor that activates T helper cells, which activate the whole cyto-immune response; C. - B cells produce antibodies; D. - killer T cells attack the affected cells and pathogens; E. - eosinophil cell produce an inflammatory cascade.

Lymphocytes, the major group of cells involved in the immune response, consist of two major subtypes (Figure 3): (i.), B-cells involved in the humoral response, and (ii.), T-cells involved in the cell-mediated immune response. While the T-cell receptor is a major histocompatibility complex (MHC) formed by a mixture of pathogen fragments and a self-receptor, the B-cell receptor is an antibody on the cell surface, which recognizes pathogens without processing them. After the specialization of a B- or T-cell line, which occurs during the first encounter with an antigen, the daughter T-cell lines are keepers of the antigen signature (memory). Every specialized B- and T-cell line is specific for a single antigen or class of antigens [14.].

Future responses are based on the antibody's capacity to recognize specific antigens, by binding to particular regions of the antigen structure, named epitopes, with a part of their own structure - the paratope. Identification of an

epitope is of crucial importance in the development of epitope based vaccines, characterization of the active sites of functional proteins e.g. enzymes, cytochrome C or in the elucidation of protein conformations and topography [13.].

Current analytical methods for epitope elucidation include: (i.) epitope screening from a library of peptides, (ii.) epitope sequence mutation screening such as alanine scan, (iii.) epitope mapping by affinity-mass spectrometric methods, (iv.) Xray structure analysis. (v.) NMR structure analysis, (vi.) computational prediction of the 3D structure [15.].

Mass spectrometric based methods of epitope analysis provide molecular structure information about the antigen and antigen binding site. Previous work in our laboratory led to the development of three individual methods for the epitope identification: proteolytic epitope excision, epitope extraction and epitope mapping using online coupled biosensor-MS[16-18.].

An example for the applicability of proteolytic epitope excision is the identification of the epitope recognized by an anti-human cystatin C (hCC) antibody. Cystatin C is a 120 amino acid soluble protein (13 kDa), which is produced by a majority of nuclear cells. hCC is a cysteine protease inhibitor found in all human body fluids, which is known to regulate extracellular cysteine protease activity during microbial invasion or release of lysosomal proteinases from dying or diseased cells [19.]. The method of epitope excision is based on the proteolytic protection of the epitope after its binding by the antibody. First, the antibody, e.g. anti-hCC, is immobilized on a stationary phase via a covalent linkage; then the hCC-antigen is non-covalently bound to the antigen. In the next step, the complex is subjected to proteolytic degradation. Due to the high association constant of antibody-antigen complex and to proteolytic stability of the native IgG in the presence of proteolytic enzymes (in short time experiments), the molecular structures involved, paratope and epitope, are shielded from the proteolytic degradation.

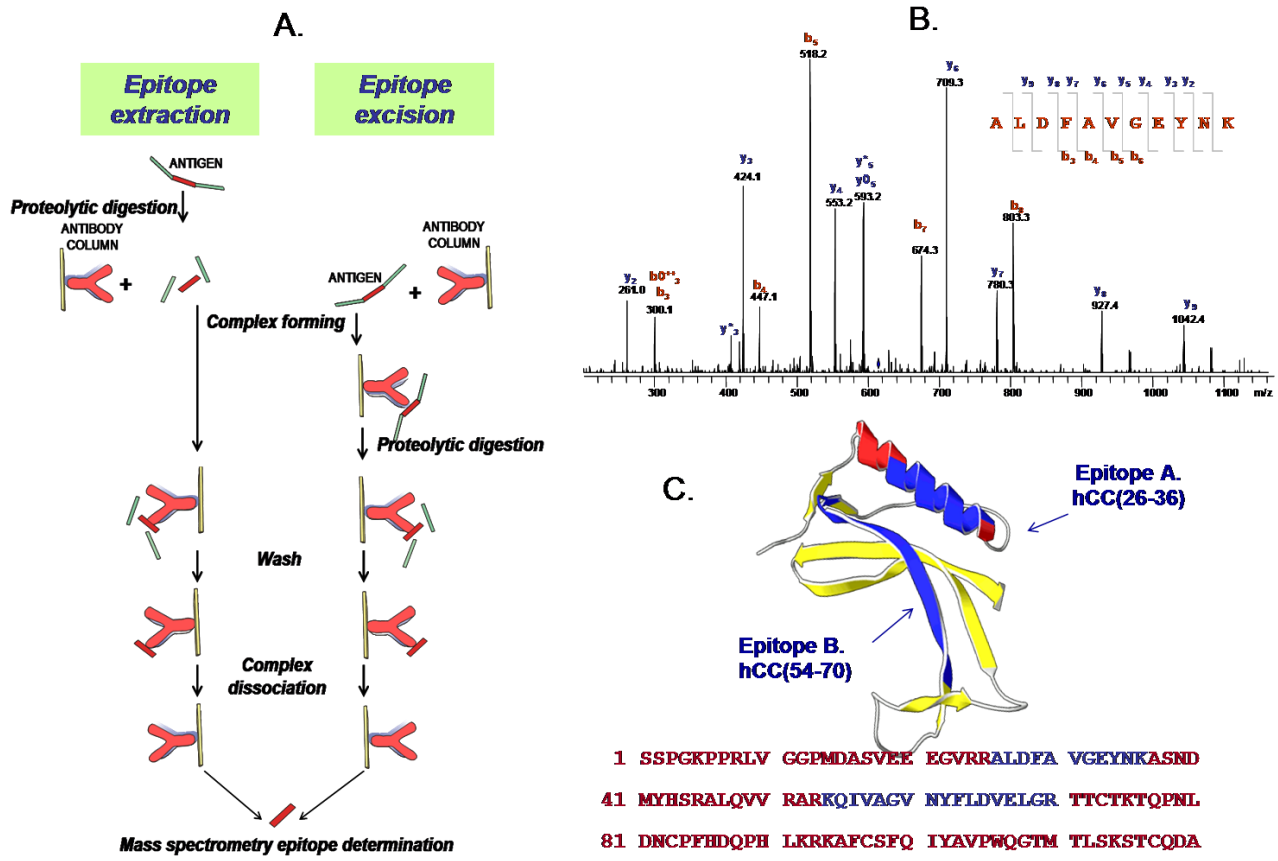

Figure 4. A. - Epitope identification by affinity mass spectrometric methods: epitope extraction and excision. B. - Example of excision experiment involving hCC and a specific hCC monoclonal antibody - epitope fragment identified in the elution fraction. C. - hCC epitope determined by epitope excision and extraction and its positioning in the polypeptide chain

The fragments cleaved from the antigen by the proteases are collected and the epitope-antibody complex is then dissociated under acidic conditions and the elution fraction is collected. Both supernatant and elution fractions are analyzed by mass spectrometry, the fragments found in the elution fragments are mapped on the antigen sequence. In the complementary experiment - epitope extraction, the antigen is first digested in solution before binding to the antibody column, the complex is formed and the unbound peptides washed away. The elution is performed as in the excision experiment and the fractions are analyzed by mass spectrometry.

In the example shown in Figure 4, two epitope peptides were found - hCC [26-36] and hCC [54-70]. 3D protein view revealed that the two epitope peptides were spatially close forming a discontinuous (conformational) epitope. The epitope mapping of the anti-hCC antibody on the hCC surface

showed a different region than the one involved in hCC-Aβ interaction, thus showing the potential of the antibody in the immunotherapy of Alzheimer's disease. In previous work [20.], it has been shown that the neuroprotective protease inhibitor Cystatin C interacts with β-amyloid (Aβ) peptide in the C-terminal domain, namely the region [101-117], the epitope being situated on the opposite side of the hCC molecule, which enables simultaneous interactions of hCC with both Aβ and anti-hCC antibody.

In the present work, the procedure used for the isolation of Aβ-autoantibodies was based on the Aβ-epitope identification performed in our laboratory [21.]. The epitope peptide was analyzed by several affinity techniques such as biosensor- MS and affinity-MS in order to identify the Aβ-core peptide involved in binding to Aβ-autoantibodies.

1.3. Structure and diversity of immunoglobulins

Antibodies form a family of plasmatic proteins, with two special functions: (i.) specific recognition of the pathogen, which initiates an immune response, and (ii.) biological function of recruiting other cells and molecules to destroy the pathogen after antibody binding. The two functions are structurally separated in the immunoglobulin molecule. The relationship between immunoglobulin structure and function is the result of the molecular evolution, by duplication and diversification of a domain in the molecule structure; there is a uniformity of the homologue domains and a diversity of the recognition domains. Antibodies consist of a constant region and a variable one. Variable regions are in more than 95 % identical for a species, but their antigenic specificity may be different even if variable regions have only one amino acid changed[13.].

The prototype immunoglobulin G1 molecule (IgG1) is formed from four polypeptide chains assembled into a macromolecular complex by disulfide bridges. Two chains are smaller and they are called light chains, and the two larger chains are called heavy chains. The two heavy chains are identical, due to the fact that only one of the two genes are expressed in B cells forming the antibody (Allelic exclusion - only one allele gene is functioning for heavy chain and for light chain) [22.].

The proteolytic digestion with papain results in the formation of 3 fragments: two identical Fab fragments (with a molecular weight of 50 kDa) containing the antigen bonding activity (fragment antigen binding, formed by a complete light chain and a part of the heavy chain); the third fragment (with a molecular weight of 80 kDa) does not bind the antigen, but can be easily crystallized (Fc - fragment crystallizable; it is formed by the two remaining parts of the heavy chains and responsible for effector biological functions of the antibodies). There are 5 types of heavy chain classes (μ, δ, γ, α, ε) and two light chain classes (κ and λ). The antibody isotype depends on the heavy chain type and light chain class (e.g., μκ). Considering that the effector functions of the antibody are the consequence of the heavy chain alone, immunoglobulin molecules are classified only by heavy chain class (IgM- μ chain, IgG- γ chain) [23.].

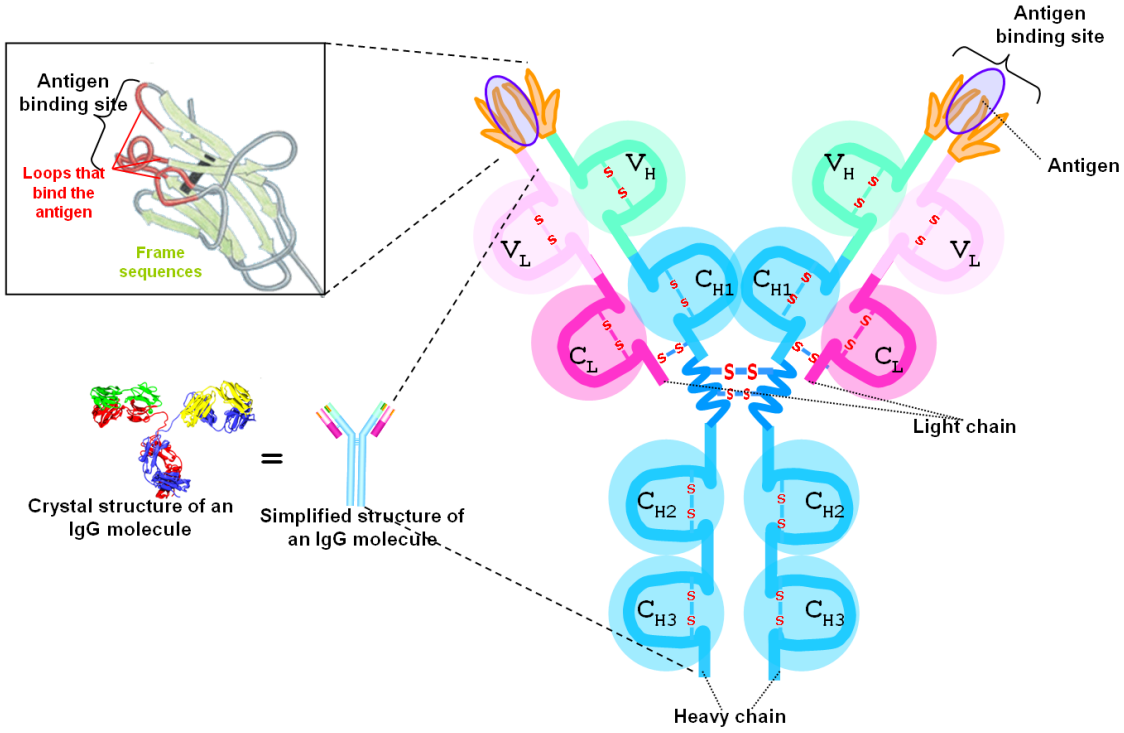

Figure 5. Schematic representation of an immunoglobulin G structure and the antigen binding site. The antibody consists of two heavy chains and two light chains bound together by disulfide bridges in the hinge region. Every heavy chain consists of three constant (C_H) and one variable region (V_H); every light chain consists of one constant (C_L) and one variable region (V_L). The variable regions contribute to the formation the antigen binding domain.

Every heavy and light chain can be divided in domains, each formed from ca. 110 amino acids. The light chain has 2 domains: V_L, for the variable region of

light chain (L) and C_L, the constant region (κ or λ). Heavy chain has 4 domains: V_H – variable region and three domains of the constant region – C_H1, C_H2, C_H3. Between C_H1 and C_H2 regions, there is a switch region, which provides to the Fab part a high mobility compared to Fc. Constant and variable regions of the light and heavy chains are coded by separated genes. Therefore, each type of V_H or V_L can combine itself with every C_H or C_L region. Each V or C domain presents a homology in sequence; which derives from an ancestral common gene. Characteristic of their domain structure is the presence of two Cys residues that form an intra-domain disulfide bridge. In general, the light chain is connected to the heavy chain by a disulfide bridge. Heavy chains are bound by disulfide bridges in the switch region. Each pair is formed by a heavy chain and a light chain and is capable to recognize the same epitope. IgG is glycosylated at the switch region and at the C_H2 domain. Carbohydrate residues are necessary for correct folding and immunoglobulin transport during the synthesis and also appear to have a role in the antibody catabolism rate [24-28.].

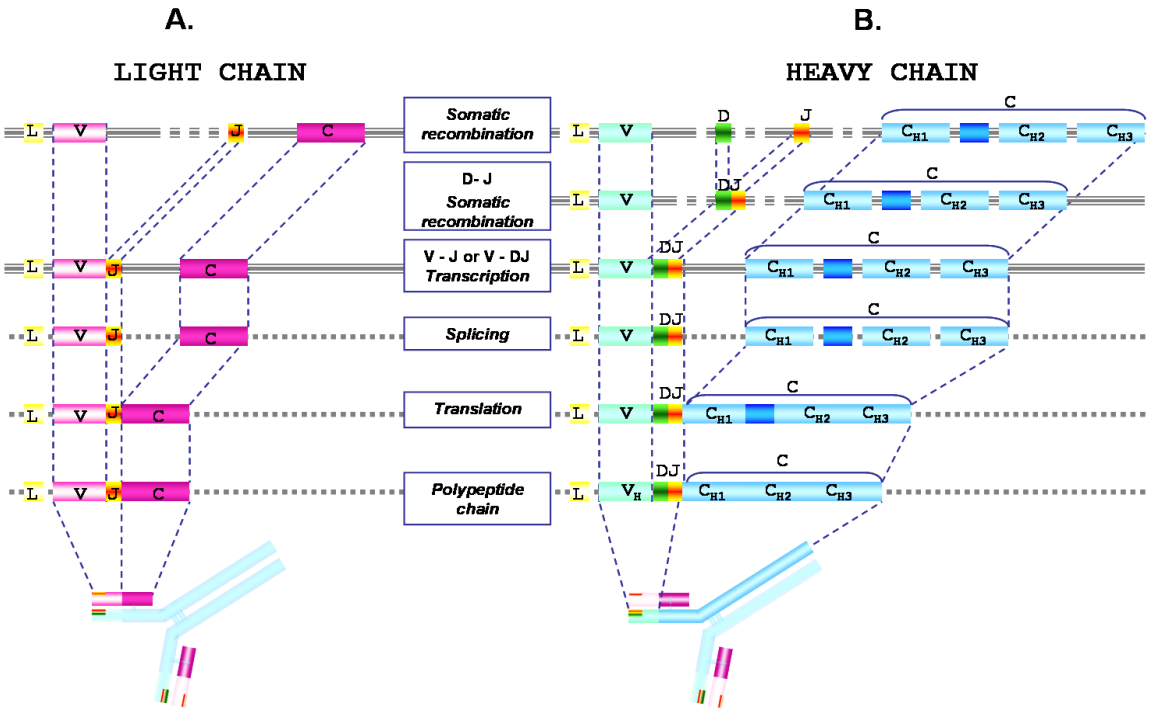

Figure 6. CDR formation in the somatic recombination process. When B cells do not produce any immunoglobulin individual gene segments coding for the V, (D) and J regions of the heavy and light chain of the immunoglobulin molecule are randomly assembled into one molecule. The recombination process is not precise and extra nucleotides are inserted; the number of possibilities of antibody V region diversity is great.

An immunoglobulin domain has a three-dimensional globular compact structure and consists of β-sheet polypeptide chains. Each domain contains two parts: one consisting of 4 β-sheet chains and the other one of 3 chains that form together a hydrophobic sandwich stabilized by an intra-domain disulfide bridge. These chains are connected by so called unstructured „loop" domains. Heavy chains bind to the light chains by the „switch" region, and their binding take place only in the constant region, but not in the variable region.

Constant regions C_H-C_L together create a hydrophobic compact core which offers a stable point for the variable domains, and V_H-V_L regions form a less hydrophobic core which delimits a small ditch in which the antigen molecules will be bound. This ditch together with the end parts of the variable region forms the combination site of the antibody molecule with the antigen or the paratope. In the variable region, the variability is not uniformly distributed, but there are some variability peaks called hypervariable regions (HVR) or complementarily determining region (CDR). There are 3 hypervariable regions for V_H, divided by 4 framework regions. The frame regions are formed by beta-sheet chains, but CDRs are in general „loop regions" forming a surface perfectly compatible with the epitope on the surface of the antigen molecule. In the formation of the antigen binding region, the hypervariable regions are not genetically coded into the general genome, but they are obtained by somatic recombination in the B-cell maturation process [24-29.]. A schematic representation of an immunoglobulin G molecule is shown in Figure 5. During the immune response a multitude of B-cell lines are formed, specific for different fragments of the antigen, each B-cell line producing only one antibody after maturation. By separating an antibody specific against for an antigen fragment from a pool of donors, one can not expect a single clone, but a variability of clones, with different affinities for the same fragment. In the structural analysis of Aβ-autoantibodies, due to the large number of donors from whom the IVIg preparations where obtained, multiple clones were expected with different CDR regions that recognize the same Aβ-peptide fragment.

1.4. Molecular pathology and immunotherapeutic perspectives of Alzheimer's Disease

Dr. Alois Alzheimer observed and documented for the first time in history a form of dementia that later received his name. He followed for a period of five years at the "*Städtische Anstalt für Irre und Epileptische"* the case of Auguste Deter who presented a series of symptoms ranging from loss of short-term memory to basic cognitive functions. At the death of the patient, he performed the autopsy and managed to identify by staining the two microscopic hallmarks of the disease later called Alzheimer's Disease (AD): neurofibrillary tangles and amyloid plaques [30-34.]. Although the last century brought a better understanding of AD, the trigger and early evolution of the disease are still poorly understood. It is known that it is a progressive type of dementia that accounts for an estimated 60 to 80 percent of all dementia cases. In the early phase, AD is characterized by an increasing difficulty in remembering recent events and names of persons and objects. In mild to moderate stages, the cortex cannot process complex calls and loses orientation; confusion is another characteristic and all lead to behavioral changes. In later stages basic functions such as walking, swallowing or speaking are impaired. At present, the diagnosis is established based on the medical and psychiatric history of the patient and family; behavioral and cognitive changes in time; neurological examinations such as magnetic resonance imaging (MRI) and biomarker tests. There are some known risk factors classified in un-modifiable and modifiable. Among the un-modifiable are genetic mutations. One of them is the presence of mutations in genes of amyloid precursor protein, presenilin 1 protein and presenilin 2 protein. Another group is represented by individuals that carry the isoform 4 of the gene apolipoprotein E. Mild Cognitive Impairment (MCI) is another group that can develop early AD. From the modifiable risk factors, early Alzheimer is promoted by cardiovascular diseases risk factors like physical inactivity, smoking, obesity. Physically, head trauma can also lead to AD [35.].

According to the reports of American National Institute of Aging for AD, the number of diagnosed American AD in 2012 was 5.4 million, of which 5.2 million of age 65 or older and the rest at early onset. Thus, one in eight

people over 65 (13%) and half of the age 85, suffer from AD. Every 68 seconds someone in America is diagnosed with AD. The number is projected to double by 2050 (one person to each 33 sec). In Germany, 1.2 million patients were registered in 2010 and by 2030, 2.8 million are expected [36.].

1.4.1. Molecular characteristics of Alzheimer's Disease

One of the changes that occur in the brain of AD patients is the accumulation of β-amyloid peptides (Aβ-peptides) in the extra-cellular space, between neurons, forming deposits known as neuritic or senile plaques together with neuritis and astrocytes from the neighboring neurons. A healthy adult brain has close to 100 billion neurons that connect to each other in a complex network through synapses. Through these connections, the information travels rapidly in form of chemical and electric signals. In AD, the information transfer is blocked at the synapses by β-amyloid plaques and the neurons eventually die [32-35.].

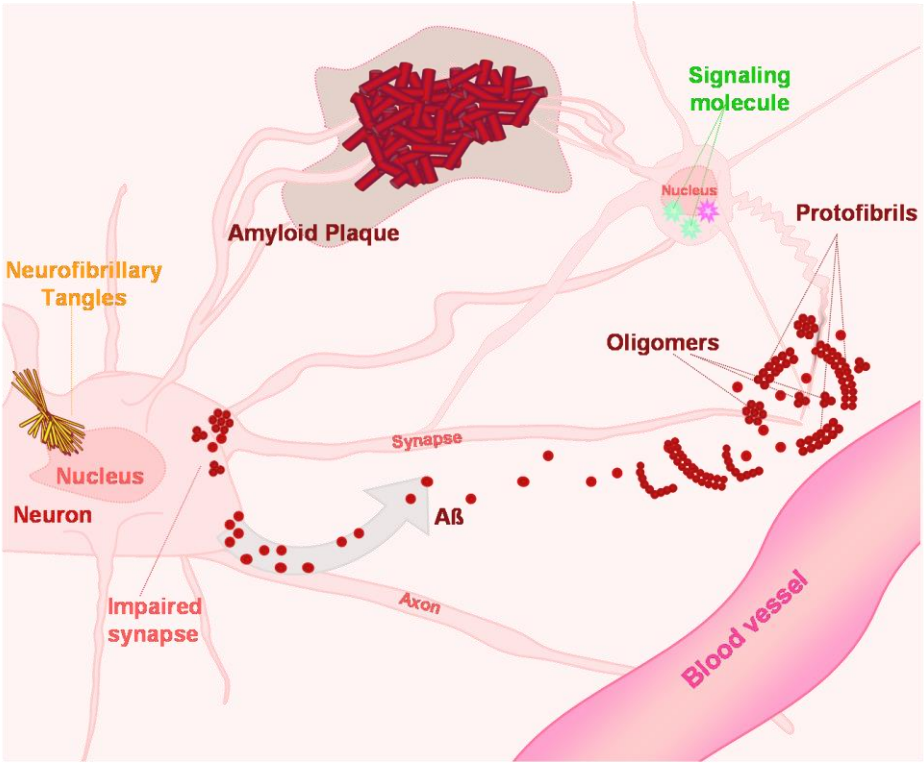

Figure 7. The major molecular hallmarks of Alzheimer's Disease: neurofibrillary tangles and β-amyloid plaques. Aβ peptides are released in inter-cellular space and, if not transported out from the CSF, they form oligomers that aggregate into fibrils and later in β-amyloid plaques blocking the synaptic communications between neurons leading to neuronal death.

Inside the neuron, Tau protein is overexpressed and forms tangles by hyper phosphorylation. Tau is a highly soluble microtubule-associated protein and its main function is to modulate the stability of axonal microtubules. Hyper-phosphorylation of Tau protein blocks the intracellular nutrient transport that contributes to neuronal death. Neuronal death is translated into macroscopic loss of neural mass and shrinkage of white and grey matter [32-35.].

1.4.2. Formation and aggregation of β-amyloid peptides

β-Amyloid is a peptide of 39 to 43 amino acids residues in length, most commonly 40 and 42. It was first found in AD patients and Down syndrome in the meningeal blood vessels, then it was isolated and sequenced from senile plaques [37-39.]. At present, it is known that the peptide is produced by proteolytic cleavage from the amyloid precursor protein (APP). APP is a trans-membrane protein found in the synaptic region of the dendrites is believed to be involved in synaptic transition [40.].

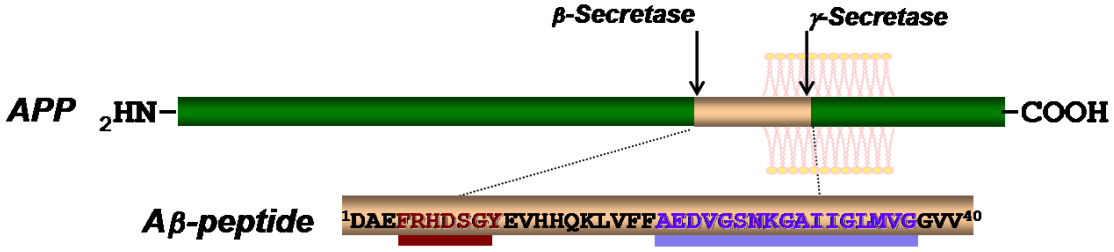

Figure 8. Proteolytic formation of amyloid peptide from APP. Aβ-peptides are produced by cleavage by γ- and β- secretases and they are released in the extracellular space where they are prone to aggregation

APP has an extracellular domain and a single membrane spanning domain. The N-terminal region of the Aβ-peptide derives from the extra-cellular domain of the APP; it is hydrophilic and unstructured. The C-terminal part of the Aβ-peptide originates from the trans-membrane region and is strongly hydrophobic. Aβ is generated from APP by proteolytic cleavage of beta-secretase at the N-terminus, and gamma-secretase at the C-terminus. Aβ42 is the most amylogenic form; Aβ40 has similar properties, but the amylogenic process is slower [40.]. Under physiological conditions in healthy brain, the Aβ-peptides generated have a half-life of 1 to 2 h [41.]. The mechanism involved in the toxicity of the released Aβ- peptides is a matter of debate in

the research community. Although the formed plaques can still exert an inhibitory effect on neuronal cell growth in vitro [42., 43.], it seems that the prefibrillary oligomeric Aβ-peptides are the most neurotoxic species that impair the synaptic function [44., 45.].

Currently, several theories are proposed in order to explain the process of amyloid plaque formation [46.]. The central dogma in amyloidogenesis predicts the formation of intermediate species between the monomers and fibrils as follows: (i.) monomeric Aβ-peptides form (ii.) small oligomers (dimers, trimers etc.), which then asociate to form (iii.) high molecular weight globular oligomers and further aggregate to (iv.) protofibrils and later to (v.) fibrils [47.].

According to another theory, Aβ undergoes a conformational change before the amyloidogenesis and forms intermediate monomeric unstructured states and amyloidogenic oligomers. Although the Aβ conformational change is not well understood, some studies suggest that oxidative stress and N-terminal cleavage might be involved, and that oligomers are the toxic species for the neurons, and not the fibrils [47.].

Both theories propose an equilibrium between the monomeric and the aggregated state of β-amyloid, an equilibrium that in AD is shifted towards the formation of fibrils, while in healthy persons towards the monomers which are cleared by different mechanisms from the brain.

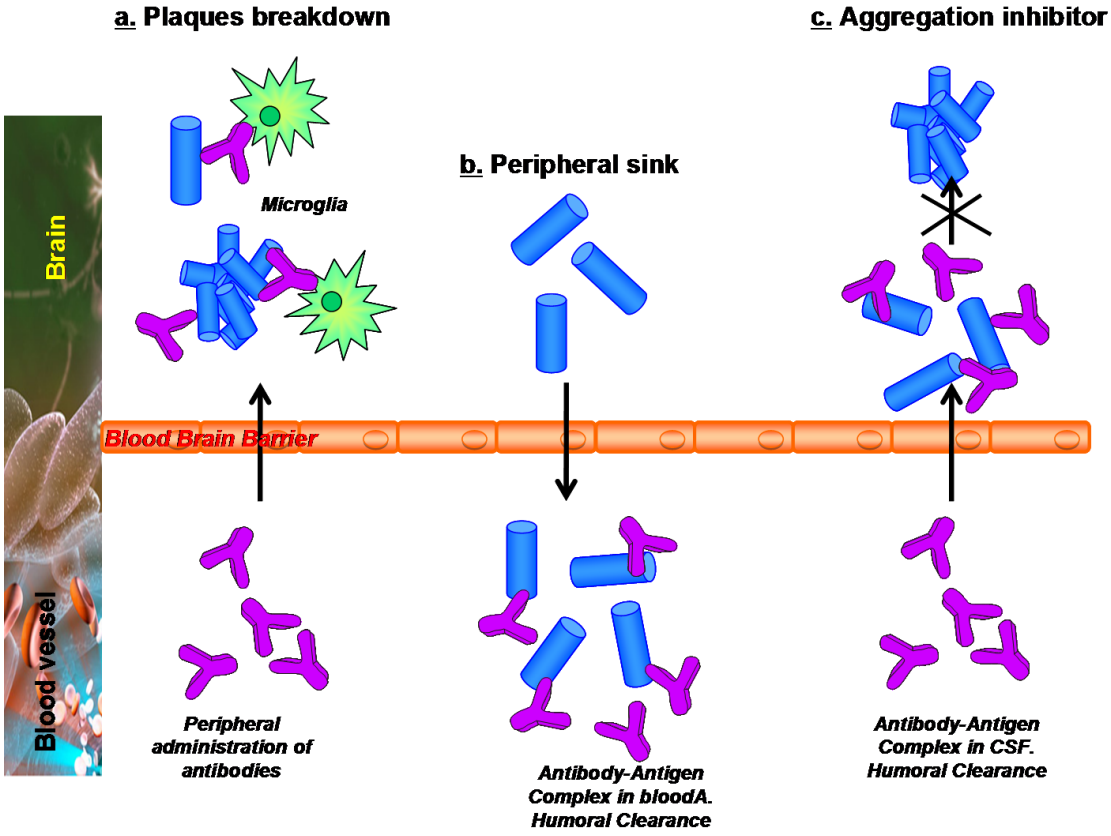

Figure 9. Proposed theories to explain Aβ clearance from the brain: a. - plaques breakdown by microglia; b. - Peripheral sink; c. - aggregation inhibition by forming the Aβ-antibody-Aβ complex [48.].

In Figure 9 different proposed mechanisms are schematically represented for [49-51.]: (i.) *the plaque breakdown hypothesis* based on the presence of antibodies in CSF, suggesting that a small amount of Aβ-autoantibodies can pass through the blood-brain-barrier (0.05 to 0.1%), bind to the Aβ peptides and promote the antibody mediated phagocytosis of the plaques [48.]; (ii.) *the plaque breakdown hypothesis* is based on the peripheral administration of Aβ-binding molecules (immunoglobulins) that bind the monomeric Aβ-peptides, shifting the equilibrium towards the passive migration of the Aβ-peptides from CSF to blood; and (iii.) *the aggregation inhibitor hypothesis* suggests the binding of the antibodies to monomeric Aβ preventing the formation of the amyloidic plaques [48.].

1.4.3. Development of immunotherapy for Alzheimer's Disease

Therapeutic approaches for the treatment of AD intervene in different oligomerization stages. Currently there are ca. 300 ongoing trials worldwide for the treatment of AD, from which 30 are in clinical phase III [52.]. In some studies it is attempted to inhibit the activity of beta- and gamma-secretases and to promote the activity of alpha-secretase, with the subsequent formation of non-amyloidogenic fragments. A possible drug that modulates the activity of gamma secretase is MPC-7869 that promotes the formation of short, less toxic Aβ-peptides [53.].

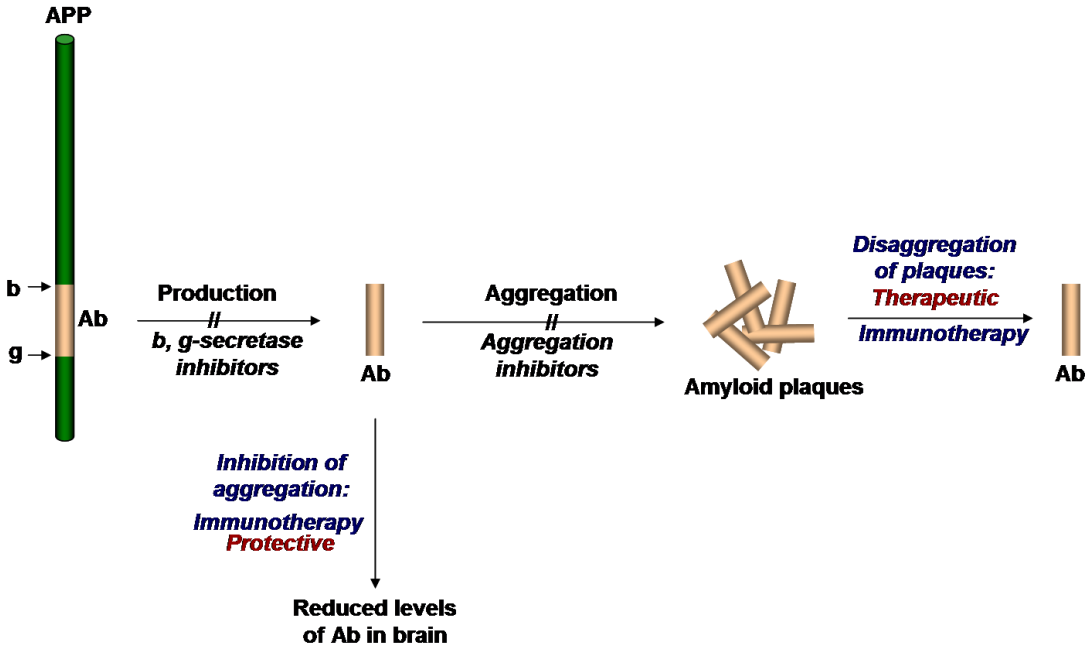

Figure 10. Therapeutic strategies of Alzheimer's Disease aim to interfere with the Aβ production and oligomerization: by inhibiting the beta- and gamma-secretases activities (in order to produce less Aβ-peptides), by inhibiting the aggregation through immunotherapy or by dis-aggregating the plaques (also by immunotherapy).

Other approaches focus on the inhibition of the aggregation process, that can be accomplished either with small molecules or proteins that bind to monomeric Aβ-peptides and thus inhibit the Aβ-Aβ interactions; e.g., cystatin C or anti-Aβ antibodies. At present, there are 3 phase III clinical trials based on antibodies that inhibit the aggregation. They are applied to moderate to late AD cases and are based on therapeutic antibodies that bind to the N-terminus of the Aβ peptide [54.].

Immunotherapy is a therapeutic approach based on “self” or “non-self” antibodies. The antibodies introduced or produced in the system activate the Aβ clearance process. Immunotherapy for AD is still in the initial phase. Although several clinical are ongoing, at present there is no immunotherapeutic agent in clinical use.

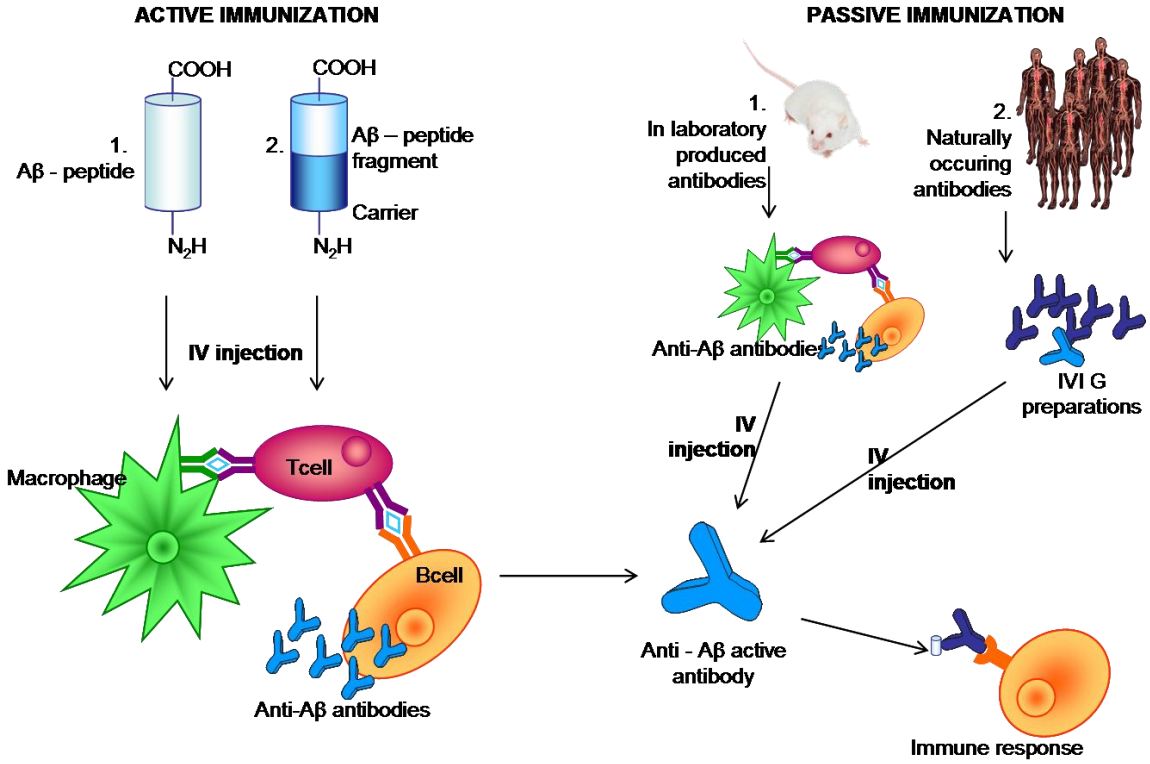

Figure 11. Immunotherapeutic approaches for Alzheimer's Disease: a.- active immunization with an Aβ-peptide or a truncated Aβ-peptide bound to a carrier molecule. The non-self Aβ-peptide fragment produces a chain immune response, with the formation of self-anti- Aβ antibodies, that bind to the self Aβ molecules and remove them from blood; b.- passive immunotherapy by introducing non-self-antibodies (either obtained in the laboratory or from human donors) that bind to the self Aβ-molecules and mediate their removal from blood.

Immunotherapy in Alzheimer's disease may be active or passive. In active immunization the Aβ-peptide fragment alone or bound to a carrier is intravenously administered. The Aβ administration produces a humoral response: Aβ is digested by macrophage which induces T cell response. T cells activate B cell lines that produce antibodies against Aβ. The active immunization is a permanent type of immunization (vaccine) that does not need a periodic administration of antibodies because it induces the formation of self-antibodies. A study of active immunization was discontinued in 2002 due to the observation that 7 % of the patients developed brain inflammation

resembling meningoencephalitis. Another study that uses a modified Aβ-peptide is in phase II clinical trial [55-59.].

In the case of passive immunization, non-self-antibodies are injected to induce the humoral response. The antibodies are either produced in the laboratory in mammalian cells, or are collected from IVIg preparations from a pool of donors. This type of immunization is temporary and repeated injection is necessary [60-62.]. Passive immunization can produce a secondary humoral response against the foreign protein (the therapeutic antibody) which can induce an inflammation (hyper-response) or a resistance (hypo-response) to that protein.

1.5. Aims of the thesis

Alzheimer's disease is the most common form of dementia with a progressive neuro-degeneration characterized by the abnormal accumulation of Aβ-peptides in the extra-cellular space between neurons, forming amyloid plaques. At present, the amyloidogenesis process is not yet understood, as well as the Aβ-peptide clearance from the brain in the healthy individuals. Aβ-autoantibodies levels and functionality may explain the inhibition of Aβ-peptide aggregation and its elimination from the brain. Design of future immunotherapies for the treatment of Alzheimer's disease must take into consideration the specific interaction between Aβ-autoantibodies and Aβ-peptides and the structural particularities of Aβ-autoantibodies.

The major objectives of the present thesis are summarized as follows:

- *Synthesis, purification and characterization of full length and truncated Aβ-peptides* as antigen peptides for Aβ-autoantibodies.
- *Isolation of natural occurring Aβ-autoantibodies from immunoglobulin preparations.* For the isolation of the Aβ-autoantibodies, specific chromatographic procedures were developed, based on an epitope containing peptide covalently bound to a matrix.
- *Primary structure determination of polyclonal Aβ-autoantibodies.* The structural characterization and sequence determination was accomplished using a strategy that combined several complementary techniques: PAGE

electrophoresis, Edman sequencing, MALDI-ToF mass spectrometry, FT-ICR mass spectrometry, proteolytic in gel digestion with specific proteases, liquid chromatography, LC/MS/MS, and de novo sequence determination. The obtained data were assembled into complete primary structures of the Aβ-autoantibodies.

- *Affinity interactions of Aβ-autoantibodies and identification of the Aβ-core epitope.* The major goals of this part were: (i.) to identify Aβ-peptide interaction with Aβ-autoantibodies using affinity methods combined with mass spectrometry; (ii.) to identify Aβ-fragments that interact with Aβ-autoantibodies using hybrid methods, especially online SAW-biosensor-mass spectrometry.

- *Synthesis and affinity interaction studies of CDR peptides derived from primary structure of Aβ-autoantibodies.* Selected CDR peptides of Aβ-autoantibodies were prepared by SPPS, purified and characterized by mass spectrometry and by analytical HPLC. Their affinities towards Aβ were evaluated using affinity-mass spectrometric methods.

2. RESULTS AND DISCUSSIONS

2.1. Epitope specificity of Aβ-autoantibody

The immunotherapy of human Alzheimer's disease is based on the production and administration of Aβ specific antibodies classified in two types according to their specific epitopes: (A.) "Plaque specific", anti-Aβ antibodies that recognize the N-terminal of Aβ and are obtained in laboratory mammals are usually monoclonal. In Western Blot they recognize both monomeric and aggregate forms of Aβ. Anti-N-terminal antibodies could help in the treatment of advanced AD by assisting in the disaggregating process.

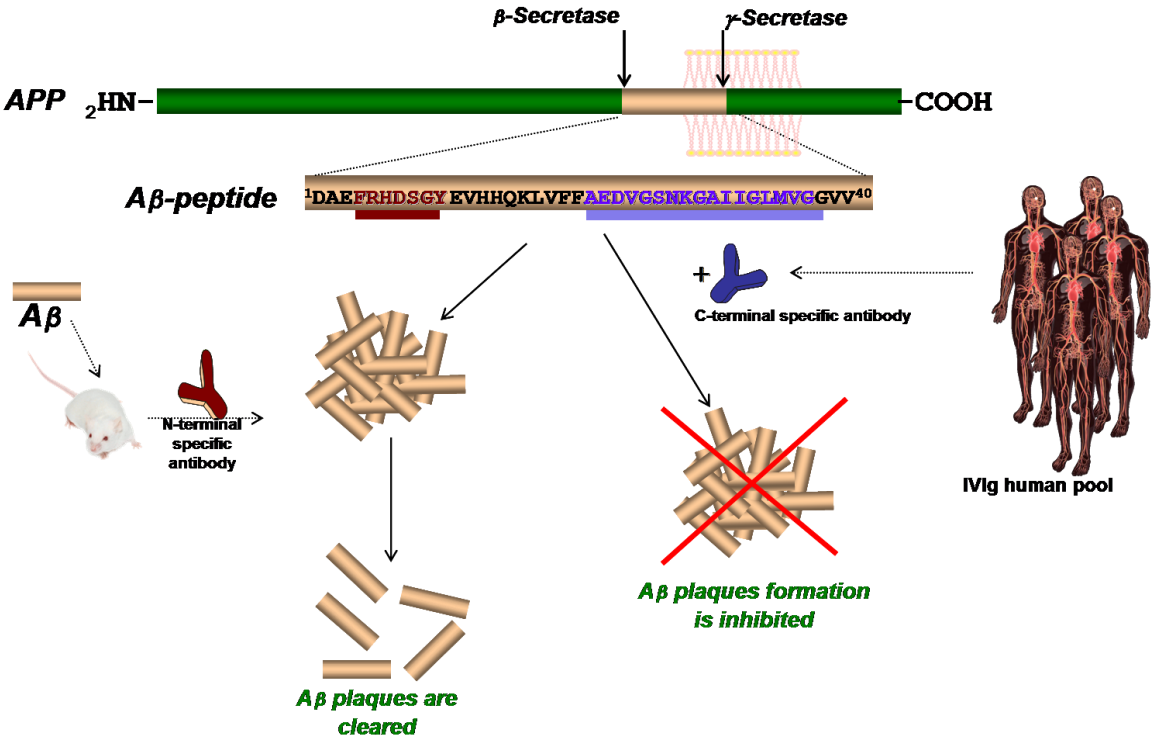

Figure 12. Types of anti-Aβ antibodies present in AD immunotherapy: A. - anti N-terminal of Aβ peptide antibodies, so called "plaque specific antibodies", that bind to the flexible part of the Aβ-molecule involved in plaques and helps clearing them; B. - anti C-terminal of Aβ-peptide antibodies, so called "plaque protective", that bind to the part of the Aβ-molecule involved in aggregation inhibiting the formation for the plaques

(B.) The second type, "Aβ protective antibodies" are specific for the C-terminal of Aβ. Generally, C-terminal antibodies are polyclonal and are obtained from human blood. The naturally occurring antibodies against the C-

terminal of Aβ are found in human individuals and usually are referred to as "Aβ-autoantibodies". Their presence in blood was hypothesited already in 1993 by Gaskin [63.], and a series of studies to elucidate their function were performed by Du et al. in early 2000 [64-66.]. The Aβ-autoantibody epitope was first identified by our laboratory after separation from IVIG [21.].

Previous studies on Aβ-autoantibody were mostly focused on quantification by affinity techniques and their value as a biomarker for AD. It was shown that in healthy individuals the levels of free Aβ-autoantibody are higher then in AD patients, while the Aβ-autoantibody - Aβ complex is present in higher amounts in AD patients, compared to healthy subjects [67.].

A phase III clinical trial was started in 2012 by passive immunization. In this study, AD patients receive a periodic injection with IVIg to replace the antibodies implicated in the Aβ-complex. By introducing an entire IVIg fraction, two major problems were considered: (i.) there is lower incidence of resistance to treatment due to the complexity of the preparation, and (ii.) the denaturation of the Aβ-autoantibody is avoided by mild acidic treatment. The clinical trial suggested some improvement in the cognitive functions of the patients [68-70.].

Previous work performed in our laboratory focused on Aβ-autoantibody that recognizes the larger epitope region[48.]. Affinity-mass spectrometric identification of the epitope region recognized by Aβ-autoantibody was carried out by epitope extraction and epitope excision. The procedures and results obtained are illustrated in Figure 13. In epitope extraction the antibody is covalently immobilized on a sepharose matrix. The antigen is digested in solution with a protease and the proteolytic mixture added on the column. After incubation, the unbound peptides are washed out and elution is performed by changing the pH to acidic and the elution fraction analyzed by mass spectrometry.

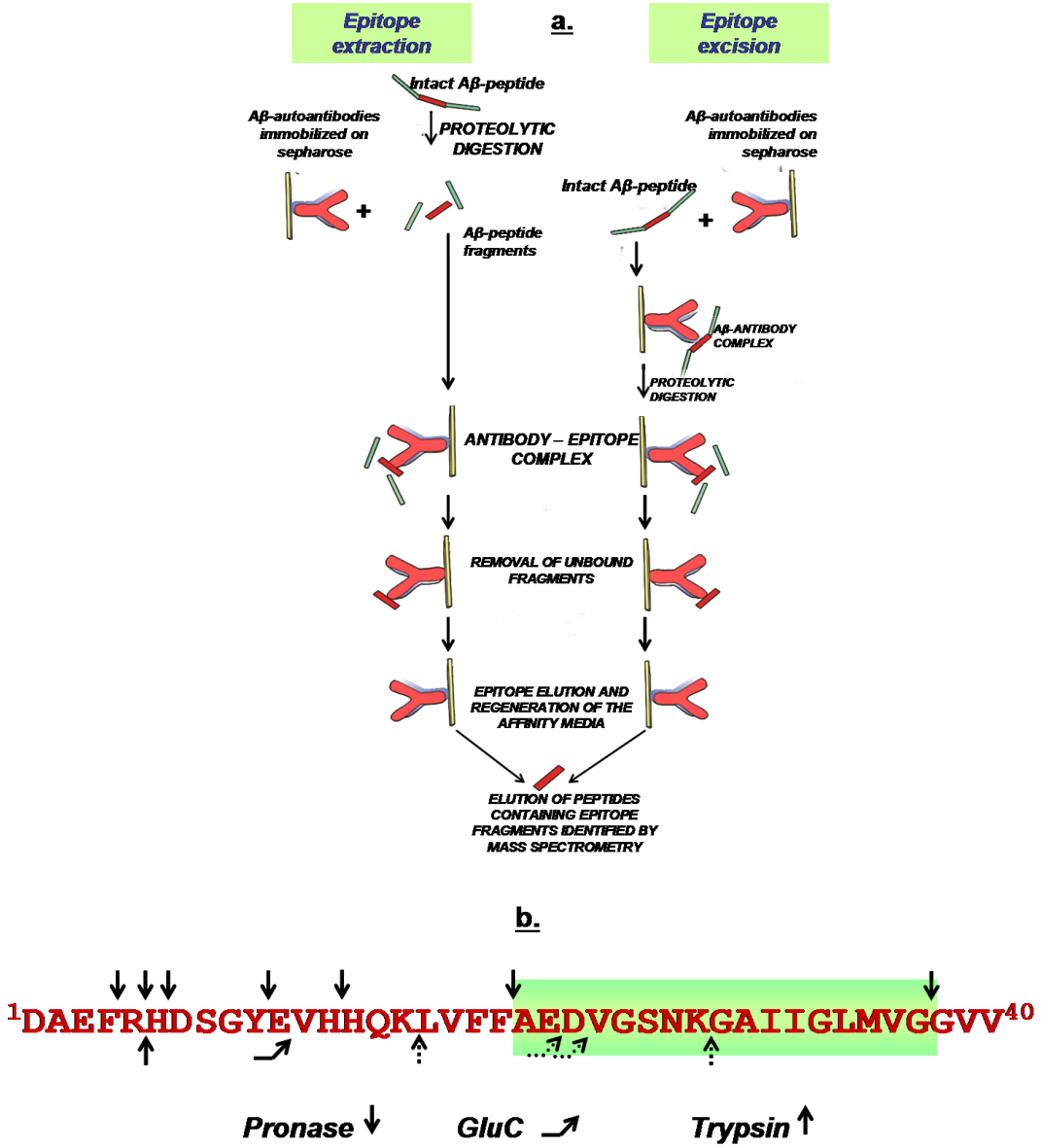

Figure 13. Aβ-autoantibody epitope determination [48.]. a. - Epitope extraction procedure & Epitope excision procedure for the determination of the epitope specific for Aβ-autoantibody; b. - Aβ-autoantibody epitope determination in region Aβ(21-37) obtained after sites E^{21} and D^{22} are protected in epitope excision with Gluc C and site K^{27} is protected in epitope excision with trypsin. Pronase gave the shortest epitope in these experiments - ^{21}EDVGSNKGAIIGLMV^{37}.

Epitope excision uses the affinity binding of the entire antigen to the immobilized antibody, and digestion of the antigen bound to the antibody[71.]. The proteolytic sites in the binding region are protected by the antibody-antigen interaction, the rest of the antigen is proteolytically digested and the fragments are washed away. By changing the pH the peptides are eluted from the column and analyzed by mass spectrometry. Mapping the peptides

present in the elution lead to the identification of the epitope of the Aβ-autoantibody. In the epitope extraction experiment, Aβ proteolytic mixtures were prepared with GluC, trypsin and chymotrypsin. Aβ-autoantibody was immobilized on a NHS - sepharose matrix and the mixtures were added. After incubation at 37°C, the supernatant was collected and analysed by mass spectrometry. The remaining unbound fragments were washed out and elution obtained by acidic pH. In the elution fractions the smallest binding fragment was Aβ (17-40).

Epitope excision was performed with Aβ (1-40). On the antibody column, Aβ (1-40) peptide was added and the column was incubated at 37°C; the complex protease was added in successive experiments (GluC, trypsin, chymotrypsin and pronase) and incubated again at 37°C. The supernatant was collected, the column washed and elution performed. By overlapping all the fragments found in the elution fraction, Aβ (21-37) was assigned as the smallest binding region [48.]. Using the information found in the epitope identification experiments, the affinity of Aβ-autoantibody towards different synthetic Aβ-peptides was tested by enzyme-linked immuno-sorbent assay (ELISA) [48.], including alanin scan to identify the epitope core. These affinity experiments showed that in ELISA, the identified epitope peptide Aβ (21-37) and smaller Aβ-fragments, did not bind to Aβ-autoantibody, but it required a longer Aβ-fragment. Another finding of the affinity experiments was that there is no difference between the affinity towards synthetic Aβ (1-40) and Aβ (12-40) peptides in ELISA experiments. To determine the core epitope was necessary to use techniques to evaluate the affinity of different truncated Aβ-peptides and Aβ-autoantibody that allows better spatial arrangement of the complex.

2.2. Isolation of Aβ-autoantibody from immunoglobulin preparations

2.2.1. Synthesis and structural characterization of Aβ-peptides

For the selection of the Aβ-peptides prepared by chemical synthesis, two parameters were considered: (i.), the positioning of the epitope region [48.]; and (ii.), the tertiary structure and orientation of the β-amyloid peptides in fibrils. β-Amyloid fibrils present an unstructured N-terminal domain ^{1}DAEFRHDSGYEVHHQKL^{17}, and a highly structured C-terminal domain ^{18}VFFAEDVGSNKGAIIGLMVGGVVIA^{42}.

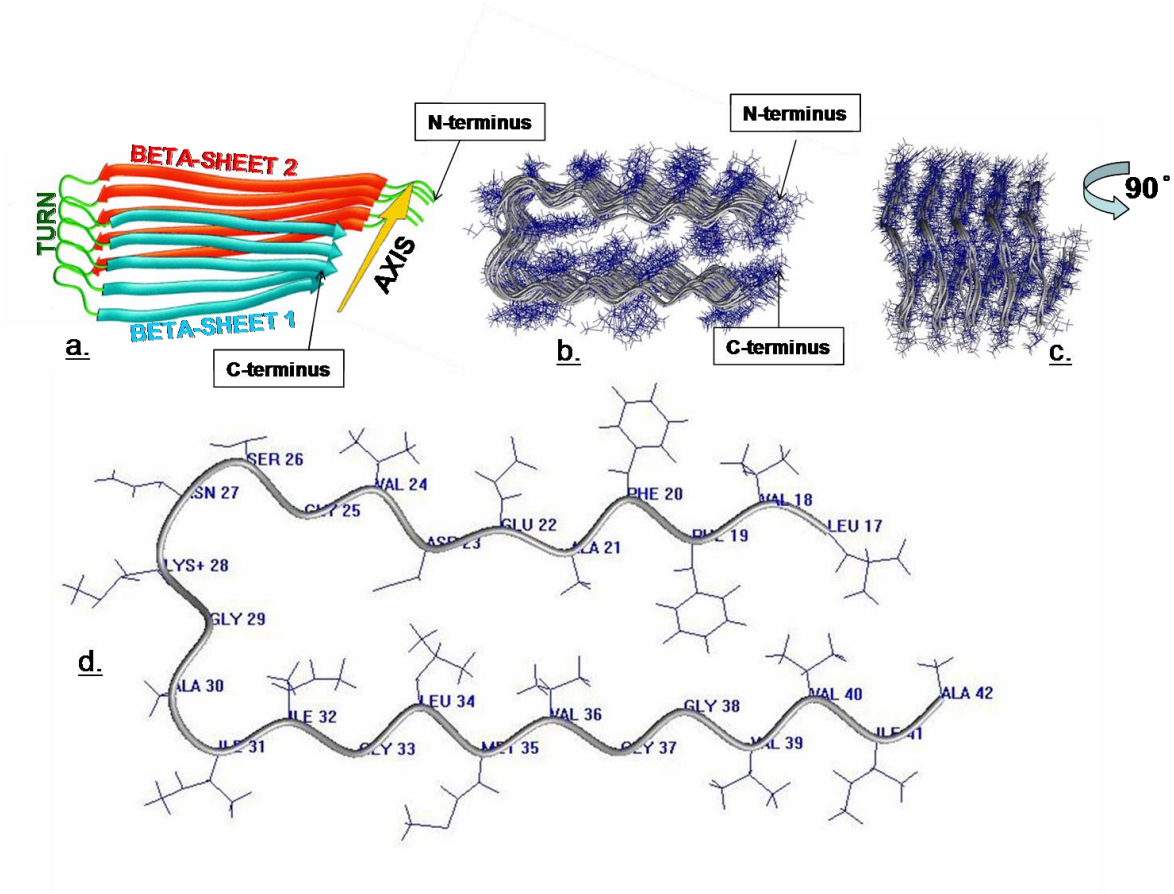

Figure 14. 3D modeling of Aβ-fibril structure: a. - representation of amyloid fibrils - the peptide molecule folded forming two complementary beta-sheets, one from Ile31 to Ala42 and one from Ser26 to Leu17; between the two beta-sheets Ala30 to Asn27 fragment forms a turn region; b. & c. - 3D modeling of the amyloid fibrils, the beta sheets are aligning; d - amino acids side chain orientation in β-amyloid fibrils; d. – Side chains orientation in a Aβ-peptide involved in aggregation.

In the structured domain the polypeptide chain forms a beta-turn-beta strand motif that contains two beta-sheets between residues 18-26

(^{18}VFFAEDVGS^{26}) and 31-42 (^{31}IIGLMVGGVVIA^{42})[66.]. The turn region is fixed in place by two beta-sheet complementary regions which suggest that in monomer form is not structured. Although there are several theories dealing with the transition monomer - oligomer - fibril, none of these has been experimentally proven, and the modification in the tertiary structure and orientation of different regions of Aβ during the oligomerization process is unknown [72-80.].

For this thesis, a series of Aβ-peptides were synthesized by manual or semiautomatic SPPS [81-83.] using NovaSyn-TGR resin and fluorenylmethyloxycarbonyl (Fmoc)/tert-Butyl (tBu) protection chemistry[84.]. Double or triple coupling was used to provide near-complete formation of peptide bonds. For the semi-automated synthesis, fresh solvents were used after each 8 amino acid coupling step. For the manual synthesis, each coupling was checked by bromophenol blue, and when necessary triple or even quadruple coupling was employed. The general protocol for synthesis is described in the Experimental Part (3.3).

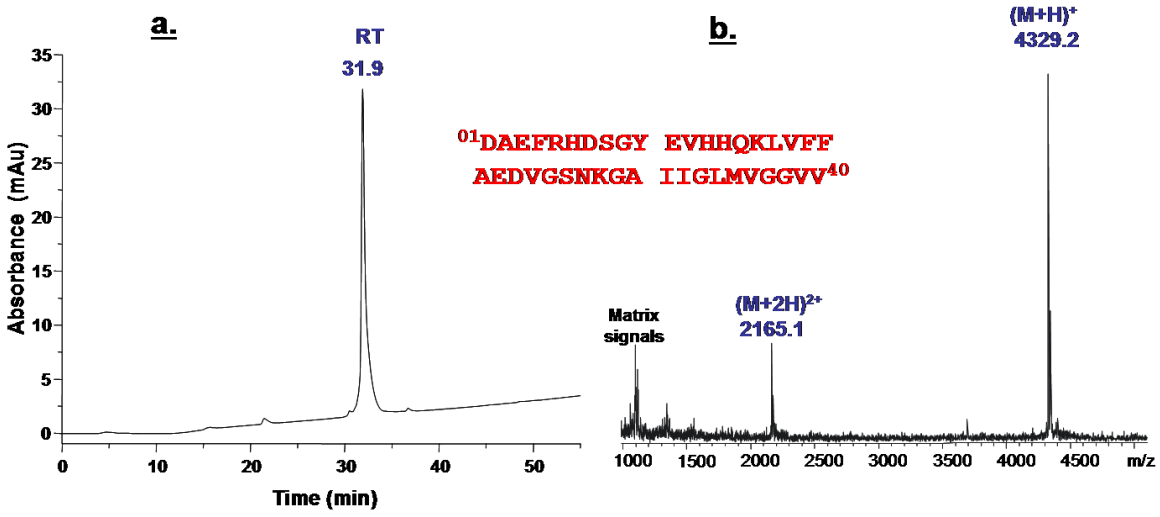

Figure 15. Characterization of synthetic Aβ (1-40): a. - RP-HPLC profile of the purified Aβ (1-40); b. - MALDI-ToF mass spectrum of synthetic Aβ (1-40).

The peptides were dried by lyophilization and purified by semi-preparative RP-HPLC, and characterized by MALDI-ToF MS and/ or ESI-ion trap MS. An example of the Aβ-peptide purification and mass spectrometric characterization is shown in Figure 15. All amino acid sequences, HPLC

retention times and masses of the synthesized Aβ-peptides are summarized in Table 1.

Table 1. Aβ-peptides synthesized by SPPS

No.	Aβ – peptides[a]	Sequence	HPLC Rt(min)[b]	$[M+H]^+_{calc}$ [c]	$[M+H]^+_{exp}$ [d]
1	Cys-Aβ(1-40)	C^{1}DAEFRHDSGYEVHHQKLV FFAEDVGSNKGAIIGLMVGG VV^{40}	33.7	4429.15	4429.38
2	Aβ(1-40)	^{1}DAEFRHDSGYEVHHQKLVF FAEDVGSNKGAIIGLMVGGV V^{40}	31.9	4329.86	4329.20
3	Cys-Aβ(12-40)	C^{12}HHQKLVFFAEDVGSNKGA IIGLMVGGVV^{40}	30.2	3124.70	3125.10
4	Aβ(12-40)	^{12}HHQKLVFFAEDVGSNKGAI IGLMVGGVV^{40}	28.9	2923.43	2923.81
5	Aβ(31-40)	^{31}IIGLMVGGVV^{40}	15.5	957.25	957.56
6	Aβ(17-28)	^{12}LVFFAEDVGSNK^{28}	13.4	1325.48	1325.84
7	Aβ(25-35)	^{25}GSNKGAIIGLM^{35}	14.2	1060.28	1060.59
8	Aβ(4-10)	^{4}FRHDSGY^{10}	10.6	880.91	881.20
9	Aβ(1-16)	^{1}DAEFRHDSGYEVHHQK^{16}	12.9	1955.03	1955.34
10	Aβ(20-37)	^{20}AEDVGSNKGAIIGLMVG^{37}	17.1	1630.88	1631.12

[a] Peptides obtained by solid phase peptide synthesis, Fmoc stategy

[b] RP-HPLC purification (Ultimate 3000, Dionex ;ThermoFisher) using a Vydac C4 column

[c] Calculated using GPMAW software (Lighthouse Data, Denmark)

[d] Mass spectrometric amalysis by ESI-ion trap (Esquire 3000) or MALDI-ToF (Micromass ToFSpec2E, Warters).

Before usage, a stock solution was prepared with a concentration of 1 µg/µL in trifluoroethanol. Trifluoroethanol (TFE) promotes the monomeric state of the Aβ-peptides by inducing the random coil and alpha helix conformation [85.]. Longer Aβ-peptides with an N-terminal cysteine residue were prepared for the affinity isolation of Aβ-autoantibody and truncated Aβ-peptides were

synthesized to be used in affinity-mass spectrometry studies and to map the core epitope.

2.2.2. Affinity isolation of Aβ-autoantibody from serum immunoglobulin

For the separation of the Aβ-autoantibody a modified affinity protocol as described previously was used [48.]. Immunoglobulin preparations from different sources (Sigma, Calbiochem) were used, after their affinity towards Aβ-peptides was ascertained. Aβ (12-40) peptide with an N-terminal cysteine residue was synthesized by SPPS. The choice of Cys-Aβ(12-40) was made for several reasons: (i.), the Aβ-autoantibody has the epitope situated between amino acids (21- 37) [48.]; however Aβ (21-37) alone loses the original conformation found in Aβ (1-40), and is not recognized by the Aβ-autoantibody; (ii.), Aβ (12-40) does not contain the epitope of the "plaque specific" antibodies that recognize the N-terminal of Aβ at amino acids (4 -10); (iii.), the cysteine at N-terminal allows flexibility of the ligand in the affinity matrix and does not interfere with the antigen-antibody interaction; (iv.) and, finally, there is no difference in affinity of the Aβ-autoantibody separated on matrices with Cys-Aβ(1-40) or Cys-Aβ(12-40). The affinity column preparation and isolation protocol are described in the Experimental Part (3.4.1-2).

The concentration of Aβ- autoantibody was established to be approximately 0,02 % of the total immunoglobulin fraction. The Aβ-autoantibody was quantified using the BCA assay according to the protocol presented in Experimental Part (3.4.3). For each separation approximately 150 μg Aβ-autoantibody were obtained.

The following structural studies were performed with approximately 3 mg in total. All separations were performed on 5 different matrixes with immobilized Cys-Aβ(12-40). After the quantification, the antibodies were subjected to reduction of the disulfide bridges using dithiothreitol (DTT). The lyophilized antibodies were re-dissolved in water and DTT was added in 10000 x molar excess. The solution was incubated at 60°C for 2 hours and then alkylation by iodoacetamide (IAA) was performed. The reaction was left overnight at

37°C and at the end the polypeptide chains were concentrated by lyophilization and reconstituted in running buffer for electrophoresis (Figure 16.).

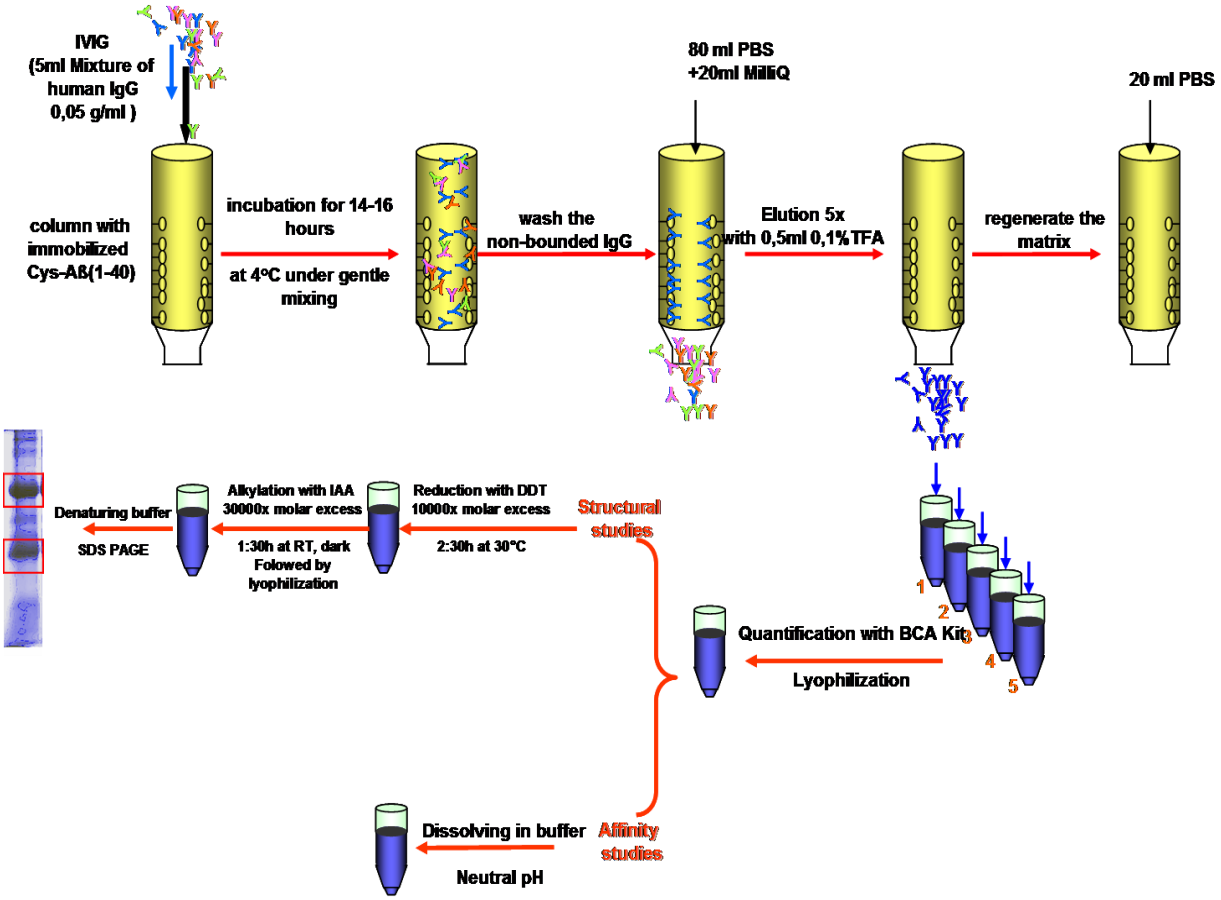

Figure 16. Affinity isolation of Aβ-autoantibody from IVIg preparations. 12mg IVIg dissolved in 5mL PBS are loaded on the affinity matrix with immobilized Cys Aβ(12-40). The column is incubated under agitation at 4°C for 16 to 18 hours and the unbound IgG molecules are removed by washing with 80ml PBS and 20mL water. Elution is performed by changing the pH at 2 with 0.1%TFA.

For the subsequent affinity experiments, the Aβ-autoantibody was suspended in trifluoroethanol, centrifuged and the dissolved antibodies were again quantified. A stock solution was prepared in TFE at a concentration of 1 µg/µL before each affinity experiment, to prevent aggregation and precipitation of Aβ-autoantibody. To verify their activity, a series of dilutions was done and the affinity against Aβ (1-40) peptide was determined by ELISA. Aβ-autoantibody separated on an affinity column with immobilized Cys-Aβ (1-40) and Cys-Aβ(12-40) were investigated in parallel, as well the entire immunoglobulin fraction.

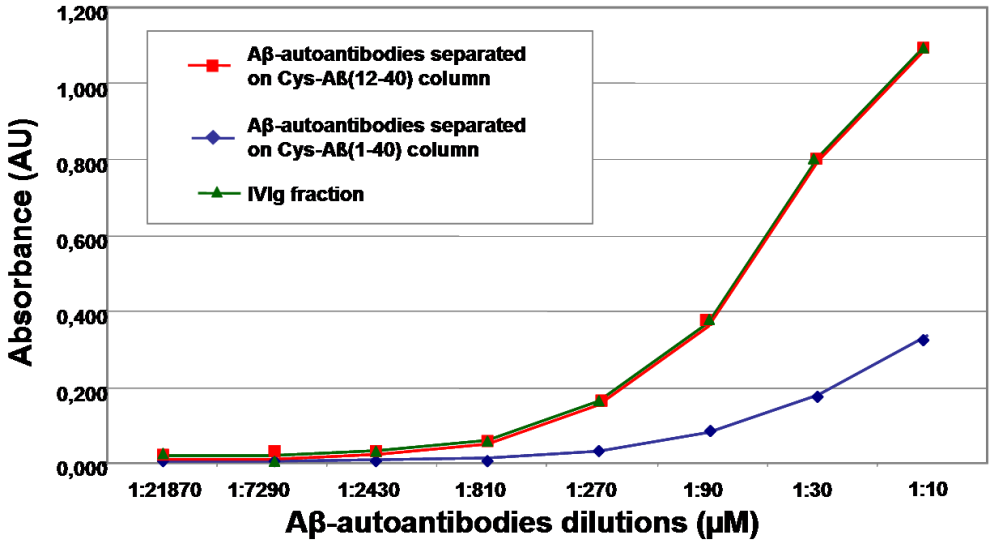

Figure 17. ELISA investigation of the autoantibody affinity towards Aβ (1-40). Aβ-autoantibody separated on Cys-Aβ (12-40) matrix presented the highest affinity for Aβ, followed by Aβ-autoantibody separated on Cys-Aβ (1-40). The whole IVIg fraction presented also affinity, but much lower.

In the direct ELISA, Aβ (1-40) was immobilized on a 96 well plate, the plate was washed and antibody dilutions were added in triplicates. After incubation, the plate was washed and the bound autoantibody was detected with an anti-human antibody conjugated with horse radish peroxidase. The substrate was added and the plate was read with a Victor2 plate reader. The results showed that Aβ-autoantibody separated on Aβ (12-40) and Aβ (1-40) have similar affinity for Aβ (1-40).

2.3. Primary structure determination of Aβ-autoantibody

Initial structural studies of the Aβ-autoantibody were carried out by 1D- and 2D-gel electrophoresis followed by in gel digestion and by mass spectrometry analysis of the mixtures. In the 2D-gel electrophoresis, the mixture was loaded on an IPG strip with a pH gradient from 3 to 10. After the first dimension of the electrophoresis, the disulfide bridges were reduced by DTT and the free –SH groups were alkylated with iodoacetamide. The IPG strip was then subjected to the second dimension for separation of light and heavy chains.

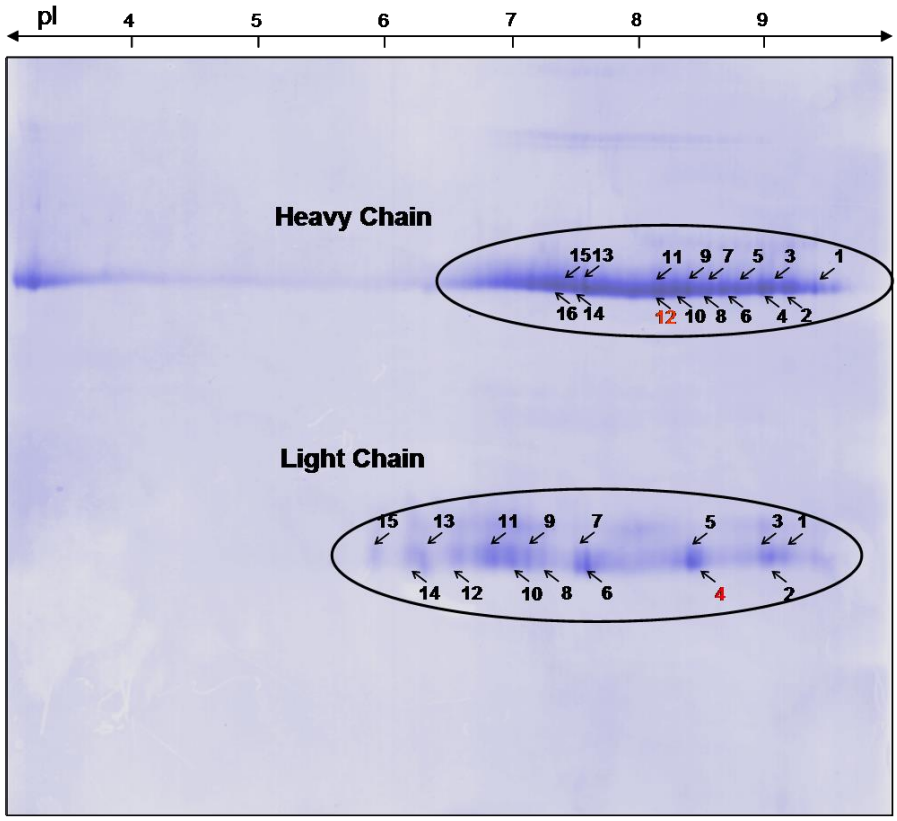

Figure 18. 2D-SDS-PAGE of Aβ-autoantibody visualized with colloidal blue reveals their heterogeneity [48.]

The 2D-electrophoresis of autoantibody showed a multitude of variants for both light and a heavy chain, clustered in patterns at pH values 6 to 10. Although the pattern in several experiments was identical, only some spots could be individualized (ca. 15 for each chain). However, these studies showed that the separation of light and heavy chains is effective and

proteomics approach led to identification of fragments from the constant regions[48.]. For the identification of variable region fragments, the 2D-gel approach was not successfully due to poor reproducibility of the 2D-gels and insufficient separation of the Aβ-autoantibody isoforms. Instead, 1D SDS-PAGE was used for separation of light and heavy chains and the strategy for identification of different variants of the chains was based on overlapping fragments.

Further studies of the Aβ-autoantibody led to the identification of their immunoglobulin types by analyzing the glycosylation pattern [86.]. After separation of the light and heavy chains, the heavy chain bands were cut, destained and subjected to proteolytic digestion. The glycopeptides were selectively detected in this mixture by monitoring the formation of the GlcNAc-oxonium ion of *m/z* 204.1 in the parent ion detection mode (Figure 19).

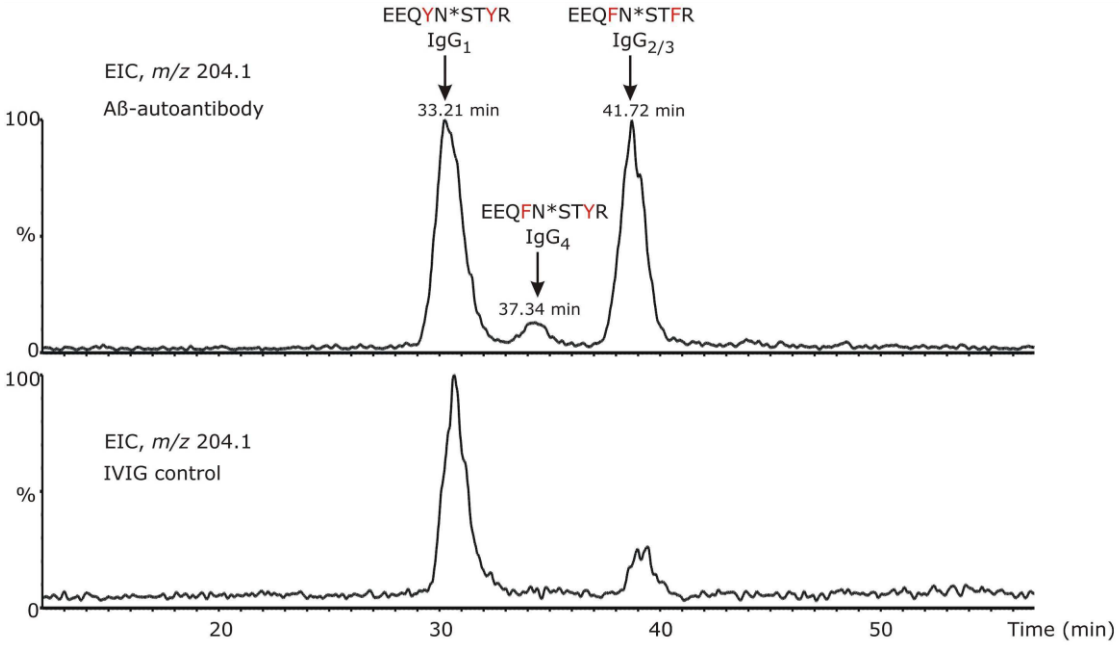

Figure 19. EIC of m/z 204.0 for a gradient of 60 minutes. The peaks observed in the chromatogram were assigned to distinct N-glycosylated peptide isoforms, corresponding to individual IgG subclasses found in the Aβ-autoantibody and IVIg, as indicated above each peak [86.].

As a reference, the total IVIg fraction, as starting material for the epitope-specific isolation of the Aβ-autoantibody, was analyzed in parallel with the Aβ-autoantibody. The human IgG subclasses showed more than 95% constant region sequence homology, but characteristic differences in the

length of the hinge region, the number of disulfide bridges, and in the C_{H2} domain around the region of *N*-linked glycosylation [86.].

For a rigorous, subclass specific glycosylation analysis of the Aβ-autoantibody, the tryptic digestion of the heavy chain was performed to completion. The concentration of each immunoglobulin in serum of healthy individuals depends on several factors, e.g. the number of plasma cells producing that antibody type. Adults exhibit highest concentrations of IgG_1 (10-12 mg/mL), followed by IgG_2 (2 - 6 mg/mL), IgA_1,IgM, IgG_3 (0.5 - 1 mg/mL), IgG_4 (0.2 - 1 mg/mL), IgA_2, IgD and IgE .Because IgG_2 and IgG_3 have identical amino acid sequences around the *N*-glycosylation site, it was not possible to separately analyze their glycosylation profile. However, the amount of IgG_3 is considerably lower than IgG_2 in human plasma. The ion current of *m/z* 204.1 indicated that the Aβ-autoantibody contains elevated levels of $IgG_{2/3}$ compared to IVIg. From the ion abundances of all glycopeptides observed in each individual subclass, the ratio $IgG_{2/3}/IgG_1$ for the Aβ-autoantibody was determined to approximately 1 and in IVIg 1:4. The levels of IgG_4 were found to be higher than those in total serum IgG [86.].

The MS/MS fragmentation of the *N*-glycosylation for each IgG subclass started with the peptide analysis that revealed the amino acid sequence EEQXNSTXR (where X = F or Y). The glycans decorating the Aβ-autoantibody constant region are almost entirely core fucosylated and the most abundant glycoform in each IgG subclass is G_1F, followed by G_0F and G_2F. The Aβ-autoantibody contains lower levels of galactosylation, as G_0F glycoform is elevated and G_2F is decreased within each subclass compared to IVIg. No significant differences were observed among the remaining glycoforms for IgG_1 and $IgG_{2/3}$, respectively [86.].

The information obtained in the previous studies can be summarized as follows: (i.) the Aβ-autoantibody epitope region is (21-37); (ii.) synthetic peptide Aβ (21-37) is not binding to Aβ-autoantibody, while Aβ (12-40) and Aβ (1-40) present high affinity towards Aβ-autoantibody, suggesting that the found epitope fragment is too small or conformationally different than the full-length Aβ-peptide; (iii.) 1D gel electrophoresis followed by a peptides separation and analysis is preferable to the 2D-gel electrophoresis followed

by a classical proteomics approach; (iv.) the Aβ-autoantibody isoforms are belonging to all IgG subclasses, according to their glycoprofiles.

2.3.1. Strategies for primary structure determination of Aβ-autoantibody

Aβ-autoantibody used for structural studies were obtained by affinity chromatography from commercially available IVIg preparations. For the structural studies, Aβ-autoantibody was denatured by reduction of the disulfide bridges and alkylation, to maintain the polypeptide chains unstructured. The separated light chains and heavy chains were isolated by one dimensional electrophoresis and afterwards, several analytical methods were applied in parallel to identify primary structures.

The N-terminus was determined by blotting followed by Edman sequencing. Several batches of light and heavy chains were subjected to proteolytic digestion with different proteases in order to obtain overlapping fragments of different length. The digestion mixtures were analyzed by mass spectrometry and peptide fingerprinting was performed by searching against data bases. The proteolytic peptides were separated by analytical HPLC and analyzed by high resolution mass spectrometry, Edman sequencing and HPLC - ion trap mass spectrometry with MS/MS capability. The primary structure information obtained from analyzing the HPLC fractions containing the proteolytic peptides was compiled manually into consensus antibody sequences.

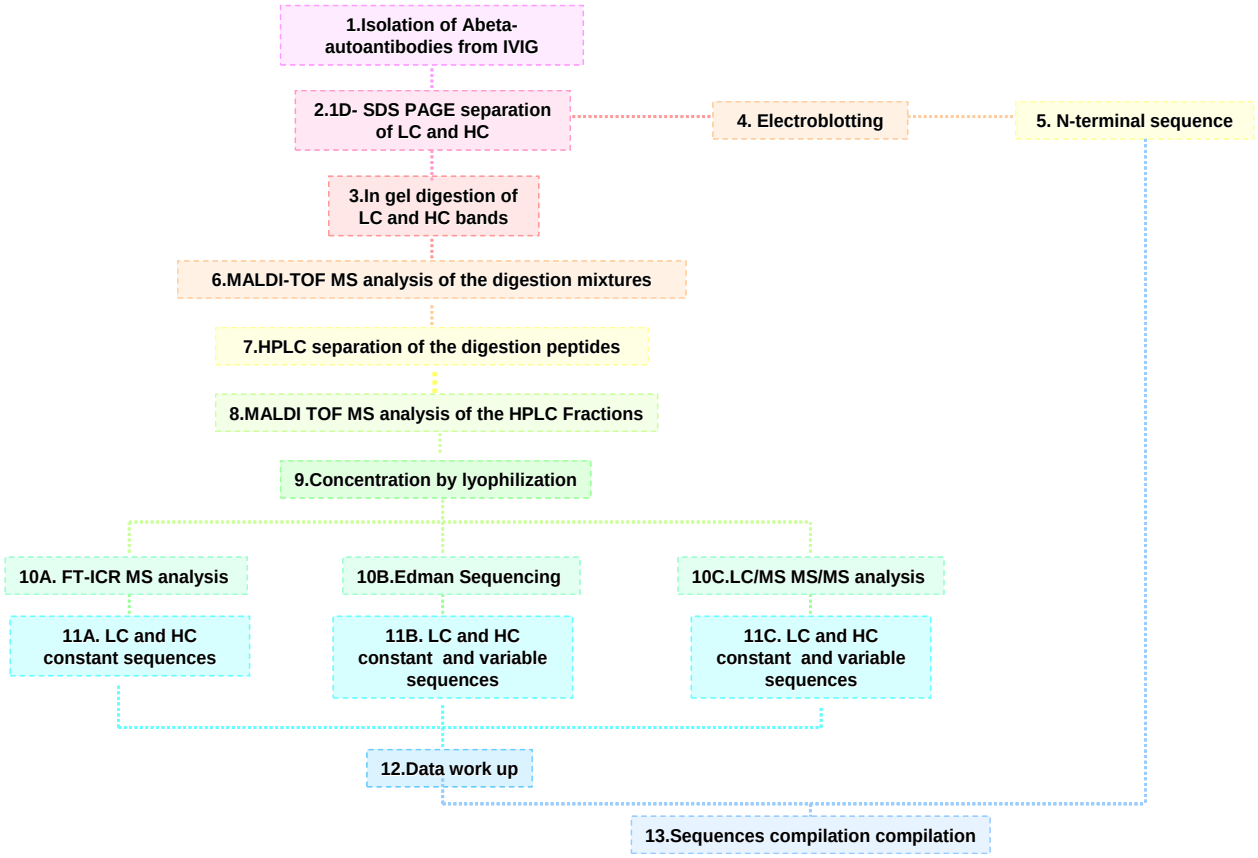

Figure 20. Experiments performed in order to obtain the primary structure of the Aβ-autoantibody. 1.- isolation of the Aβ-autoantibody; 2.- separation of light chain and heavy chain; 3.- in gel digestion of polypeptide chain; 4.- blotting to nitrocellulose membrane; 5.- Edman sequencing of the N-terminal; 6.- mass spectrometric analysis of the peptide mixtures; 7.- HPLC separation of the proteolytic peptides; 8.- mass spectrometric analysis of the separated peptides; 9.- concentration of the HPLC fractions; 10.- parallel analysis of the HPLC fractions; 11.- obtaining primary structure information from light and heavy chain variable and constant regions; 12.- data workup by search against data base or/and de novo sequence determination; 13.- Aβ-autoantibody sequence compilations and summing up of the variations.

2.3.2. Separation of heavy and light chains by SDS-PAGE

Immunoglobulins have a very stable 3D structure, both to proteolysis and chemical degradation. After the isolation, the light and heavy chains were separated by reduction of disulfide bonds followed by alkylation with iodoacetamide. The reaction mixture was lyophilized. The running buffer for electrophoresis in, which the light and heavy chains were reconstituted, contained urea and thiourea for further denaturation of tertiary and secondary structures for better electrophoresis separation of light and heavy chains.

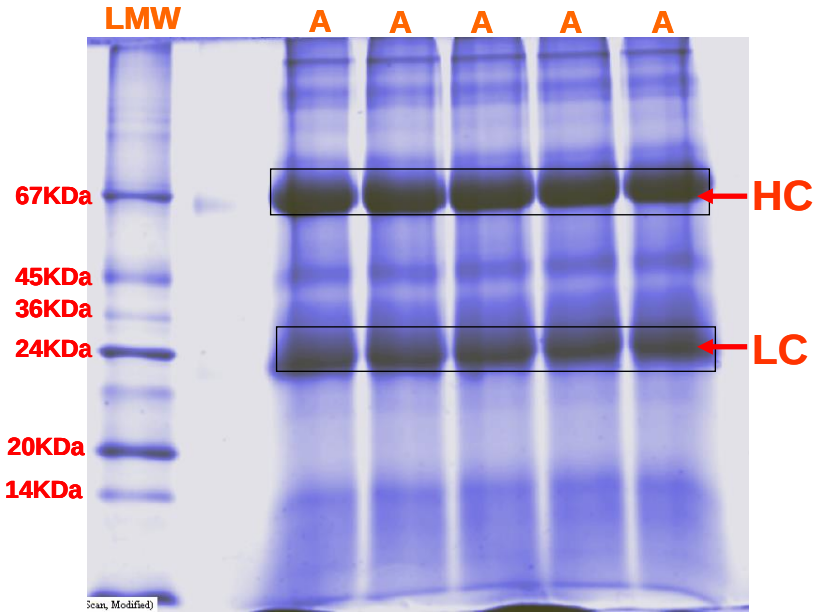

Figure 21. 1D SDS-PAGE separation of light ad heavy chain. The molecular marker (LMW) showed the light chain running at 25 kDa and heavy chain at 60 kDa

20 µg antibodies were loaded in each well on a 10% polyacrylamide gel, for each experiment batches of 250 - 300 µg were prepared (3 gels). After Coomassie staining, the gel revealed two major bands for each sample, one at 25 kDa corresponding to light chain and one at 67 kDa corresponding to heavy chain. Although the heavy chain was expected at ca. 50 kDa, the corresponding band was very faint and is retarded due to the glycosylation in the hinge region. The gel bands were cut and dried, destained and prepared for proteolytic digestion.

2.3.3. Identification of N-terminal sequences of light and heavy chains by Edman sequencing

For initial structure determination of Aβ-autoantibody, the N-terminal residues were sequenced by Edman degradation in three stages, each requiring different conditions. Amino acid residues can therefore be sequentially removed from the N-terminus in a controlled, stepwise approach. Subsequent to electrophoretic separation, the light and heavy chain bands were transferred onto membranes and subjected to Edman sequencing. For this experiment, the polyacrylamide gel was electroblotted onto membranes using a semi-dry transfer procedure. Membranes were stained with Coomassie Brilliant Blue R-250 in methanol/ water until protein bands became visible, and subsequently air dried.

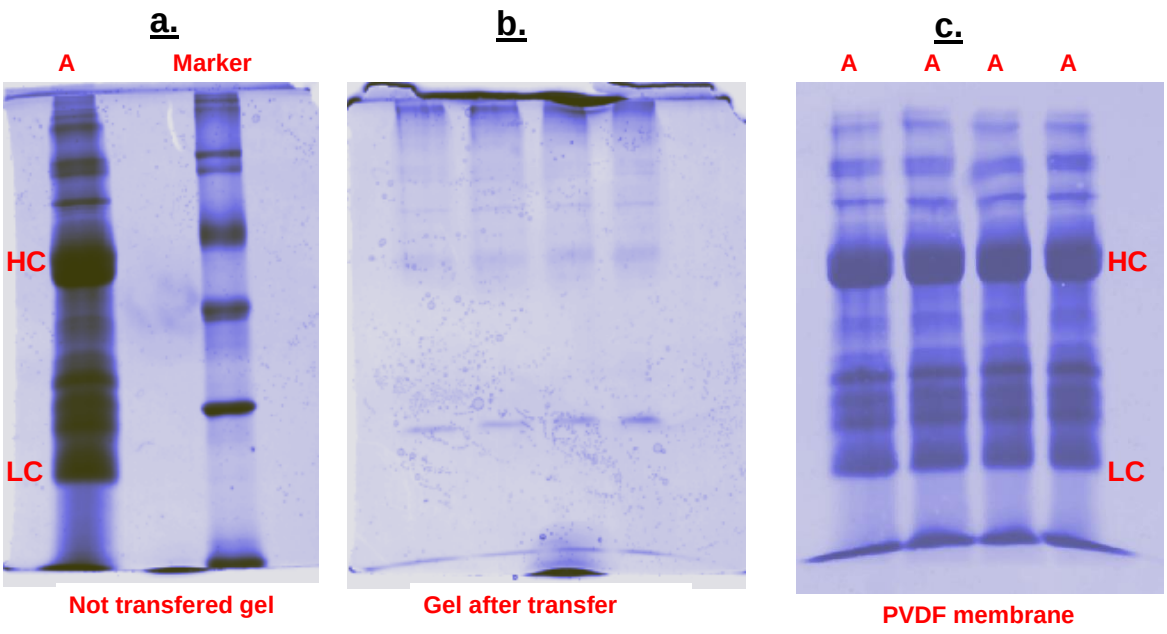

Figure 22. Eletroblotting transfer of light and heavy chain. a. - Coomassie staining of a 1D-SDS-PAGE of light and heavy chain separation; b. - Coomassie staining of a 1D-SDS-PAGE of light and heavy chain separation after transfer; c. - Coomassie staining of a PVDF membrane after transfer for Edman sequencing

Membranes were then destained in 50 % methanol and bands were excised and applied into the sequencing cartridge. Figure 22 shows an example of an original gel, gel after transfer and a PVDF membrane stained with 0.1 % Coomassie Brilliant Blue R-250 of light chain and heavy chain bands. The Edman sequencing of the heavy chain band was carried out for 25 cycles

and showed a single dominant variant: [1]EVQLVEGGGVVQPGGSLRLSCAAS[24].

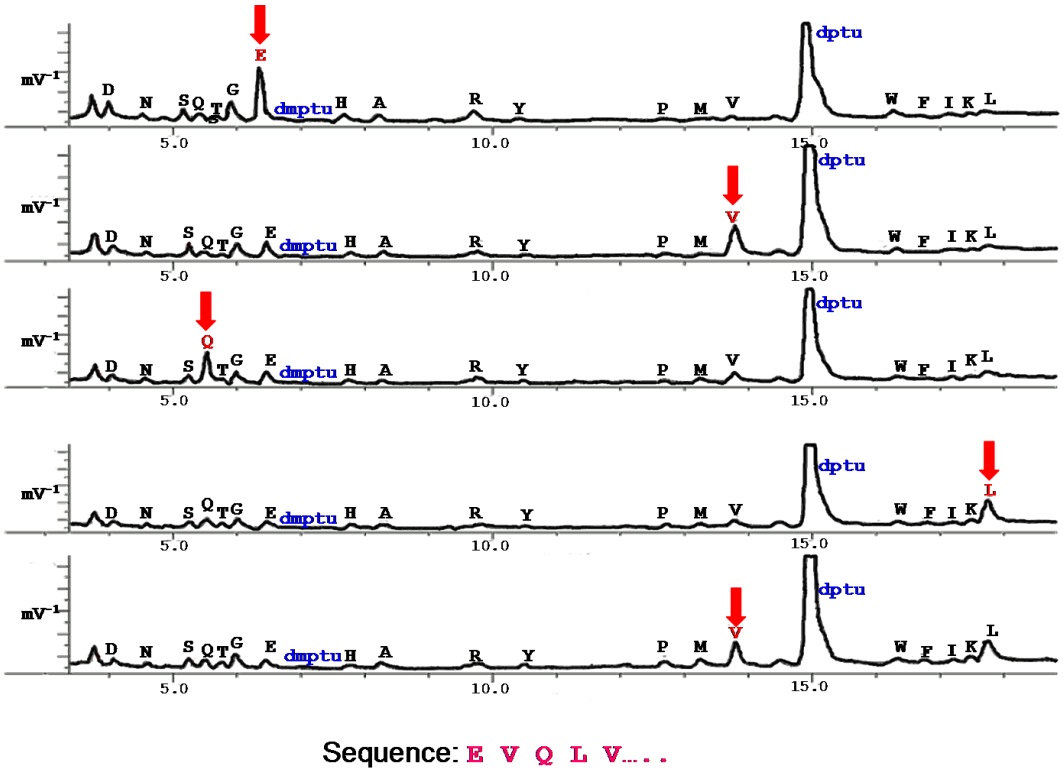

Figure 23. Example of Edman N-terminal sequencing of Aβ-autoantibody heavy chain

For the light chain 7 biologically relevant sequences were obtained, as seen in data base search. The obtained sequences were searched against data base using BLAST alignment tool and showed the presence of both kappa and gamma light chains. The sequence analyzed revealed a conserved amino acid pattern: position 1 is an acidic amino acid (E or D), position 2 - a hydrophobic (Leu or Ile) residue; 3rd position - Val or Gln; position 4th - Leu or Met; residues in positions 5 to 8 are conserved (Thr- Gln- Ser- Pro) and mark a turn in the polypeptide orientation due to the presence of proline residue; in 9th position is a small amino acid that stabilizes the turn (Ala, Ser or Gly); 10th position provides a hydroxyl group for the stabilization of the secondary structure of the framework 1; position 12th - Leu followed by hydrophobic amino acid (Ala or Leu) and another conserved residue -Ser - in position 14; position 16 brings another turn with the a further Pro residue. The Edman

sequencing could not be carried out for more than 18/24 cycles (depending of the antibody quantity).

Table 2. N-terminal sequencing of light and heavy chain results. For heavy chain Edman analysis revealed a single chain, while the light chain presents variations at amino acids 1, 2, 3, 4, 9, 10, 13, 15. Although the amino acids are different their type (amino acids, aliphatic amino acids etc.) is conserved.

N-terminal sequencing of heavy chain										
Position	1	2	3	4	5	6	7	8	9	10
Amino acids	**E**	**V**	**Q**	**L**	**V**	**E**	**G**	**G**	**G**	**V**
Position	11	12	13	14	15	16	17	18	19	20
Amino acids	**V**	**Q**	**P**	**G**	**G**	**S**	**L**	**R**	**L**	**S**
Position	21	22	23	24						
Amino acids	**C**	**A**	**A**	**S**						
Consensus heavy chain sequence:										
^{1}**EVQLVEGGGVVQPGGSLRLSCAAS**^{24}										
N-terminal sequencing of light chain										
Position	1	2	3	4	5	6	7	8	9	10
Amino acids	**E** **D**	**I** **V**	**V** **Q**	**S**	**P**	**A** **S** **G**	**S** **T**	**L**	**S**	**A** **L**
Position	11	12	13	14	15	16	17	18	19	20
Amino acids	**S**	**P** **V**	**G**	**D** **E**	**R**	**V**	**T**	**I**	**T**	**C**
Position	21									
Amino acids	**R**									
Consensus light chain sequences:										
^{1}**EIVLTQSPATLSLSPGERVTITCR**^{21}										
^{1}**DIQMTQSPATLSLSPGER**^{15}										
^{1}**EIVMTQSPATLSLSPGER**^{15}										
^{1}**DVVMTQSPSSLSASVGDRVTITCR**^{21}										
^{1}**DIVLTQSPATLSLSPGERVTITCR**^{21}										
^{1}**DIQMTQSPGTLSLSPGER**^{15}										
^{1}**DVVMTQSPSSLSASVGDRVTITCR**^{21}										

According to Kabat rules, all assembled sequences belong to the conserved framework1 of the immunoglobulin structure. They are mapped already in data bases, and therefore were confirmed as biological consensus sequences after BLAST search.

2.3.4. In gel digestion of light and heavy chains and mass spectrometric analysis of proteolytic mixtures

Light and heavy chain bands from each batch were cut from the gel and pooled in light and heavy chain bands to obtain necessary amounts for analytical HPLC separation. Gel pieces were destained and crushed for a better penetration of the enzyme solutions. Destained gel pieces were dried out and soaked in enzyme solutions and incubated at 37°C for 16 hours before extraction of the proteolytic peptides.

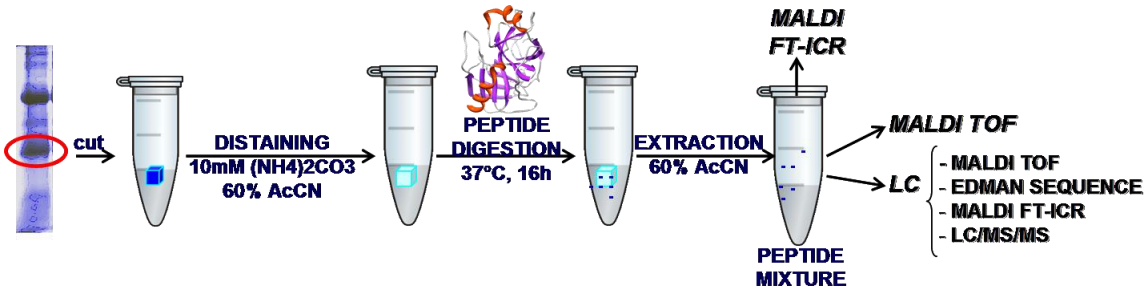

Figure 24. Sample preparation for structure analysis. The gel bands were cut, detained, incubated with enzyme solution before MS analysis

For different batches, different enzymes were employed for in gel proteolytic digestion. The first experiments were performed with trypsin, obtaining small fragments ending in arginine and lysine. Their masses were ranged up to 4 kDa and all could be subjected to MALDI-FTICR, LC-MS/MS analysis and/or to Edman Sequencing. To obtain larger fragments with overlapping regions Lys-C protease was used (cuts specifically after lysine residues). Chymotrypsin was used for smaller fragments, more feasible to MS/MS fragmentation (it cuts specific after aromatic amino acids and unspecific after methionine, leucine and other hydrophobic amino acids).

A sample from each of the peptide mixtures was loaded on a MALDI target for MALDI-ToF mass spectrometry, and the signals searched against the data base for peptide fingerprinting. The data obtained in this experiment were used for enzymatic reaction monitoring and for further orientation in the structure determination; however they were not considered in the final sequence alignment due to the low resolution of MALDI ToF-MS.

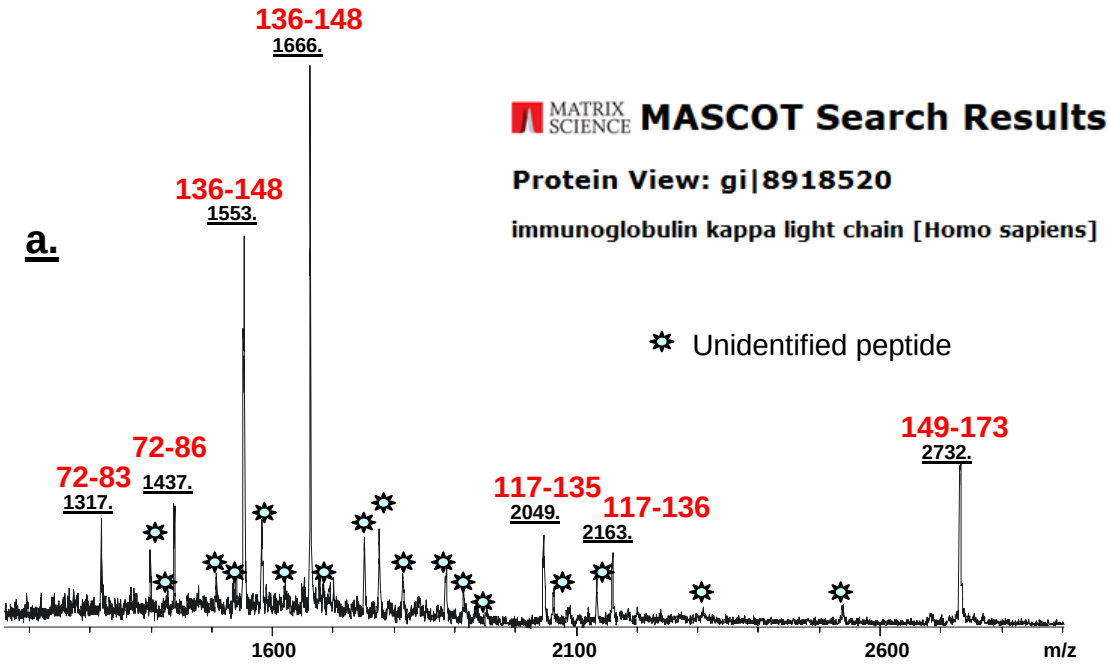

Figure 25. MALDI-ToF-MS analysis of light chain chymotryptic mixture. a. – MALDI-ToF spectrum of proteolytic mixture - fragments found in data base by the mascot search engine were assigned with red and unidentified signals are marked blue star; b. - Peptide mapping - fragments identified by data base are highlighted in red and the context (the sequence given by data base) is presented in black

Light chain spectra for trypsin and LysC showed dominant signals of peptides from the constant region C_L, common for immunoglobulin G from both kappa (κ) and lambda (λ) subclasses and were identified with high identification scores using SwissProt data base. Examples of spectra for trypsin and LysC digestion are listed in the Experimental Part (3.7., Figure 68). The chymotrypsin digestion yielded smaller fragments that resulted in a more abundant number of signals with comparable intensity, most of which could not be identified by searching against data bases. One example of the light chain spectra of a chymotrypsin digestion and the data base search is shown in Figure 25 . Heavy chain spectra of trypsin and LysC digestion mixtures follow the same pattern with dominant signals of the constant region C_H, common for immunoglobulin G1 and G2, while smaller signals remain

unidentified. Examples of spectra for trypsin and LysC digestion are listed in the Experimental Part (3.7., Figure 69).

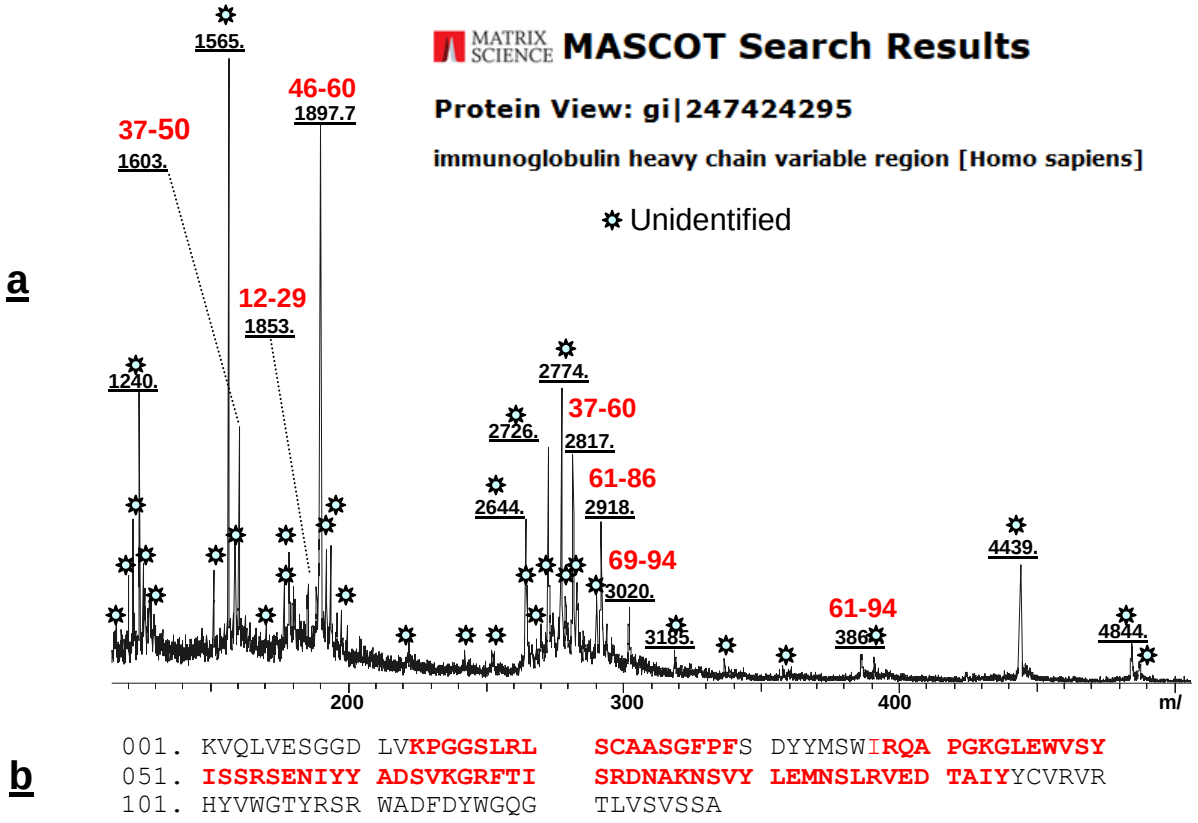

Figure 26. MALDI-ToF MS analysis of heavy chain chymotryptic mixture. a. - MALDI ToF spectrum of proteolytic mixture - fragments found in data base by the mascot search engine were assigned with red and unidentified signals are marked blue star; b. - Peptide mapping - fragments identified by data base are highlighted in red and the context (the sequence given by data base) is presented in black

The chymotrypsin digestion yielded, as in the case of light chain, smaller fragments that gave signals with comparable intensity. One example of the light chain spectra of a chymotrypsin digestion and the data base search is shown in Figure 26. After confirmation of the digestion reaction by MALDI-ToF MS, the solutions were concentrated by lyophilization and subjected to further analysis to confirm the sequences obtained by peptide fingerprinting and to identify the unassigned signals.

2.3.5. Separation of Peptides by analytical HPLC and analysis by MALDI mass spectrometry

Analytical HPLC on a C18 analytical column and an UV detector (220 nm) was employed to reduce the complexity of the samples since each proteolytic mixture contains between 50 and 500 different peptides. The amount of sample loaded on the column for each run (both light and heavy chain) was 100 - 200 µg (2-4 nmol for heavy chain; 4-8 nmol for light chain).

The number of fractions (in the chromatographic profile was depending on the type of enzyme and the amount of sample). For the same enzyme and comparable amount of sample the chromatographic profile was reproducible. For the tryptic digestion of the light chain, the number of fractions obtained was in the range of 45 to 50, for lysC digestion 95-100 and for chymotrypsin 145-150.

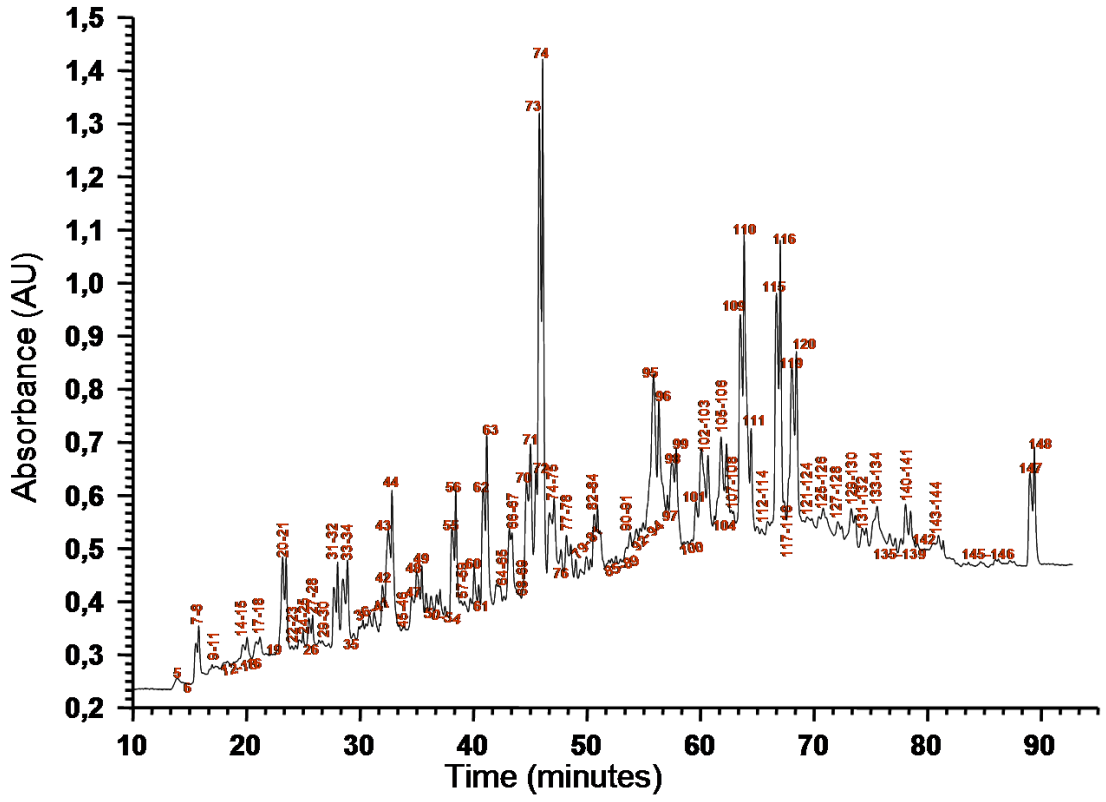

Figure 27. RP-HPLC chromatogram of light chain chymotryptic mixture of the Aβ-autoantibody. Separation was performed on a analytical C18 stationary phase, with a gradient starting at 0 % B with an increment of 0, 5 % per minute for 95 minutes.

In the case of the heavy chain, the number of fractions obtained by tryptic digestion was approximately of 60 to 97, for LysC digestion 180-195 and for chymotrypsin 164-175. Examples of RP-HPLC separation of an Aβ-autoantibody proteolytic mixture are presented in Figure 27 (light chain) and in Figure 28 (heavy chain). The peptides were separated using a linear gradient from 0 to 65% solvent B (80% acetonitrile in 0,1 % trifluoroacetic acid) over 100 minutes. The HPLC fractions were analyzed by MALDI-ToF-MS to identify the constant region fragments and then lyophilized and reconstituted for further sequence analysis. Again the data obtained from the peptide fingerprint with the MALDI-ToF were used only for obtaining orientation in further analysis, not for the final data compilation.

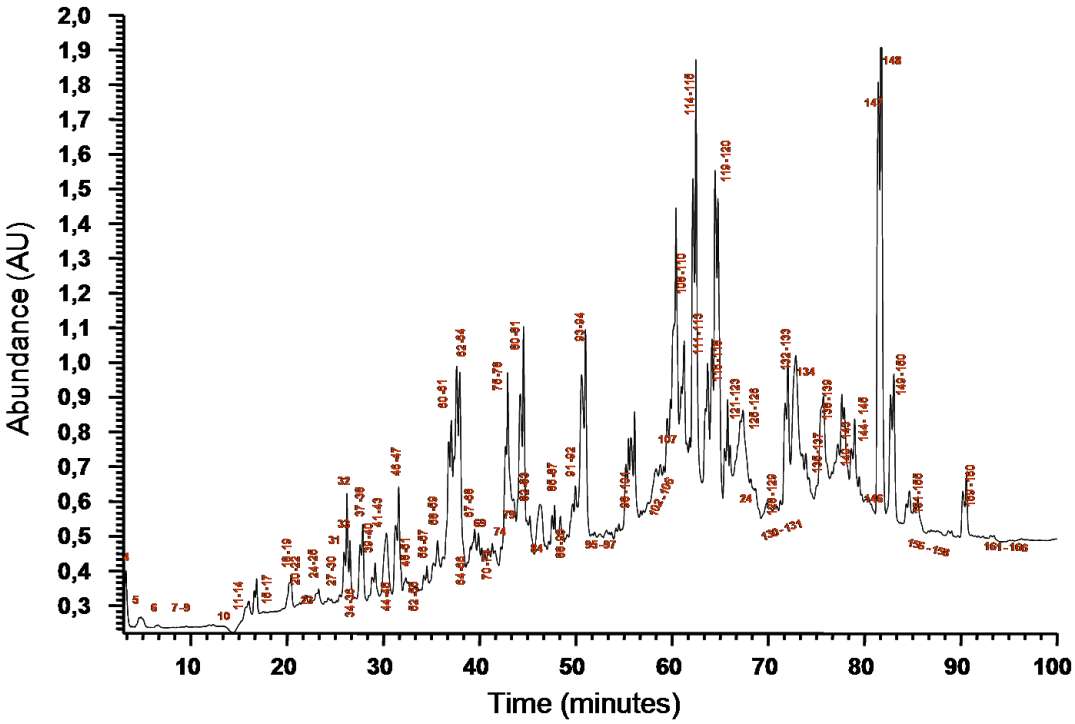

Figure 28 RP-HPLC chromatogram of heavy chain chymotryptic mixture of the Aβ-autoantibody. Separation was performed on a analytical C18 stationary phase, with a gradient starting at 0% B with an increment of 0,5 % per minute for 100 minutes

All fractions were analyzed by MALDI-ToF MS, before concentration by lyophilization. Three different cases were present in each experimental batch: (i.), a peptide was found in the data base corresponding m/z value; (ii.),

signals were found but no identification was obtained by data base search; (iii.), no signals were found. The higher peaks in the chromatogram contained peptide fragments from the constant region that dominate the spectrum of the mixture due to their presence in all variants of Aβ-autoantibody, and could be found by search against data bases and confirmed by fragmentation analysis.

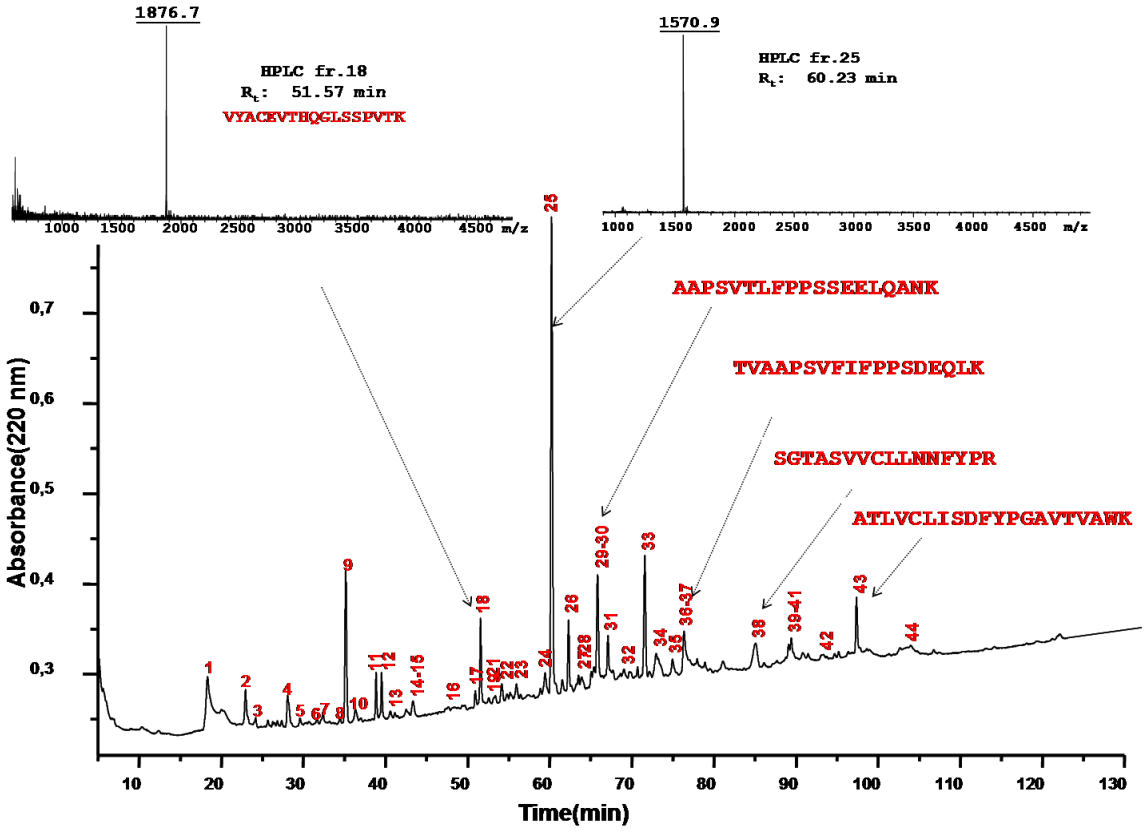

Figure 29. MALDI-ToF mass spectrometric analysis of light chain proteolytic peptides isolated by RP-HPLC. Peptide fingerprint results are indicated by arrows to the corresponding fraction in the chromatogram. The inserted spectra in upper part of the chromatogram show the 2 different cases (i.) identification was made by search against data base and (ii.) signals were present, but no identification was possible.

The low intensity signals were peptides from the variable regions of the antibodies, which could not be identified in data base. Examples of the results obtained by the MALDI-ToF MS of the HPLC fractions are presented in Figure 29 (light chain) and Figure 30 (heavy chain).

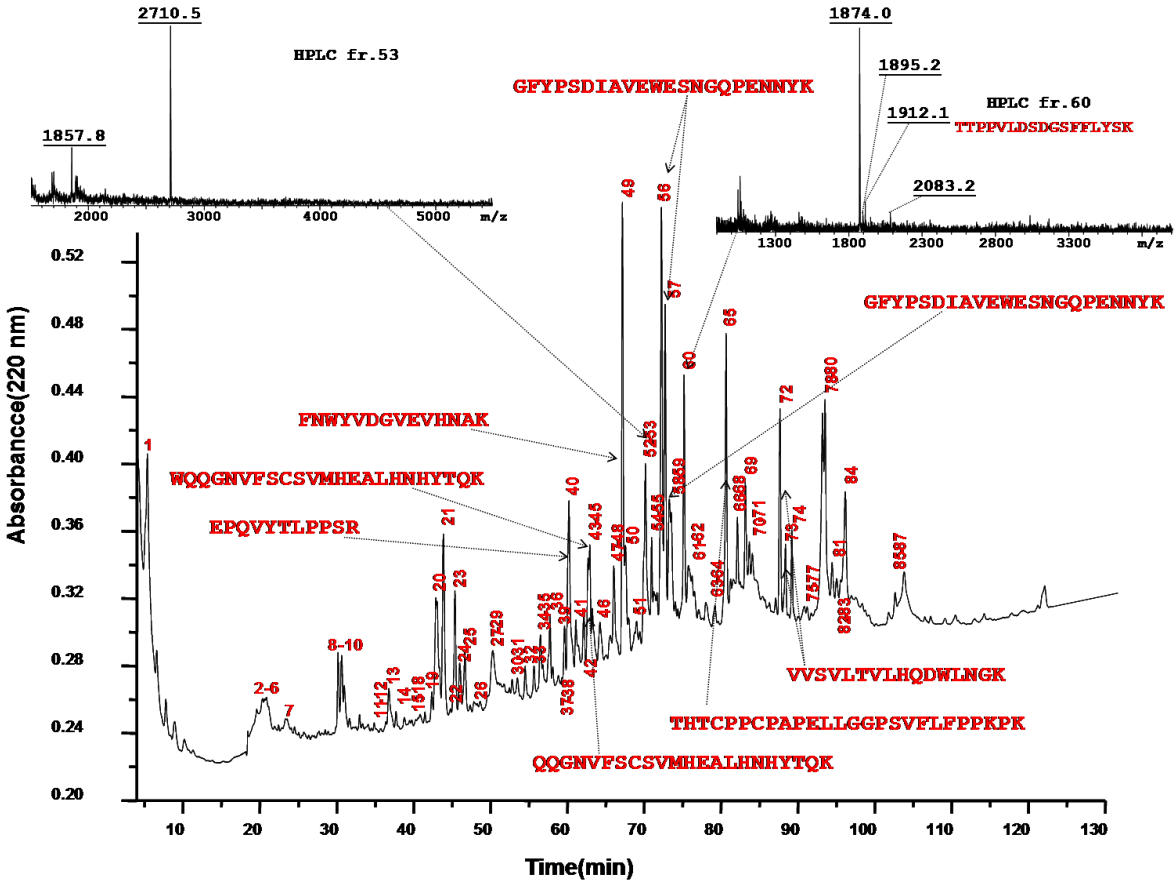

Figure 30. MALDI-ToF mass spectrometric analysis of heavy chain proteolytic peptides isolated by RP-HPLC. Peptide fingerprint results are indicated by arrows to the corresponding fraction in the chromatogram. The inserted spectra in upper part of the chromatogram show the two different cases (i.) identification was made by search against data base and (ii.) signals were present, but no identification was possible.

2.3.6. High resolution mass spectrometric analysis of tryptic mixtures and isolated peptides

A batch of trypsin proteolytic mixture was used to ascertain the composition by high resolution FT-ICR mass spectrometry. After in gel trypsin digestion of the light and heavy chain, the extraction mixture was lyophilised and reconstituted in 10 µL MALDI solvent and 0.5 µL of mixture was loaded on a MALDI target and measured by MALDI-FT-ICR. FT-ICR-MS was chosen due to the high mass resolution. MALDI-FT-ICR spectra of the tryptic mixtures are shown in Figure 31. The m/z values obtained were used for peptide fingerprinting and the identified peptides are summarized in

Table 3 for heavy chain, and in Table 29 (Experimental part, 3.8.1) for light chain sequences.

The rest of the peptide mixtures was re-lyophilized and reconstituted in 0.1 % TFA, and peptides isolated by analytical HPLC. The fractions were lyophilized and loaded into MALDI-FT-ICR MS. The identified signals were searched again in databases. The results were used to amend the sequence tables and, together with the sequencing data, for final sequence compilation.

The MALDI-FTICR mass spectrometric analysis of the tryptic peptides provided accurate masses and identification of the fragments present in data bases NCBInr and SwissProt. The identified fragments provided a frame of constant regions common with antibodies already present in these data bases or encoded in genes sequenced and stored in libraries. These analyses did not provide new sequences, but provided exact ion masses for unidentified peptides present in HPLC fractions.

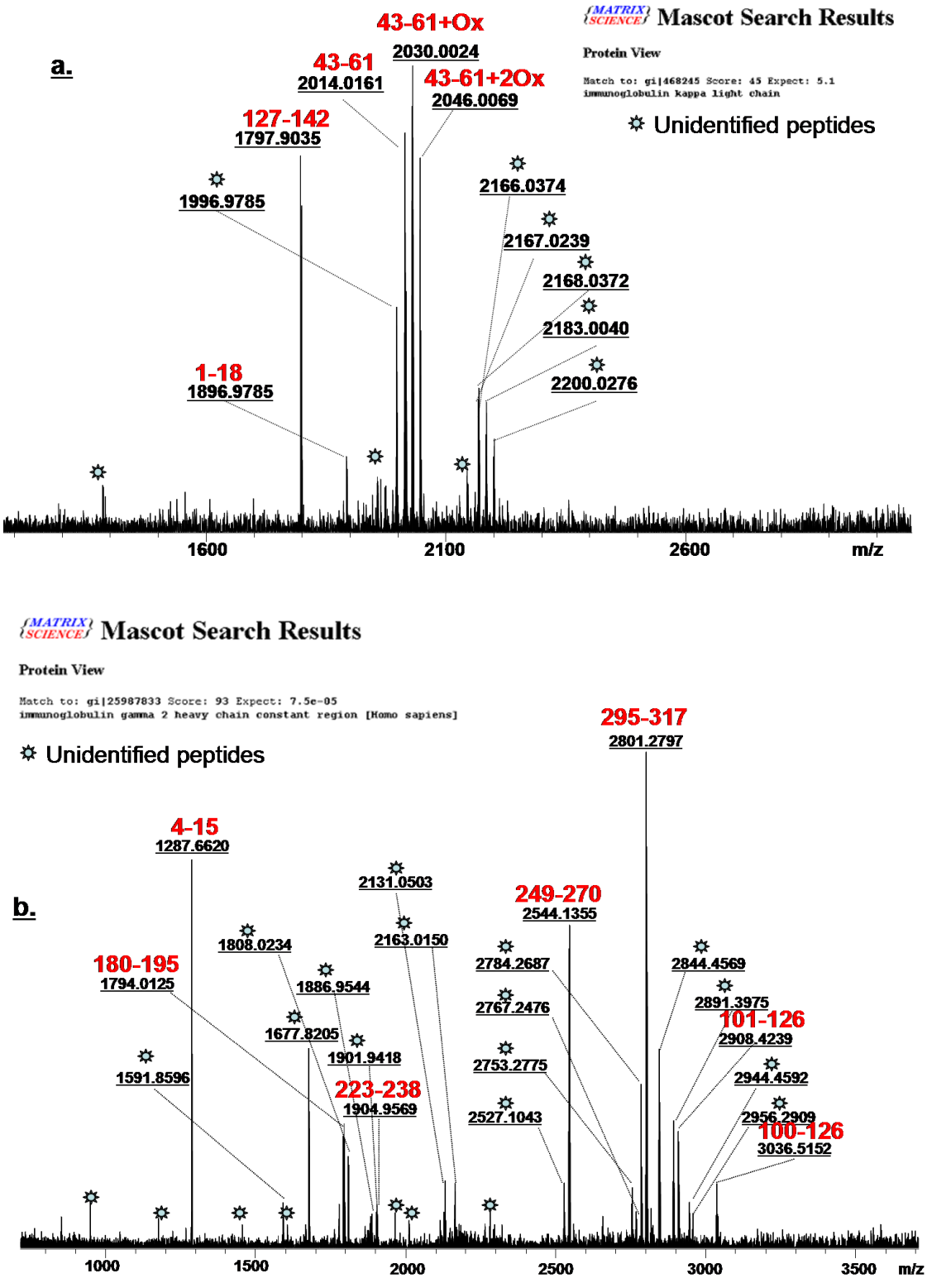

Figure 31. MALDI-FT-ICR spectrum tryptic mixture: a. - light chain; b. - heavy chain. Fragments found in data base by the mascot search engine were assigned with red and unidentified signals are marked blue star;

Table 3. Aβ-autoantibody heavy chain tryptic peptides identified by MALDI-FTICR and peptide mass fingerprint and list of unassigned m/z values.

Nr. Crt.	Position	Sequence	$[M+H]^+_{calc}$	$[M+H]^+_{exp}$	Δm (ppm)
1	126-137	GPSVFPLAPCSR	1287.6227	1287.6223	0
2	137-151	STSGGTAALGCLVK	1321.6493	1321.6761	20
3	138-151	STSESTAALGCLVK	1423.6810	1423.7091	20
4	260-278	TPEVTCVVVDVSHEDPEVK	2138.9987	2139.0163	8
5	227-252	THTCPPCPAPELLGGPSVFLFPPKPK	2844.4073	2844.4550	17
6	279-292	FNWYVDGVEVHNAK	1677.7947	1677.7983	2
7	294-320	KCCVECPPCPAPPVAGPSVFLFPPKPK	3036.4035	3036.5152	37
8	295-320	CCVECPPCPAPPVAGPSVFLFPPKPK	2908.3085	2908.4239	40
9	306-321	VVSVLTVLHQDWLNGK	1807.9992	1808.0019	1
10	349-359	EPQVYTLPPSR	1286.6666	1286.6738	6
11	349-364	EPQVYTLPPSRDELTK	1872.9629	1872.9540	5
12	365-374	NQVSLTCLVK	1161.6009	1161.6299	25
13	375-396	GFYPSDIAVEWESNGQPENNYK	2544.1241	2544.1086	6
14	397-413	TTPPVLDSDSFFLYSK	1815.8931	1816.9021	5
15	421-443	WQQGNVFSCSVMHEALHNHYTQK	2806.2384	2806.3381	36

Unsigned ion masses	543.3249	1076.6465	1317.5981	1563.9331	1864.0224	2602.0437
	682.3370	1089.5339	1330.7038	1566.2070	1886.9544	2644.2507
	718.3741	1110.5740	1331.7504	1567.7470	1887.9065	2753.2775
	816.4351	1111.5176	1343.6565	1591.8974	1896.0220	2862.2683
	853.4520	1178.5470	1385.8664	1605.8246	1901.9418	2948.5675
	949.4372	1183.6132	1388.6005	1624.8604	1993.9772	3456.7984
	976.4868	1191.6717	1390.1900	1667.7508	2026.1678	3598.8407
	994.2520	1199.7732	1445.6903	1789.9968	2121.9851	3690.8830
	997.4855	1215.5662	1452.7150	1824.0013	2131.0503	3799.7478
	1001.5876	1234.7321	1490.8372	1839.9935	2163.0150	4412.1520
	1039.5048	1240.5596	1506.6577	1857.8880	2527.1043	4430.1559
	1044.5936	1305.7130	1543.8954	1863.9975		

An example of MALDI-FT-ICR spectrum of a PR-HPLC fraction containing tryptic peptides of heavy chain is presented in Figure 32. The initial complexity of the heavy chain is much reduced; two peptides are present in the spectrum, one monoisotopic mass obtained - 1667.7983 - resulted in the identification of a constant region peptide ^{157}FNWYVDGVEVNHNAK^{170}.

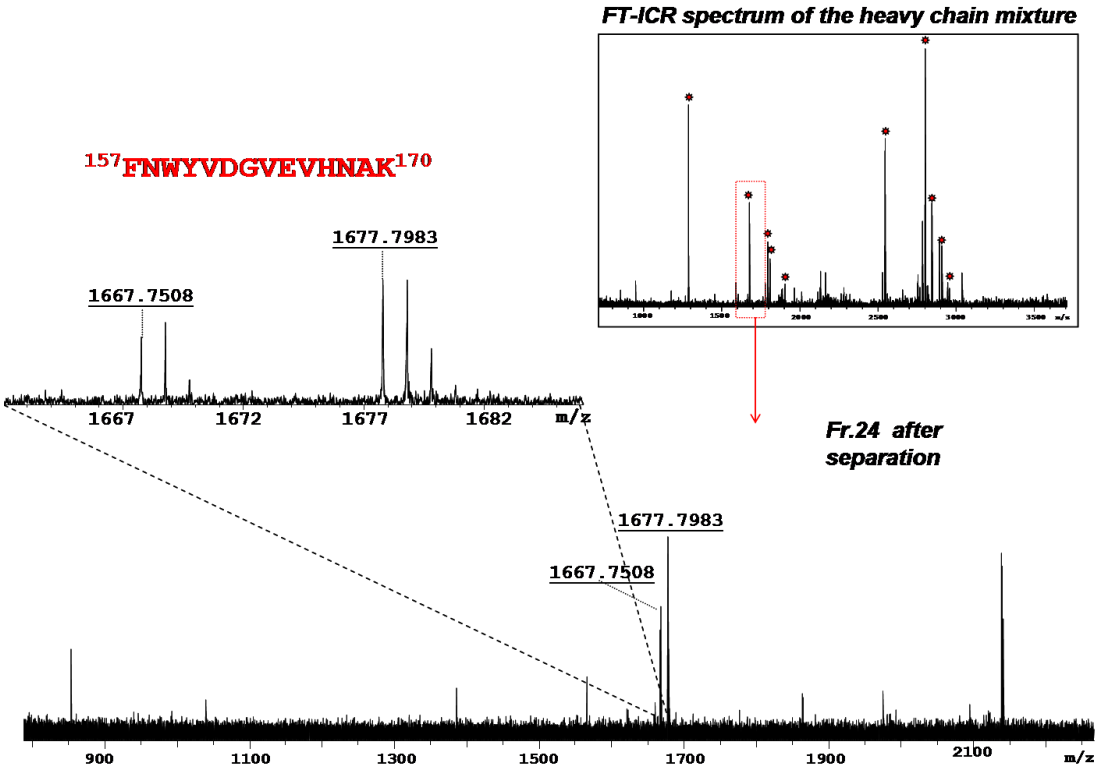

Figure 32. FT-ICR-MS spectrum of an isolated multi-component fraction obtains by HPLC separation of heavy chain tryptic mixture. The HPLC separation reduced the complexity of the sample (upper spectrum right) and the FTICR analyzer provides an accurate monoisotopic mass of the peptide (upper spectrum left) which in turn provides a data base identification

2.3.7. Edman sequencing of the isolated proteolytic peptides

Second batch of tryptic peptides fractions and fractions from LysC experiments were undergone Edman sequencing analysis using an automated sequencer that sequentially cleaved N-terminal amino acids analyzed the resulting phenylthiohydantoin (PTH)-amino acid residues. Fractions were lyophilized and re-dissolved in methanol and applied on polyvinylidene difluoride membrane. The membrane was air-dried and applied on sequencing cartridges. The number of cycles on each sample was limited only by the amount of peptide in each sample and the equilibrium point of the technique.

The results were search in data bases with BLAST alignment tool and, and when possible, the probable position in the antibody sequence was found. Using the sequences and their position, antibody sequences variants were

compiled as bases to build on the real sequences. In the construction of the variants, the Kabat rules were taken in consideration. A complete list of identified peptides by Edman Sequencing is presented in Table 4 (light chain peptides) and Table 5 (heavy chain peptides).

Table 4. Aβ-autoantibody heavy chain variable and constant region proteolytic peptides identified by RP-HPLC separation and individual analysis of each fraction by Edman analysis

No.	Position	Sequence	Number of cycles	$[M+H]^+_{exp}$ *
1	001-018	DIQMTQSPATLSLSPGER	14	1931.1
2	001-024	EIVLTQSPATLSLSPGERVTITCR	18	2630.1
3	001-024	EIVMTQSPATLSLSPGERVTITCR	18	2649.2
4	019-024	VTITCR	6	-
5	030-039	NYLAWYQQK	9	1212.9
6	039-045	PGQAPR	6	-
7	046-051	LLIYK	5	-
8	055-061	ATGIPDR	7	-
9	062-079	FSGSGSGTDFTLTISR	14	1633.4
10	106-111	VDIK	4	-
11	110-128	RTVAAPSVFIFPPSDEQLK	17	2102.9
12	111-128	TVAAPSVFIFPPSDEQLK	18	1946.4
13	113-131	AAPSVTLFPPSSEELQANK	15	1985.7
14	129-147	SGTASVVCLLNNFYPREAK	16	2127.0
15	137-151	YAASSYLSLTPEQWK	15	1744.1
16	137-156	ATLVCLISDFYPGAVTVAWK	4	2212.0
17	148-151	VQWK	4	-
18	152-171	VDNALQSGNSQESVTEQDSK	16	2136.2
19	164-173	AGVETTTPSK	9	-
20	172-185	DSTYSLSSTLTLSK	14	1503.1
21	186-190	ADYEK	5	-
22	193-209	LYACEVTHQGLSSPVTK	17	1890.1
23	193-209	VYACEVTHQGLSSPVTK	17	1875.2
24	197-211	SYSCQVTHEGSTVEK	14	1711.1
25	210-216	SFNRGEC	7	-

* Ion masses obtained by MALDI-ToF mass spectrometry analysis of the RP-HPLC fractions

Table 5. Aβ-autoantibody heavy chain variable and constant region proteolytic peptides identified by RP-HPLC separation and individual analysis of each fraction by Edman analysis

No.	Position	Sequence	Number of cycles	$[M+H]^+_{exp}$ *
1	001-019	EVQLVESGGGLVQPGGSLR	12	1882.1
2	044-050	GLVWVSR	7	816.9
3	044-048	GLEWV_	6	-
4	087-097	AEDTAVYYCAR	8	1318.4
5	126-137	GPSVFPLAPCSR	10	1287.5
6	126-137	GPSVFPLAPSSK	8	1187.3
7	138-151	STSESTAALGCLVK	12	1424.3
8	138-151	STSGGTAALGCLVK	12	1322.4
9	152-214	DYFPEPVTVSWNSGALTSGVHTFPAVLQSSG LYSLSSVVTVPSSSLGTQTYICNVNHKPSNTK	12	*6718.4*
10	201-214	TYTCNVDHKPSNTK	10	1665.7
11	216-227	EKKDF*KDGKRL	10	-
12	227-252	THTCPPCPAPELLGGPSVFLFPPKPK	19	2846.1
13	253-259	DTLMISR	8	835.1
14	297-305	EEQFASTFR	9	1115.1
15	306-321	VVSVLTVVHQDWLNGK	14	1795.6
16	306-321	VVSVLTVLHQDWLNGK	12	1810.1
17	306-321	VVSVLTVVHQDWLDGK	15	1796.1
18	331-338	GLPAPIEK	9	824.1
19	332-334	EYK	4	-
20	347-413	TTPGLLDSDGSFFLYSK	15	1849.0
21	347-413	TTPPMLDSDGSFFLYSK	12	1906.1
22	349-359	EPQVYTLPPSR	8	1285.7
23	349-364	EPQVYTLPPSREEMTK	10	1906.1
24	375-389	GFYPSDIAVEWESN_	12	-
25	375-396	GFYPSDIAVEWESNGPENNYK	15	2416.6
26	397-413	TTPPMLDSDGSFFLYSK	16	1906.6
27	414-418	LTVDK	6	-
28	420-438	SQIIINVFS	10	-
29	421-443	WQQGNVFSCSVMHEALHNHYTQK	12	2802.1
30	444-450	SLSLSPG_	8	-
32	445-364	GQPREPQVYTLPPSRDELTK	10	2312.1

* Ion masses obtained by MALDI ToF mass spectrometry analysis of the RP-HPLC fractions

The sequences provided by Edman degradation were sufficient to provide new information about the hypervariable regions, frames in variable regions V_L and V_C and the confirmation of sequences identified by MALDI mass spectrometry (both FTICR and ToF), however they were insufficient to obtain a complete and continuous sequence of Aβ-autoantibody.

2.3.8. LC/MS/MS analysis of HPLC isolated proteolytic peptides

For the LC-MS/MS analysis the peptides mixtures were subjected to analytical HPLC to reduce the complexity of the sample. Each HPLC fraction (of a total of ca. 1600) was concentrated by lyophilization, and re-dissolved in 2 % formic acid to be injected on a HPLC with micro flow connected with an Esquire 3000+. For the HPLC a 120 minutes gradient was used and for the mass spectrometric analysis, a method that scanned alternatively in MS and MS/MS mode. Both parent ions and fragment ions were registered for all peptides in the samples.

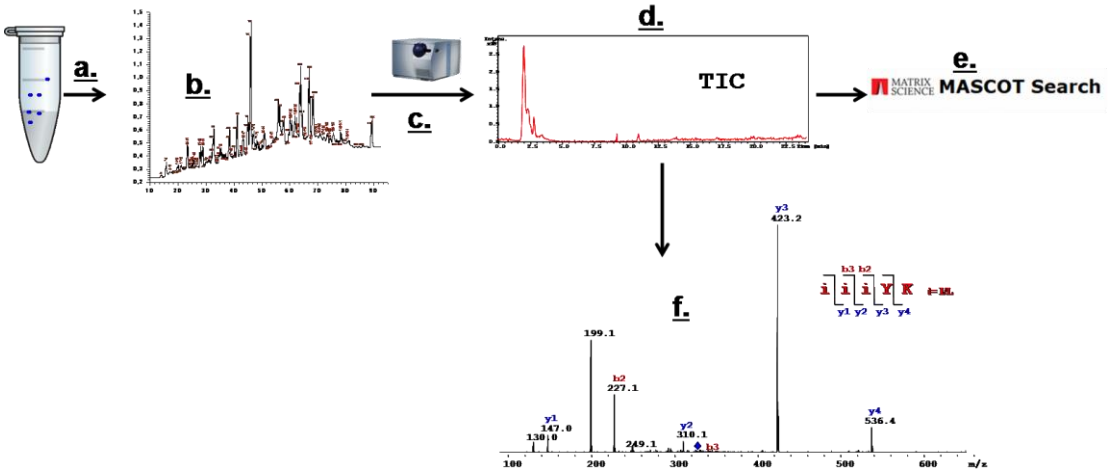

Figure 33. Scheme of proteolytic digestion sample processing for the LC-MS/MS analysis: a. - the proteolytic mixture is subjected to analytical HPLC; b. - separate fraction with low complexity are obtained; c. - HPLC fractions are lyophilized and injected in the LC-MS/MS system; d. - a data set is obtained containing fragmentation spectra of the proteolytic peptides; e. - MS/MS spectra are searched against data base, for constant region and frame sequences; f. - valid MS/MS spectra with no correspondence in data base are subjected to manual *de novo* sequencing.

The MS data were visualized and interpreted using the Data Analysis software (Bruker Daltonik). Each MS/MS spectra was saved as *.mgf file. These data were searched against databases with Mascot MS/MS Ion Search engine (www.matrixscience.com), using a precursor tolerance of 0.6 Da and a MS/MS tolerance of 0.5 Da[87.]. The protein identifications were validated by comparing the theoretical peptide ions and their fragments with the observed m/z values and corresponding charge states. For the MS/MS data that had no correspondence in the database, manual *de novo* MS/MS

data interpretation was performed, using the protocol for the peptide fragmentation characteristic for in ion trap fragmentations (b and y ions).

The MS/MS revealed sequence data on all regions of the antibody for both light and heavy chains. There were found in the fragmentation spectra information from constant (C_L, C_H) and variable regions (V_L, V_H), such as N-terminus, CDRs, and frame regions.

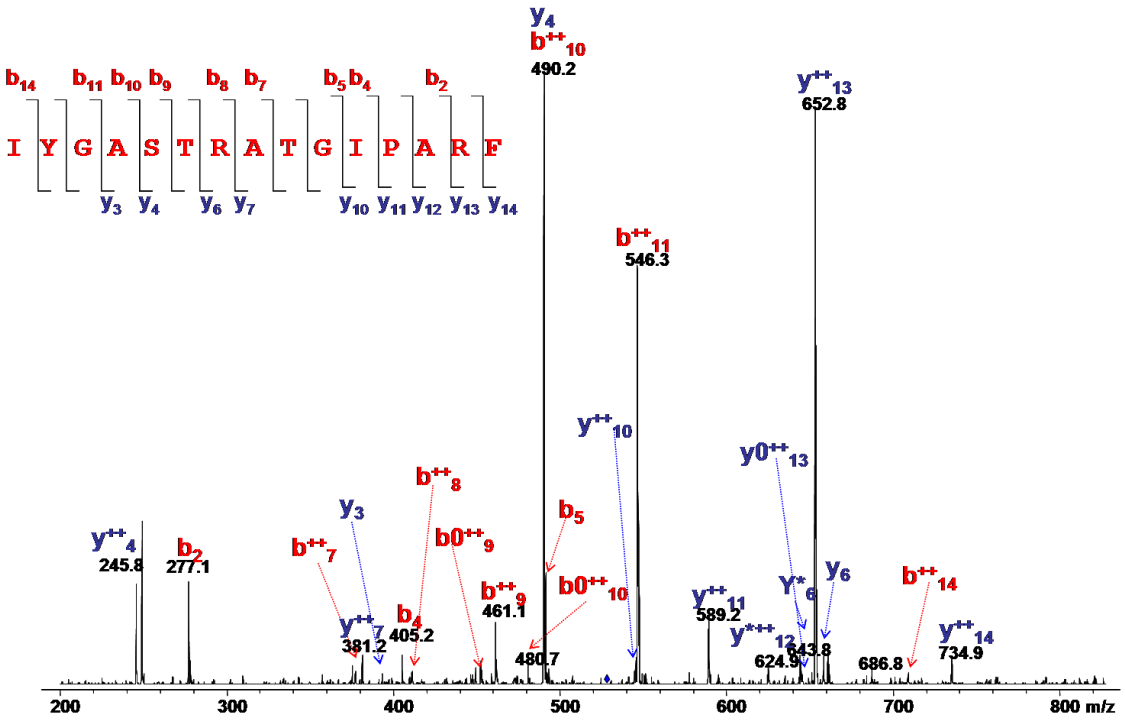

Figure 34. LC-MS/MS fragmentation mass spectrum of ion 527.9 (3+) which led to identification of peptide ^{48}IYGASTRATGIPARF^{62} that contain a variant of light chain CDR 2.

Figure 34 show an example of CDR peptide found by de novo sequencing of a chymotryptic peptide. The MS/MS fragmentation spectrum of triple charged ion 527.3 led to the identification of CDR2 light chain contained in peptide ^{48}IYGASTRATGIPARF^{62}. For each CDR of each chain, light and heavy, a list of peptides that contain fragments of CDR was compiled. Peptides containing CDR1 fragments are listed in Table 6, and showed a complete coverage of the CDR1 (amino acids 24-34) by overlapping the sequences of proteolytic peptides. Light chain CDR1 presented a low degree of variation.

Table 6. Aβ-autoantibody light chain CDR1 peptides identified by HPLC separation and individual analysis of each fraction by LC-MS/MS

No.	Position	Sequence	$[M+H]^+_{calc}$ [a]	$[M+H]^+_{exp}$	Δm (Da)
1	016-037	GQPASISCRSSQ	1277.5	1277.3	0.2
2	019-024	VTITCR	749.3	748.4	0.9
3	022-033	SCRASQSVSSNY	1345.5	1345.4	0.1
4	022-033	SCRASQSVSSIY	1344.6	1344.1	0.5
5	022-033	SCRASQSVSSYL	1344.6	1344.2	0.4
6	022-033	SCRASQSVSSSF	1302.5	1302.4	0.1
7	022-033	SCRASQSVSSAY	1302.5	1302.5	0.0
8	022-033	SCRASQSVSSNF	1329.5	1329.8	0.3
9	023-031	CKSSQSVLY	1071.5	1071.9	0.4
10	031-039	NYLAWYQQK	1213.6	1213.1	0.5

[a] Calculated using GPMAW software (Lighthouse Data, Denmark)

[b] RED -frame regions; BLUE - CDR s

Peptides containing CDR2 (amino acids 50-56) fragments are listed in Table 25 (Experimetal Part, 3.8.2) and they showed a complete coverage of the CDR2 by overlapping the sequences of proteolytic peptides. Proteolytic peptides containing parts of the light chain CDR2 showed a consistency in the frame sequences and a conservation of the amino acid types.

Peptides containing CDR3 (amino acids 91-99) fragments are listed in Table 26 (Experimetal Part, 3.8.2). For CDR3 light chain, only one peptide covered the entire CDR region, but the ion analyzed had a very low intensity suggesting a variant of Aβ-autoantibody of low abundance. The rest of the peptides covering adjacent frame sequences or part of the CDR were not sufficient to cover the entire CDR3 region.

An example of heavy chain CDR peptide found by de novo sequencing of a chemotryptic peptide is presented in Figure 35. The MS/MS fragmentation spectrum of triple charged ion 451.1 led to the identification of CDR2 heavy chain contained in peptide ^{49}VANIKQDGGERY^{59}.

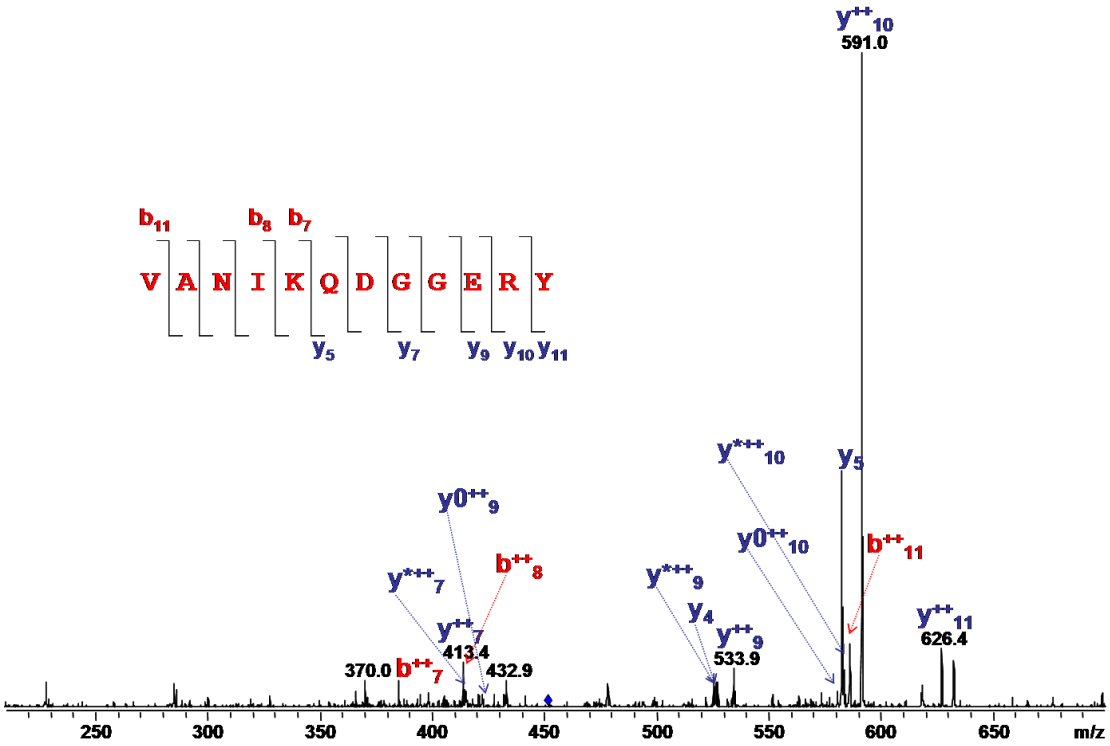

Figure 35. LC-MS/MS fragmentation mass spectrum of ion 451.1 (3+) which led to identification of peptide ^{48}VANIKQDGGERY^{62} that contain a variant of light chain CDR 2.

Peptides containing heavy chain CDR1 fragments are listed in Table 7 and they show a complete coverage of the CDR1 (amino acids 26-36) by overlapping the sequences of proteolytic peptides. Light chain CDR1 presented a high degree of variation, although the frame regions in the same sequences present a high amino acids conservation.

Table 7. Aβ-autoantibody heavy chain CDR1 containing peptides identified by HPLC separation and individual analysis of each fraction by LC-MS/MS.

No.	Position	Sequence	$[M+H]^+_{calc}$ [a]	$[M+H]^+_{exp}$	Δm (Da)
1	005-030	VESGGGLVQPGGSLRLSCAAS*GFNL*	2433.2	2434.8	1.6
2	018-032	LGLIKRSGR*LMTSY*	1594.9	1594.8	0.1
3	019-027	RLSCAAS*GF*	968.4	967.4	1.0
4	019-027	RKSCAAS*GF*	983.4	982.8	0.6
5	019-027	KVSCKAS*GF*	983.4	982.8	0.6
6	019-027	RLSCKAS*GF*	1025.5	1025.6	0.1

7	019-027	RISCQASGF	1025.4	1025.6	0.2
8	019-032	RLSCTASAFNLSDY	1604.7	1605.6	0.9
9	019-036	RLCCAASGFTFRTYSMHW	2250.9	2251.2	0.3
10	019-03 6	RLSCAASGFTLSSSAMSW	1918.8	1919.1	0.3
11	020-030	LSCAASGFTFR	1215.0	1215.5	0.5
12	020-038	VSCTASGFDFDYYFHWVR	2256.9	2256.5	0.4
13	020-037	LSCAASGFTFSKYWMHWVR	2334.0	2333.7	0.3
14	020-037	LSCAASGFTFTNYWMNWVR	2311.0	2310.8	0.2
15	020-037	LSCAASGFTFNTCWMTWVR + Ox	2310.9	2310.9	0.0
16	020-037	LSCAASGFTFSKYFMHWVR + Ox	2311.0	2310.7	0.3
17	020-037	LSCAASGFTFSKYFMHFVR + Ox	2272.0	2271.7	0.3
18	020-042	LSCAASGFGFGGQALSWVRQAPGK	2452.2	2451.6	0.6
19	021-036	SCAASGFTLINYRHNW	1896.8	1896.5	0.3
20	021-036	SCAASGFTFKDYGMHW	1864.7	1864.9	0.2
21	028-036	IFSNFGMHW	1138.5	1138.6	0.1
22	028-036	IFSNFGFHW	1154.5	1154.7	0.2
23	028-036	IFSMNGMHW	1122.5	1122.8	0.3
24	030-045	TSYDIDWVRQATGQGL	1809.8	1810.8	1.0
25	030-045	STYGMSWVRQAAGKGL	1710.8	1710.8	0.0
26	030-047	SSYEMNWVRQAPGKGLERF	2255.1	2256.0	0.9
27	032-050	TFISWVRQAPGQGLEWMGW	2249.1	2250.0	0.9
28	033-047	GMHWPRQAPGKGLEW + Ox	1764.8	1765.0	0.2
29	033-047	AMHWIRQAWGKGLEW + Ox	1883.9	1885.8	1.9
30	033-047	AMHWIRQATGKGLEW	1783.9	1784.7	0.8
31	033-047	GMHWNRQAPGKGLEW	1765.8	1767.0	1.2
32	033-050	YVHWVRQAPGQGLEWMGW + Ox	2216.1	2216.7	0.6
33	033-041	GVSFTDYSW	1061.4	1061.4	0.0
34	033-045	GVSWVRQGPGQGL	1340.7	1340.4	0.3
35	034-047	WEWVRQPPGKGLEW	1767.9	1767.2	0.7
36	034-047	WKWVRQPPGKGLEW	1766.9	1767.2	0.3
37	034-047	WQWVRQPPGKGLEW	1766.9	1767.2	0.3

[a] Calculated using GPMAW software (Lighthouse Data, Denmark)

[b] RED -frame regions; BLUE - CDR s

Peptides containing CDR2 (amino acids 50-65) fragments are listed in Table 27 (Experimetal Part, 3.8.2). Heavy chain CDR2 of the Aβ-autoantibody was obtained by overlapping the sequences of proteolytic peptides, all sequences found showing a high variability of the amino acid sequence. The frame

sequences surrounding heavy chain CDR2 present relatively fixed primary structure. Peptides containing CDR3 (amino acids 98-110) fragments are listed in Table 28 (Experimetal part, 3.8.2). For heavy chain CDR3 of the Aβ-autoantibody were determined multiple fragments but could not be obtain an overlapping of the sequences due to high variability in the primary structure of the fragments found by LC-MS/MS. The frame sequences adjacent to heavy chain CDR3 have a relatively constant sequence and in a few samples make the connection with C_H domain. Examples of fragmentation spectra that resulted in the identification of N-terminal sequences, of frame regions V_L and V_H, and of constant regions C_L and C_H are shown in the Experimental Part (Figure 72-79). All data from the LC-MS/MS experiments were summarized in two lists presented in Appendix 1 (light chain) and Appendix 2 (heavy chain). All sequences determined by LC-MS/MS analysis provided the missing and overlapping fragments necessary to complete the Aβ-autoantibody sequences.

2.4. Aβ- Autoantibody sequences alignments

2.4.1. Kabat rules for alignment of antibody sequences

The antibody sequences found in different experiments were searched against data bases using BLAST alignment to find homologue sequences and the relative peptides positions in the polypeptide chains of the antibodies [88.]. Aβ-autoantibody sequence compilation was performed manually by overlapping fragments of different lengths.

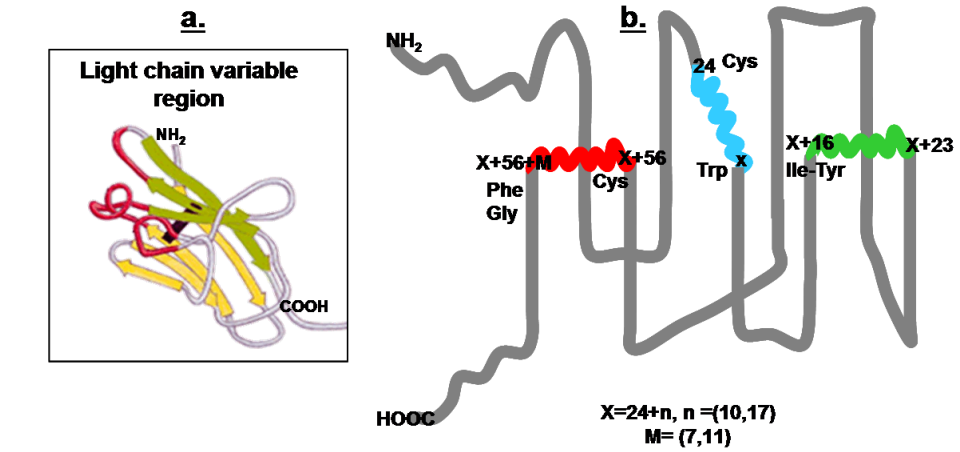

CDR LC	Start	Lenght	Residues before	Residues after
CDR1	approx residue 24	10 to 17 residues	always Cys	always a Trp. Trp-Tyr-Gln, Trp-Leu-Gln, Trp-Phe-Gln, Trp-Tyr-Leu
CRD2	always 16 residues after the end of L1	always 7 residues	Ile-Tyr Val-Tyr, Ile-Lys, Ile-Phe	
CRD3	always 33 residues after end of L2	7 to 11 residues	always Cys	Always Phe-Gly-XXX-Gly

Figure 36. Kabat numbering scheme light chain of antibodies. a. - Light chain of autoantibody modeling structure show a rigid beta sheet conformation for frame regions bound together by flexible loop regions that coincide with CDR regions; b. - The orientation of the polypeptide chain is visualized in the lower right scheme - frame 1 and 3 changed chain direction, maintaining the CDR position in the same

plane to form the antigen interaction surface (light chain part of the paratope); c. - Kabat, later revised by Chothia, postulated the exact positioning of the CDRs in the variable region sequence summarized in the table.

In the sequence compilations, Kabat rules applied. The Kabat numbering scheme postulates the positions of hypervariable regions (HVRs or CDRs) in the polypeptide chains of the antibodies [89-94.]. For both light and heavy chains, the CDR positions follow fixed rules. In light chain, frame 1 (FR 1) is approximately 24 residues followed by CDR 1 of 10 to 17 amino acids, which is finished with a Trp residues changing the orientation of the backbone. Usually the Trp is part of a triad motif: WYQ, WLQ, WFQ, and WYL. Frame 2 is formed of 16 residues and CDR 2 begins with a Tyr for 7 amino acids. CDR 3 starts after exactly 33 amino acids after the end of CDR 2 with a Cys, and lasts for 7 to 11 residues, finishing with a Gly. The position of the Trp, Tyr His and Cys residues determine the changes in the backbone orientation to form the secondary and tertiary structure of the variable region. The structure is stabilized by the formation of beta-sheets in the frame regions illustrated in Figure 36 [95-106.].

The heavy chain of the immunoglobulin follows the same structure as the light chain, with three frame regions and three CDR regions. CDR 1 starts after amino acid 26 with a Cys and lasts for 10 to 12, finishing with a Trp. CDR 2 starts exactly 15 residues after CDR 1, lasts for 16 to19 amino acids and finishes is a limited number of motifs. CDR 3 starts always 33 amino acids after the end of CDR2 with a Cys and ends with a Gly (Figure 37) [95-106.].

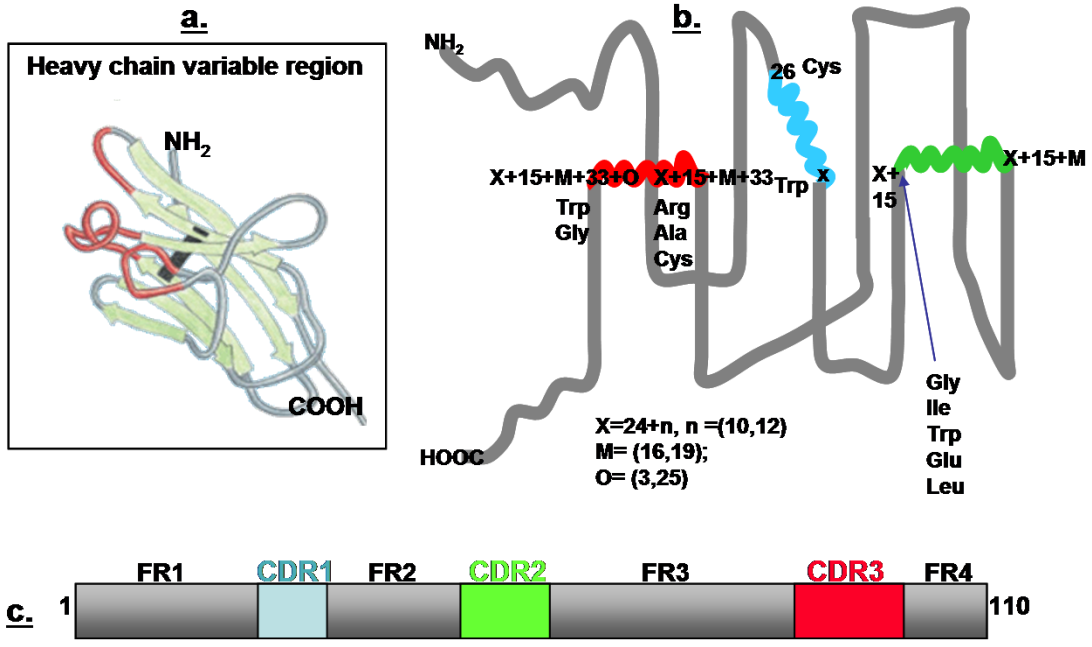

CDR HC	Start	Lenght	Residues before	Residues after
CDR1	Approx residue 26 (always 4 after a Cys)	10 to 12 residues	Cys-XXX-XXX-XXX	always a Trp. Typically Trp-Val, but also, Trp-Ile, Trp-Ala
CRD2	always 15 residues after H1	16 to 19 residues	Typically Leu-Glu-Trp-Ile-Gly, but a number of variations	Lys/Arg-Leu/Ile/Val/Phe/Thr/Ala-Thr/Ser/Ile/Ala
CRD3	always 33 residues after end of H2	3 to 25(!) residues	Cys-XXX-XXX (typically Cys-Ala-Arg)	Trp-Gly-XXX-Gly

Figure 37. Kabat numbering scheme of antibodies heavy chain. a. - heavy chain of autoantibody modeling structure show a rigid beta sheet conformation for frame

regions bound together by flexible loop regions that coincide with CDR regions; b. - The orientation of the polypeptide chain is visualized in the lower right scheme - frame 1 and 3 changed chain direction, maintaining the CDR position in the same plane to form the antigen interaction surface (light chain part of the paratope); c. - Kabat, later revised by Chothia, postulated the exact positioning of the CDRs in the variable region sequence summarized in the table.

2.4.2. Complete light and heavy chain sequences of Aβ-autoantibody

For light chain, three complete sequences were assembled with full sequence coverage, and 33 incomplete sequences. The sequences belong to lambda and kappa types. An example of light chain is presented in Figure 38a. In the case of heavy chain, two types were found in the Aβ-autoantibody, IgG1 and IgG2. In Figure 38b. an example of a heavy chain is presented.

a.

001. EIVLTQSPGT LSLSPGERAT LSCRASQSVS SNYLWYQQKP GKPPKLLIYG
051. ASTRATGIPA RFSGSGSGSG TDFTLTISRL QPEDFAVYYC QQSYSSQLTF
101. GQGTKVDIKR TVAAPSVFIF PPSDEQLKSG TASVVCLLNN FYPREAKVQW
151. KVDNALQSGN SQESVTEQDS KDSTYSLSST LTLSKADYEK HKVYACEVTH
201. QGLSSPVTKS FNRGEC

b.

01. EVQLVESGGG LVKPGGSLRL SCAASGFTFS KYWMNWVRQA PGKGLEWVAN
51. IKQDGGERYA NSVQGRFTIS RDNAKNSLYL QMNSLRAEDT AVYYCARGAA
101. RLDYYYGMDL WGQGTLVSVS SASTKGPSVF PLAPSSKSTS GGTAALGCLV
151. KDYFPEPVTV SWNSGALTSG VHTFPAVLES SGLYSLSSVV TVPSSSLGTQ
201. TYICNVNHKP SNTKVDKKVE PKSCDKTHTC PPCPAPELLG GPSVFLFPPK
251. PKDTLMISRT PEVTCVVVDV SHEDPEVKFN WYVDGVEVHN AKTKPREEQF
301. NSTFRVVSVL TVLHQDWLNG KEYKCKVSNK GLPAPIEKTI SKAKGQPREP
351. QVYTLPPSRE EMTKNQVSLT CLVKGFYPSD IAVEWESNGQ PENNYKTTPP
401. VLDSDGSFFL YSKLTVDKSR WQQGNVFSCS VMHEALHNHY TQKSLSLSPG
451. K

Figure 38. Amino acid sequence of the Aβ-autoantibody light (a.) and heavy (b.) chains assembled with proteolytic peptides determined by LC-MS/MS summarized in Tables 30-31 and Edman sequencing listed in Table 4 and Table 5 by overlapping fragments with at least two common amino acids at one end. Color code: BLACK-

constant region sequences (C_L, C_{H1}, C_{H2}, C_{H3}); BLUE - complementary determining regions according to Kabat and Chothia rules (CDRs); RED - constant sequences (V_L and V_H); GREY - Sequences obtained only by homology with other sequences present in data bases

Although a large number of peptides were found in the HPLC fractions, only a limited number of complete sequences could be assembled due to the difficulty to find uninterrupted overlapping fragments. The two sequences presented in Figure 38 were written in FASTA files and used for 3D modeling of the Aβ-autoantibody using a homology model strategy. Homology modeling aims to build three-dimensional protein structure models using experimentally determined structures of related family members as templates, in this case a crystal structure of an immunoglobulin from Protein Data Base (PDB). The Aβ-autoantibody 3D model was visualized using BallView and RasMol programs as shown in Figure 39. The antibody structure is formed of two polypeptide chains: one heavy and one light linked by a disulfide bond C216 of C_L and C224 of C_{H2}.

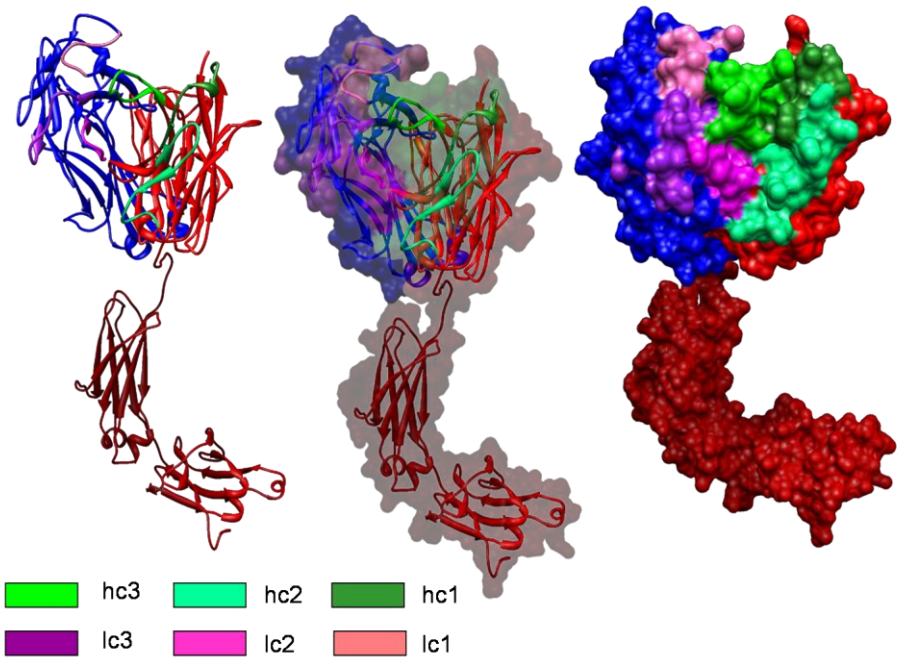

Figure 39. Molecular modeling of the structure of Aβ-autoantibody obtained by homology model and visualized using BalView program. Left - ribbon diagram with beta sheet and loops of Aβ-autoantibody; Middle mixed diagram backbone and surface of Aβ-autoantibody; Right - Molecular surface model of Aβ-autoantibody.

Color code: red- CH regions and constant frames of VH; blue - CL region and constant frames of VL; purple colors - light chain CDRs; green colors - heavy chain CDRs

The surface exposure of the CDRs of the light and heavy chains is illustrated in Figure 39 in a Van der Waals surface model showing a series of cross-sections of the antigen binding site. All CDRs regions have surface exposure, with light chain CDRs 1 and 2 and heavy chain CDR1 having the highest. Although the model is a theoretical one and without further improvements such as single loop optimization or molecular dynamic simulations, it offers a view into the 3D structure of Aβ-autoantibody and a starting point for the determination of the Aβ recognition region of autoantibody.

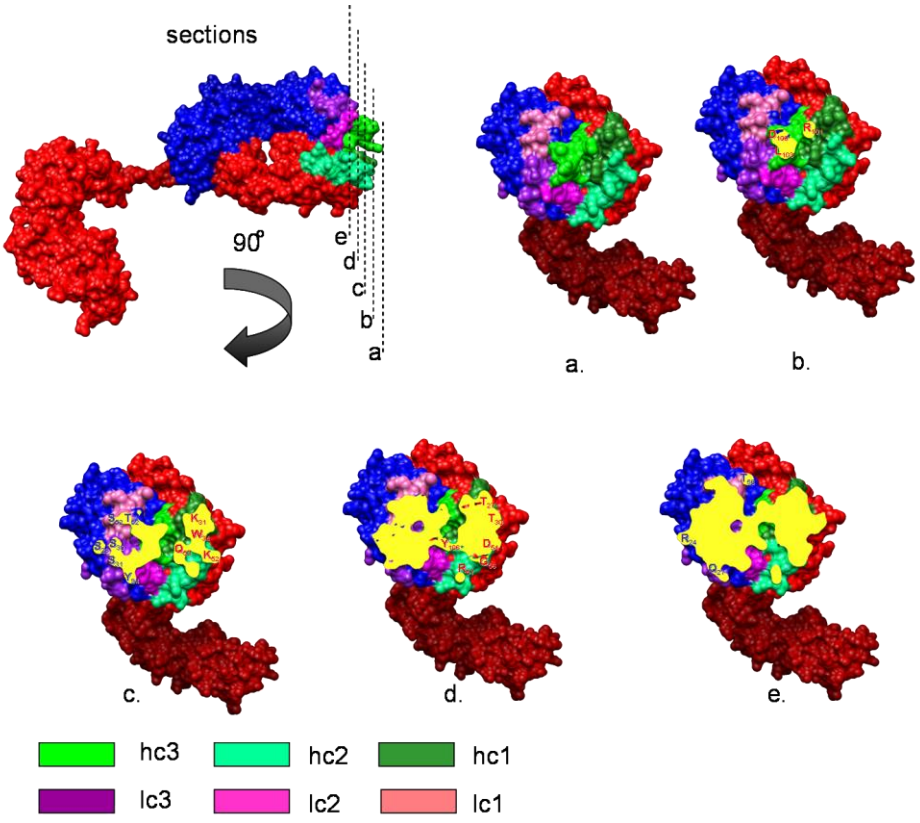

Figure 40. Van der Waals surface model of the Aβ-autoantibody from two different perspectives typical for immunoglobulin molecule - side view plane of the molecule and 90° of the side view. 5 different theoretical cross sections (a to e) show that light chain CDRs 1 and 2 and heavy chain CDR1 have the highest surface exposure. Color code: red- C_H regions and constant frames of V_H; blue - C_L and region and constant frames of V_L; purple colors - light chain colors; green colors - heavy chain CDRs

2.4.3. Sequence variations of light chains

The compilation started with the results obtained by Edman sequencing for the first 24 amino acids. The same amino acids were confirmed by MS/MS fragmentation. The first 4 amino acid presented each 2 different variants: aa1 (secondary carboxyl group – E or D), aa2 (hydrophobic amino acid – I or V), aa3 (Q or V), aa4 (L or M - similar side chain). Amino acids aa5 to aa8 are constant ^{5}TQSP^{8}, in position 9 there is short amino acid (A or S), followed by a frame constant region from aa 10 to aa 12 - ^{10}TLS^{12}.

Table 8. Aβ-autoantibody light chain amino acids variations in the primary structure of the variable region. For each position from 1 to 40 all the possible variations are listed as determinate by fragmentation techniques of the proteolytic peptides.

Amino acid position	1	2	3	4	5	6	7	8	9	10
Conserved amino acids					T	Q	S	P		T
Amino acid level variations	E D	I V	V Q	L M					A S	
Amino acid position	**11**	**12**	**13**	**14**	**15**	**16**	**17**	**18**	**19**	**20**
Conserved amino acids	L	S		S						T
Amino acid level variations			L A E V		P V	G D	E D Q N	R S G	V A	
Amino acid position	**21**	**22**	**23**	**24**	**25**	**26**	**27**	**28**	**29**	**30**
Conserved amino acids			C	R		S	Q			
Amino acid level variations	I L	T S			E A			G S	I V	R S
Amino acid position	**31**	**32**	**33**	**34**	**35**	**36**	**37**	**38**	**39**	**40**
Conserved amino acids					W	Y	Q	Q		P
Amino acid level variations	N S	Y S A N	L F Y	A L					K L	

In the position 13 the variability is very high, preferably being a hydrophobic amino acid (L, A, E or V), followed again by a frame amino acid - S. In the position 15, is preferred a P, rarely a V and in 16th a G to a D. Position 17 is polar, preferred being acids E or D to N or Q. Aa18 is highly variable (R, S or G) and is followed by a small hydrophobic position (V or A) and a frame amino acid T. In position 21 one can find a hydrophobic (I or L) and immediately after a polar amino acid (S or T).The C in position 23 is

predicted by Kabat rules and found also in the sequence, followed by the first amino acid of the CDR 1 - a Arg residue.

Table 9. Aβ-autoantibody light chain amino acids variations in the primary structure of the variable region. For each position from 41 to 80 all the possible variations are listed as determinate by fragmentation techniques of the proteolytic peptides.

Amino acid position	41	42	43	44	45	46	47	48	49	50
Conserved amino acids	G			P		L	L	I	Y	
Amino acid level variations		Q T K	A P		R K					K G D A
Amino acid position	**51**	**52**	**53**	**54**	**55**	**56**	**57**	**58**	**59**	**60**
Conserved amino acids		S					G		P	
Amino acid level variations	A V		T N S D	R L	A T Q N	T S R		I V		D A S
Amino acid position	**61**	**62**	**63**	**64**	**65**	**66**	**67**	**68**	**69**	**70**
Conserved amino acids	R	F	S	G	S		S	G		
Amino acid level variations						G S N D T Q			T N D	D T K
Amino acid position	**71**	**72**	**73**	**74**	**75**	**76**	**77**	**78**	**79**	**80**
Conserved amino acids			L	T	I	S		L		
Amino acid level variations	F V A	T S					R G S		E Q K R	P S T A

From this position were searched at least 2 overlapping peptide fragments determined by MS/MS or Edman sequencing for each amino acid, to confirm their position in the peptide chain. In the CDR 1 (aa24-34) only a a24 (R), aa 26 (S) and aa 27 (Q) are conserved; aa 25 has two variants (E or A), aa 28 a small amino acid (G or S), aa 29 is hydrophobic (I or V), 30 is polar (R or s), 31 also (N or S). The aa32 is highly variable (Y, S, A or N) and the 33 is big (L, F or Y), wile the last one is hydrophobic (A or L).

After the CDR 1, a constant region is predicted by the Kabat rule, ^{35}WYQQ^{38}. This constant region is part of frame 2, which contains also other two constant amino acids: ^{40}P and ^{41}G. The first amino variable amino acid from frame 2 is a bulky one (K or L), followed in position 42 by a highly variable one (Q, T or K) and A or P in the 43rd. The rest of the frame is relatively conserved ^{44}PXLLIY^{49}, where X is a basic residue.

CDR 2 lies between residues 50 – 56 and has only one fix amino acid in position 42 – Ser. The nature of the residues in CDR 2 of the Aβ – autoantibody are as follows: aa 50 is highly variable; aa 51 is a small hydrophobic; aa 53 has a positive small side chain; aa 54 is a bulky and basic; aa 55 is a variable one; aa 56 has a hydroxyl group. Frame 3 has a few constant parts: ^{57}G, ^{59}P, ^{61}RFSGS^{49}, ^{67}SG^{69}, ^{73}LTIS^{76}, ^{78}L, ^{84}A, ^{86}YYC^{88}. The variable amino acids are positioned as following: aa 58 is a hydrophobic one, I or V; aa 60 is small; aa66 highly variable; aa 69 is hydrophilic; aa 70 is charged; aa 71 is hydrophobic; aa 72 has a hydroxyl group; aa 77 is variable; aa 79 is a bulky one with an amino group on side chain; aa 80 is small; aa 81 is Q or E; aa 82 is N or D; aa 83 and aa 85 is variable.

For CDR 3 only a single sequence was found ^{89}QQSYT^{93} (representing the first part). Positions 94 to 96 were not covered by sequencing data. For this reason alignment tools were employed for the obtaining of the sequences, such as BLAST to search for the similar sequences of antibodies to predict the missing amino acids. The last amino acid in the CDR is a variable one (T, Y or V). The last constant frame from the variable region presents no variations: ^{98}FGQGTKVDIKR^{108}.

Table 10. Aβ-autoantibody light chain amino acids variations in the primary structure of the variable region. For each position from 81 to 108 all the possible variations are listed as determinate by fragmentation techniques of the proteolytic peptides.

Amino acid position	81	82	83	84	85	86	87	88	89	90
Conserved amino acids				A		Y	Y	C	Q	Q
Amino acid level variations	E Q	D N	F E A D V		V D T I					
Amino acid position	91	92	93	94	95	96	97	98	99	100
Conserved amino acids	S	Y	T					F	G	Q
Amino acid level variations				X	X	X	T Y V			
Amino acid position	101	102	103	104	105	106	107	108		
Conserved amino acids	G	T	K	V	D	I	K	R		
Amino acid level variations										

2.4.4. Sequence variations of heavy chains

In the heavy chain, the variations in the variable region are counting for over 5 % of the sequence, both CDRs and frames. The N-terminus was assigned by Edman sequencing and confirmed by tandem mass spectrometry. The sequence starts with a Gln or Glu, aa 2 is a hydrophobic with an iso – side chain, aa 3 Q or L, aa 4 was hydrophobic (L or V), aa 5 is V or Q followed by aa 6 E or S. In frame 1, constant amino acids are situated in positions: ^{7}G, ^{8}G, ^{13}P, ^{16}S, ^{17}L, ^{18}R and ^{24}S; hydrophobic amino acids in positions: ^{10}X (X = V or L) and ^{19}Y (Y = I or L).

In positions 9, 11 and 14 variable amino acids are present. Position 12 in polypeptide chain is occupied by a large amino acid Gln and Lys, position 15 by Gly or Lys. In position 20 there is a charged amino acid (S or Q) as in 21 (C or Q). Positions 22 and 23 are filled either with Ala or Lys.

Table 11. Aβ-autoantibody heavy chain amino acids variations in the primary structure of the variable region. For each position from 1 to 40 all the possible

variations are listed as determinate by fragmentation techniques of the proteolytic peptides.

Amino acid position	1	2	3	4	5	6	7	8	9	10
Conserved amino acids							G	G		
Amino acid level variations	E Q L	V I	Q L	L V	V Q	E S			G D V L	V L
Amino acid position	11	12	13	14	15	16	17	18	19	20
Conserved amino acids			P			S	L	R		
Amino acid level variations	V L V H A	Q K		G E Q R	G K				L I	S Q
Amino acid position	21	22	23	24	25	26	27	28	29	30
Conserved amino acids				S	G	F				
Amino acid level variations	C Q	A K	A K				T S	F T L	R S K I	S T G S D N
Amino acid position	31	32	33	34	35	36	37	38	39	40
Conserved amino acids					W					
Amino acid level variations	Y T	D S G A R E Y F	M V N H I Y W	S H G N M H V K Q E		V I	R Q	Q K R	A T P	P A

The CDR 1 of the heavy chain starts with 2 conserved amino acids ^{25}GF^{26}. Aa 27 has a hydroxyl- group on the side chain (T or S) just like aa 31 (Y or T), while aa 29, aa 30, aa 31, aa 32, aa 33, aa 34 are highly variable.

^{35}W marks the turn in the polypeptide chain and the start of frame 2 of the light chain, followed by a hydrophobic amino acid (V or I). In position 37 and 38, the side chains of the residues have free amino group (R, Q or K). Ala or Pro occupies next positions 39 – 40.

Table 12**.** Aβ-autoantibody heavy chain amino acids variations in the primary structure of the variable region. For each position from 41 to 80 all the possible

variations are listed as determinate by fragmentation techniques of the proteolytic peptides.

Amino acid position	41	42	43	44	45	46	47	48	49	50
Conserved amino acids						W				
Amino acid level variations	G D	K Q	G A	L V	E Q K		V L I M	A S G I	S D I V R N Y G	V T G I D M N
Amino acid position	**51**	**52**	**53**	**54**	**55**	**56**	**57**	**58**	**59**	**60**
Conserved amino acids										
Amino acid level variations	K Y S G T V	Q Y M G S D F	F N D A E I S	F L H S G A T	S D G	G Y T S E K N	S I Y G R K T	A S Y T N	A Y T	T Y N D L
Amino acid position	**61**	**62**	**63**	**64**	**65**	**66**	**67**	**68**	**69**	**70**
Conserved amino acids						R				
Amino acid level variations	G P S	S V	V L R K Q	K Q G	G K Q		F V L	T A S	I M T	S T R
Amino acid position	**71**	**72**	**73**	**74**	**75**	**76**	**77**	**78**	**79**	**80**
Conserved amino acids										
Amino acid level variations	R V A N T	D S N T	T N V K L	S N A D T	K T I	N S	T Q K S	L V N A	Y L Q	L F

From aa 41 to aa 44 there are 2 options for each position: aa 41 = G or D, aa 42 = K or Q, aa 43 = G or A, aa 44 = L or V. In position 45 is E, Q or K followed by another turn with ^{46}W, a hydrophobic in aa 47 (V, L, I or M) and the frame 2 is ending with a small amino acid (A, S or G).

The CDR2 is mainly formed by highly variable residues from aa 49 – 60, as the first part frame 3 from aa 61 - 65 and from aa 67 - 90; all variations found are listed in Table 12. Position 82 is occupied by similar residues Met and Leu. Aa84 presents small amino acids with hydroxyl group on the side chains (Ser or Thr). Position 85 is filled up by an aliphatic amino acid (L, A or V).

Table 13. Aβ-autoantibody heavy chain amino acids variations in the primary structure of the variable region. For each position from 81 to 100 all the possible

variations are listed as determinate by fragmentation techniques of the proteolytic peptides.

Amino acid position	81	82	83	84	85	86	87	88	89	90
Conserved amino acids										
Amino acid level variations	Q H D	M L	N T I S R K D	S N T	L A V	R T K E Q	A S T G V D	E D A K Q	D G N	T A E
Amino acid position	91	92	93	94	95	96	97	98	99	100
Conserved amino acids	A		Y	Y	C	A	R			
Amino acid level variations		V I						G V S D	A L G R D S E	A T Y K F R A G

Table 14. Aβ-autoantibody heavy chain amino acids variations in the primary structure of the variable region. For each position from 101 to 120 all the possible variations are listed as determinate by fragmentation techniques of the proteolytic peptides.

Amino acid position	101	102	103	104	105	106	107	108	109	110
Conserved amino acids										
Amino acid level variations	R D A Y T G E	L A G Y D K	D S M G A I D F Y	Y W G S G K	Y V S L D W	Y I L S R F	G L T D D Y	M T Y L D S F G	D N L G Y	V N A G L
Amino acid position	111	112	113	114	115	116	117	118	119	120
Conserved amino acids	W				T	L	V			
Amino acid level variations		G T	Q E	G V				T G S	V Q	S P

The second part of frame 3 is a highly conserved sequence ^{91}AXYYCAR^{97}, where X is either Val or Ile. This part of the frame 3 is involved in the 3D structure stabilization being involved in intra-domain disulfide bonds. CDR3 is

composed of hypervariable residues from position 98 to 110. The CDR is preponderant hydrophobic and/or aromatic. The last amino acid, ^{111}W sets the last turn in the polypeptide chain of variable region.

The last frame, the forth, makes the transition to constant region and has 2 variants: ^{112}GQGTLVTVS^{120}, characteristic for IgG_1 and ^{112}TEVTLVGQP^{120}, characteristic for $IgG_{2/3}$.

2.5. Characterization of affinity interactions between Aβ-autoantibody and Aβ-peptides

The biological activity of Aβ-autoantibody led to its initial discovery in human serum [107, 108.]. Their correlation with the molecular pathology and with the symptoms of AD was the subject of a series of studies on their possible role in the treatment of AD patients. Based on the finding that Aβ-autoantibody recognizes the Aβ (21–37) epitope, in a recent study carried out in our laboratory, a sandwich ELISA for the determination of intact Aβ-IgG immune complexes was developed and applied for the analysis of serum samples from healthy individuals of different age [67.]. A similar study on AD patients and age-matched healthy individuals was also performed [109.] and it was found that both serum and CSF levels of Aβ-IgG immune complexes were significantly higher in AD patients compared to control subjects. Moreover, the levels of Aβ-IgG complexes were negatively correlated with the cognitive status across the groups, increasing with declining cognitive test performance of the subjects.

Comparative binding studies of human Aβ-antibody with Aβ (1-16), Aβ (1-40), Aβ (12-40) and Aβ (17-28), each synthesized with a pentaglycine spacer and biotin at the N-terminal end, were performed by an indirect ELISA assay. The results indicated that Aβ (1-16) and Aβ (17-28) did not bind to the Aβ – autoantibody, while Aβ (12-40) and Aβ (1-40) showed binding affinity towards polyclonal Aβ - autoantibody in a concentration-dependent manner. Similar results were obtained by analyzing samples of the anti-Aβ-autoantibody isolated from AD patients[109.]. For a more detailed analysis of the molecular interaction between Aβ-autoantibody and Aβ-peptides and the molecular topography of the interaction, a panel of analytical methods was employed in the present thesis, such as affinity-mass spectrometry, SAW-biosensor and SAW-biosensor-mass spectrometry.

2.5.1 Affinity-mass spectrometric characterization of Aβ-autoantibody

Affinity-mass spectrometry experiments were based on the immobilization of the Aβ-autoantibody on a sepharose matrix, through a linker that offers flexibility for the affinity binding with the ligand. Aβ-peptides were synthesized by solid phase peptide synthesis, purified by RP-HPLC and used as a stock solution of 1 µg/µL in trifluoroethanol. The peptide was diluted with PBS (pH 7.5) and incubated with the matrix containing immobilized Aβ-autoantibody. After incubation, the supernatant was collected and the excess of peptide was washed away with 50 mL PBS. The immune complex was then dissociated under acidic conditions - the elution was performed three times and collected.

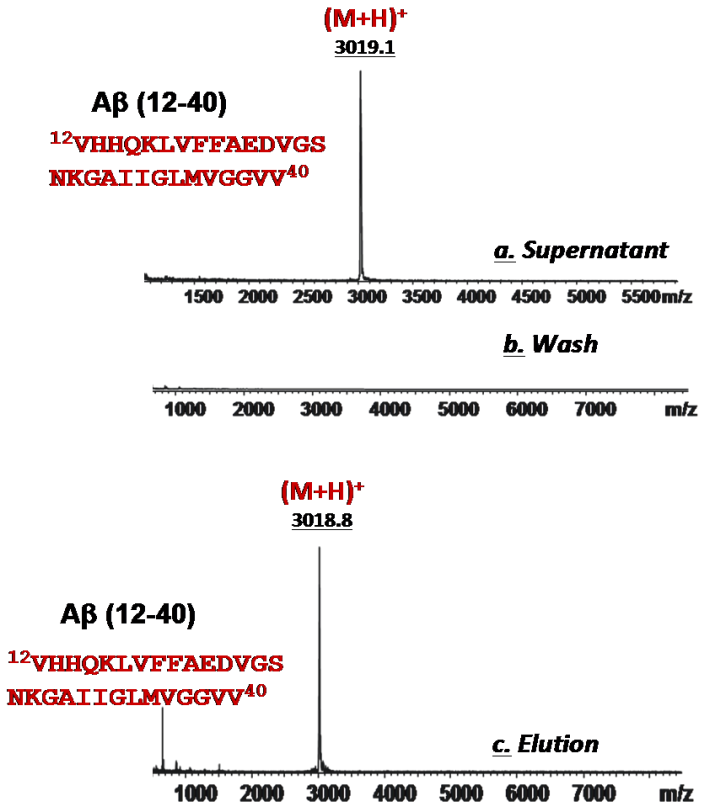

Figure 41. Binding Aβ (12-40) to Aβ-autoantibody column by affinity-mass spectrometry using MALDI-ToF MS: a. - Supernatant fraction; b. - Washing fraction; c. - Elution fraction showing $(M+H)^+$ of Aβ-peptide.

After desalting and concentration, the supernatant, last wash and elution fractions were loaded on a MALDI-ToF target and analyzed by mass

spectrometry. An example of the affinity-mass spectrometry analysis of Aβ (12-40) and the Aβ-autoantibody is shown in Figure 41.

The results from overlapping affinity-MS experiments provided a core fragment containing peptides that have affinity towards the Aβ-autoantibody. The shorter fragment found to bind to the Aβ-autoantibody was Aβ (25-35) as shown in Table 15.

Table 15. Results of affinity-mass spectrometry binding studies of Aβ-autoantibody with Aβ peptide fragments. The smallest Aβ fragment that bound to Aβ-autoantibody was Aβ (25-35)

No.	Aβ-peptide[a.]	Molecular Mass $(M+H)^{+}$ [b.]	Affinity towards Aβ
1	Aβ (1-40)	4329.86	+
2	Aβ (1-16)	1955.03	-
3	Aβ (4-10)	880.92	-
4	Aβ (20-37)	1778.06	-
5	Aβ (12-40)	3022.56	+
6	Aβ (17-28)	1325.48	-
7	Aβ (25-35)	1060.28	+
8	Aβ(31-40)	957.25	-

[a.] Peptides obtained by solid phase peptide synthesis, Fmoc strategy

[b.] Mass spectrometry analysis by ESI-ion trap (Esquire 3000) or MALDI-ToF (Micromass ToFSpec2E)

2.5.2. Characterization of Aβ-autoantibody - Aβ-peptide interaction using SAW-Biosensor

A biosensor converts a biological response into an electrical signal with applications e.g. in medical diagnostics, drug detection and food quality. The principle of surface acoustic wave biosensor (SAW-biosensor) is based on the transformation of an electric signal into a mechanical wave through piezoelectricity. The viscosity of the analyte modifies the amplitude and phase of the wave, and the wave is converted back into an electrical signal for processing and quantification. The high sensitivity, simultaneous measurement of two types of signals and resistance to buffer changes render SAW technique highly suitable for affinity biomolecular interaction studies. The SAW-biosensor has five sensor elements on one chip operated in Lowe/wave geometry, operating at two fixed frequencies that differ by about 0.3 MHz, with φ(f1)-φ(2) of approx. 180° at a frequency range between 130 and 170 MHz, optimized to reduce the influence of physical parameters on the sensor signal such as temperature, salts and viscosity of the analyte solution [110-112.].

The interaction between the Aβ-autoantibody and Aβ-peptides was tested in two systems: (i.), direct analysis with immobilized Aβ-peptide and Aβ-autoantibody in mobile phase and (ii.), a reverse system in which the Aβ-autoantibody were immobilized on the chip and Aβ was in the mobile phase. In the first step, the SAM-carboxyl groups were activated with N-(3-dimethylaminopropyl)-N-ethylcarbodiimide (EDC); further, the coupling of Aβ(1-40) was carried out using 50 mM NHS followed by washing of the chip surface with 40 µL/ min H_2O for several minutes. The remaining NHS groups were blocked with 1 M ethanolamine (pH 8.5). After stabilization of the signal, 150 µL of 200 nM Aβ-autoantibody solution were injected and run over the chip. In the last step, the antibody-antigen complex was dissociated by changing the pH. A schematic view of the phase shift in an ideal experiment is shown in Figure 42.

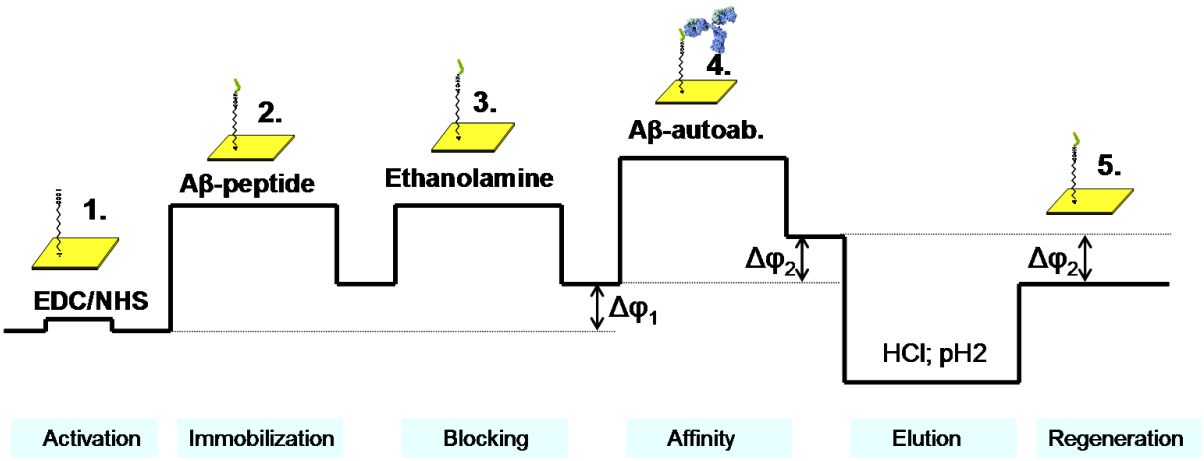

Figure 42. Principle of the SAW biosensor affinity experiment. 1- The gold surface of the chip is activated by EDC/NHS; 2 – Aβ-peptide is covalently immobilized on the surface and the excess is washed away with PBS; 3 - the free remaining sites are blocked with ethanolamine; 4 – Aβ-autoantibody is passed through the system and bind to the antigen and the excess is washed away with PBS. The phase shift is read; 5 - Elution is performed under acidic conditions and after equilibration with PBS, the phase shift is read again.

Aβ-autoantibody was injected in the system and the affinity binding was performed. The elution was performed and the eluted antibody subjected to reduction of the disulfide bridges with DDT and alkylation of the free sulfhydryl group with IAA. The solution was loaded on an SDS-PAGE to check the content of the elution fraction. The direct experiment showed that the Aβ-autoantibody had high affinity towards Aβ-peptide. Although the elution was performed three times, more than half of the antibody amount remained bound to Aβ on the chip. Upon repetition of the experiment another three times on different gold chips with higher blocking time, the same result was obtained, which confirmed the Aβ-autoantibody avidity towards Aβ. The sensogram of immobilization of Aβ (1-40) and the biosensor affinity experiment are presented in Figure 43.

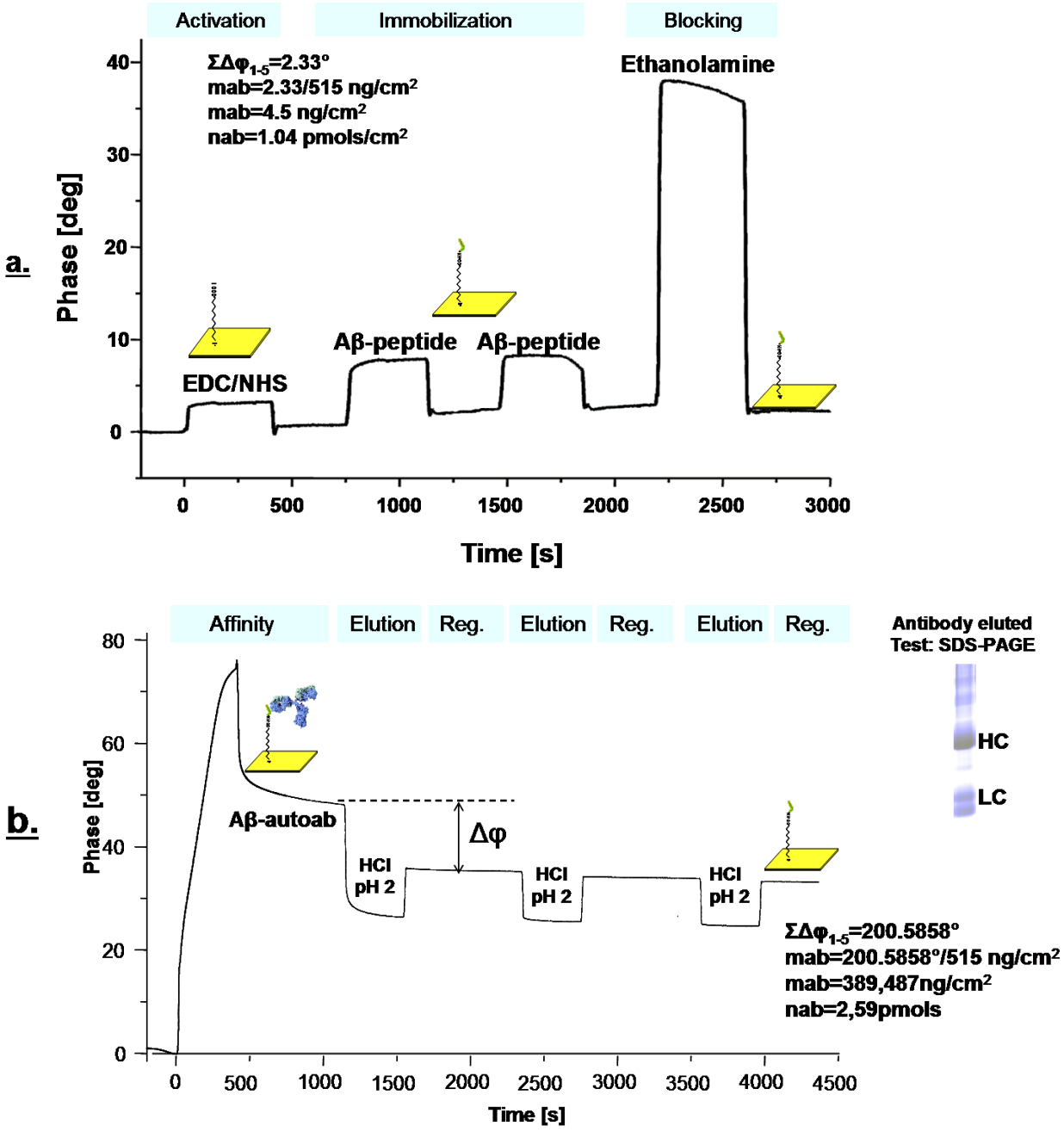

Figure 43. Interaction between Aβ (1-40) and Aβ-autoantibody analyzed by SAW-biosensor. a. - Biosensor sensogram of Aβ (1-40) immobilization on self-assembled monolayer (SAM) gold chip present the following signals: activation with EDC/NHS, Aβ (1-40) immobilization and blocking with ethanolamine. The change in phase shift suggests a binding to the gold chip surface. b. - biosensor profile of bio-affinity interaction between Aβ and Aβ-autoantibody. Differences in phase shift appear at affinity with Aβ-autoantibody and at the 3 elutions performed. The insert in upper right part is the gel lane visualization of the elution fractions

2.5.3. Epitope mapping of Aβ-autoantibody by online SAW-Biosensor-Mass Spectrometry

The interaction between Aβ-autoantibody and different truncated Aβ-peptides and Aβ was characterized using a SAW-biosensor system coupled with an ion trap mass spectrometer to confirm the results from epitope extraction experiments previously performed using the reverse system with Aβ-autoantibody immobilized on the gold chip, as schematically shown in Figure 44. The interface used for on-line coupling of SAW with ESI-MS included a six-port valve unit and C18-micro guard column and micro-injector for desalting and concentration of dissociated ligand samples [113.]. The Aβ-autoantibody was diluted with 7% TFE in PBS just before performing the SAW affinity experiments. Using this solution, the antibody was immobilized on the gold chip after an a priori formation of a self assembled monolayer (SAM) of 16-mercaptohexadecanoic acid, for 12 h at 25 °C. SAM-carboxyl groups were activated with N-(3- dimethylaminopropyl)-N-ethylcarbodiimide (EDC); coupling was carried out using NHS, followed by washing the chip surface with 40 µL/ min H_2O for several minutes. The remaining NHS groups were blocked with 1 M ethanolamine (pH 8.5) as shown in Figure 45a.

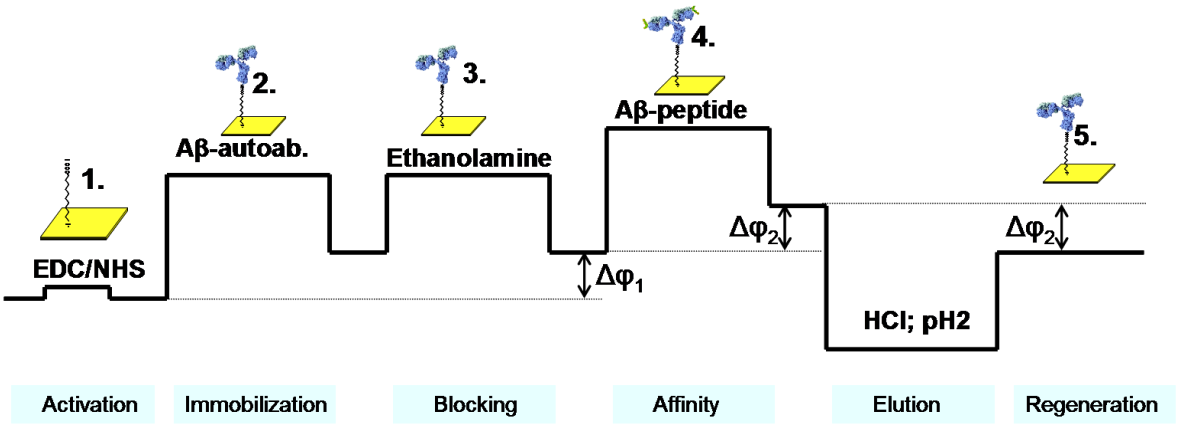

Figure 44. Experimental procedure to determine the Aβ-autoantibody – Aβ-peptide interaction by SAW-biosensor: 1.- Gold surface of the chip was activated by EDC/NHS; 2. - Aβ-autoantibody was covalently immobilized on the surface and the excess was washed away with PBS; 3. - the free remaining sites were blocked by ethanolamine; 4. – Aβ-peptide was passed through the system and it bound to the antibody and the excess was washed away with PBS . The phase shift was read; 5 - Elution was performed under acidic conditions and after equilibration with PBS the Phase shift was read

A 10 µM solution of two different Aβ-peptide fragments in equimolar mixture was added and the affinity binding performed at a flow rate of 20 µL/min. All affinity binding experiments were carried out at RT in PBS binding buffer, pH 7.5. Following the association of the ligand, the elution was carried out with 0,1% TFA in d.i. water, as shown in the sensogram presented in Figure 45b. Removal of buffer salts was performed by washing with 0.5% aqueous HCOOH and the elution and transfer into the ESI source was done with 0.5% HCOOH in acetonitrile (elution). A Bruker Esquire 3000+ ion trap mass spectrometer was used for on-line SAW-ESI-MS. Mass spectra were recorded in full-scan mode, mass range 200–2000 Th, with 20 psi nebulizer gas, 10.0 L min^{-1} drying gas, and 200 °C ion source temperature. The difference in the phase multiplied with the conversion factor $(515 * cm^3)^{-1}$, the exact amount in ng of Aβ-autoantibody immobilized on the gold surface could be calculated in the range of 271 ng/cm^3 to 292 ng/cm^3 in different experiments. Quantification of Aβ-autoantibody coupled on the surface of the chip was important not only to verify the experiment, but also to calculate the binding ratio of the different Aβ-peptide fragments, the amount of which could be also calculated from the phase shift of the affinity experiment.

A typical on-line SAW-biosensor-mass spectrometry experiment performed using a mixture of Aβ-peptides is presented in Figure 46. A peptide mixture of 2 to 4 different Aβ peptides was characterized by ESI-ion trap mass spectrometry before the bio-affinity experiment (Figure 46a). The mixture was passed through the SAW-biosensor with a gold chip with Aβ-autoantibody immobilized on the surface. The peptides that had affinity towards the antibodies remained bound to the surface, leading to a shift in the phase and amplitude of the sensogram (Figure 46b.).

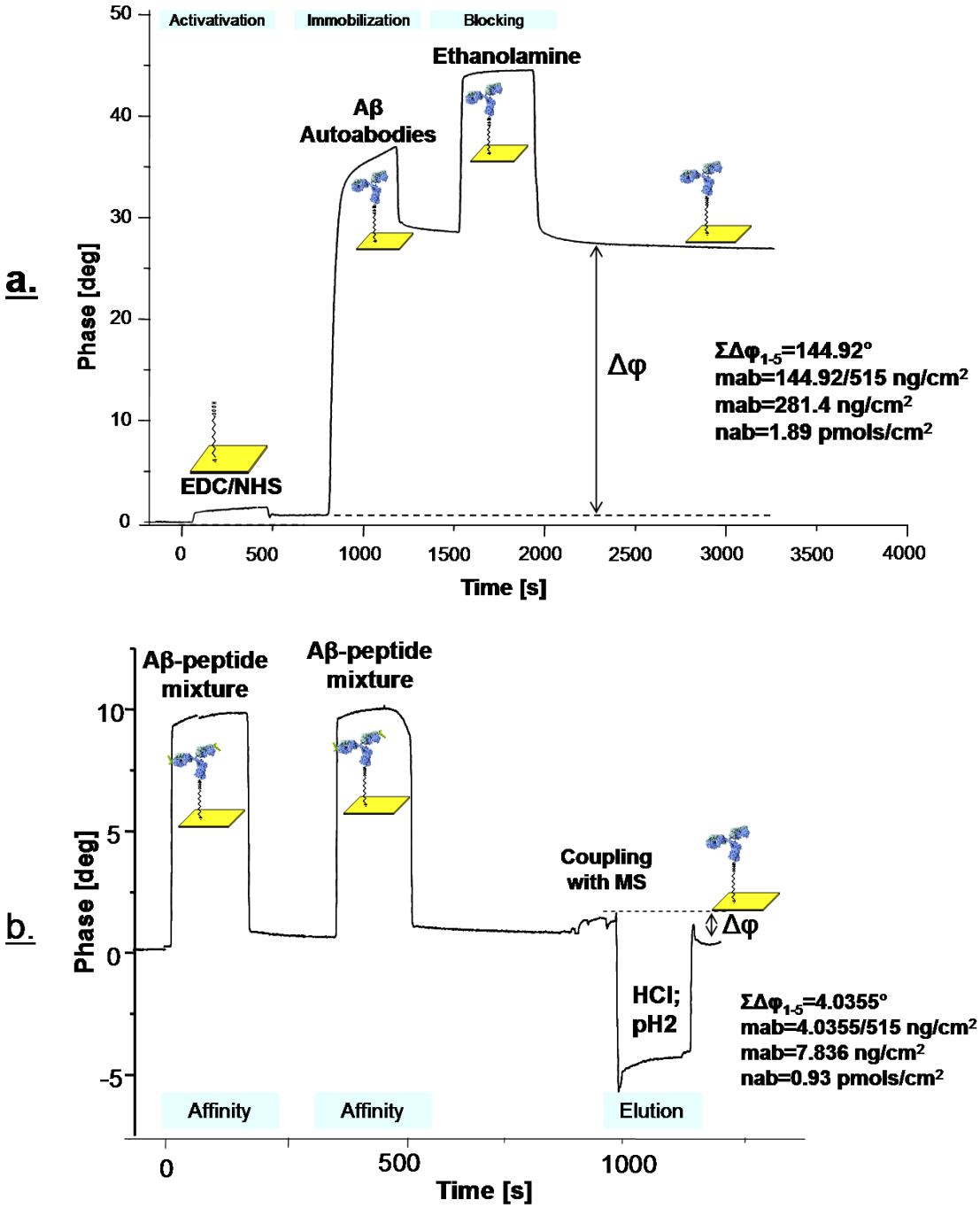

Figure 45. SAW-biosensor sensogram of the affinity interaction between Aβ-autoantibody and Aβ (1-40). a. - Biosensor sensogram of Aβ -autoantibody immobilization on self-assembled monolayer (SAM) gold chip presents the following signals: activation with EDC/NHS, Aβ (1-40) immobilization and blocking with ethanolamine. The change in phase shift suggests a binding to the gold chip surface, the high amplitude of the signal is due to the high molecular mass of the antibody. b. - biosensor profile of bio-affinity interaction between Aβ-autoantibody and Aβ. Differences in the phase shift occur during binding with Aβ-peptides and during elution. By measuring the phase shift, the amount of the antigen bound to the antibodies can be calculated.

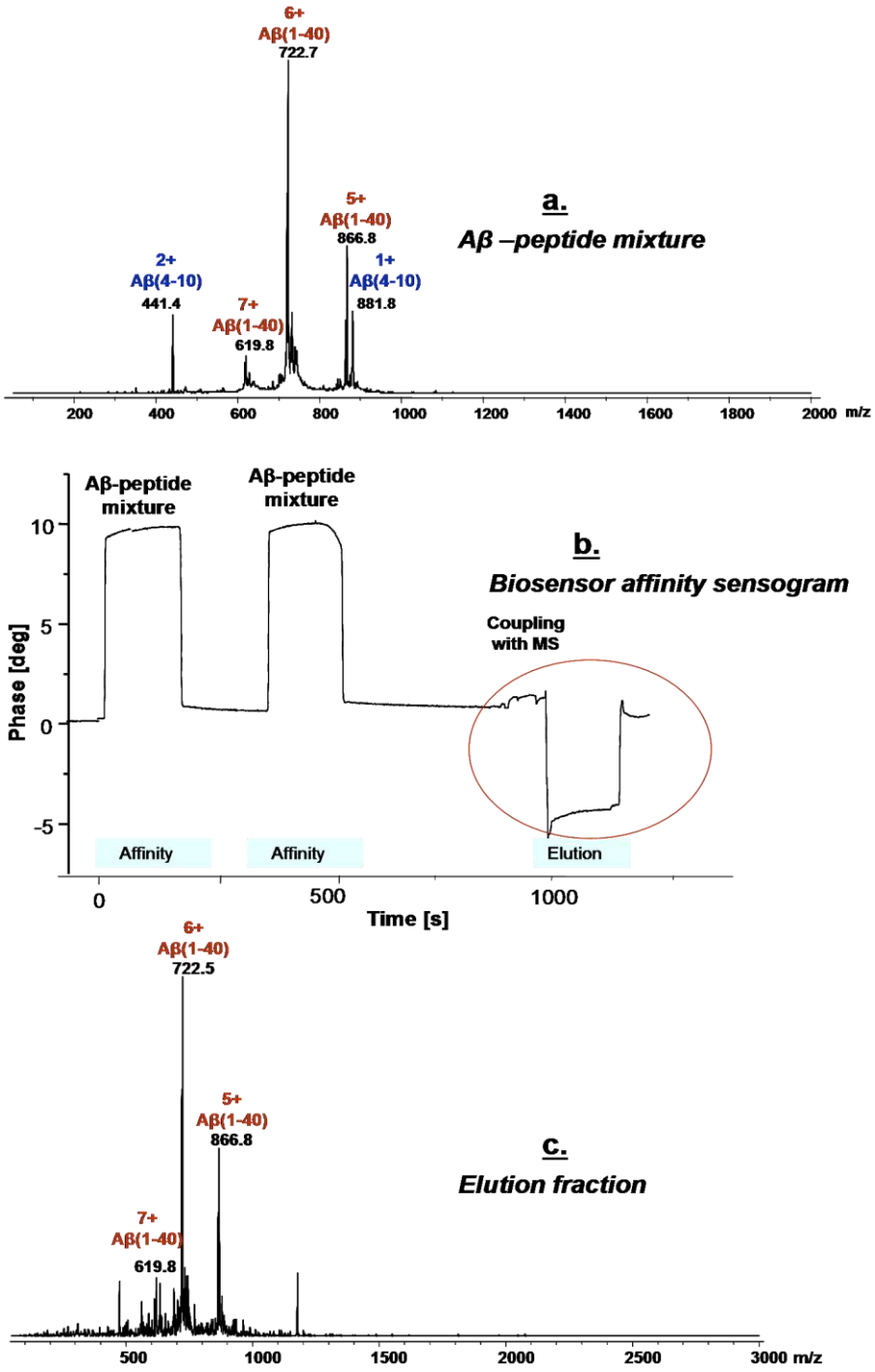

Figure 46. Example of Aβ-peptides - Aβ-autoantibody interaction investigated by biosensor-MS. a. – Esi-ion trap mass spectrum of a mixture of Aβ (1-40) and Aβ (1-16) before injection on the biosensor chip; b. - Biosensor sensogram with the phase shift recorded when the mixture passes on the surface; c. – Esi-ion trap mass spectrum of the desalted elution fraction showing that only Aβ(1-40) binds to autoantibody, but not Aβ (1-16).

By changing the pH of the mobile phase, the affinity interaction between peptides and antibody is disrupted, and the peptides are eluted from the chip surface. The online interface captures the eluted peptides, desalts and

concentrates the elution, delivering them directly to the mass spectrometer, where a mass spectrum is recorded (Figure 46c.). In case the spectrum of the elution fraction contained signals, the affinity experiments were repeated with the individual Aβ-peptide to calculate de exact mass bound to the autoantibody. The mass shifts gave the Aβ-peptides that bind to autoantibody and the amounts, which after conversion in mols, gave the binding affinity for each fragment, listed in Table 16. From all Aβ-fragments, the highest affinity was shown by Aβ (12-40), followed by Aβ (1-40). The lowest affinity is presented by the smallest peptides that contain the fragment Aβ (25-28). If the fragment is situated in the middle of Aβ peptide, the affinity is increased, so the core peptide is ^{25}GSNK^{28}; however, the neighbor amino acids are important in the binding, possible by structuring the Aβ peptide spatial configuration.

The overlapping of the fragments of the Aβ-peptides that bind to the autoantibody revealed a common fragment situated in the region 25-28 (^{25}GSNK^{28}). After mapping on the 3D structure of Aβ-molecule [114.] the fragment indicated the turn region involved in the aggregation of the Aβ-molecule (Figure 47). This result provides an explanation for the binding of autoantibody to the Aβ-peptide in monomeric and low oligomeric states, but not to high molecular aggregates, in which the turn region is masked.

Table 16. Aβ-peptides and their binding affinities to Aβ-autoantbody determined by biosensor-MS. The smallest Aβ-fragment common to all peptides that bind to Aβ-autoantibody was Aβ (25-28).

No.	Aβ-peptide[a.]	Molecular mass[b.]	Affinity towards Aβ	Binding affinity to Aβ-autoantibody (molar ratio)
1	Aβ (1-40)	4329.86	+	1:1
2	Aβ (1-16)	1955.03	-	-
3	Aβ (4-10)	880.92	-	-
4	Aβ (20-37)	1778.06	+	1:0.7
5	Aβ (12-40)	3022.56	+	1:1.3
6	Aβ (17-28)	1325.48	+	1:0.82
7	Aβ (25-35)	1060.28	+	1:0.56
8	Aβ (31-40)	957.25	-	-

[a.] Peptides obtained by solid phase peptide synthesis, Fmoc stategy

[b.] Mass spectrometry analysis by ESI-ion trap (Esquire 3000) or MALDI-ToF (Micromass ToFSpec2E, Warters)

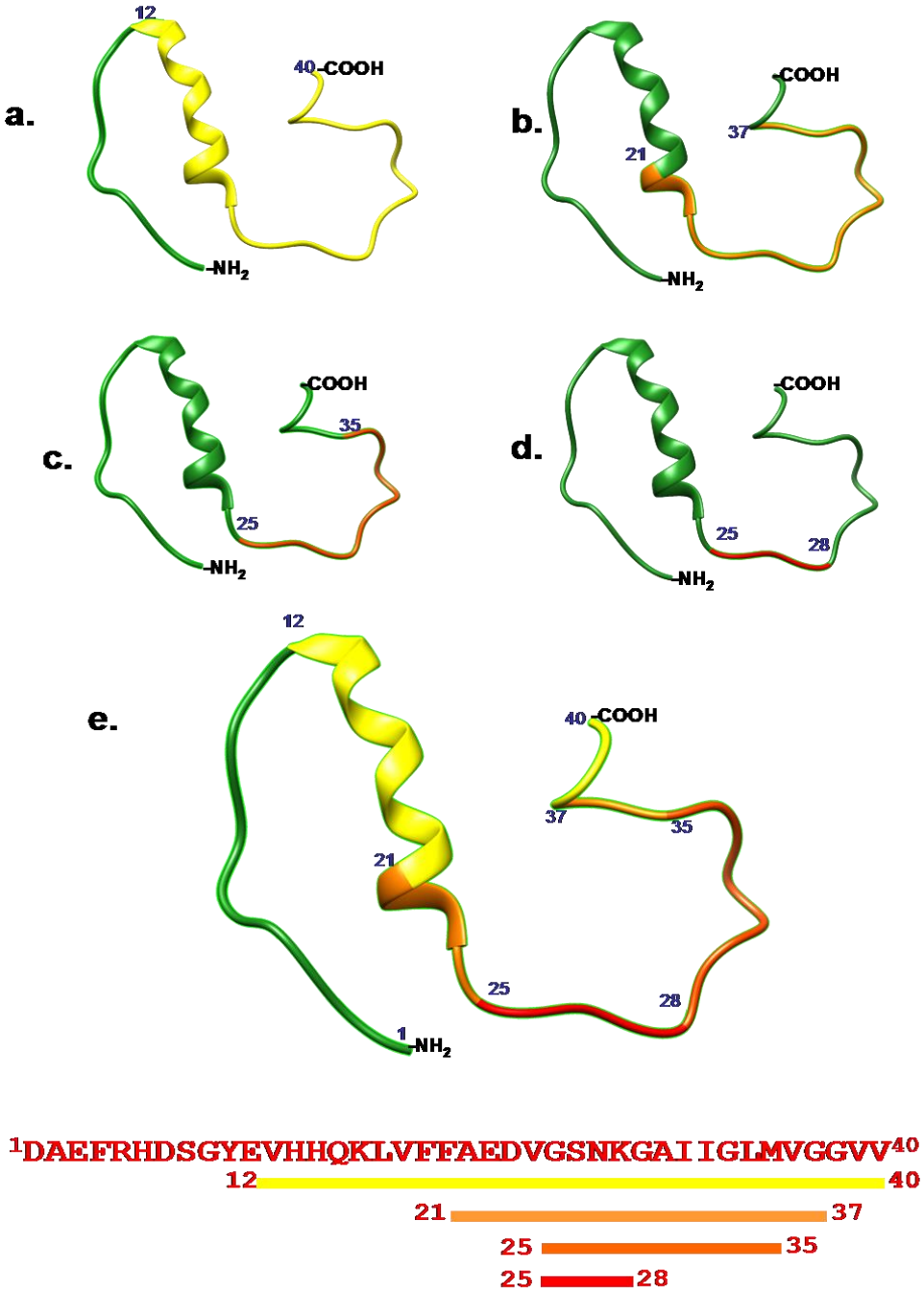

Figure 47. Summarized results of the epitope mapping experiments: a. – results of direct ELISA experiments showing that Aβ (12-40) is the smallest fragments that binds to autoantibody[48.]; b. – epitope excision and extraction experiments led to the identification of Aβ (21-37) as the the smallest epitope fragment[48, 115.]; c. – affinity-mass spectrometry analysis provided a shorter binding fragment, namely Aβ (25-35); d. - SAW-biosensor-mass spectrometry provided the core epitope ^{25}GSNK^{28}; e. – summary of all experiments. Color code: GREEN – part of the peptide not involved in the affinity interaction with Aβ-autoantibody; YELLOW – fragment determined by ELISA; ORANGE – fragment identified by epitope excision; ORANGE-RED - fragment determined by affinity-MS; RED - core epitope identified by SAW-MS.

2.5.4. Determination of dissociation constant of Aβ-autoantibody - Aβ-peptide complex by SAW-Biosensor

The K_D value for the polyclonal Aβ-autoantibody and Aβ (1-40) was determined using the system: the Aβ (1-40) peptide was immobilized as described in the Experimental Part; after the blocking step with ethanolamine, affinity binding experiments were performed using solutions of Aβ-autoantibody with increasing concentrations from 0.87 nM to 1 µM, followed by successive surface regeneration with 0.1% TFA, pH 1.9. The experiments were repeated four times and a typical sensogram is depicted in Figure 48. For further evaluation, the resulting curves were exported into Origin and then the integrated FitMaster was applied. The resulting overlay plot and individual fitting are following with a 1:1 residue - binding model. The pseudo-first order kinetic constant k_{obs} was determined by the FitMaster and plotted versus the concentrations of the Aβ-autoantibody. A best linear fit was applied using the equation $K_{obs} = k_{off} + k_{on} * C$. The K_D value was determined from $K_D = k_{off} / k_{on}$ and calculated to be in average 0.8 µM. The experiments were repeated with similar results and the K_D was calculated for all channels of the chip separately.

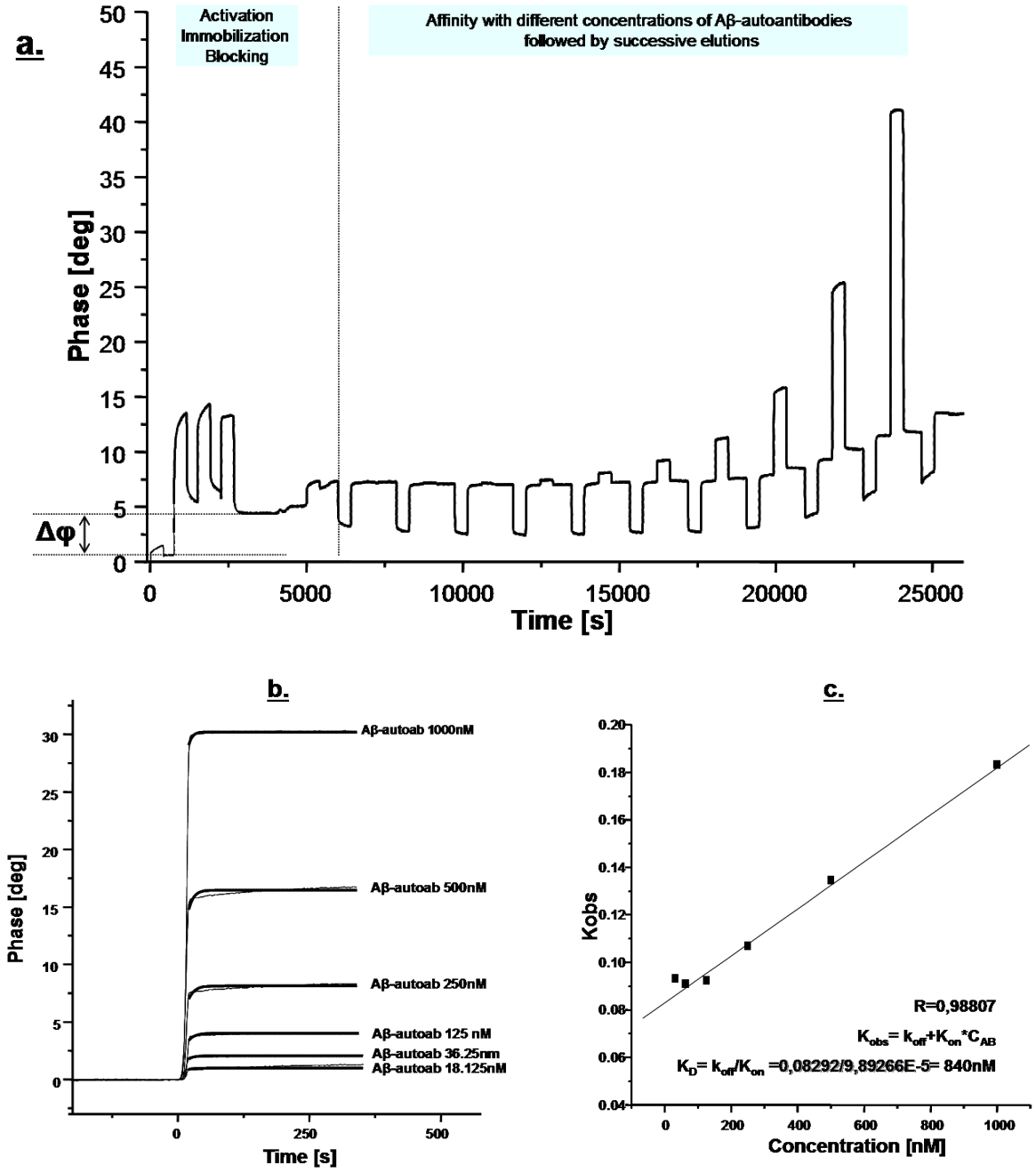

Figure 48. K_D determination for the Aβ-autoantibody - Aβ-peptide complex. a. - Sensogram profile used in the K_D determination for the characterization of Aβ-peptide – Aβ-autoantibody complex recorded with the SAW-biosensor; b. - The fitted curves of the increased binding concentrations; c. - Pseudo first-order kinetic constant plotted versus concentration. The linear regression was applied for KD of 840 ± 24.54 nM.

2.6. Characterization of Aβ-peptide – Aβ-autoantibody CDR-peptides interaction

The interactions between Aβ (1-40) peptide and the synthesized CDR peptides were investigated by affinity-mass spectrometry, online biosensor-mass spectrometry and the dissociation constants were determined by the SAW-biosensor.

2.6.1 Synthesis and mass spectrometric characterization of Aβ-autoantibody CDR-peptides

To determine the affinity of the recognition domains of the Aβ-autoantibody to Aβ (1-40) peptide, a series of peptides containing the CDR regions were synthesized by solid phase peptide synthesis (SPPS) on a semi-automated synthesizer using a NovaSyn-TGR resin and Fmoc/tBu strategy. Each peptide was synthesized in steps of 10 amino acid residues using the general protocol detailed in the Experimental Part. After completion of the synthesis, the cleavage was performed in the presence of trifluoroacetic acid, triisopropylsilane and water for 3 h; precipitated with ice cold diethyl-ether, filtered, redissolved with glacial acetic acid, lyophilized and analysed by MALDI-ToF MS. The crude CDR peptides were purified by semi-preparative RP-HPLC, using 0.5 % TFA in water (solvent A) and 0.5 % TFA in acetonitrile (solvent B) as mobile phases and a gradient specific for each peptide. The pure CDR peptides were characterized by MALDI-ToF-MS and ESI-ion trap MS. An example of a synthetic CDR peptide characterized by RP-HPLC and mass spectrometry is shown in Figure 49.

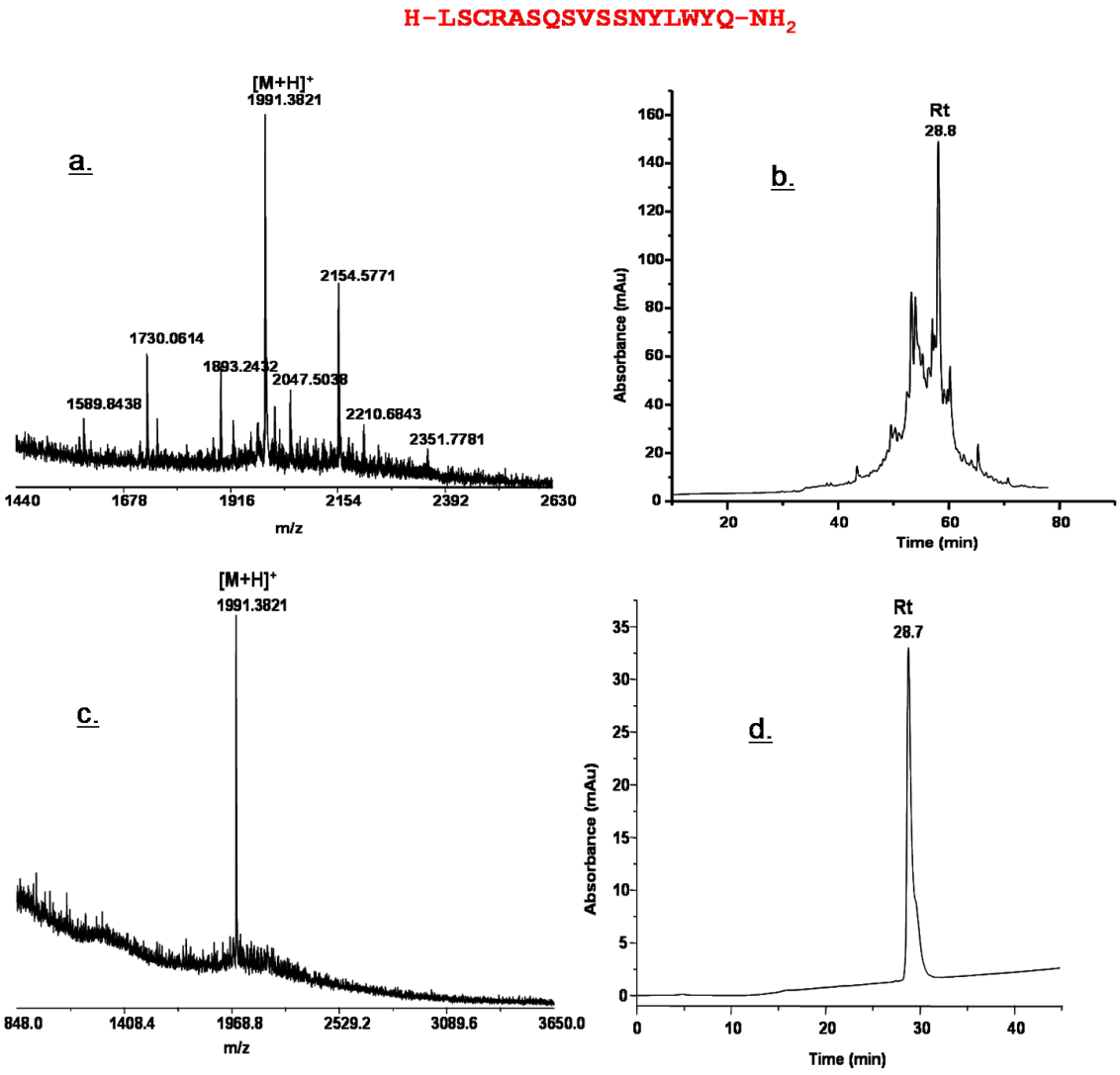

Figure 49. Example of a synthetic CDR-peptide from Aβ-autoantibody: a. – MALDI-TOF mass spectrum of the crude synthetic CDR peptide; b. – RP-HPLC chromatogram obtained during CDR peptide purification; c. - MALDI-TOF mass spectrum of the pure synthetic CDR peptide; d. – RP-HPLC characterization of the pure CDR peptide

From each CDR region specific for light and heavy chains found in the structural studies were chosen peptides to be synthetized. The amino acid sequences, the HPLC chromatograms and $[M+H]^+$ values of CDR peptides obtained by ESI-ion trap mass spectrometry are summarized in Table 17.

Table 17. Characterization of Aβ-autoantibody CDR-peptides synthesized by SPPS for the affinity experiments with Aβ-peptides:

No.	CDR peptide position[a]	Sequence	HPLC Rt (min)[b]	$[M+H]^+_{calc}$ [c]	$[M+H]^+_{exp}$ [d]
Pep.A	LC1a Light chain (21-37)	**H-LSCRASQSVSSNYLWYQ-NH2**	28.7	1991.19	1991.38
Pep. B	LC1b Light chain (22-40)	**H-TCRESQGIRNYLAWYQQLP-NH2**	34.2	2325.61	2325.95
Pep. C	LC2 Light chain (46-59)	**H-LIYGASTRATGIP-NH2**	15.4	1319.52	1319.66
Pep.D	LC3 Light chain (87-102)	**H-YYCQQSYSSQLTFGQ-NH2**	26.9	1801.93	1802.00
Pep. E	HC1a Heavy chain (23-38)	**H-AASGFTFSKYWMNWVR-NH2**	29.3	1951.24	1921.31
Pep. F	HC1+2b Heavy chain (39-57)	**H-FRGYWMSWVRQAPGKGLEWVASVKQFFSG-NH2**	44.9	3405.93	3406.04
Pep. G	HC2 Heavy chain (44-68)	**H-GLEWVANIKQDGGERYANSVQGRFT-NH2**	38.5	2796.05	2796.24
Pep. H	HC3 Heavy chain (94-113)	**H-YCARGAARLDYYYGMDLWGQ-NH2**	37.7	2371.66	2371.95

[a]Synthetized by Fmoc/tBu solid phase peptide synthesis (EPS 221, Abimed)

[b]Semi-preparative RP-HPLC purification (UltiMate 3000, Dionex) using a Vydac C4 column

[c]GPMAW software 5.0 (Lighthouse Data, Denmark)

[d]Mass spectrometry analysis by MADI-TOF-MS

2.6.2. Affinity-mass spectrometry and online-bioaffinity-mass spectrometry characterization of Aβ-peptide - CDR-peptides interactions

For the affinity - mass spectrometry experiments, Aβ (1-40) was immobilized on a sepharose matrix through a linker providing flexibility for further affinity binding. All CDR-peptides were synthesized by solid phase peptide synthesis, purified by RP-HPLC and used as stock solutions of 1 µg/µL in trifluoroethanol.

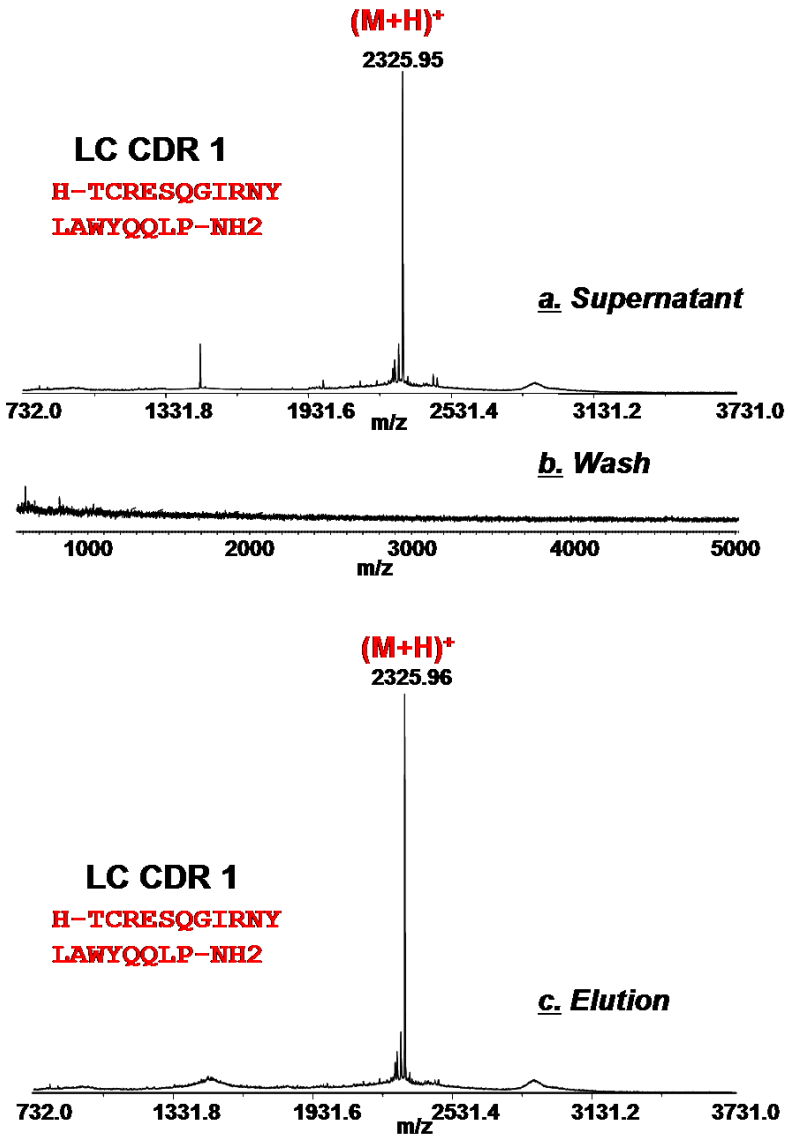

Figure 50. Affinity-MS mass experiment with Aβ-peptide and synthetic light chain CDR-peptide H-TCRESQGIRNYLAWYQQLP-NH2: a. – MALDI-ToF mass spectrum of the supernatant fraction; b. – MALDI-ToF mass spectrum of the last wash fraction; c. – MALDI-ToF mass spectrum of the elution fraction

The peptide was diluted in PBS (pH 7.5) and incubated with the Aβ-matrix. After incubation, the supernatant was collected and the excess was washed away with 50 mL PBS. The complex was dissociated under acidic conditions by performing the elution three times with 0.1 % TFA. After desalting and concentration, the supernatant, last wash and elution fractions were loaded on a MALDI-ToF target and subjected to mass spectrometry analysis. The results of the affinity-MS experiments showed that all synthesized CDR1 and CDR2 peptides, from light and heavy chains, had affinity towards Aβ (1-40); in contrast, the light and heavy chain CDR3 peptides did not bind to Aβ-peptide (

Table **17**).

Furthermore, the interactions between synthetic CDR-peptides and Aβ-peptides were also characterized by the SAW-biosensor system, coupled with an ion trap mass spectrometer. The interface used for on-line coupling of SAW with ESI-MS included a six-port valve unit, a C18-microguardcolumn and micro-injector for desalting and concentration of dissociated ligand samples. Aβ (1-40) was diluted in 7% TFE in PBS fresh before the SAW-affinity-experiments to a concentration of 10µM. Using this solution the Aβ-peptide was immobilized on a gold chip (Figure 51).

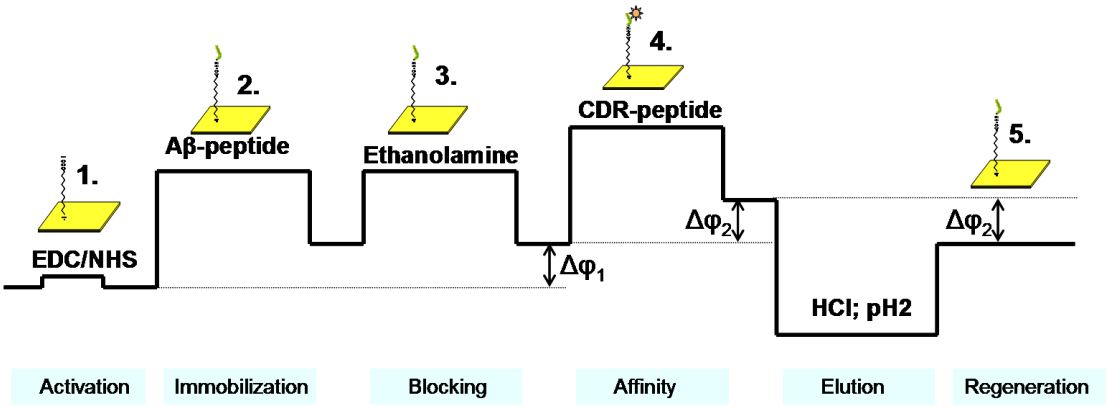

Figure 51- Experimental procedure to characterize the CDR-peptide – Aβ-peptide interaction by SAW- biosensor. 1.- Gold surface of the chip was activated by EDC/NHS; 2. - Aβ peptide was covalently immobilized on the surface and the excess was washed away with PBS; 3. - the free remaining active sites were blocked by ethanolamine; 4. – CDR-peptide was passed through the system and bound to the antibodies; the excess was washed away with PBS. The phase shift

was read; 5. - Elution was performed under acidic conditions and after equilibration with PBS the phase shift was read

A 10 µM solution of synthetic CDR-peptide was added and affinity binding performed at a flow rate of 15 µL per min (the detailed experimental procedure is described in the Experimental Part). Following the binding of the ligand, the elution was carried out with 0.1% TFA and the removal of buffer salts was performed a priori transfer into the ESI source.

The difference in the phase multiplied with the conversion factor $(515 * cm^3)^{-1}$, the exact amount in ng of Aβ peptide immobilized on the gold surface could be calculated in the range of 5.9 pmols/cm^3 to 6.9 pmols/cm^3 in different experiments. Quantification of Aβ-peptide coupled on the surface of the chip was important not only to verify the experiment, but also to calculate the binding ratio of the different CDR-peptides, the amount of which could be also calculated from the phase shift of the affinity experiment. An example of online-SAW-biosensor-mass spectrometry experiment performed with a CDR-peptide is presented in Figure 52. A 10 µM solution of CDR-peptide was initially characterized by ESI-ion trap mass spectrometry (Figure 52a.). The solution was passed through the SAW-biosensor with a gold chip containing Aβ-peptide immobilized on its surface. The peptides that had affinity towards the antibody fragments remained bound to the surface, producing a shift in the phase and amplitude of the wave (Figure 52b.). Elution was performed and the online interface captured the eluted peptides, desalted and concentrated the elution fractions, delivering them directly to the mass spectrometer where another mass spectrum was recorded (Figure 52c.). The phase shifts showed the CDR-peptides that bound to Aβ and the amounts of the CDR-peptide bound to Aβ. The mass of each CDR-peptide bound to Aβ expressed in mols gave the binding stoichiometry of each fragment (listed in Table 17) which in turn provided a comparative affinity towards Aβ for all CDR peptides.

The binding stoichiometry of CDR-peptides to Aβ in SAW-MS experiments, using the same concentration of CDR-peptide (10 µM) showed a higher affinity of light chain peptides containing CDR1 and CDR2. In the case of CDR- peptides containing a Cys residue, the stoichiometry was >1 due to the

dimerization of the peptide during the affinity experiment at pH 7.5. The dimerization of the CDR peptides was confirmed by the ion trap mass spectrum of the elution fraction; an example of such online SAW-MS experiment in which the dimerization of the CDR peptide was observed is presented in Figure 52. To accurately ascertain the binding affinity, the K_D at different ligand concentrations must be calculated.

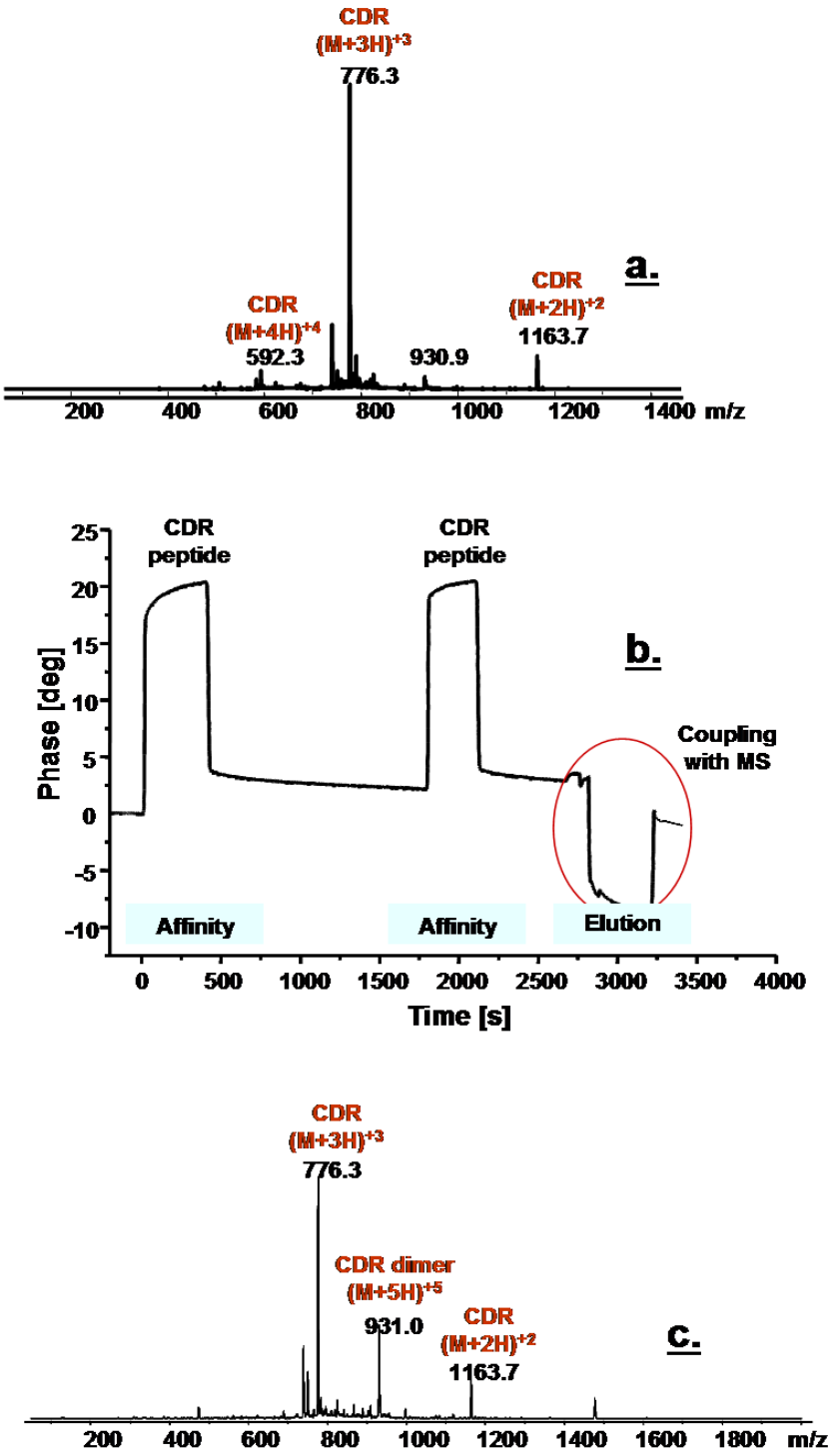

Figure 52. Example of CDR-peptide - Aβ-autoantibody interaction investigated by SAW-MS. a. – Esi-ion trap mass spectrum of CDR-peptide (Peptide B; H-TCRESQGIRNYLAWYQQLP-NH2) before injection on the biosensor chip; b. - Biosensor sensogram with the phase shift registered when the peptide solution passes through cell; c. – Esi-ion trap mass spectrum of the desalted elution showing that CDR-peptide bound to Aβ (1-40) immobilized on the chip.

Table 18. Results of affinity-mass spectrometry experiments with Aβ-peptide and Aβ-autoantibody CDR peptides

No.	CDR peptide position[a]	Sequence	$[M+H]^+_{exp}$[b]	Affinity towards Aβ(1-40) by affinity-MS	Affinity towards Aβ1-40) by SAW-MS Binding stoichiometry
Pep. A	LC1a Light chain (21-37)	H-LSCRASQSVSSNYLWYQ-NH2	1991.38	+	**Yes** **1:1.5**
Pep. B	LC1b Light chain (22-40)	H-TCRESQGIRNYLAWYQQLP-NH2	2325.95	+	**Yes** **1:1.4**
Pep. C	LC2 Light chain (46-59)	H-LIYGASTRATGIP-NH2	1319.66	+	**Yes** **1:0.95**
Pep. D	LC3 Light chain (87-102)	H-YYCQQSYSSQLTFGQ-NH2	1802.00	-	**No** -
Pep. E	HC1a Heavy chain (23-38)	H-AASGFTFSKYWMNWVR-NH2	1921.31	+	**Yes** **1:0.75**
Pep. F	HC Fr.1+2b Heavy chain (39-57)	H-FRGYWMSWVRQAPGKGLEWVASVKQFFSG-NH2	3406.04	+	**Yes** **1:0.43**
Pep. G	HC2 Heavy chain (44-68)	H-GLEWVANIKQDGGERYANSVQGRFT-NH2	2796.24	+	**Yes** **1:0.69**
Pep. H	HC3 Heavy chain (94-113)	H-YCARGAARLDYYYGMDLWGQ-NH2	2371.95	-	**No** -

[a]Synthesized by Fmoc/tBu solid phase peptide synthesis (EPS 221, Abimed)

[b]Mass spectrometry analysis by MADI-ToF-MS

2.6.3. K_D Determination of Aβ - CDR peptides complexes by SAW biosensor

The dissociation constants (K_D) for the synthetic CDR-peptides - Aβ (1-40) complexes were determined using the following experimental system: the Aβ (1-40) peptide was first immobilized on the gold chip; after blocking with ethanolamine, the binding experiments were performed using solutions of CDR-peptides with increasing concentrations (from 50 nM to 100 µM). For further evaluation, the resulting curves were exported into Origin software and the integrated FitMaster function was applied. The resulting overlay plot and individual fitting is following with a 1:1+residue - binding model. The pseudo-first order kinetic constants k_{obs} were calculated with FitMaster and plotted versus the concentrations of the CDR-peptides. An example of K_D determination of a CDR-peptide - Aβ-peptide complex is shown in Figure 53 (peptide E, H-AASGFTFSKYWMNWVR-NH2). A linear best fit was applied using the equation $K_{obs} = k_{off} + k_{on} * C$. The K_D value was determined from $K_D = k_{off} / k_{on}$ and the results are listed in Table 19.

Light chain CDR peptides1 and 2 have a K_D value situated in low micromolar range, while CDR 3 synthetic peptide is not binding at all to Aβ-peptide. The heavy chain CDR peptides 1 and 2 have a K_D also in low micromolar range, while the frame containing peptide and CDR 3 present a lower affinity towards Aβ-peptide. Although the size of the synthetic peptides is quite small comparing to the entire Aβ-autoantibody molecule and the 3D structure is not as rigid and fix as an immunoglobulin, their K_D are comparable, leading to the conclusion that these synthetic CDR 1 and CDR2 peptides from both light and heavy chains have the potential to be used as lead structures in future studies as Aβ binding molecules used in the treatment of AD.

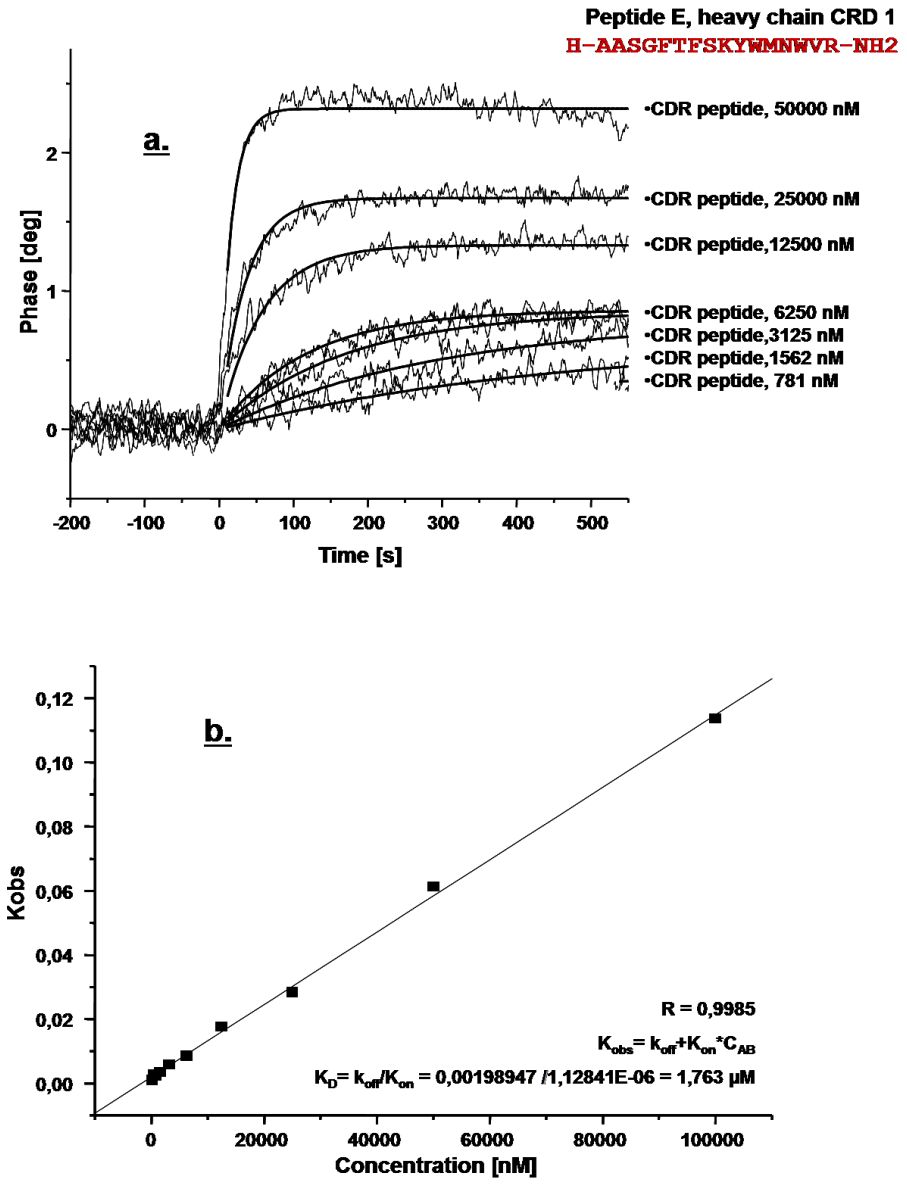

Figure 53. K_D determination of CDR-peptide - Aβ-peptide complex: a. - The fitted curves of the increased binding concentrations; b. - Pseudo first-order kinetic constant plotted versus concentration. The linear regression was applied for K_D of 1,76 µM.

Table 19. Kinetic rate and equilibrium dissociation constants of synthetic CDR peptides of Aβ-autoantibody and Aβ-peptide:

No.	CDR peptide position[a]	Sequence	kon (nM^{-1} sec^{-1})	koff (sec^{-1})	KD (μM)
Pep. A	LC1a Light chain (21-37)	H-LSCRASQSVSSNYLWYQ-NH2	2169E-05	1,12E-05	1,936
Pep. B	LC1b Light chain (22-40)	H-TCRESQGIRNYLAWYQQLP-NH2	2806 E-05	1,48E-05	1,895
Pep. C	LC2 Light chain (46-59)	H-LIYGASTRATGIP-NH2	1484E-05	1,12E-05	1,325
Pep. D	LC3 Light chain (87-102)	H-YYCQQSYSSQLTFGQ-NH2	Negative	53,8E-05	-
Pep. E	HC1a Heavy chain (23-38)	H-AASGFTFSKYWMNWVR-NH2	317E-05	0,15E-05	2,113
Pep. F	HC Fr.1+2b Heavy chain (39-57)	H-FRGYWMSWVRQAPGKGLEWVASVKQFFSG-NH2	4349 E-05	0,31E-05	14,029
Pep. G	HC2 Heavy chain (44-68)	H-GLEWVANIKQDGGERYANSVQGRFT-NH2	40227E-05	17,1E-05	2,352
Pep. H	HC3 Heavy chain (94-113)	H-YCARGAARLDYYYGMDLWGQ-NH2	1514E-05	0,28E-05	5,426

[a]Synthesized by Fmoc/tBu solid phase peptide synthesis (EPS 221, Abimed)

[b]Mass spectrometry analysis by MADI-ToF-MS

3. EXPERIMENTAL PART

3.1. Materials and reagents

In this work the following commercially available materials were used: protein Cards Whatman (Germany); 96 well Optiplate black: Perkin Elmer; Low binding test tubes: Sigma Aldrich; Omix Pipette Tips C4 and C18: Varian, Inc.;

In this work the following commercially available reagents (of analytical grade or highest available purity) were used: NHS-activated Sepharose (*Sigma Aldrich*), Coomassie Brilliant Blue G250 (*Sigma Aldrich*), Tween 20 - Polyoxyethylensorbitanmonolaureat (*Sigma Aldrich*), diethanolamine (*Sigma Aldrich*), HCCA - α-cyano-4-hydroxycinnamic acid (*Sigma Aldrich*), deionised water (*Millipore*), Hydrochloric acid (*Sigma Aldrich*), sodium hydroxide (*Merk*), Trypsin (*Promega*), t-buthyl-methyl-ether (*Fluka*), DMF - dimethylformamide (*Fluka*), NMM - N-Methylmorpholine (*Fluka*), piperidine (*Fluka*), trifluoroacetic acid (*Fluka*), TES - triethylsilane (*Fluka*), DHB - dihydroxybenzoic acid (*Fluka*), N-α-protected amino acids (*NovaBiochem*), TRG resins (*NovaBiochem*), PyBOP (*NovaBiochem*).

3.2. Buffers and stock solutions

Table 20. Composition of buffers and stock solutions used in presented work

No.	Buffer	Solution Composition
1	SDS-PAGE sample buffer	4% SDS 25% Glycerin 50 mM Tris 0.02% Coomasie 6M Urea pH 6.8
2	SDS-PAGE separation gel	0.5 M Tris 0.4% SDS pH 6.8
3	SDS-PAGE stacking gel	1.5 M Tris 0.4% SDS

		pH 8.8
4	SDS-PAGE running buffer	25 mM Tris 192 mM glycine 0.1% SDS
5	Buffer A for Coomassie staining	10% NH_4SO_4 2% H_3PO_4
6	Coomassie Blue Staining Solution	20% methanol 0.1% Coomassie brillant blue G-250 in Buffer A
7	Fixing solution	30% ethanol 10% acetic acid
8	PBS ELISA	5 mM Na_2HPO_4 x 2 H_2O 150 mM NaCl pH 7.5
9	High ionic strength PBS	5 mM Na_2HPO_4 x 2 H_2O 136 mM NaCl 2.7 mM KCl 0.01 % NaN_3 pH 7.5
10	Affinity column coupling buffer	500 mM NaCl 200 mM $NaHCO_3$ pH 8.3
11	Affinity column blocking buffer	500 mM NaCl 100 mM Ethanolamine pH 8.3
12	Affinity column washing buffer	500 mM NaCl 200 mM CH_3COONa x 3 H_2O pH 4
13	Solvent A for HPLC	0.1% TFA in H_2O
14	Solvent B for HPLC	80% ACN 0.1% TFA in H_2O
15	MALDI solvent	ACN/ 0.1% TFA in H_2O (2:1)
16	Aβ-peptide stock solutions	1 mg/mL inTFE
17	SPPS base solution	1.3 NMM inDMF
18	SPPS activation solution	0.9 M PyBOP in DMF
19	SPPS deprotection solution	2% piperidine; 2% DBU in DMF
20	SPPS cleavage solution	90% TFA 5% TIPS 5% MilliQ
21	Enzyme solution	12 ng/uL in buffer
22	Matrix solution for MALDI-FTICR	100 uM of 2,5 DHB in MALDI solvent
23	Matrix solution for MALDI-ToF	Saturated solution of HCCA in MALDI solvent
24	Solvent A for HPLC	2 % HCOOH in H_2O
25	Solvent B for HPLC	2 % HCOOH in AcCN

26	SAM solution	10 uM 16-mercaptohexadecanoic acid in $CHCl_3$
27	SAW activation solution	50 mM NHS 200 mM EDC in buffer
28	SAW blocking solution	1 M ethanolamine
29	Piranha solution	H_2O_2/H_2SO_4 (1:1, vol.)

3.3. Solid phase peptide synthesis

SPPS (Solid phase peptide synthesis) is used for the synthesis of peptides and small proteins. The C-terminal amino acid is attached to a solid support via an acid labile bond with a linker molecule. The resin is insoluble in the solvents used for synthesis, making it relatively simple and fast to wash away excess reagents and by-products. The solid support is a synthetic polymer with reactive groups which react covalently with the carboxyl group of an N-α-protected amino acid. The amino protecting groups can then be removed and a second N-α-protected amino acid can be coupled to the attached amino acid. These steps are repeated until the desired sequence is obtained [82, 83, 85.].

The peptides were synthesized manually and semi-automatically (with a semi-automated peptide synthesizer EPS 221 from Abimed, Germany) on NovaSynTGR resin (0.23 mmol/g loading capacity) in accord to Fmoc/tBu strategy, on a 50 µM scale, using a double coupling method (60 min/coupling, 19 min/deprotection).

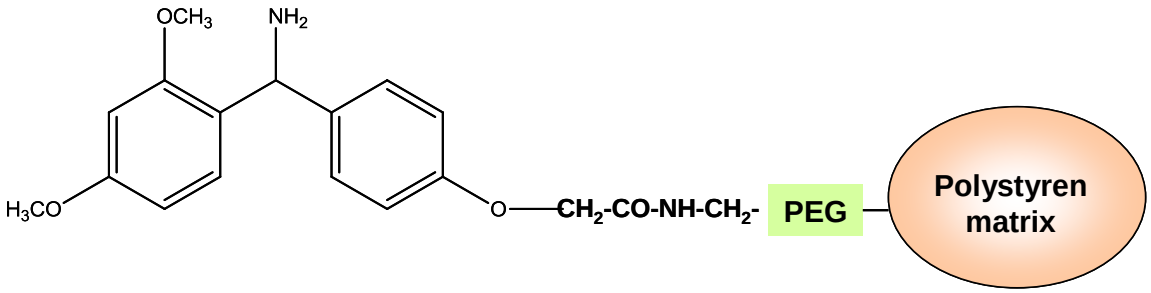

Figure 54. Structure of NovaSynTGR resin

The resin was first swelled with DMF for 30 minutes to reach the maximum volume and to assure the entire surface accessibility.

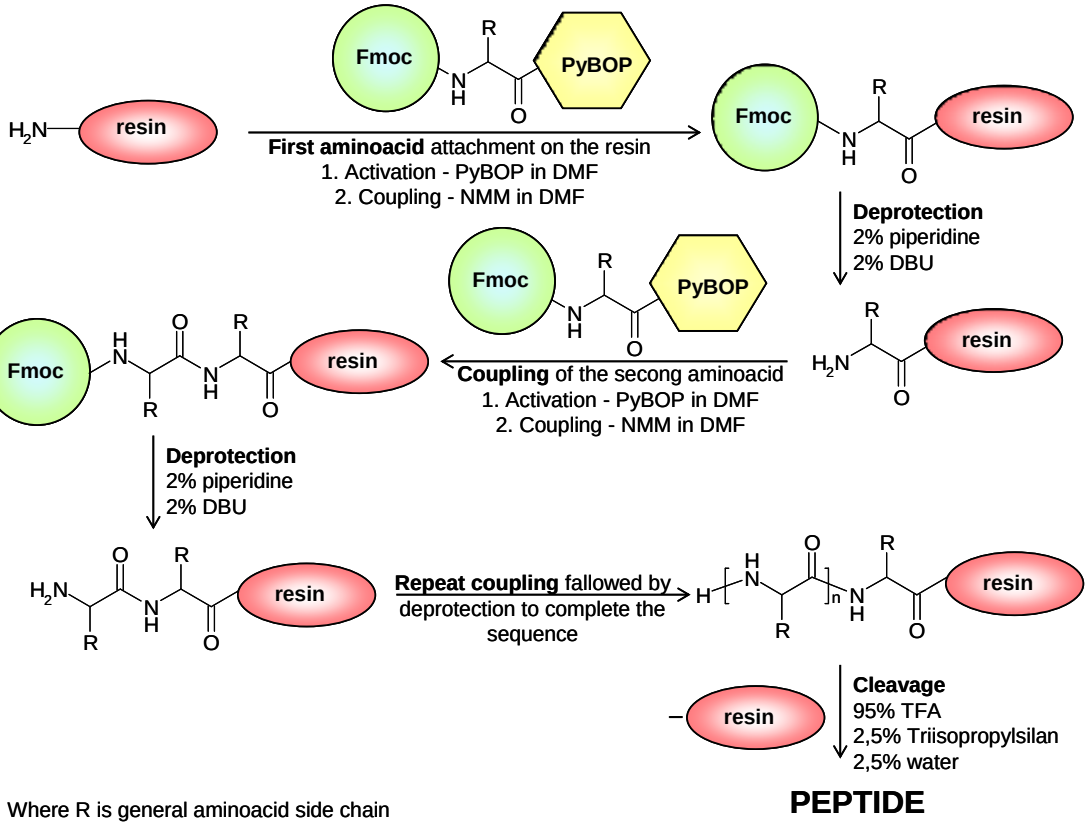

Figure 55. Fmoc solid phase peptide synthesis.

Solutions needed for peptide synthesis: A. - deprotection solution: 2% piperidine, 2% DBU in DMF; B. - activation solution: PyBop in DMF 0.9 M; C. - base solution: NMM in DMF 1.3 M; D. - washing solution: DMF. Every amino acid cycle followed next steps: a. - washing (4times with DMF, 2 ml each); b. - deprotection 19 minutes (4 steps 5/10/2/2 min); c. - washing (10 times with DMF, 2 ml each); d. - coupling (60 min with 280 µL activation solution + 126 µL base solution + 300 µL DMF + 5 times amino acid excess); e. - washing (10times with DMF, 2 ml each); f. - coupling (60 min with 280 µL activation solution + 126 µL base solution + 300 µL DMF + 5 times amino acid excess); g. - washing (10times with DMF, 2 ml each) - end of cycle.

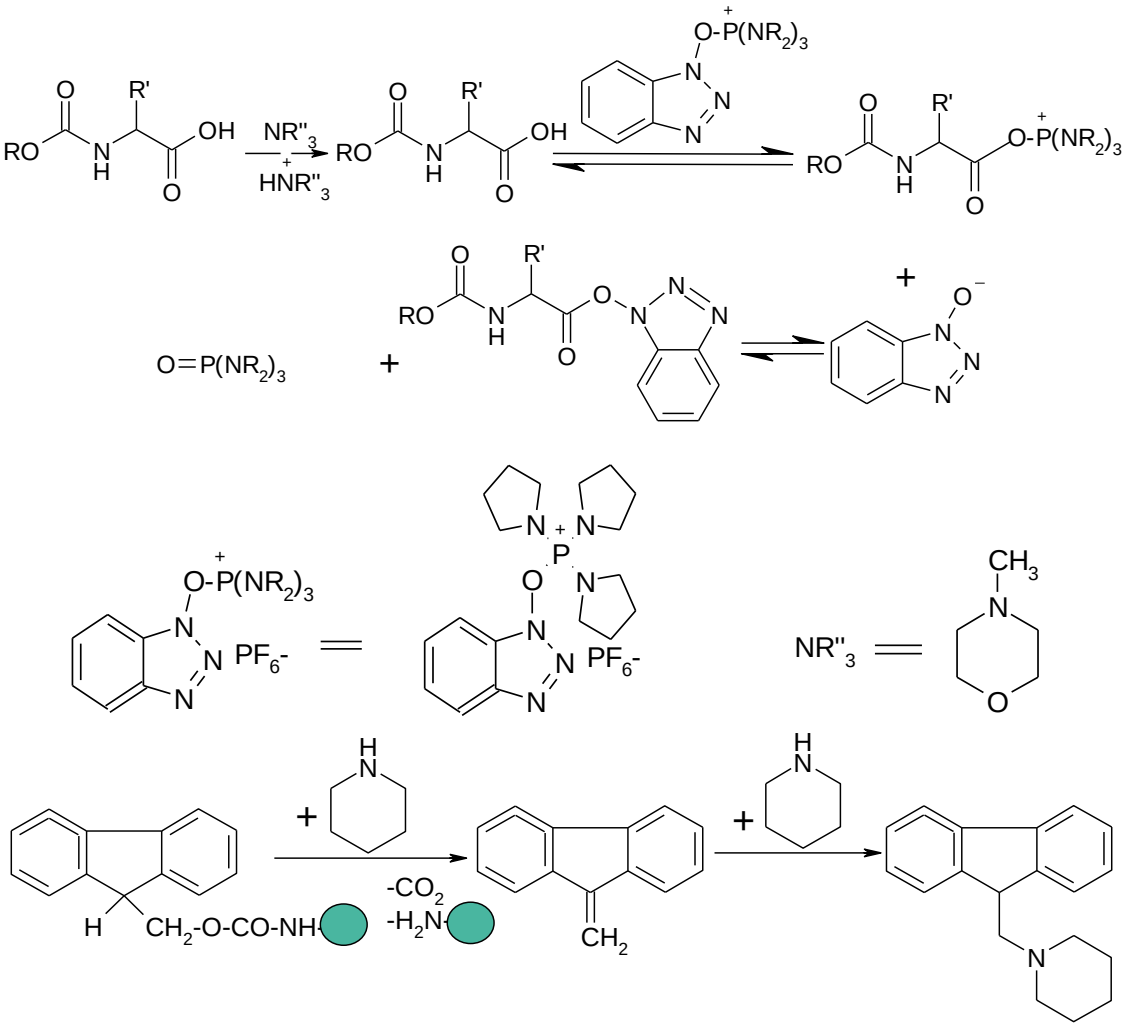

Figure 56. PyBOP activation of the amino acids in basic conditions before coupling in solid phase peptide synthesis

The amino acids used: N-α-Fmoc-L-alanine (Fmoc-Ala-OH), N-α-Fmoc-S-trityl-L-cysteine (Fmoc-Cys(Trt)-OH), N-α-Fmoc-L-aspartic acid-β-t-butylester (Fmoc-Asp(OtBu)-OH), N-α-Fmoc-L- glutamic acid-γ-t-butylester (Fmoc-Glu(OtBu)-OH), N-α-Fmoc-L-fenyl-alanine (Fmoc-Phe-OH), N-α-Fmoc-glycine (Fmoc-Gly-OH), N-α-Fmoc-N-im-trityl-L-histidin (Fmoc-His (Trt)-OH), N-α-Fmoc-L-izoleucine (Fmoc-Ile-OH), N-α-Fmoc-N-ε-t-Boc-L-lisine (Fmoc-Lys(Boc)-OH), N-α-Fmoc-N-β-trityl-L-asparagin (Fmoc-Asn(Trt)-OH), N-α-Fmoc-L-proline (Fmoc-Pro-OH) N-α-Fmoc-N-γ-trityl-L-glutamin (Fmoc-Gln(Trt)-OH), N-α-Fmoc-NG-(2,2,4,6,7-

pentametildihidrobenzofuran-5-sulfonil)-L-arginin (Fmoc-Arg(Pbf)-OH), N-α-Fmoc-O-t-butil-L-serine (Fmoc-Ser(tBu)-OH), Nα-Fmoc-L-valine (Fmoc-Val-OH), N-α-Fmoc-O-t-butil-L-tirozine (Fmoc-Tyr(tBu)-OH), N-α-Fmoc-L-metionine (Fmoc-Met-OH) (GL Shangai Lt, Shangai, China).

For the final cleavage 2.5 mL cleavage solution (90 % TFA, 5 % TIPS, 5 % MilliQ) for each 100 mg resin were needed. The resin was incubated at room temperature for 2 h, and then the peptides were precipitated with diethyleter at -28°C for 1 h. The precipitate was filtered and washed on the filter with 50 mL diethylether. At the end it was diluted with 100% acetic acid and lyophilized. The crude peptides were purified by reverse phase-high performance liquid chromatography (RP-HPLC) on a preparative or semipreparative C_4 or C_{18} columns (Vydac) depending on their hydrophobicity. Purified peptides were characterized by analytical RP-HPLC and mass spectrometry.

3.4. Isolation of Aβ-autoantibody from serum IVIG

3.4.1 Preparation of Aβ affinity columns for the isolation of Aβ-autoantibody

Because Aβ (12-40) contains two lysine residues, a special protocol was laid down for the purification column, using a cysteine attached at the N-terminal end of the peptide. This cysteine gave a similar orientation of the peptide molecule on the column matrix after immobilization. The matrix activated with azlactone contains an iodo-acetyl group (UltraLink; Perbio, Bonn, Germany) at the end of 15 carbon atoms spacer which reacts with the sulfhydryl of the cysteine to produce a stable covalent bound, thioetheric type. The spacer is used to produce a steric flexibility of the antibody-antigen interaction.

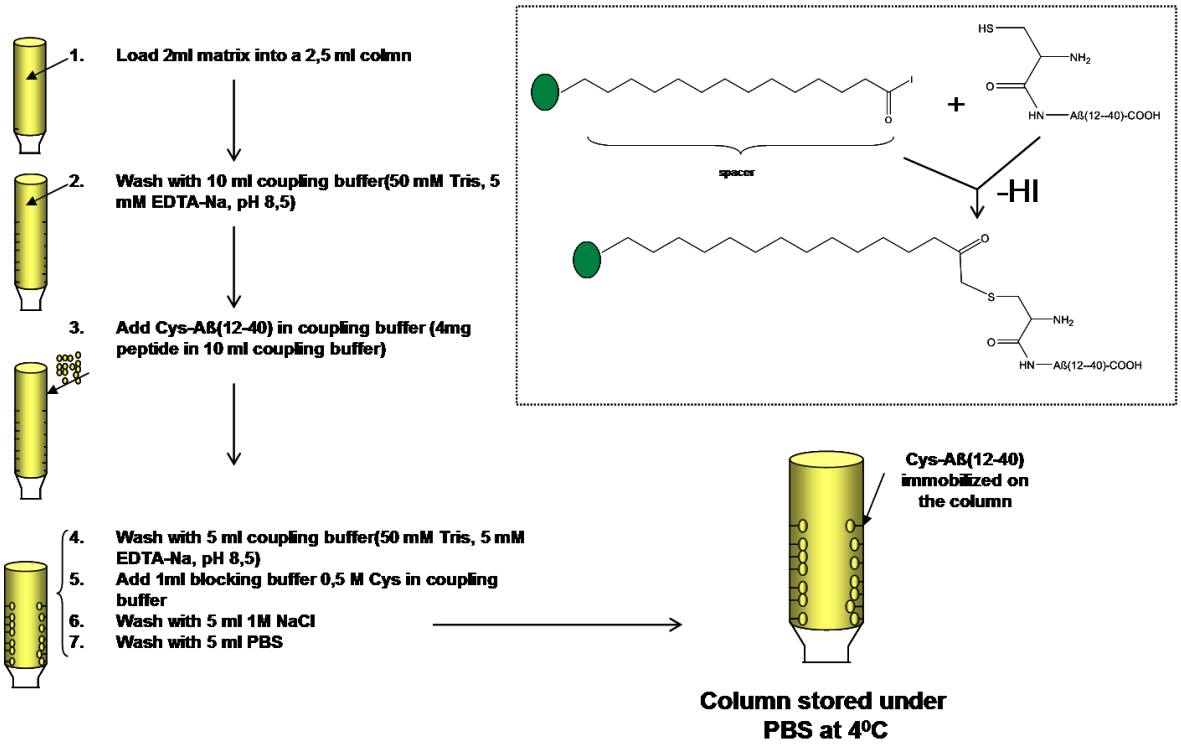

Figure 57. Column preparation for the isolation of Aβ-autoantibody. The matrix is loaded on a column and coupling buffer (pH 8.5) and Cys-Aβ-(12-40) are added. The column is incubated for 16 h at 4 °C and then washed alternatively with coupling and blocking buffer and at the end with PBS and stored at 4 °C. In medallion: specific reaction between iodo – acetyl group of the spacer and sulfhydric group of the N-terminal cysteine.

2 mL slurry matrix (UltraLink; Perbio, Bonn, Germany) were loaded into a 2,5 mL syringe. The liquid was pushed out and washed with 5 mL coupling buffer (50 mM tris, 5 mM EDTA-Na, pH 8.5). 4 mg Cys-Aβ(12-40) were solved in coupling buffer and added on the column. The peptide was added in high quantity due to the competition reaction between the matrix formation reaction and the dimerization of the peptide. The coupling reaction was performed at room temperature for 30 minutes under gentle mixing, followed by 30 minutes without mixing. The free iodoacetyl groups were blocked with 5 mL solution of 0.5 M L-cysteine in blocking buffer. The blocking solution was washed out with 5 mL 1M NaCl and the matrix was equilibrated with 5 mL PBS. The column was stored under PBS at 4 °C.

3.4.2. Affinity isolation of Aβ-autoantibody

0.5 mL of the Cys-Aβ(12-40) coupled support was packed into a column (2.5 mL, MoBiTec, Göttingen, Germany) and equilibrated with 20 mL PBS (0.1 M sodium phosphate, 0.15 M NaCl, pH 7.2). The support was transferred into a 15 mL Falcon vial using 5 mL PBS and mixed with 12.5 mg IVIg (Calbiochem) dissolved in 5 mL PBS. The diluted gel slurry was slowly rotated overnight (16h) at 4°C. The suspension was transferred to a column using the effluent to completely rinse the matrix back into the column. The column was washed four times with 10 mL of PBS followed by 4 wash cycles with 10 mL 5 mM Na_2HPO_4, 150 mM NaCl, pH 6.8 and two wash cycles with water (MilliQ). The affinity-bound antibodies were eluted from the column with 10 x 0.5 mL 0.1% TFA (aqueous solution, pH 2). The IgG preparation for the following experiments was performed using two different protocols. To regenerate the column, the matrix was washed with 10 mL 0.1% TFA and 40 mL of PBS.

3.4.3. Quantification of Aβ-autoantibody by BCA assay

Antibody concentration in the elution fractions was determinate by micro-BCA protein assay (Thermo Fisher Scientific, Rockford, IL, USA). BCA Protein Assay is based on bicinchoninic acid (BCA) for the colorimetric detection and quantization of total protein[116.]. The bovine serum albumin (BSA) stock solution of 2 mg/ml received in the Micro BCA™ Kit was used to prepare 150 µL fresh standard dilutions into the concentrations range 40-0.5 µg/ml and then to make a standard curve. From each antibody fraction 15 µL were taken and diluted with buffer to a final volume of 150 µL (vol. dilution 1:10). On top the standard dilutions and fraction dilution, 150 µL coloring buffer containing Cu^{2+} ions was added. Coloring reagent is a mixture of reagent A (sodium carbonate, sodium bicarbonate, bicinchoninic acid and sodium tartrate in 0.1 M sodium hydroxide) plus reagent B (4% cupric sulfate) in a ratio 50:1. The reaction was incubated for 1h at 60 °C, changing the solution color from green to purple. The

samples were loaded into an ELISA 96 well plate and measured with a Victor 2 (PerkinElmer) plate reader equipped with a 562 nm filter. The fraction concentration was established by plotting the results into the standard curve and multiplying by a factor of 10.

Table 21. Preparation of diluted BSA standard curve

	Concentration (µg/mL)	BSA stock (µL)	Buffer (µL)
A	200	25	225
B	40	200 A	800
C	20	150 B	150
D	10	150 C	150
E	5	150 D	150
F	2.5	150 E	150
G	1	150 F	150
H	0.5	150 G	150
I	0	-	150

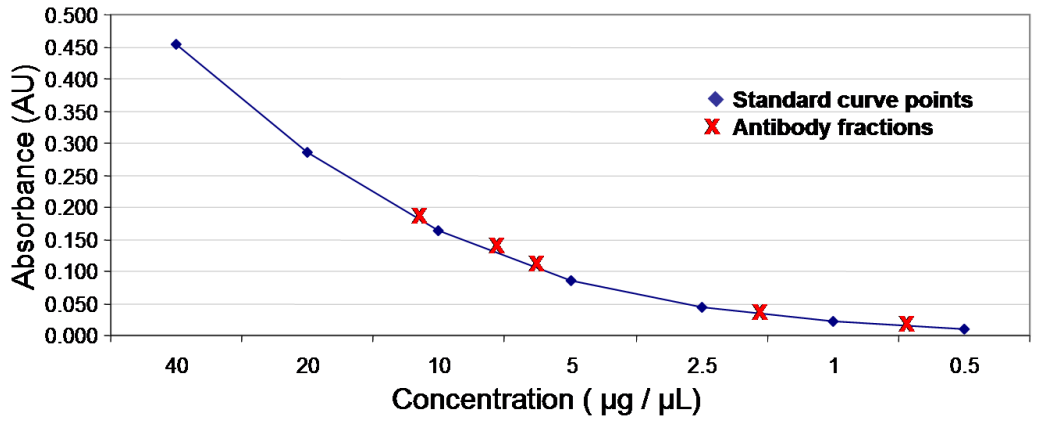

Figure 58. BSA standard curve obtained by plotting the OD (562 nm) measurement for each BSA standard vs. its concentration in µg/mL.

3.5. Chromatographic and electrophoretic separation methods

3.5.1. High performance liquid-chromatography (HPLC)

Biomolecules possessing characteristic mass, shape and surface charge, may also differ from each other in terms of their hydrophobicity. Also

soluble proteins will often possess regions of their structure which are rather hydrophobic. These regions depend on the primary structure of the protein and may be used to separate otherwise very similar proteins or peptides. When passed through stationary phase with immobilized hydrocarbon chains, sample components bind to these chains as a result of these hydrophobic parts of their structure. This is the basis of reversed-phase chromatography (RP-HPLC).

Analytical RP-HPLC was performed on a Bio-Rad instrument (Bio-Rad Laboratories, Richmond, CA) and on UltiMate 3000 system (Dionex, Germering, Germany), equipped with LPG-3400A pumps using: a - Vydac C4 column (250 × 4.6 mm I.D.) with 5 µm silica (300 Å pore size) (Hesperia CA) or b - analytical Nucleosil 300-7 C18 column (250 × 4 mm I.D.) with 7 µm silica and 300 Å pore size (Macherey-Nagel, Düren, Germany) as a stationary phase. It was used at a flow rate of 1 mL/min and peptides were detected at 220 nm, employing the VWD-3400 variable wavelength detector of the UltiMate system, with a flow cell of PEEK, 0.4 mm long and an internal volume of 0.7 µL. For synthetic peptides linear gradient elution (0 min 0% B; 5 min 0% B; 50 min 90% B) with eluent A (0.1% TFA in water) and eluent B (0.1% TFA in acetonitrile- water,80:20, v/v). For the separation of light or heavy chain tryptic peptides, the following gradient was used: 0 min 0% B; 5 min 0% B; 135 min 65% B, 150 min 100% B, 160 min 100% B, 160 min 0% B.

Crude peptides were purified by RP-HPLC. Preparative purification of the peptide was carried out on a Knauer HPLC system (Knauer, Berlin, Germany) using a preparative Vydac C_4 column (250 × 20 mm, 10 µm, 120 Å; Vydac, Hesperia, CA) or a C18 column (GROM-SIL 120 ODS-4 HE, 10 µm, 250 x 20 mm, pore size 120 Å; Herrenberg-Kayh, Germany). Semipreparative purification of the peptide was carried out on a Dionex HPLC system (Dionex, Germany) using a preparative Vydac C_4 column (250 × 10 mm, 15 µm, 120 Å; Vydac, Hesperia, CA). Linear gradient elution (0 min 20% B; 5 min 20% B; 65 min 85% B) was employed using

the same mobile phases as described above, with a flow rate of 3 to 10 mL/min. The peak detection was performed at 220 nm.

3.5.2. ZipTip desalting

Desalting ZipTip procedure was performed using ZipTip® C18 and C4 pipette tips from Omix (Varian) and from Millipore[117.]. The ZipTip pipette tip was a 10 µL pipette tip with a bed of chromatography media fixed at its end. The C4 or C18 reverse phase media is used for desalting and concentrating peptide and protein samples. ZipTip C18 pipette tips are most applicable for peptides and low molecular weight proteins (under 50 kDa), while ZipTip C4 pipette tips are most suitable for low to intermediate molecular weight proteins (also over 50 kDa). The procedure contains five steps: a.- wetting of the ZipTip pipette tip; b.- equilibration of the ZipTip pipette tip, c.- binding of the peptides and/or proteins to ZipTip pipette tip, d.- washing and e.- elution. For these steps the solutions are listed in the following table.

Table 22. Solutions required for use with ZipTip pipette tips containing C18 media.

ZipTip procedure step	Solution needed
Wetting	50% ACN in MilliQ water
Equilibration	0.1% TFA in MilliQ water
Sample preparation	0.1% TFA in MilliQ water
Washing	0.1% TFA in MilliQ water
Elution	0.1% TFA / 80% ACN

3.5.3. 1D-gel electrophoresis

Electrophoresis is based on the migration of positively or negatively charged molecules into an electric field and is applied in analytical studies of proteins. Biopolymers such as proteins and nucleic acids are folded into compact tri-dimensional structures held together by a variety of non-

covalent, ionic interactions such as hydrogen bonding and salt bridges. These ionic interactions are disrupted by denaturation, a treatment used before electrophoretically separate the biopolymers in structural studies. SDS-PAGE (polyacylamide-gel electrophoresis) was performed according to Laemmli method. The detergent SDS consists of a hydrophobic 12-carbon chain and a polar sulfated head. The hydrophobic chain can intercalate into hydrophobic parts of the protein disrupting its compact folded structure. Additionally, SDS coats proteins with a uniform layer of negative charges which causes them to migrate towards the anode when placed in an electrical field, regardless of the net intrinsic charge of the proteins. The unique dimension remaining in the SDS-PAGE analysis is the mass of the analyte [118., 119.].

The gels were prepared using the mini-gel instrument MiniProtean from BioRad. In the next table are presented the solutions for SDSPAGE separation and stacking gels.

Table 23. Solution needed for a SDS-PAGE with 1mm – thick gel.

Solution	**Gel concentration**	
	5%	**10%**
Stacking gel buffer	2.5 mL	-
Separation gel buffer	-	6 mL
Milli Q	5.8 mL	10 mL
Acrylamide solution	1.7 mL	8 mL
APS (a)	85 µL	125 µL
TEMED (b)	20 µL	20 µL

(a) 10% Ammonium peroxydisulfate

(b) N',N',N',N'- tetramethylethylenediamine

Prior to SDS-PAGE, all antibodies used in the present work were treated as follows: antibody aliquots (200-400 µg) were incubated with DTT solution with a molar excess of 10000 vs antibody quantity for 2.5 hours at 37°C. Subsequently, iodoacetamide was added to a final DTT/IAA molar ratio of 1:3, and the reaction mixture was incubated for one additional hour

at room temperature before loading lyophilization. The reduced and alkylated antibodies were reconstituted in running buffer. The Power/PAC 1000 instrument from Bio-Rad at constant current in two steps was used for SDS-PAGE: a) 60 V when the samples were in the stacking gel and b) 120 V when the sample was in the separating gel. The molecular weights of unknown proteins were estimated by running standard proteins of known molecular weights from 14 to 67 kDa in the same gel. Afterwards the gels were a. - stained by Coomassie blue or b. - transferred on the PVDF membranes to perform Edman sequencing analysis.

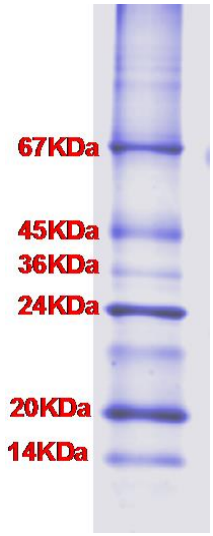

Figure 59. Molecular weight marker- PageRulerTM Unstained Protein Ladder (Fermentas) [120.]

a. Colloidal Coomassie Brilliant Blue staining. After PAGE, the gels were shacked overnight immersed in Coomassie staining solution. Further, the gels were washed with 25% methanol and scanned with GS-710 Calibrated Imaging Densitometer from BIO-RAD. Colloidal Coomassie blue staining has a detection limit of 0.1 to 1 μg protein/spot. This procedure is based on the binding of the dye Coomassie Brilliant Blue G-250, which binds non-specifically to virtually all proteins in acid solution. This binding results in a spectral shift from reddish / brown (λ= 465 nm) to blue (λ= 610 nm). The protein-Coomassie complex absorbs at 595 nm, and this wavelength is optimal for spectral determination to measure the

blue color from the Coomassie–protein complex. Coomassie Blue binds roughly stoichiometrically to proteins, so this staining method is well suited for densitometry determinations. The proteins are detected as blue bands on a clear background, after fixing the gel with TCA for obtaining maximum sensitivity [121.] .

To overcome the lengthy procedure of Colloidal Coomassie blue staining, a shorter protocol has been employed, which is based on the binding of the dye Coomassie Brilliant Blue R-250 (CBB R-250) to proteins. This dye differs from Coomassie Brilliant Blue G-250 by the lack of two methyl groups. This method is faster and compatible with mass spectrometry.

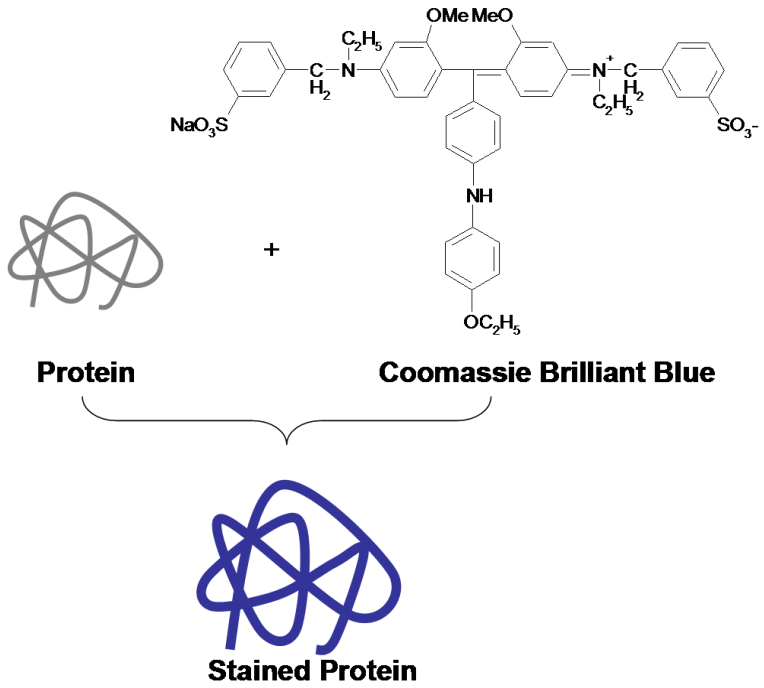

Figure 60. Scheme of protein staining with Coomassie blue

First the gel was shacked in Coomassie staining solution (50% methanol, 10% acetic acid, 0.05% CBB R- 250) for 10 min at 25°C and then 30 min at 60°C. Then the gel was shacked in distaining solution (30% methanol, 10% acetic acid) for 30 min at 25°C. This last step was repeated until the best contrast was achieved.

b. Blotting on a PVDF membrane. The term “blotting” refers to the transfer of biological samples from a gel to a membrane and their subsequent detection on the surface of the membrane [122.]. The gel is placed on a PVDF membrane and the two are covered ("sandwiched") with blotting paper and placed in the blotting setup were a current is applied. Proteins are migrating from cathode to anode, from the gel into the membrane.

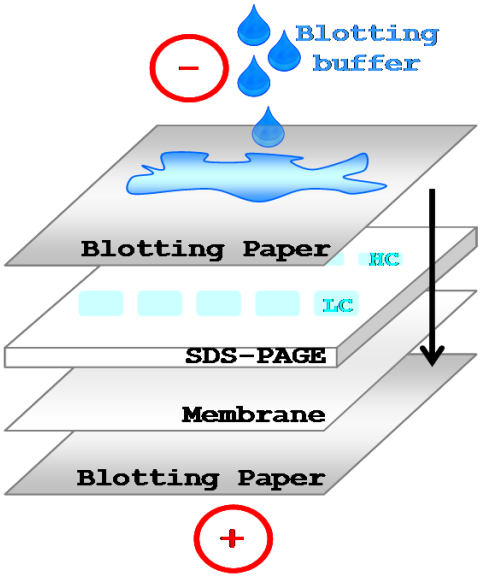

Figure 61 Protein blotting with a wet transfer unit.

One-dimensional gels containing light and heavy chain bands were transferred on PVDF membranes using a wet-transfer procedure (70 V, 2 h). The transfer was performed with Towbin buffer: 25 mM Tris, 192 mM Glycine, 20 %, methanol, 0.1 % SDS, pH 8.3 (gel and membrane were also soaked in this buffer, before applying them inside the transfer sandwich).

3.6. Edman sequencing

Automated amino acid sequence analysis was performed on an Applied Biosystems Model 494 Procise Sequencer attached to a Model 140C Microgradient System, a 785A Programmable Absorbance Detector and a

610A Data Analysis System. All solvents and reagents used were of highest analytical grade purity (Applied Biosystems. For sequencing both blotted and lyophilized samples the corresponding standard pulsed liquid methods were used. Edman degradation occurs in three stages, amino acid residues can therefore be sequentially removed from the N-terminus of a polypeptide in a controlled stepwise fashion [123.].

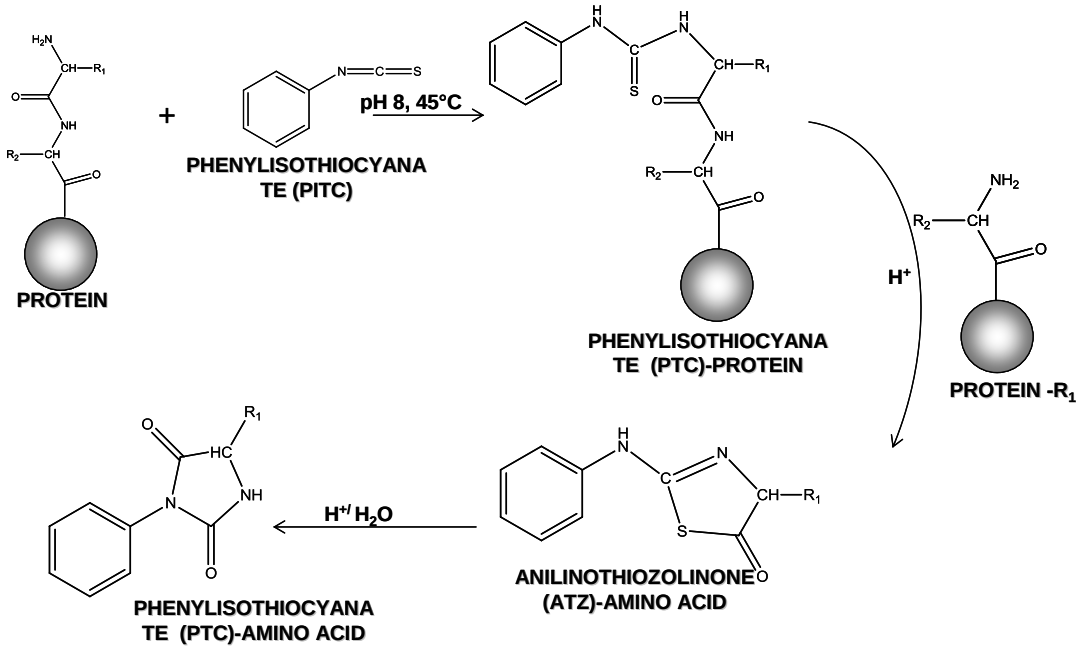

Figure 62. Edman degradation in 3 steps with different reaction conditions: 1) mildly alkaline conditions; 2) anhydrous hydrofluoric acid; 3) aqueous acid.

The phenyl isothiocyanate (PITC) reacts with the N-terminal amino groups of proteins under mildly alkaline conditions to form their phenylthiocarbamyl (PTC) adduct. This product is treated with anhydrous hydrofluoric acid, which cleaves the N-terminal residue as its thiazolinone derivative but does not hydrolyze other peptide bonds. The thiazolinone-amino acid is selectively extracted into an organic solvent and by treatment with aqueous acid is converted to the more stable phenylthiohydantoin (PTH) derivative that can be identified by RP-HPLC with detection at 270 nm. The sequencing experiments were performed by Adrian Moise and Marius Ionut Iurascu, Laboratory of Analytical Chemistry

and Biopolymer Structure Analysis, department of Chemistry of the University of Konstanz.

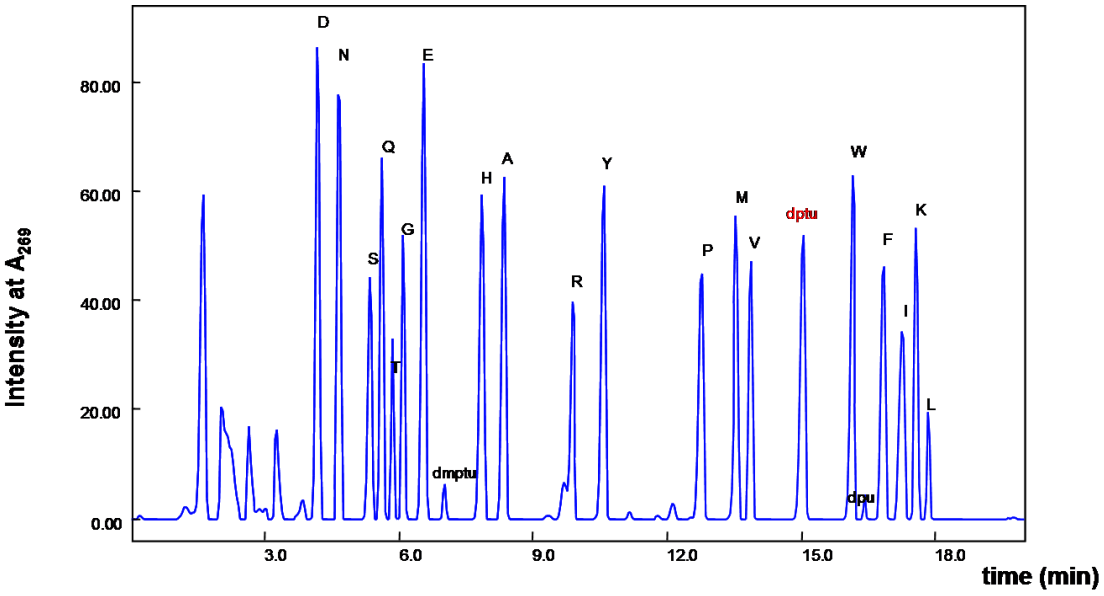

Figure 63. Standard chromatogram for phenylthiohydantoin (PTH) derivatives standards registered at RP-HPLC with detection at 270 nm.

a. Preparation of blotted samples for sequencing

Staining solution: 0.1 % Coomassie Brilliant Blue R-250 in 40 % methanol in water. Distaining solution: 50 % methanol in water, prepared freshly before use. After transfer the PVDF membrane was washed with water for 15 minutes then with methanol for 5-10 seconds and incubated the in staining solution until spots are visible. The membrane was then destained in distaining solution until the background decreases and the spots were clearly visible. The membrane was air-dried. The spots of interest were cut and fully distained. After distaining the spots were dried and kept at 4 degrees in Eppendorf tubes. For sequencing, the distained protein spots were wetted with 100 % methanol and applied in the sequencing cartridge.

b. Preparation of HPLC fractions for sequencing

Lyophilized HPLC fractions were dissolved in 20 µL 20 % ACN, 0.1 % TFA. The solved sample was applied on glass fiber filters (Applied Biosystems) in aliquots of 5 µL, each application followed by drying under a stream of argon (in order to assure a distribution as close to the centre of the glass fiber filter as possible).

3.7. Proteolytic digestion of Aβ-autoantibody polypeptide chains

Proteases used in the present work have different substrate specificities and cleave preferentially different peptide bonds. For example trypsin cleaves at the C-terminal bonds of lysine (Lys) and arginine (Arg) residues (basic amino acids), but has a preference for Arg particularly at high pH values. In the sequences Arg-X, Lys-X, cleavage is inhibited if there is a proline (Pro) residue at positionX; Glu-C cleaves mostly at the C-terminus of acidic amino acids; Lys-C at the C-terminal of lysine[124.].

All serine proteases (e.g. trypsin, Lys-C) have the same general mechanism, which involves into the reaction three specific amino acids known as the catalytic triad: histidine 57, aspartate 102 and serine 195 residues. The peptide substrate molecule attaches to the catalytic site of trypsin (or other serine protease) by binding of its hydrophobic group to a specific non-polar pocket such as the carbonyl carbon atom of the peptide bond to be attached which is close to the serine-OH. The hydrogen atom of the serine transfers to the histidine nitrogen atom and the oxygen atom forms a bond with the carbonyl atom of the substrate.

Table 24. The endo-proteases and their specific cleavage sites.

Protease	**Cleavage site**
Trypsin	Specific after K, R not before P
Lys-C	Specific after K, not before P
Chymotrypsin	Specific W, F, H, Y, not specific after M, L, I and other hdrophobic amino acids

The proton is transferred to the tetrahedral intermediate causing the breakage of the first product R'-NH_2 and form the acyl-enzyme intermediate. The next step is to hydrolyze the ester bond of the acyl-enzyme intermediate, and liberate the second product of the peptide hydrolysis R-COOH and restore the original enzyme state ready for reaction with the next substrate molecule.

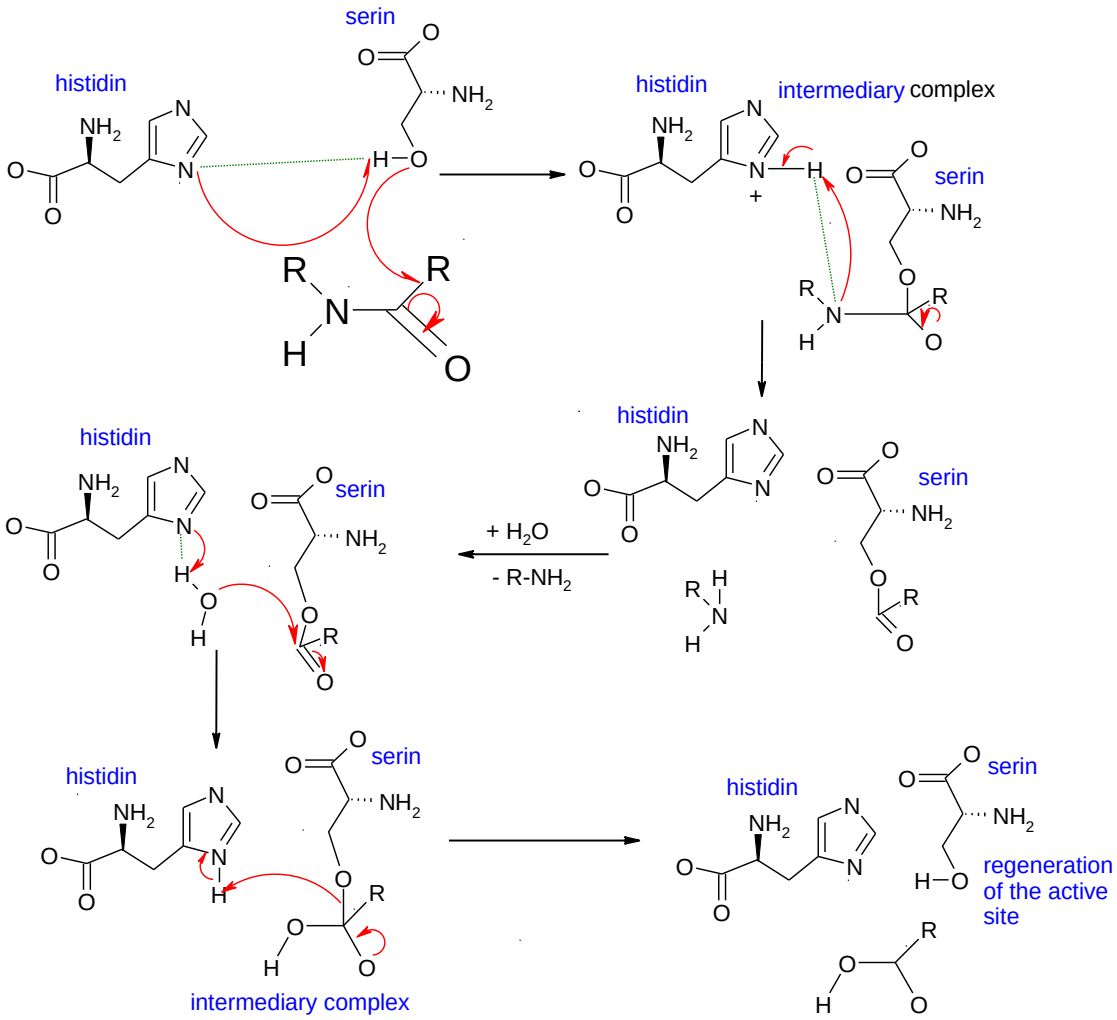

Figure 64. Reaction mechanisms at the catalytic centre of the serine protease [125.]: nucleophilic attack of the side chain oxygen of Ser on the carbonyl carbon forming a tetrahedral intermediate; breakage of the peptide bond with assistance from His 57 (proton transfer to the new amino terminus); it is release the first product; nucleophilic attack of water and formation of the tetrahedral intermediate; decomposition of acyl intermediate and release of the second product.

Bands were excised manually from the gel and under went to digestion with trypsin, chymotrypsin or Lys-C according to Mortz et al and peptide extraction. The gel pieces were washed with ultra pure water (MilliQ, Millipore) for 15 min and shaken with acetonitrile (ACN) to dehydrate the gel. After drying the gel pieces in a vacuum centrifuge, they were distained with 50 mM NH_4HCO_3 for about 15 min and dehydrated with 3:2 acetonitrile/ MilliQ (15 min), followed by drying in a vacuum centrifuge. The gel pieces were swollen in digestion buffer (12 ng/µL TPCK-trypsin in 50 mM NH_4HCO_3) at 4°C (on ice) for 45 min; the gel pieces were incubated at 37°C overnight (12 h); at last, the peptides were extracted twice with ACN/ 0.1% TFA 3:2. The samples containing the extracted peptides were lyophilized after the digestion stage was checked by MALDI-TOF MS. The batches with proteolytic mixture and fractions: trypsin batches for FT-ICR, Edman Sequencing and LC-MS/MS; chymotrypsin batches for Edman Sequencing and LC-MS/MS; Lys-C bathes for Edman Sequencing and LC-MS/MS. All were checked by MALDI-ToF.

3.8. Mass spectrometric methods

Mass spectrometry is wildly used as analytical method to identify proteins. The techniques offers speed, sensitivity and versatility making possible a real fast development of proteomics and related fields and the complexity of the studied biosystems is increasing everyday. A mass spectrometer consists of an ion source, a mass analyzer that measures the mass to charge ratio (m/z) of the ionized analytes, and a detector that registers the number of ions at each m/z.

Ionization types and analyzers are freely mixed for a better analysis, but some combinations are preferred: MALDI is usually coupled to ToF analyzers, whereas ESI is mostly coupled to ion traps and triple quadrupole instruments and used to generate fragment ion spectra (collision induced dissociation or CID spectra). One key advantage of mass spectrometric analyses over other analytical techniques is its

capability to study extremely small quantities of molecules with high sensitivity. Ionization techniques such as electrospray (ESI) and matrix assisted laser desorption and ionization (MALDI) are directly responsible for these advanced possibilities. ESI, as well as MALDI have demonstrated their capabilities for mass spectrometric analysis of biopolymers up to several hundred thousand Daltons.

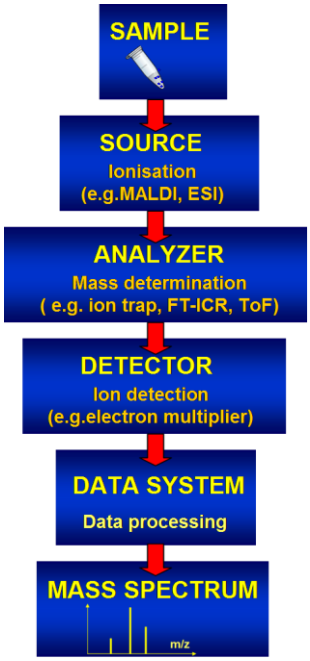

Figure 65. General components of a mass spectrometer: source, analyser, detector

3.8.1. Electrospray and MALDI ionization methods

MALDI-MS is a preferred technique for analysis of biological samples and complex mixtures, due to high sensitivity and the tolerance of many biological buffer solvents. In MALDI-MS the sample with an organic matrix (usually aromatic acids) is applied on a target and desorbed by laser irradiation. Ionization takes place bombarding the sample with short-duration (1 - 10 ns) pulses of UV light from nitrogen. The ionization process is poorly understood. The sample is crystallized with the matrix molecules and when the laser strikes the matrix crystals, the energy

deposition is thought to cause rapid heating of the crystals brought about by matrix molecules emitting absorbed energy in the form of heat. The rapid heating causes sublimation of the matrix crystals and expansion of the matrix and analyte into gas phase. Ions might be formed through gas-phase proton-transfer reactions in the expanding gas phase plume with photoionized matrix molecules. MALDI-matrix plays a key role in MALDI and is a non-volatile solid material that absorbs the laser radiation resulting in the vaporization of the matrix and sample embedded in the matrix. The matrix also serves to minimize sample damage from the laser radiation and to facilitate the ionization process[126.].

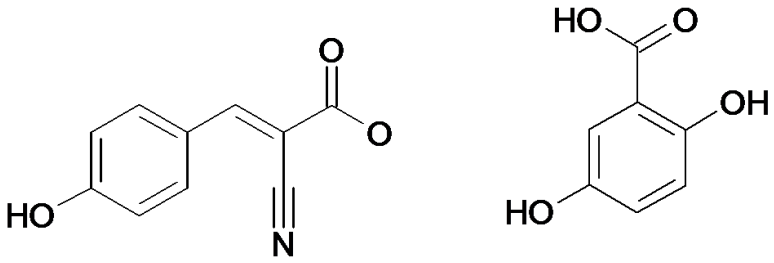

a. **b.**

Figure 66. Matrices used in MALDI-TOF-MS: (a), α-Cyano-4-hydroxycinnamic acid, (HCCA) and (b), in MALDI-FTICR-MS 2,5-Dihydroxybenzoic acid (DHB).

The most common matrices α-cyano-4-hydroxycinnamic and 2, 5-dihydroxy benzoic acid. α-cyano-4-hydroxycinnamic acid (HCCA) is recommended for peptides and proteins under 10 kDa of mass. Best results are obtained in the 1500-5000 Da range and therefore HCCA is the matrix of choice for peptide mass fingerprinting, being usually used for MALDI-TOF mass spectrometry; 2, 5- dihydroxy benzoic acid (DHB): is used for the analysis of small molecules and peptides (200 to 1000 Da), and DHB is usually used in MALDI-FTICR mass spectrometry. A good matrix should fulfill the following requirements: absorption at the wavelength of the laser radiation (λ = 337 nm) to provide sufficient energy deposition in the sample; and to be soluble in the same solvent as the analyte. They have to crystallize upon sample preparation. A mixture of

matrix and sample is applied on the target and desorbed by laser ionization. The desorbed ions are moved in an electric field and separated in a time of flight analyzer.

Electrospray ionization is generally leading to the formation of multiply charged molecules. This is an important feature since the mass spectrometer measures m/z, thus making it possible to analyze large molecules with an instrument of a relatively small mass range and it is the principal difference with the MALDI ionization which produces with predilection single charges ions[127.].

3.8.2. Mass spectrometric analyzers

The mass analyzer is responsible for the accuracy, range, and sensitivity of a mass spectrometer.

a.Time of flight mass spectrometry (ToF MS)

Time-of-flight analysis is based on accelerating a set of ions to a detector with the same amount of energy. With MALDI-ToF analyte ions gain additional activation energy and fragmentation occurs by collisions with matrix molecules and residual gas molecules during their flight in the field free drift path; this post source decay creates metastable ions.

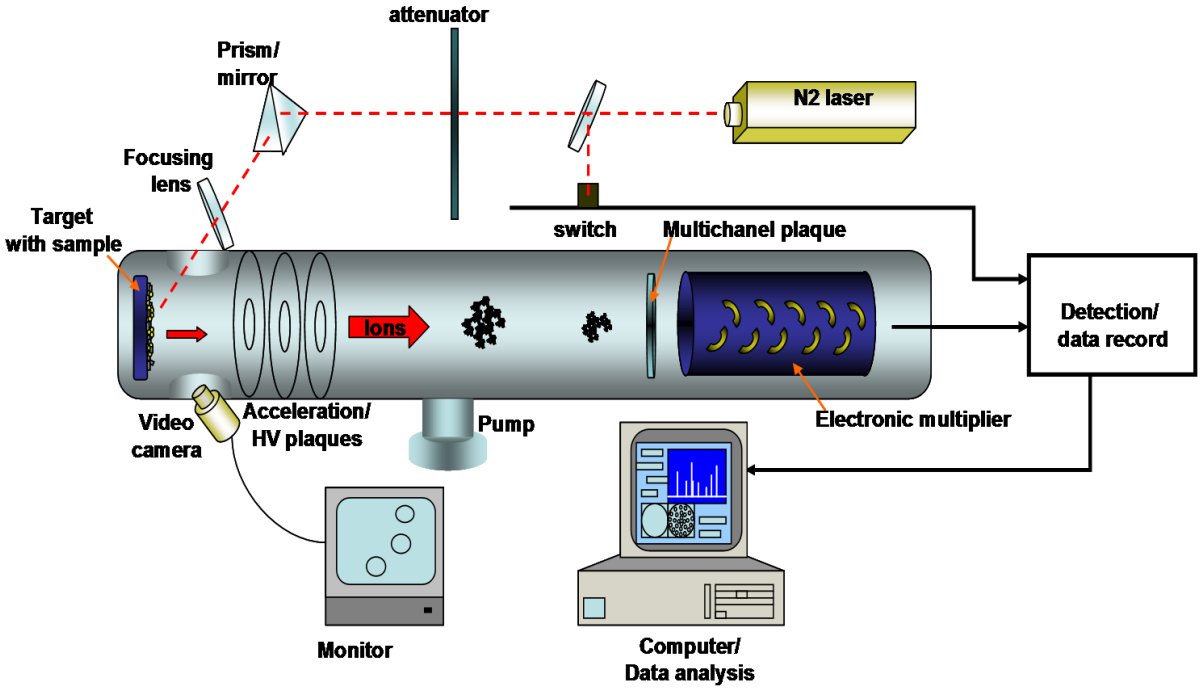

Figure 67. Time of flight mass spectrometer. The analyte is loaded on a MALDI target and it desorbed by the laser, the masses formed ions are calculated by measuring the time necessary to reach to detector (the size of the molecules are inverse proportional with the time of flight), the resolution of the technique depends on the type of matrix and of the size off the flight pathway[128.].

The metastable ions are brought into the detector and their fragment masses can be analyzed. Because the ions have the same energy, yet a different mass, the ions reach the detector at different times. The smaller ions reach the detector faster because of their greater velocity and the larger ions take longer, thus the analyzer is called time-of-flight because the m/z is determine from the ions time of arrival [129, 130.]. The arrival time of an ion at the detector is dependent upon the mass charge, and kinetic energy of the ion. MALDI-ToF mass spectrometry was performed using a Bruker (Bruker Daltonics, Germany) Biflex ITM linear ToF mass spectrometer with a SCOUT-26-ionization source video system, nitrogen UV laser (337 nm), and a dual channel plate detector. Each spot on the target was prepared using mixture between matrix and sample. 0.6 μL of a freshly prepared saturated solution of HCCA (α-cyano-4- hydroxycinnamic

acid) in ACN: 0.1% TFA (2:1, v/v) was applied onto the dried target, and then 0.8 µL of the peptide (sample) solution was applied over.

Internal or external mass calibration was performed using a peptide mixture with a concentration of 1 pmol/µL. The spectra were registered using an accelerating voltage of 20 kV and a laser attenuation power of 45%. A number off 40 laser shots were applied for accumulating one spectrum.

MALDI-ToF mass spectrometry was employed in the analysis all the proteolytic peptide mixtures for the reaction monitoring and all of the HPLC fractions containing separated peptides. All the resulting ion masses were searched in data base and used as starting point in further fragmentation analyses. Examples of digestion peptide mixtures of are presented in Figure 25, Figure 26, Figure 68 and Figure 69.

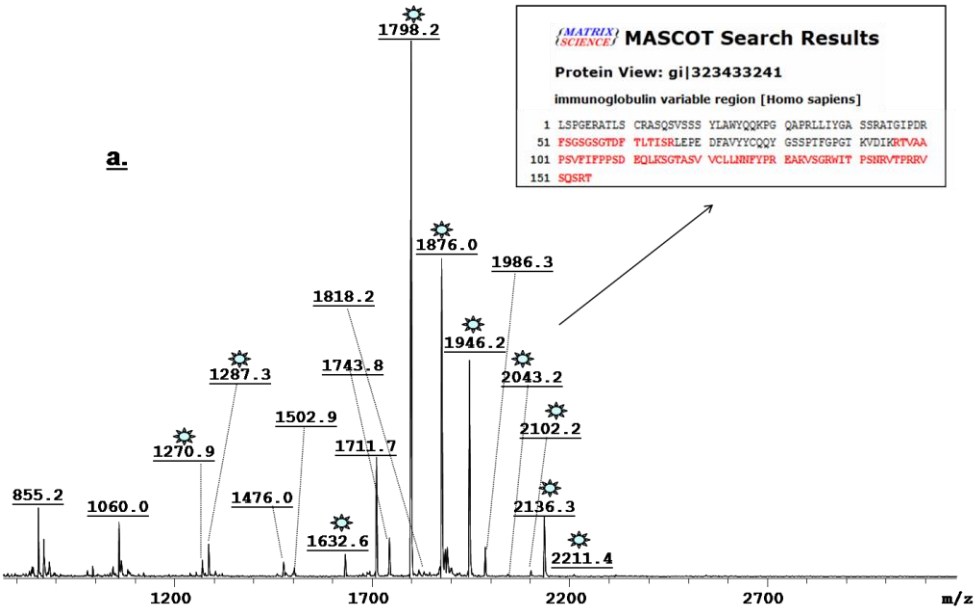

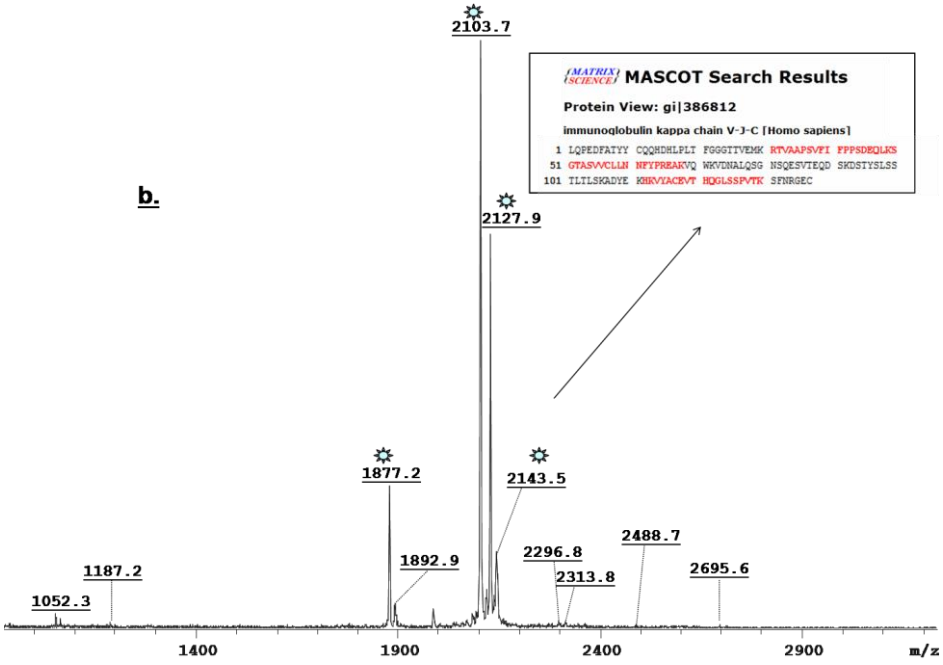

Figure 68. MALDI -ToF MS analysis of light chain tryptic mixtures. a. - MALDI ToF spectrum of tryptic mixture - fragments found in data base by the mascot search engine were assigned with a blue star; b. - MALDI ToF spectrum of Lys-C mixture - fragments found in data base by the mascot search engine were assigned with a blue star

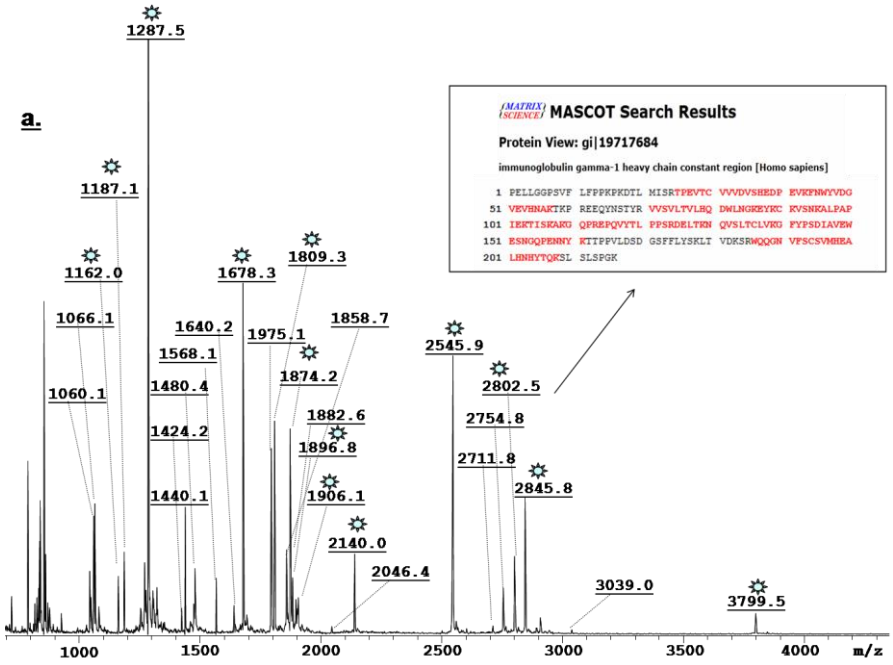

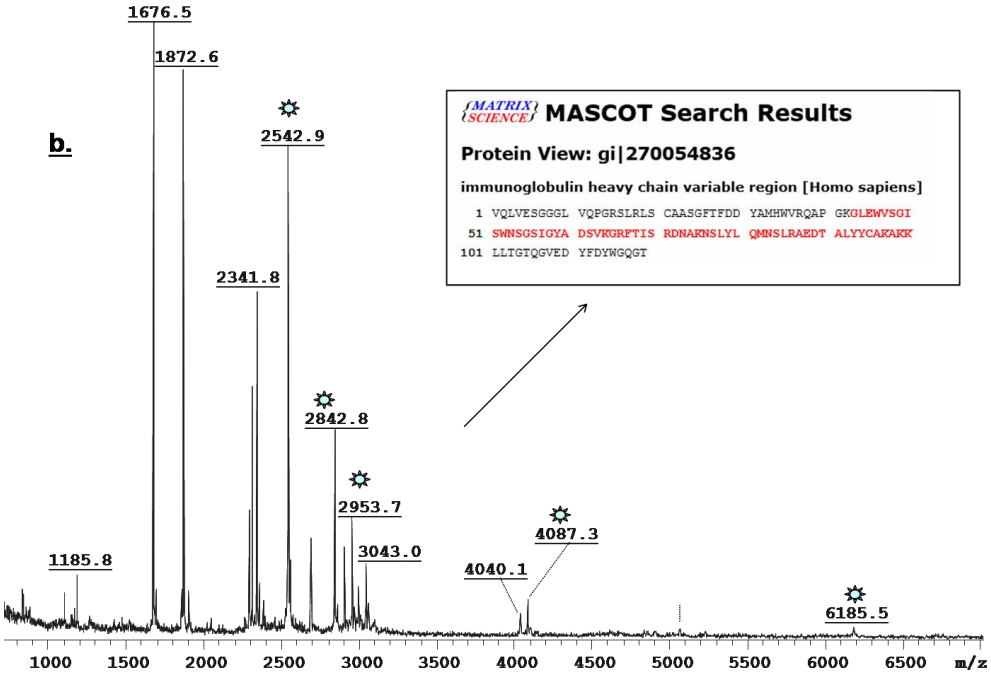

Figure 69. MALDI -ToF MS analysis of heavy chain LysC proteolytic mixtures. a. - MALDI ToF spectrum of tryptic mixture - fragments found in data base by the mascot search engine were assigned with a blue star; b. - MALDI ToF spectrum of Lys-C mixture - fragments found in data base by the mascot search engine were assigned with a blue star

b. Ion trap mass spectrometry

The ion trap mass analyzer is the three dimensional analogue of the linear quadrupole mass filter and is based on the motion of ions in a radio frequency electric field. Ions are subjected to forces applied by a radio frequency field in all three directions.

The ion trap is formed with three electrodes with hyperbolic surfaces: two end-cap electrodes at ground potential and a ring electrode between them to which a radio frequency voltage is applied. The device is radial symmetrical. The ion trap uses an alternating electric field to stabilize and destabilize the passing ions. In the case of ion trap the electric field is used to store ions and to release them in time to be analyzed. The ion trap mass analyzer applied to peptide sequencing generally are combined with

an ESI ion source[131.]. In an MS/MS experiment ions are injected into the ion trap. The parent ion is isolated and the fragmentation take place by collision-induced dissociation (CID) when helium molecules collide with the resonating excited ions. After fragmentation, the CID spectrum of the selected precursor ion is recorded by sequentially ejecting the product ions; only masses higher than 28% of the parent ion can be stabilized inside the ion trap. Ion trap is about 50 times more sensitive than a triple quadrupole mass spectrometer and the resolution can be improved using a multiple reaction monitoring scan mode. In the fragmentation of the proteins or peptides, peptide bonds are commonly broken releasing mostly intact amino acid residues. In MS experiments, however, there may also be fragmentation at other localization in addition to peptide bonds resulting in a complex pattern of ions. The nomenclature proposed by Roepstorff describe polypeptide fragmentation, ions formed from a polypeptide during MS may retain a positive or negative charge either on their C- or N-terminus[132.].

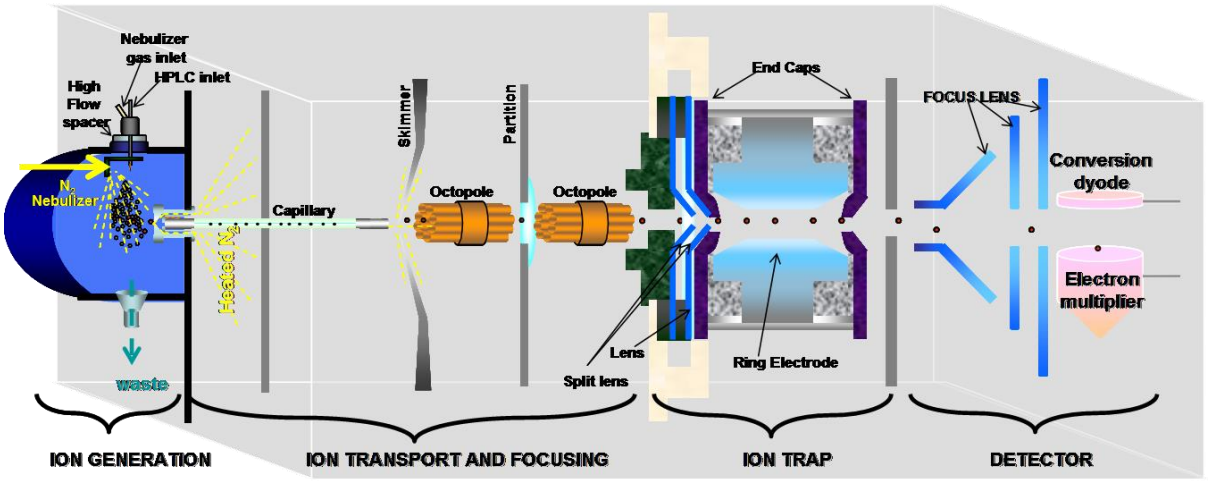

Figure 70. Schematic of ion trap mass spectrometer. This mass spectrometer is equipped with an ESI source, pass through the capillary and HV octopoles in gas phase to get to the ring electrode. The ring electrode has the capacity to screen in MS mode for m/z up to 4000 or to resonate only with ions of interest by trapping them into an electric field. The trapped ions can be fragmented with the formation of b and y type ions [133.].

A horizontal line pointing towards the C- or N-terminus at the breakage point is used to denote which fragment carries the charge in that particular ion. For the N-terminal ions there are a_n, b_n, c_n and d_n (numbered from the N-terminus) while the C-terminal ions are designated x_n, y_n and z_n (numbered from the C-terminus). The ion represented by a_1 represents the first residue in the sequence (minus the CO group) while a_2 represents the first two residues (minus the CO group) and so on. Identical main-chain breakage points are denoted by the pairs a/x, b/y, c/z (each member of a pair referring to a positive charge retained either on the N- or C-terminus, respectively).

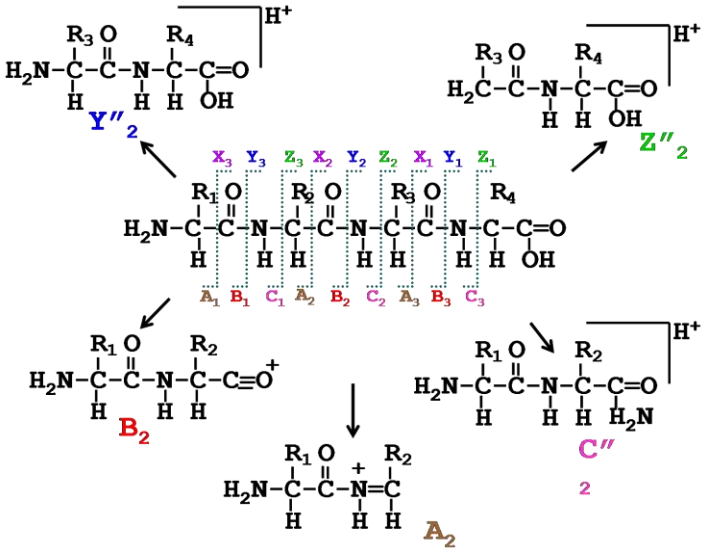

Figure 71. Peptide mass spectrometric fragmentation pattern. In ion trap the only b and y ions are formed, fact used in de novo interpretation of MS/MS data obtained with Esquire 3000+ mass spectrometer [134.].

The peptide fractions analysis was done on an Esquire 3000+ (Bruker Daltonics, Bremen, Germany). This instrument has a superior MS/MS performance and resolution throughout the whole mass range 50-3,000 m/z. Standard resolution mode resolving 2+ ions is at 13,000 u/sec and maximum resolution mode resolving 3+ and 4+ ions at 1,650 u/sec. All MS results were obtained using atmospheric pressure chemical ionization (APCI) in the positive ion mode. Mass spectra were recorded in the full scan mode, scanning from m/z 100 to 2500. Ion source parameters were

19 psi nebulizer gas and 7 L/ min of drying gas with a temperature of 250°C.

Examples of MS/MS spectra used for the de novo identification of peptide sequences from N-terminus, frame and constant regions of the Aβ-autoantibody light and heavy chains are shown in Figure 72-79. All sequences containing CDR peptides (complete or partial) are listed in Table 6, Table 7, Table 25-28.

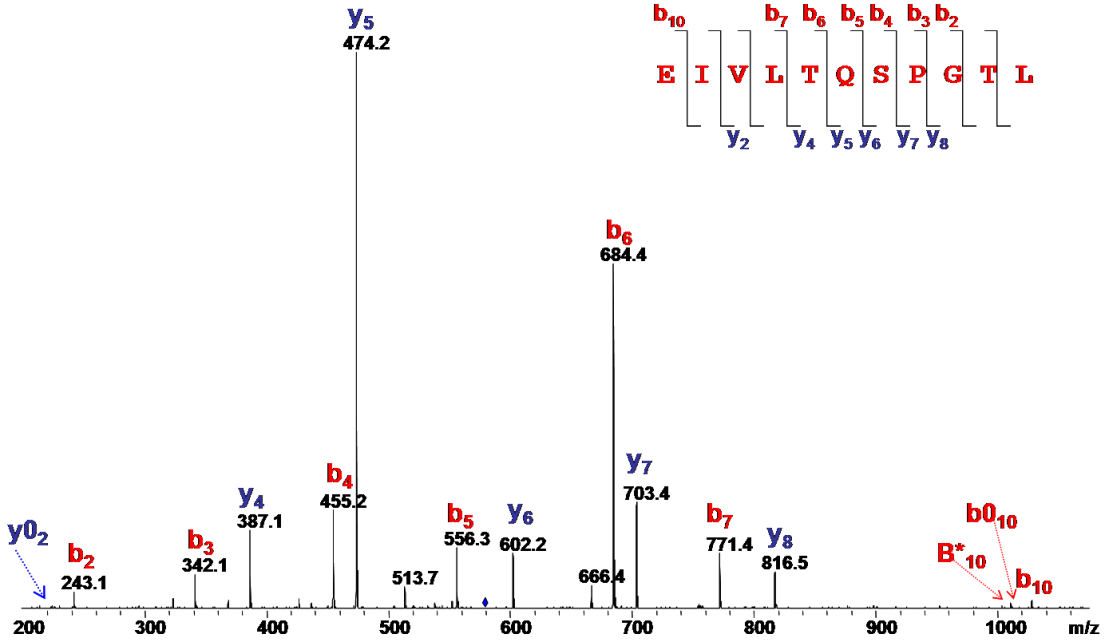

Figure 72. LC-MS/MS fragmentation mass spectrum of ion 579.8 (2+) which led to identification of a peptide containing N-terminus fragment of light chain.

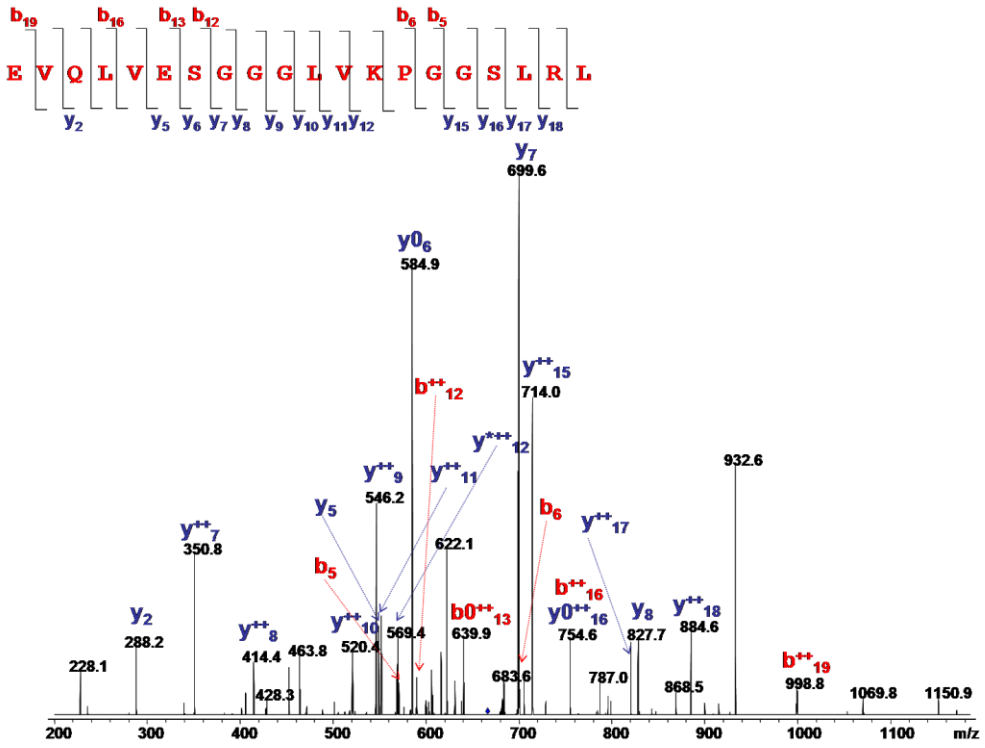

Figure 73. LC-MS/MS fragmentation mass spectrum of ion 661.3 (3+) which led to identification of a peptide containing N-terminus fragment of heavy chain

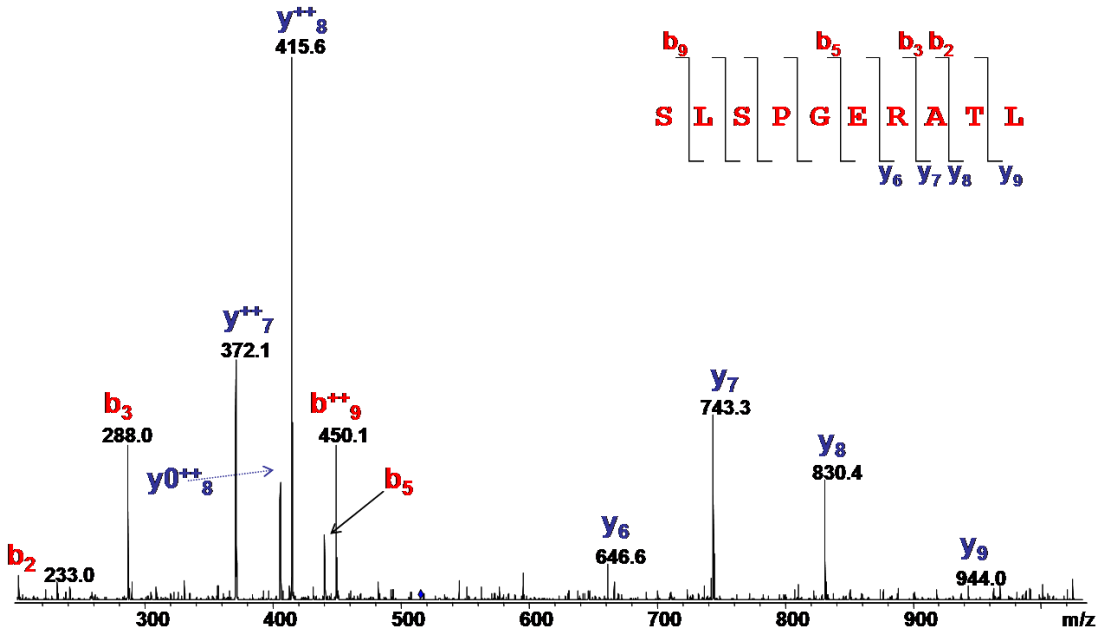

Figure 74. LC-MS/MS fragmentation mass spectrum of ion 516.1 (2+) which led to identification of a peptide containing frame region fragment of light chain

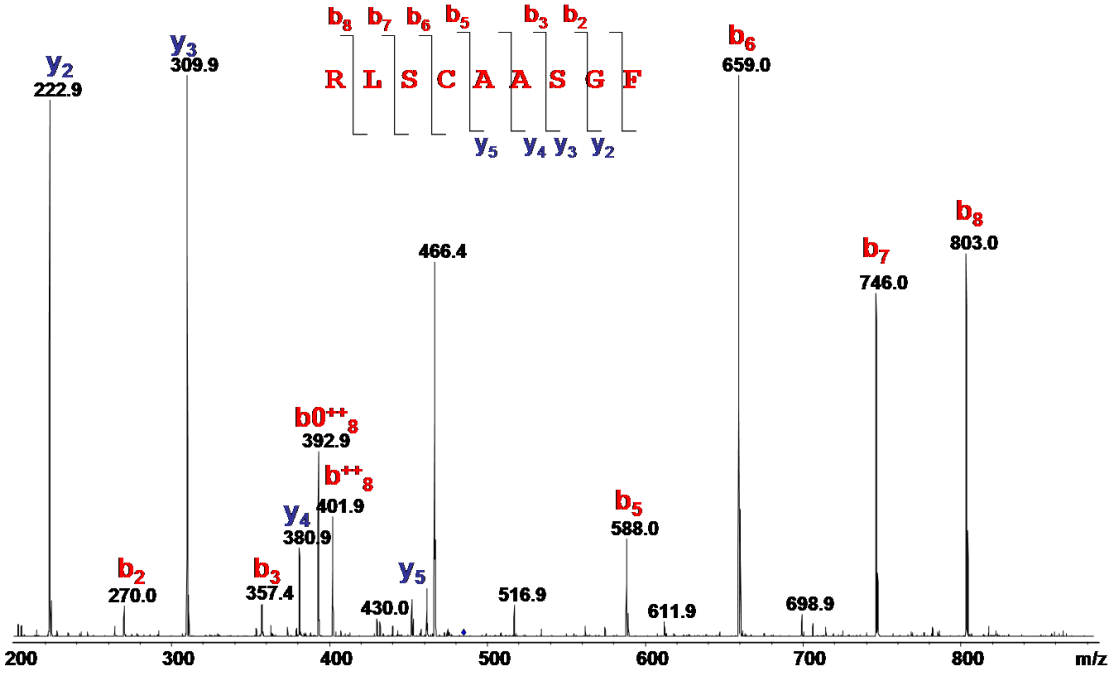

Figure 75. LC-MS/MS fragmentation mass spectrum of ion 485.2 (2+) which led to identification of a peptide containing frame region fragment of heavy chain

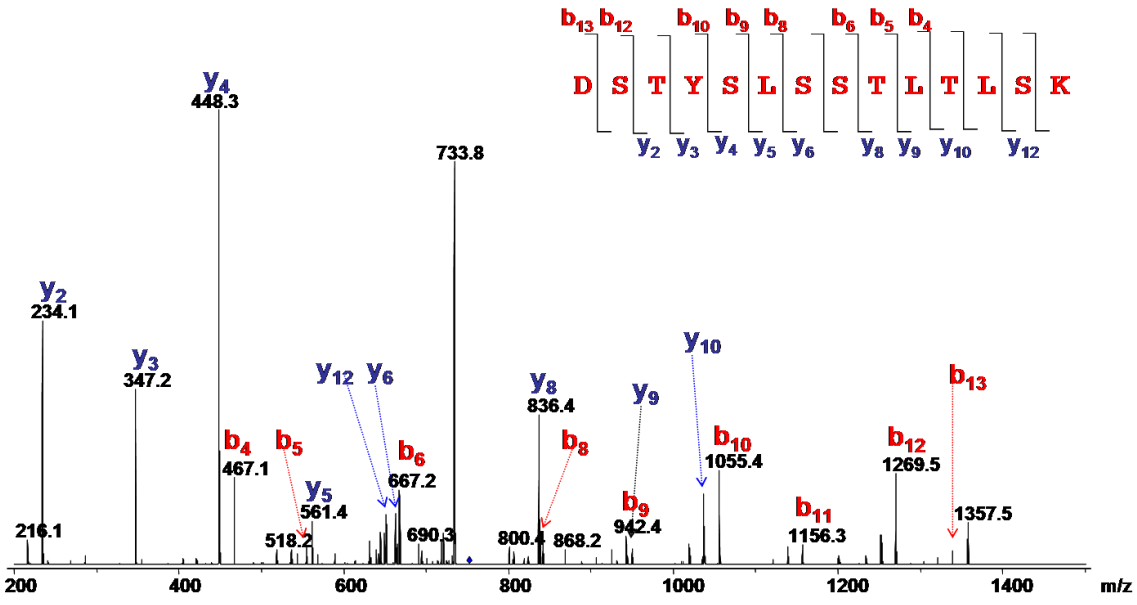

Figure 76. LC-MS/MS fragmentation mass spectrum of ion 501.9 (3+) which led to identification of a peptide containing constant region fragment of light chain

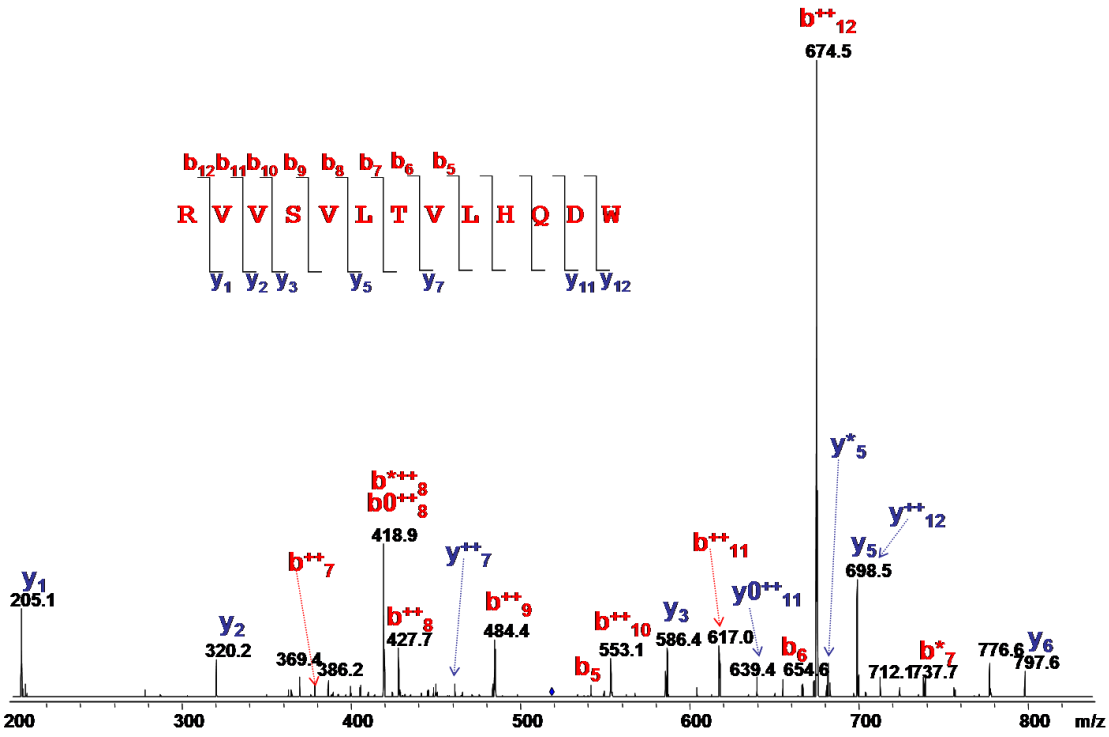

Figure 77. LC-MS/MS fragmentation mass spectrum of ion 518.3 (3+) which led to identification of a peptide containing constant region fragment of heavy chain

Table 25. Aβ-autoantibody light chain CDR2 containing peptides identified by HPLC separation and individual analysis of each fraction by LC-MS/MS

No.	Position	Sequence	$[M+H]^+_{calc}$ [a]	$[M+H]^+_{exp}$	Δm (Da)
1	042-050	SQPKNPTV*T*	971.5	971.4	0.1
2	039-050	HSGKAPKLMIY*D*	1359.7	1360.2	0.5
3	039-050	QSGKAPKLMIY*D*	1350.7	1351.5	0.8
4	043-052	SPQPLIY*LG*Y	1150.6	1151.3	0.7
5	043-052	APKLLIY*GN*Y	1151.6	1151.9	0.3
6	046-050	LLIY*K*	648.4	648.4	0.0
7	046-053	LIIY*DVTK*	964.5	965.0	0.5
8	046-053	LIIY*EVSK*	964.5	963.9	0.6
9	046-053	LLIY*DDNK*	993.5	992.4	1.1
10	046-053	LLIY*DISK*	964.5	963.9	0.6
11	046-053	LLIY*EVSK*	964.5	963.9	0.6
12	046-053	IIIY*EVSK*	964.5	965.0	0.5

13	046-053	LMLTNYIK + Ox	1011.5	1012.1	0.6
14	046-053	LMIYDVTK + Ox	998.5	998.0	0.5
15	046-054	LLISDASNR	988.5	987.4	1.1
16	046-054	LLIYGASAR	963.5	962.5	1.0
17	046-054	LLIYAGSTR	993.5	992.5	1.0
18	046-054	LLIYWASTR	1122.6	1121.7	0.9
19	046-054	LIIYDVYKR	1182.6	1183.1	0.5
20	046-054	LLMYDALKR + Ox	1138.6	1138.9	0.3
21	048-054	IYDASTR	825.4	825.7	0.3
22	048-062	IYGASSRATGIPDRF	1610.8	1610.5	0.3
23	048-062	IYGASTRATGIPARF	1580.8	1581.3	0.5
24	050-062	AVSSLQSGVPSRF	1334.7	1334.9	0.2
25	050-062	AASSLQSGVPSRF	1306.6	1306.5	0.1
26	050-062	SASVLQSGVPSRF	1334.7	1334.5	0.2
27	050-073	AASDLQSGVPSRFSGSGSGTDTTL	2298.0	2298.8	0.8
28	055-061	ATGIPAR	685.4	684.4	1.0
29	055-061	ATDIPAR	743.4	743.4	0.0
30	055-061	ATGIPDR	729.4	729.4	0.0
31	055-061	APGIPDR	725.4	725.4	0.0

[a] Calculated using GPMAW software (Lighthouse Data, Denmark)

[b] RED -frame regions; BLUE - CDR s

Table 26. Aβ-autoantibody light chain CDR3 containing peptides identified by HPLC separation and individual analysis of each fraction by LC-MS/MS

No.	Position	Sequence	$[M+H]^+_{calc}$ [a]	$[M+H]^+_{exp}$	Δm (Da)
42	087-106	DYYCSSYAGSNNLVFGGGTS	2118.8	2119.1	0.3
43	089-094	YCQQSY	791.3	791.5	0.2
44	097-106	TRVFGTGTKV	1065.6	1065.7	0.1
45	098-105	LTELGQPK	885.5	885.4	0.1
46	098-105	VTVLGQPK	841.5	840.6	0.9
47	098-105	LTVLGQPK	855.5	854.4	1.1
48	098-105	LTVNGQPK	856.5	855.6	0.9

[a] Calculated using GPMAW software (Lighthouse Data, Denmark)

[b] RED -frame regions; BLUE - CDR s

Table 27. Aβ-autoantibody heavy chain CDR2 containing peptides identified by HPLC separation and individual analysis of each fraction by LC-MS/MS.

No.	Position	Sequence	$[M+H]^+_{calc}$ [a]	$[M+H]^+_{exp}$	Δm (Da)
1	037-050	VRQAPGKGLEWVSL	1539.8	1539.9	0.1
2	037-050	VRQAPGKGLEWLSY	1603.8	1603.8	0.0
3	037-050	VRQAPGKGLEWISY	1603.8	1604.1	0.3
4	037-050	FRQAPGKGLEWVGF	1591.8	1591.5	0.3
5	037-050	IRQPPGKGLEWIGY	1613.8	1614.2	0.4
6	037-050	IRKPPGQGLEWIGY	1613.8	1614.2	0.4
7	044-050	GLVWVSR	816.4	815.7	0.7
8	044-050	GLEWVGR	816.4	815.6	0.8
9	044-052	GLEWLAVLK	1028.6	1028.0	0.6
10	044-052	GLQWVALIK	1027.6	1028.0	0.4
1	044-052	GLQWVANIK	1028.6	1028.0	0.6
12	044-052	GLEWVALIK	1028.6	1028.0	0.6
13	044-052	GLEWVAIIK	1028.6	1028.0	0.6
14	044-052	GLEWIGLIK	1028.6	1028.0	0.6
15	044-052	GLEWLGLIK	1028.6	1028.0	0.6
16	044-052	GLQWVGQIK	1028.5	1028.0	0.5
17	044-053	GLEWVAMISK	1133.6	1133.1	0.5
18	044-058	ALEWLAVVYWNDYK	1769.9	1770.2	0.3
19	044-063	GLEWASAIRGDGGFQYADAVK	2211.1	2211.5	0.4
20	046-056	EWLAYMSSSGSY	1380.5	1380.1	0.4
21	046-059	EYLSAISSDGETTY	1535.6	1535.2	0.4
22	046-059	EWVSSISRSGDNTY	1600.7	1599.6	1.1
23	046-058	EWVSVIGSAGDTYY	1546.7	1546.1	0.6
24	046-059	EWVSTIVGSGDATF	1468.7	1467.9	0.8
25	046-061	EWVGRIKSEADGGTTDY	1883.8	1884.8	1.0
26	046-063	EWIGHVSGSGVAKYNPSL	1900.9	1900.6	0.3
27	046-063	EWIGNVFSSGSTNYNPSL	1971.9	1972.8	0.9
28	048-059	VANIKQDGGERY	1349.6	1350.3	0.7
29	048-059	VANIKQDGSKKY	1350.7	1350.3	0.4
30	048-064	MGRIFPLLGVAKYAQKF	1939.1	1939.4	0.3
31	048-064	MGTIYGGDSDTRYNPSF	1880.8	1880.9	0.1
32	048-064	MGGIIPLSETPNYAQKF	1865.9	1866.0	0.1
33	048-064	MGWSSTDTGNTNHAQKF + Ox	1897.8	1897.5	0.3

34	050-065	***FTVSSGSAFGPTLFPL***	1627.8	1627.6	0.2
35	051-071	***IYYSGSSNYNPSLKS*RVTMSL + Ox**	2383.1	2383.8	0.7
36	052-060	***FNGDTYYNL***	1106.4	1106.2	0.2
37	053-080	***NPSLKGRLTMSVD*TSKNQLLL + Ox**	2331.2	2332.4	1.2
38	057-064	***TNYNPSLK***	936.4	936.4	0.0

[a] Calculated using GPMAW software (Lighthouse Data, Denmark)

[b] RED -frame regions; BLUE - CDR s

Table 28. Aβ-autoantibody heavy chain CDR3 containing peptides identified by HPLC separation and individual analysis of each fraction by LC-MS/MS.

No.	Position	Sequence	$[M+H]^+_{calc}$ [a]	$[M+H]^+_{exp}$	Δm (Da)
1	086-106	**RSEDTAVYYCAR*VMVRGVISLDY***	2724.3	2725.2	0.9
2	086-099	**RVEDTGMYYCAR*DF*+ Ox**	1798.7	1799.0	0.3
3	086-099	**SPEDTAMYFCAR*DL***	1675.7	1675.6	0.1
4	086-100	**QVRGVTLYYQSL*DVW***	1826.9	1826.1	0.8
5	086-108	**TSDDAAVYYCAV*DSGAKAGNYY***	2360.9	2361.0	0.1
6	087-105	**SYSTAYLQWSS*LKASDTAM***	2109.9	2110.0	0.1
7	092-104	**IYYSGS*TKYNSSL***	1482.7	1482.5	0.2
8	092-104	**IYYSGT*TNYNSSL***	1482.7	1482.4	0.3
9	092-104	IYYTGS*TNYNSSL*	1482.7	1482.5	0.2
10	093-099	YYVDS*VK*	872.4	872.3	0.1
11	094-107	YCAR*GEYYGSGSL*	1482.6	1482.5	0.1
12	094-109	YCAR*GRKSYFDVGGYY*	1961.8	1961.9	0.1
13	094-109	YCAR*DESEYSSSSLDL*	1881.7	1881.6	0.1
14	095-104	CAR*GAARLDY*	1151.5	1151.4	0.1
15	095-105	CAR*GLVERRTW*	1403.7	1403.9	0.2
16	095-105	CAR*VGYYGSGY*	1253.5	1253.4	0.1
17	095-105	CAR*SDFSGMDV*	1244.4	1244.6	0.2
18	095-106	CAR*VGYYGSGVY*	1315.6	1314.0	1.6
19	095-106	CAR*VHRGGSYYL*	1338.6	1338.9	0.3
20	095-107	CAR*HRPTYGVYYY*	1706.7	1706.1	0.6
21	095-109	CAR*GAGMVQGVITTL*	1533.7	1534.0	0.3
22	095-111	CAR*VRSGGGSSFPSDAF*	1757.7	1758.4	0.7
23	095-112	CAR*DFVVVVGGTQWDMNY* + Ox	2132.9	2132.8	0.1
24	096-107	DS*SGYSAYYYYY*	1500.9	1500.4	0.5
25	098-107	*QGLLKPSETL*	1085.6	1085.8	0.2

26	098-108	*GAGLLKPSETL*	1085.6	1085.4	0.2
27	098-108	*FGEVILRAGWF*	1294.7	1294.2	0.5
28	098-110	*QFFSGALATGSVK*	1311.7	1311.6	0.1
29	098-110	*QFFSGSPATGSVK*	1311.7	1311.6	0.1
30	101-112	*NDAYGGGIDY*WG	1286.5	1286.1	0.4
31	101-122	*FYYYYGMDV*WGQGTTVTVSSG + Ox	2397.0	2398.0	1.0
32	102-121	*DGPYAYDI*WGQGTMVAVSL	2059.9	2060.3	0.4
33	104-116	*GGWFDP*WGQGTL	1320.6	1321.0	0.4
34	105-116	*NWFDP*WGQGTL	1320.6	1321.0	0.4
35	106-116	*WFDP*WGQGTL	1206.5	1206.6	0.1
36	107-116	*ELDY*WGTGTL	1154.5	1154.6	0.1
37	107-116	*IDN*WGQGTL	1003.4	1003.0	0.4
38	107-116	*LND*WGQGTL	1003.5	1003.0	0.5
39	108-116	*DY*WGQGTL	939.9	939.0	0.9
40	108-116	*DY*WGKGTL	939.4	939.0	0.4
41	108-116	*DF*WGQGTL	923.4	923.2	0.2
42	108-116	*YD*WGQGTL	939.4	939.2	0.2

[a] Calculated using GPMAW software (Lighthouse Data, Denmark)

[b] RED -frame regions; BLUE - CDR s

c. Fourier Transform - Ion Cyclotron Resonance Mass Spectrometry

Fourier-Transform-Ion-Cyclotron-Resonance (FTICR) is based on charged particle orbiting in the presence of a magnetic field in a stable cyclic motion. The analyzer cell is an ultra high vacuum (<10^{-10} mbar) trap in which ions can be stored for extended periods of time. In a FTICR mass spectrometer, the mass analysis is performed in a cubic or cylindrical cell placed in a strong magnetic field[135-137.].

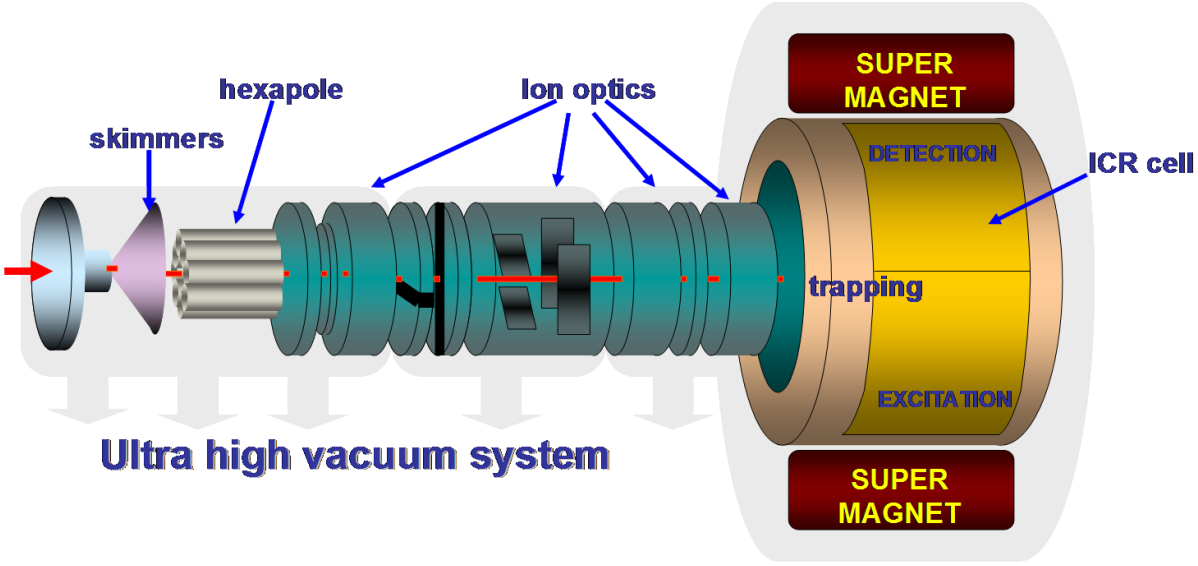

Figure 78. FT-ICR mass spectrometer. Coupled either with MALDI or ESI source (micro and nano flow) the ions are passing through a complex ion optics under high vacuum to reach the ion cyclotron cell. Here the molecules of analyte resonate in the magnetic field and the resulting vibrations are measured at translated into a mass spectrum by FT. The resolution of the instrument is higher than other MS techniques and depends only on the magnetic field strength[138.].

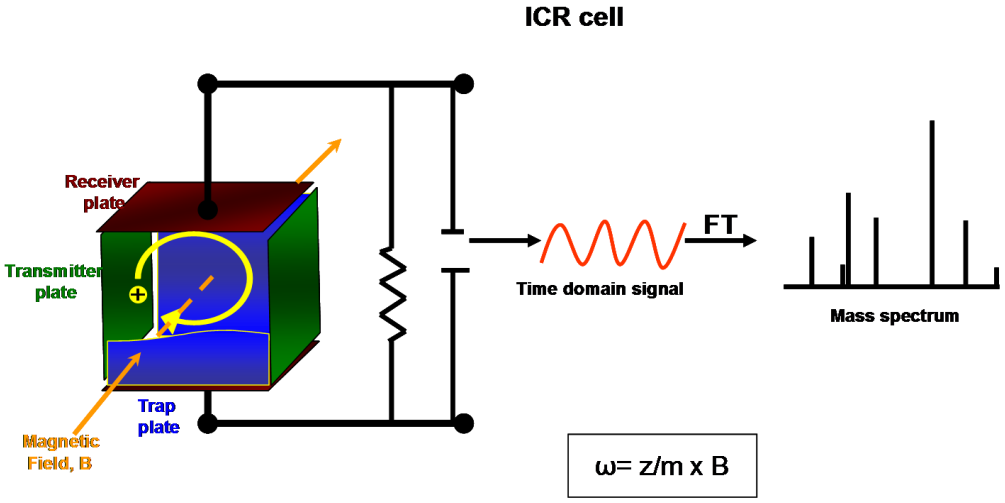

Figure 79 Schematic representation of ICR cell, a cubic trapped ion cell used in FTMS. Coherent motion of the ions in the cell induces an image current in the receiver plates. The time domain signal is subjected to a Fourier transform algorithm to yield a mass spectrum[139.].

The cell consist of two opposite trapping plates, two opposite excitation plates and two opposite detection plates. Each ion moving in a spatially

uniform magnetic field will describe a circular cyclotron motion as a result of the Lorenz force and the centrifugal force operating on it in opposite directions. The cyclotron frequency is dependent only on the mass over charge and magnetic field, as described by the general equation $\omega_c = z/m \times B$, where ω_c is the unperturbed cyclotron frequency, z is the charge, B is the magnetic field strength and m the mass of the ion. The FTICR's advantage is that the cyclotron frequency is independent from the kinetic energy and the velocity of ions that could be influenced by the ionization process. MALDI-FTICR mass spectrometric analysis was performed with a Bruker APEX II FTICR instrument (Bruker Daltonics, Bremen, Germany) equipped with an actively shielded 7T superconducting magnet (Magnex, Oxford, UK), a cylindrical infinity ICR analyzer cell, and an external Scout 100 fully automated X-Y target stage MALDI source.

Table 29. Aβ-autoantibody light chain tryptic peptides identified by MALDI FTICR and peptide mass fingerprint and list of unassigned m/z values.

No.	Position	Sequence			$[M+H]^+_{calc}$ [c]	$[M+H]^+_{exp}$ [d]	Δm (ppm)
1	001-018	**ELQMTQSPSSLSASVGDR**			1892.8946	1892.9591	34
2	043-061	**APTLLIYAVSNLQDGVPSR**			2014.0088	2014.0894	40
3	127-142	**SGTASVVCLLNNFYPR**			1797.8962	1797.8879	5
Unassigned		575.6534	818.3732	1384.6877	1765.8309	1996.9729	2150.007
ion masses		696.6266	881.2606	1390.6466	1875.9224	1996.9785	2168.0238
		701.9165	936.3846	1539.8254	1896.3908	2003.0024	2184.0143
		736.9808	1242.7327	1555.8152	1899.9592	2029.9967	2200.0276
		742.8391	1268.9288	1585.8371	1956.9867	2046.0069	2352.8257
		801.3043	1358.7074	1743.8523	1963.6492	2102.1231	3413.8983

As matrix was used a solution 100 mg/mL solution of 2,5-dihydroxybenzoic acid in acetonitrile/0.1% TFA in water (2:1). 0.5 µl of matrix solution and 2 x 0.5 µl of sample solution were mixed on the stainless steel MALDI target and allowed to dry. A pulsed nitrogen laser of 337 nm was used to desorb

the ions from the target. External calibration was carried out using the monoisotopic masses of singly protonated reference peptides in the mass range, m/z 100 – 5000. Acquisition and processing of spectra were performed with the XMASS software (Bruker Daltonics). The results of the MALDI-FT-ICR-MS measurements are listed in

Table 3 and Table 29.

3.8.3. Hybrid analytical techniques

Mass spectrometry alone in an indispensable analysis method in several science fields, but for a more comprehensive analysis in biology it is coupled with other techniques as liquid or gas chromatography, biosensors, fluorescence detectors etc. In present work, mass spectrometry was used on its own but also coupled liquid chromatography and sound acoustic waves biosensor.

a. Liquid chromatography tandem mass spectrometry (LC/MS/MS)

An LC-MS set up has three major components: an LC (to resolve a complex mixture of compounds), an interface (to transport the analyte into the ion source of a mass spectrometer) and a mass spectrometer (to ionize and mass analyze the individually resolved components). The electrospray ionization is optimized to accept flow rates up to 0.01 to 1 mL/min. The nebulization process for both of these ion sources is assisted with nebulizing gas and counter current drying gas [140.].

Elution fractions were pooled and lyophilized. After lyophilization, they were re-dissolved in 50 µL 0.2 % formic acid. LC was performed on Agilent 1100 Series binary pump system (Agilent Technologies, Waldbronn, Germany) equipped with C18 column (Vydac 100 x 1mm, 3µm) at a flow rate of 50µl/min. The gradient used for LC method: equilibration step with 2 % B for 5 min, linear gradient from 2 % B to 6 5% B in 63 min,

from 65%B to 98 % B in 10 min, 10 min washing step 98 % B, 10 min to return to the initial concentration of 2 % B (solvent A was 0.2 % formic acid in water, solvent B was 0.2 % formic acid in acetonitrile).

Electrospray mass spectrometry was performed on Esquire 3000+ instrument (Bruker Daltonik, Bremen, Germany) ESI conditions were as it follows: capillary temperature 250°C, nebulizer gas 20 psi (Ar), dry gas 9 l/min (N2), potential difference of 4kV (positive ion mode), endplate offset 500V, skimmer 40V, capillary exit 136V. The ion trap was locked on automatic gain control, six microscans were collected for each full MS scan and 20 for each MS/MS scan, with a maximum accumulation time of 200ms for each ion. Complete lists of all Aβ-autoantibody peptides identified by HPLC separation and individual analysis of each fraction by LC-MS/MS are presented in Table 30 and in Table 31.

b. Surface-acoustic-wave-biosensor mass spectrometry (SAW-MS)

Dragusanu et all developed in our laboratory the coupling interface with online combination of a surface acoustic wave biosensor with electrospray ionization mass spectrometry, SAW-ESI-MS, which enables the direct detection, identification, and quantification of affinity-bound ligands together with dissociation constant (KD) determination in a wide range of affinities. The online coupling between the SAW-sensor chip and the ESI-MS source was achieved by interfacing the two instruments with a guard column, installed on a Rheodyne six-port valve, to which also an HPLC instrument was connected, used for obtaining precise composition and constant flow of solvents for the sample elution from the guard column[113.].

The interface provides both ligand concentration and in situ desalting step for the dissociated complex. In a typical coupling experiment, the antibody was immobilized on the chip surface by injecting a solution of 200 nM. Then, the peptide or protein was allowed to interact with the antibody at a concentration of 10 µM in PBS buffer. The affinity bound peptide or protein was eluted with at pH 2 at a flow rate of 20 µL/min. During the elution injection, the exit capillary of the biosensor was connected to the inject unit, and the liquid that washed the chip was allowed to flow through the guard column. The analyte on the column was then washed at a flow rate of 40 µL/min with a mixture containing 5% solvent B, delivered by the HPLC system. After one minute, the composition of the mixture was changed to 75 % solvent B. The eluted peptide or protein sample from the column was directed to the ESI source of the mass spectrometer. After acquiring the MS signal, the guard column was washed thoroughly with solvent B and then equilibrated with solvent A, for a new experiment.

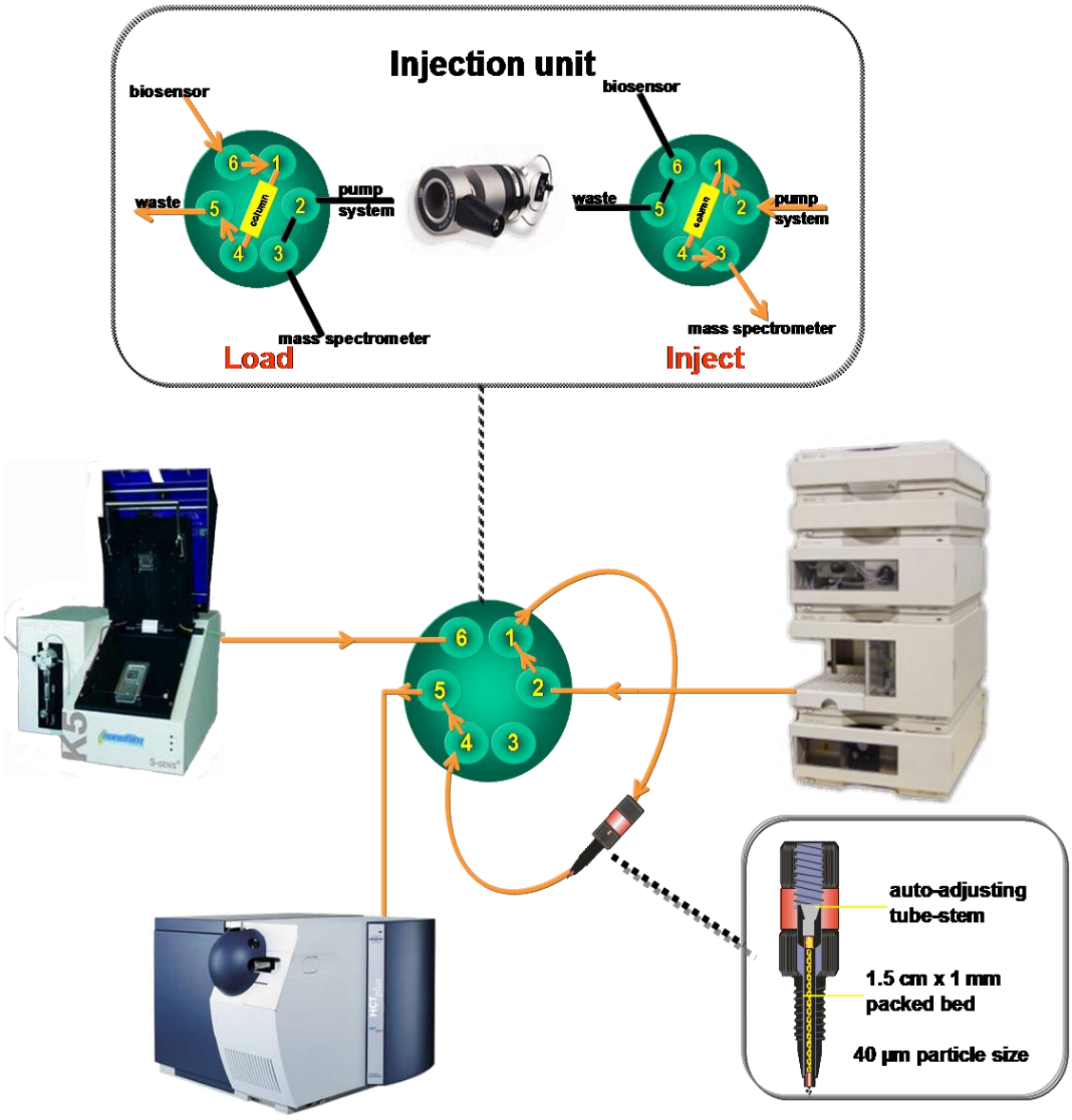

Figure 80. SAW-ESI-MS system: the SAW-biosensor (containing the gold covered quartz chip) is connected to ESI-MS through an interface consisting of a Rheodyne six ports injection valve, with an extra front needle port. A guard column for sample desalting and concentration is inserted in the loop of the injection valve, being the central element of the interface. An HPLC instrument is also connected to the interface, used as solvent delivery system. In the medallion, the arrows indicate the path of the analyte from SAW-biosensor (where the bioaffinity is investigated) through the guard column (where the desalting occurs) to the ESI-MS (for ligand identification). The flow rates are given on the path arrows.

3.9. Immunoanalytical methods

Immunological methods are based on the affinity interactions between biological partners. The affinity bounds are weaker than covalent bounds and can be altered by changing the environmental conditions. If one of the partners is immobilized on a matrix or a surface the second partner can be isolated and identified from a complex mixture[141.].

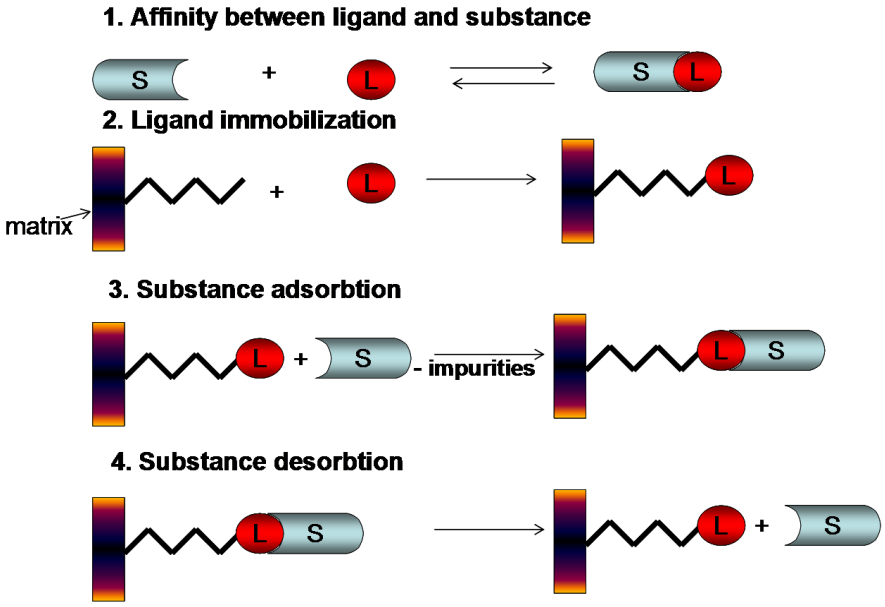

Figure 81. Affinity principle. A ligand is immobilized on a surface or a matrix, the partner is "fished out" from a complex and the matrix/surface is washed. The complex is disrupted by changing the conditions (pH, ionic strength, hydrophobicity) and analyzed.

The immunological methods employed in this work are: ELISA, SAW biosensor, affinity chromatography, and affinity-MS.

3.9.1. Enzyme-linked immunosorbent assay

ELISA (enzyme-linked immunosorbent assay) is testing the binding affinity by coating a target molecule onto a plastic plate, the analyte is added (alone or in a complex mixture), and a third molecule is used to detect binding of the analyte. ELISA is rapid and convenient, and the specificity is in nano or even atto molar range for peptides and proteins. The assay is

based on the antigen-antiboy-antibody recognition, the later being conjugated with a peroxidase that oxidate o-phenylenediamine with the production of a orange-brown color detectable at 450 nm [142, 143.].

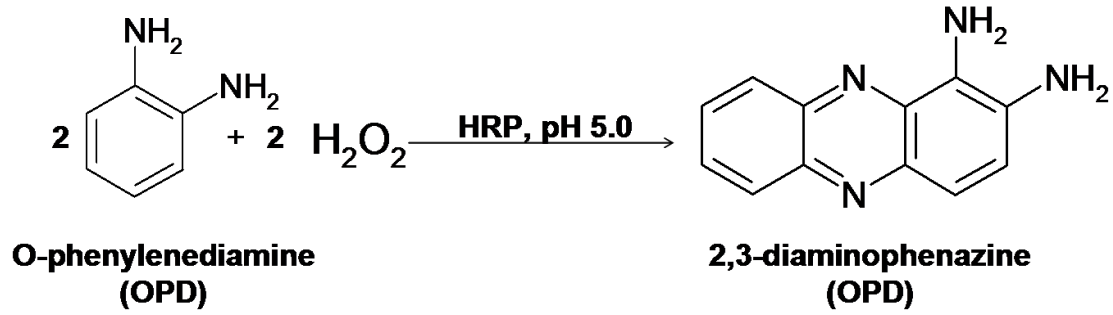

Figure 82. Reaction catalysed by horseradish peroxidase: oxidation product of o-phenylenediamine is converted into 2,3-diaminophenazine.

For Aβ - antibodies indirect ELISA was performed. The titration plate with 96 wells was covered with 100 µL/well of 1.5 µM Aβ (1-40) solution in PBS (pH 7.5) overnight at 4° C. The peptide solution was washed 4x for 15 minutes with 200 µL/well PBS-Tween (pH 7.5). The remaining free sites were blocked with 200 µL/well 5 % BSA in PBS-Tween 3 h at room temperature. Anti Aβ (12-40) antibody separated by affinity was diluted from 1:10 µg/µL to 1:21870 (dilution 1:3 for each step) in 5 % BSA in PBS-Tween (blocking solution). The plate with the antibody solution was incubated 2 h at room temperature. The antibody solution is removed and the plaque was washed 4x15 min with 200 µL /well PBS-Tween (pH 7.5). The second antibody (HRP-conjugated mouse anti human antibodies) was diluted 1:5000 (µg/µL) in blocking solution and it was incubated for 2 h at room temperature on the plates. The antibody solution was removed and the plaque is washed 4x15 min with 200 µL/well PBS-Tween (pH 7.5). The solution was removed and the plaque was washed 1x15 min with 200 µL /well citrate-phosphate solution (pH 5).100µl/well substrate solution were added (1 mg ODP/ml citrate solution, 2 µL H_2O_2/10 mL citrate-phosphate solution). The absorbance was read immediately at 450 nm using ELISA Wallac Reader.

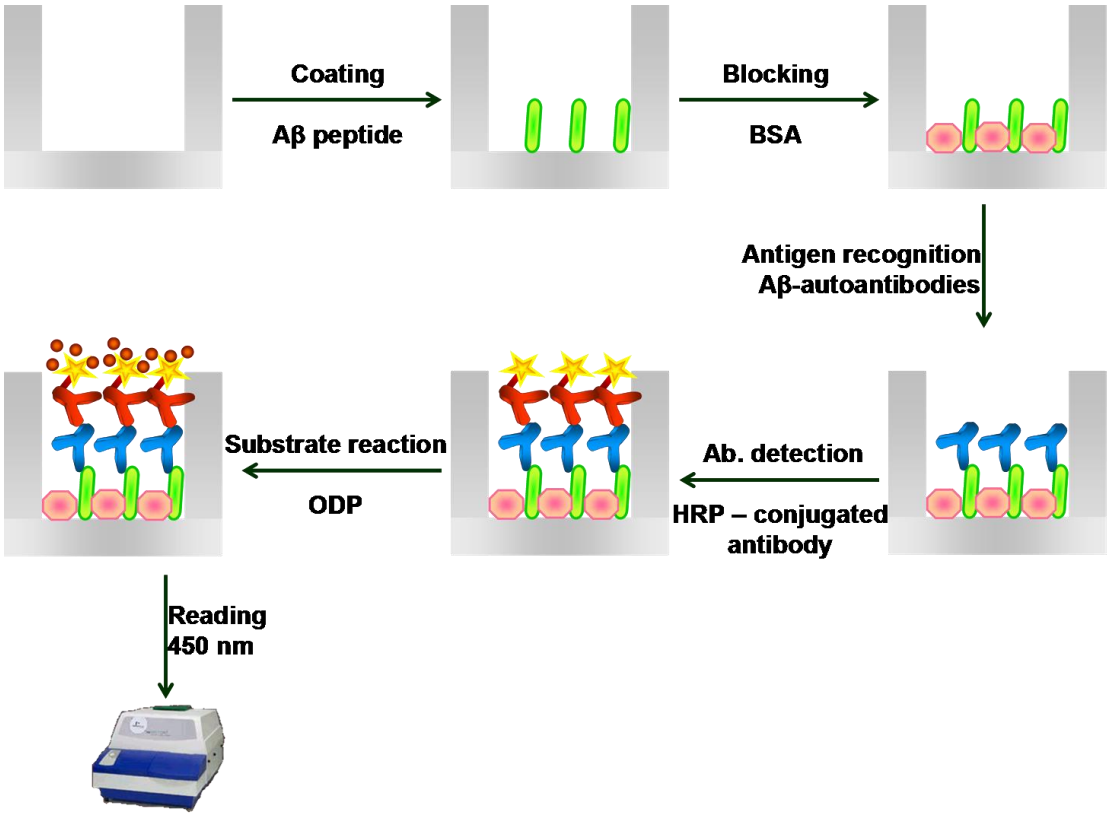

Figure 83. Schematic representation of indirect ELISA.

3.9.2. Preparation of antibody columns used in affinity–mass spectrometric studies

The affinity material (NHS-activated 6-aminohexanoic acid-coupled Sepharose 4B) containing NHS-esters reacts with accessible α-anime groups of the peptides or proteins. A covalent amide bond is formed when the NHS-ester cross-linking agent reacts with a primary amine, releasing N-hydroxysuccinimide (NHS) [71, 144, 145.].

Activated CH-Sepharose® 4B" (SIGMA) was used as matrix for the affinity column. 100 µg Antibody was dissolved in coupling buffer (0.1M NaHCO3; 0.5M NaCl; pH 8,3) and mixed with 66.6 mg NHS-activated Sepharose for 2h at room temperature. The entire matrix is transferred into a micro-column. The uncoupled antibody is removed and the matrix is washed alternatively 3 times with 6 mL washing buffer (0.1 M NaOAc; 0.5 M NaCl,

pH 4) and with 6 mL blocking buffer (0.1 M Ethanolamine; 0.5 M NaCl, pH 8.3).

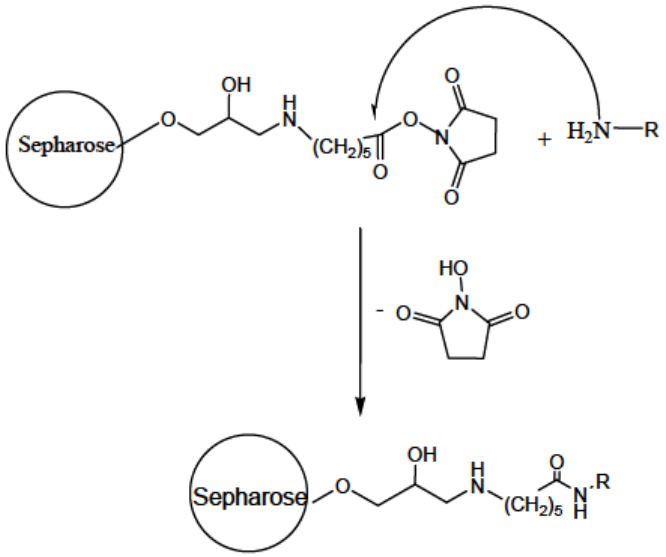

Figure 84. Principle of the antibody immobilization to the NHS-Sepharose.

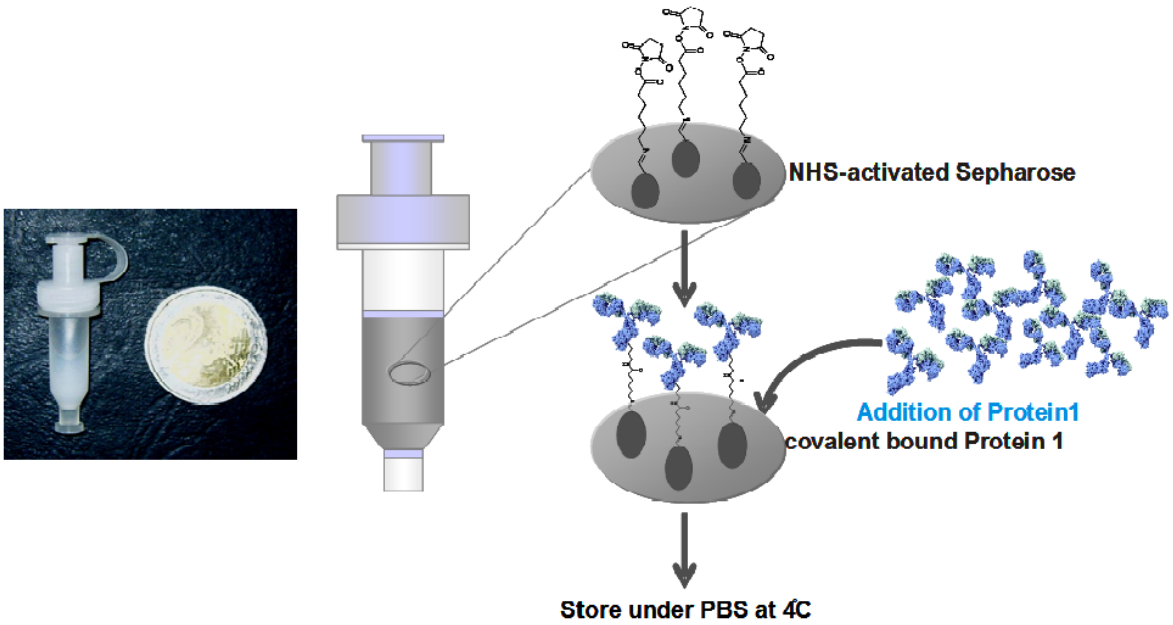

Figure 85. Antibody column preparation for the affinity-mass spectrometry experiments

The remaining free NHS-activated carboxy-groups of the Sepharose were inactivated with blocking buffer at room temperature for 2h. The matrix is then washed again alternatively 3 times with 6 ml washing buffer (0,1M NaOAc; 0,5M NaCl, pH 4) and with 6ml blocking buffer (0,1M Ethanolamine; 0,5M NaCl, pH 8, 3). For usage the column was washed with 10 ml PBS saline and store at 4°C. For long time storage at 4 °C, 1 mM Na_2HPO_4, 136 mM NaCl, 2.7 mM KCl and 0.01% NaN_3 (pH 7.3) was used.

3.9.3. Affinity-mass spectrometry

Affinity-mass spectrometry was carried out on the antibody micro-column which contains Aβ-autoantibody specific antibody immobilized on Sepharose 4B. The affinity procedure is developing as follows: a mixture containing antigens was loaded on the column and after binding, the solution was drained and collected; the column was washed for impurities and the last washing fraction was collected before the elution; the elution was performed and the fractions collected; at the end, the collected solutions were desalted and concentrated by lyophilization and analyzed by mass spectrometry [71, 145.].

A priori the affinity experiment, the column was washed with 20 mL PBS. 10 µg Aβ-peptide in 500 µL PBS is added on the column. The antibody column with Aβ-peptide is incubated at 37 °C for 3 h and in the end the supernatant was collected. Column was washed with 80 mL PBS and with 20 mL MilliQ. Last mL was collected. Elution was performed 3x with 0.5 mL 0.1 % TFA pH 1.9. At the end the column was regenerated with 10 mL PBS and stored at 4°C. The supernatant, last wash and elution fractions were lyophilized and desalting was performed on ZipTip micro column. The desalted samples were loaded on a MALDI target and measured by MALDI-ToF-MS.

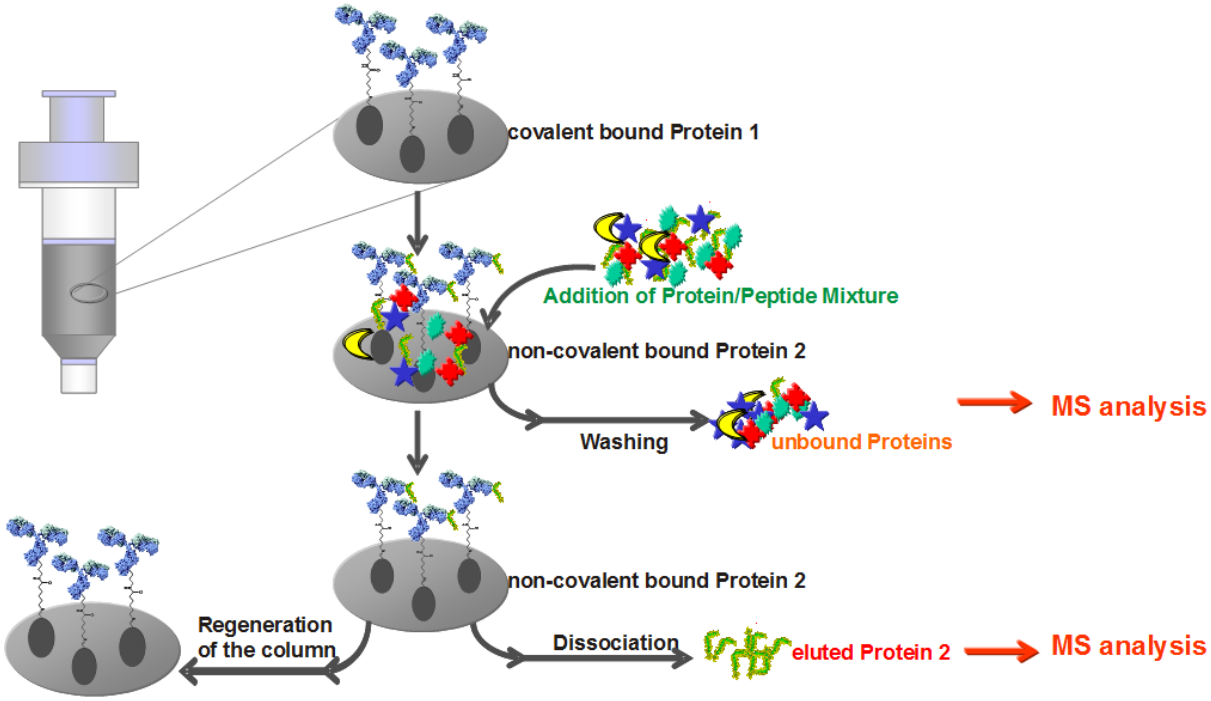

Figure 86. Schematic representation of affinity-mass spectrometry principle.

3.9.4. SAW-biosensor

The biosensor system used (S-Sens® K5 System, Biosensor GmbH, Bonn, Germany) is based on surface acoustic waves. The waves are produced through inverse piezoelectric effect on the surface of quartz chip covered with a thin layer of gold. Viscosity changes and mass loadings on the chip's surface affect the phase and amplitude of the acoustic waves, which are transformed back into electrical signal through direct piezoelectric effect [146, 147.]. The biosensor employs special shear waves of Love type to achieve high sensitivity in detecting interactions that take place in solution. Love waves, proper to a very thin layer of substance, coupled with displacement of matter parallel to the interface solid-liquid permit a high conservation of wave energy making them very sensible to surface effects (i.e. mass loading and viscosity changes) and lowers the noise level in the signal.

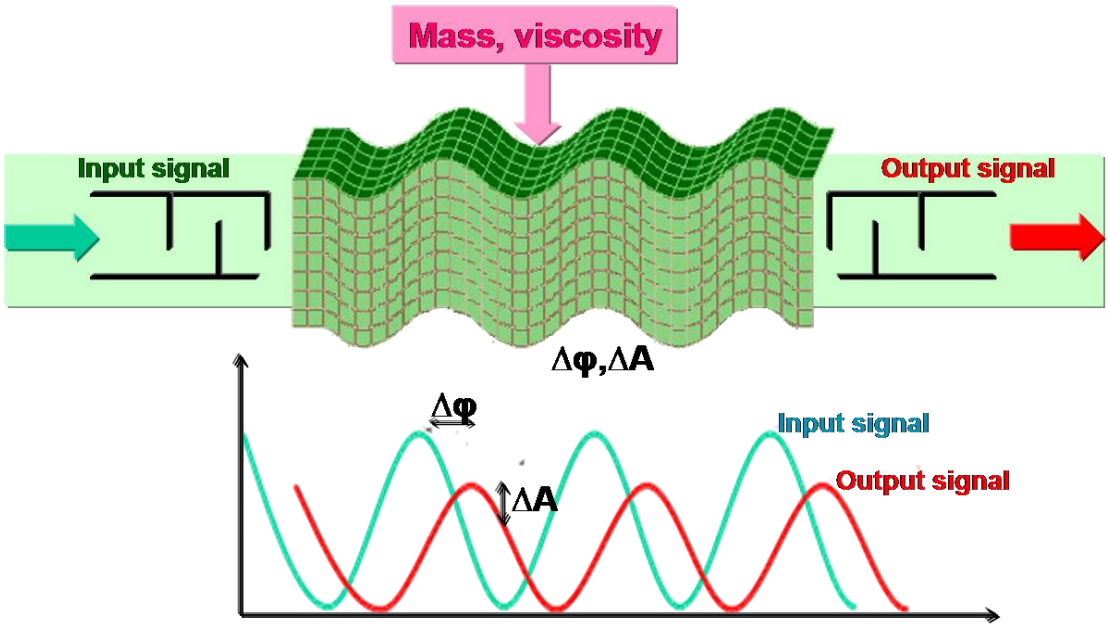

Figure 87. Principle of the surface acoustic wave (SAW) biosensor. An electric field is converted into a mechanical wave through a piezoelectric effect. When the surface mass loading and/or liquid viscosity change, the wave will change its amplitude and phase and it is converted into electrical signal for processing. Δφ represents the phase shift and ΔA the amplitude difference.

The central element in the instrument structure is the quartz sensor chip containing five sensor elements, where the surface acoustic waves are produced, allowed to travel along the surface and transformed back into electrical signal for analysis[148-150.]. Mass loading on the chip's surface and liquid viscosity changes in the liquid running on it will induce modifications in the amplitude and phase of the acoustic wave. In particular, mass loading will cause phase shifts, whereas viscosity changes produces modifications in both phase and amplitude [110, 112, 151-154.]. The quartz chips are covered with a thin gold coating, used for immobilization of different compounds containing sulphur (i.e. thiol groups). In the present work 16-mercaptohexadecanoic acid was used as a linker.

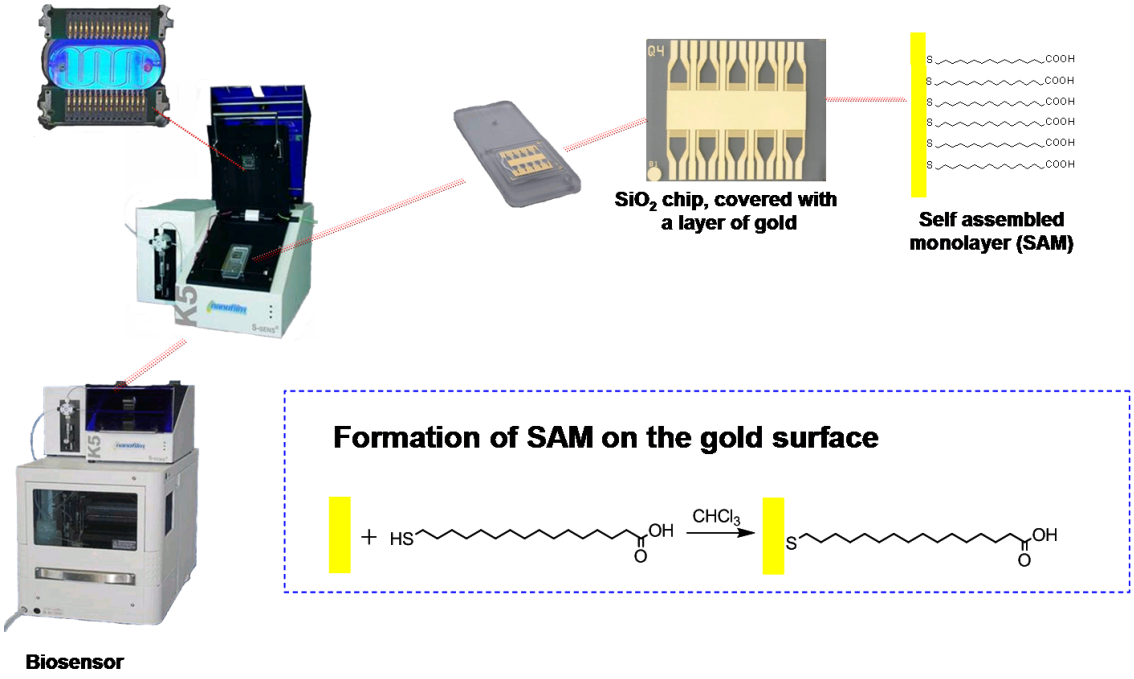

Figure 88. S-Sens® K5 Biosensor System. The instrument has 2 main parts: autosampler and main biosensor containing the quartz- sensor system, electronics and syringe pump. The quart-sensor system is complementary with the SiO_2 chip, covered with a thin layer or gold forming 5 different channels. On gold reacts with -SH group of 16-mercaptohexadecanoic acid to form Self Assembled Monolayer (SAM).

The chip is kept overnight in a 10 μM solution of 16-mercaptohexadecanoic acid (5.77 mg acid in 2 mL chloroform) to form a so called self assembled monolayer (SAM) after the reaction of the thiol groups with the gold surface. The hydrocarbonated chains align parallel one to anther due to hydrophobic effect, and the carboxyl groups orient themselves at the free surface. Different compounds containing free amino groups can be covalently immobilized by forming a peptide bond with these groups. However, the reactivity of the carboxyl groups must be enhanced for the formation of the peptide bond. This can be achieved by modifying the carboxyl into an active ester.

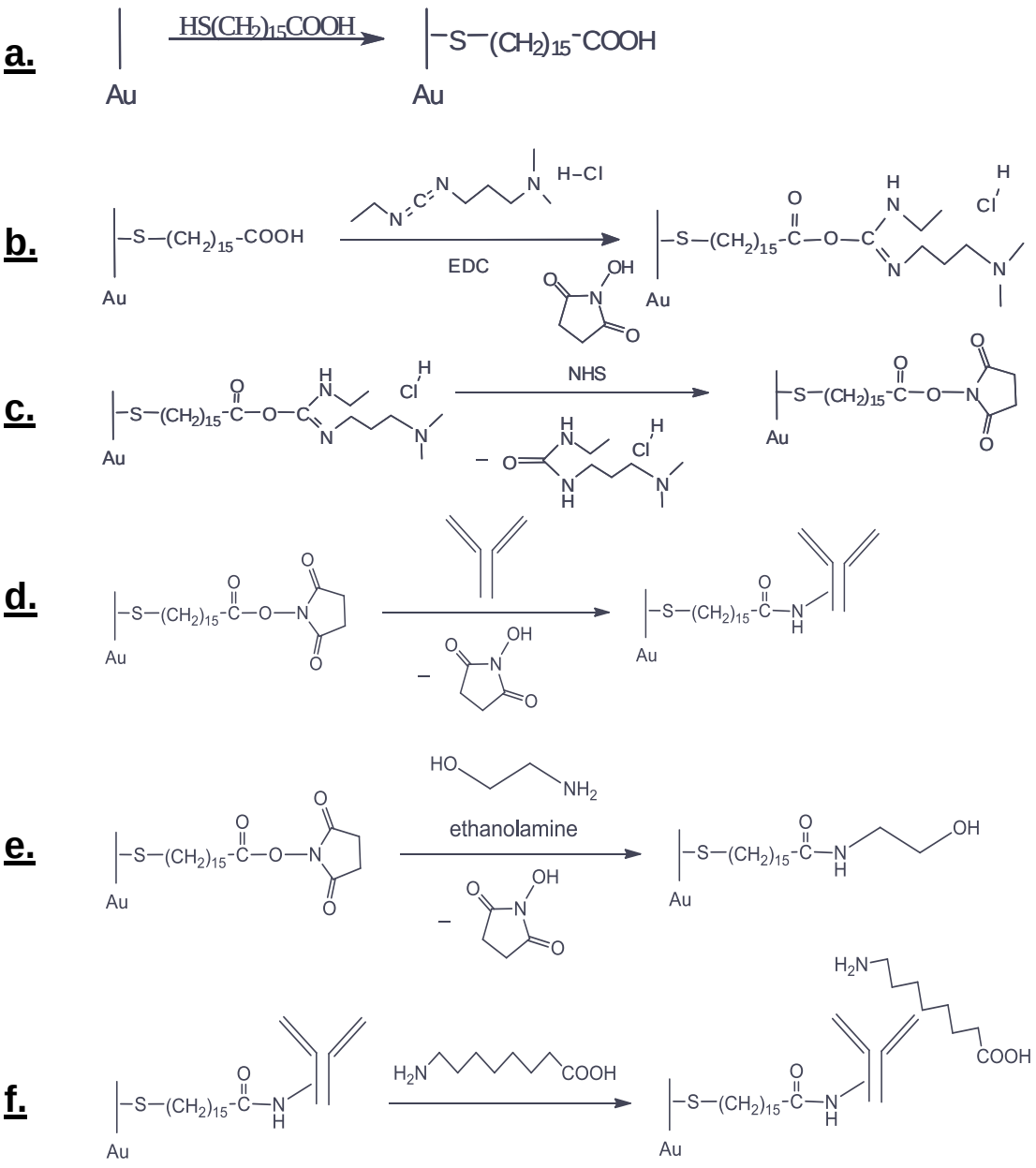

Figure 89. Chemistry involved in biosensor experiments. a. - formation of self assembled monolayer; b.&c. - activation of the carboxyl groups of SAM; d. - covalently bound protein (in this case antibody) via ammino group; e. - blocking of the remaining free sites with ethanolamine; f. - affinity bound partner (in this case peptide antigen) to be quantified by Biosensor instrument. **[110, 112, 151-154.]**

After the chip is placed in the instrument under air free liquid, first injection will contain a mixture of 200 mM EDC (1-ethyl-3-(3-dimethylaminopropyl) carbodiimide) and 50 mM NHS (N-hydroxysuccinimide) solutions, in a volumetric ratio of 1:1. The resulting hydroxysuccinimide ester reacts with

the compound to be immobilized (peptide, protein or antibody), injections of different concentrations and volumes being used. The free remaining active ester groups are blocked with 1M solution of ethanolamine, pH 8.5. By injecting solutions of different compounds, their affinity to the immobilized partner can be observed. To elute the affinity bound compounds from the chip the pH of the buffer is changed to 2,5 from 7.

$$515 = \frac{\varphi\ (^{\circ})}{m\ (\mu g) \times A(cm^2)}$$

This was possible by injecting acidic solutions as 0,1 % trifluoroacetic acid, 2 % formic acid, glycine 50 mM (adjusted to pH 2.0) or HCl 0.1 M (pH 1.0). The gold coated chips can be reused after a thorough cleaning step with Piranha-solution (H_2O_2 30 % / H_2SO_4 98 % 1:1) for 45 min, that would each all organic compounds on the surface. The quantity of bound compound to the chip can be evaluated from the measured phase shift (recorded with the K15 software) using the following sensitivity calibration factor:

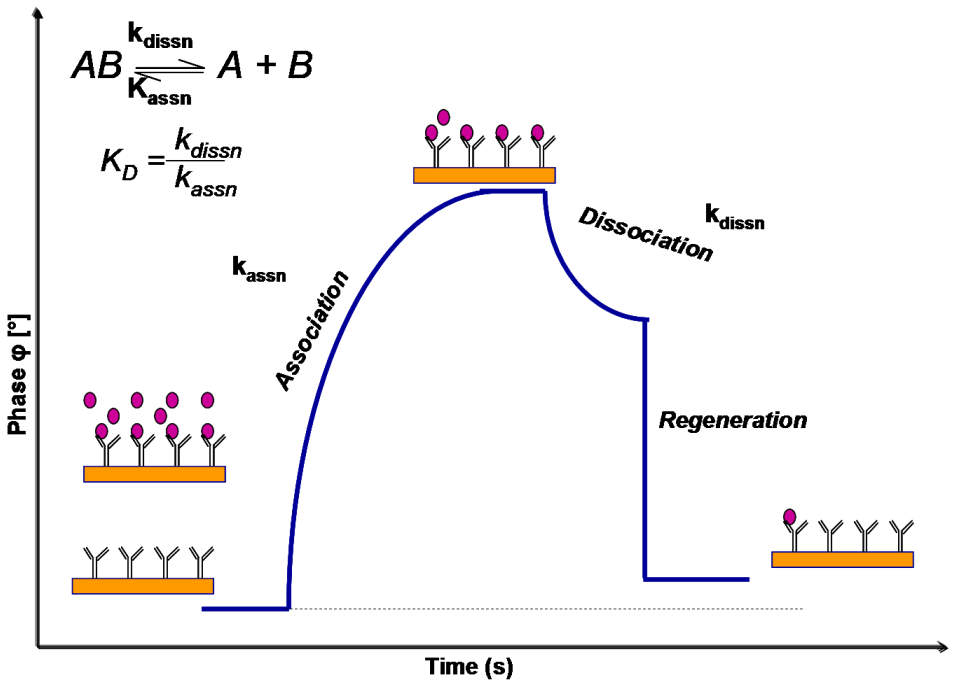

Figure 90. Biosensor sensogram used for the determination of K_D [110, 112, 151-154.].

For K_D determinations, Aβ (1-40) was immobilized on the chip and the affinity was investigated at different concentrations of Aβ-autoantibody found in solution, in a sequential series of injections, each of them followed by an acidic elution step (regeneration of the antibody surface).The measurements were recorded and the instrument was controlled by the Biosense K12 software. The series of injections from autosampler was programmed using the SequenceMaster 6.0 software. The binding curves were analyzed with Origin Pro 7.5 and its engine was also employed by FitMaster for fitting the binding curves according to a mathematical model that considered a remaining residue affinity bound to the surface even after the acidic elution step, as well as for determining the dissociation and association reaction rates (k_{off} and k_{on}) from the shape of the fitted curves. A linear best fit was applied using the equation $K_{obs} = k_{off} + k_{on} * C$. The average k_{off} [Unit in sec-1] equals the intersection with the y-axis. The slope of the fitted straight line is a measure of the k_{on} rate [Unit in Conc-1 sec-1]. The K_D value was calculated with $K_D = k_{off} / k_{on}$[110, 112, 151-154.].

3.10. Software for data acquisition and processing

3.10.1. GPMAW

GPMAW 5.0 (General Protein/ Mass Analysis for Windows) (Lighthouse Data, Denmark) was used for the molecular weight determination of the peptides. The program made the calculation of the monoisotopic and average masses of the peptides or proteins possible in known MS conditions, also prediction of the proteolytic digestion of peptides and proteins, followed by searching for different fragments having a known mass [155.]. Using this program is possible to introduce different modifications at certain amino acid positions. One can obtain the average and the monoisotopic values for $[M+H]^+$ ions and also the values of fragment ions having different charges. GPMAW 5.0 program may predict

the secondary structure and the hydrophobic nature of a given protein or peptide sequence.

3.10.2. Data Analysis

The Bruker Daltonics DataAnalysis 3.3 was used for processing advanced data acquired on Bruker Daltonics mass spectrometers. Data Analysis was used in multiple analyses at a time and allowed peptide analysis, structural elucidation, and compound identification based on MS and MS/MS spectra [156.].

3.10.3. PDQuest software

PDQuest software was used to scan the Coomassie blue gels, advanced algorithms are available to remove background noise, gel artifacts, and horizontal or vertical streaking from the image [157.].

3.10.4. OriginPro 7.5 with FitMaster plugin

OriginPro 7.5 with FitMaster plug-in was used to fit the sensograms from the biosensor and to calculate the dissociation constant of interactions Aβ-autoantibody - Aβ-peptide and Aβ-peptides – CDR-peptides [158.].

3.10.5. UCSF Chimera

UCSF Chimera is a free visualization system employed in this work for the visualization and modelling of molecular structures [159.]. The program is able to import structures from the most common molecular structure formats such as .pdb. Structures can be visualized with all standards graphical models and coloring methods. Different parts of a molecule can be freely visualized and selected for special tasks.

3.10.6. Online search engines and data bases

a. MascotScience

The MS/MS data were submitted to be compared with the fragmentation spectra of peptides deposited in protein databases. Fragment ions from the acquired data were matched, based on their *m/z* ratio, when possible, with theoretical spectra of peptides derived from *in-silico* digestion of proteins. The MS/MS ion search was performed indicating the experimental conditions: the protease; fix(e.g. carbamidomethyl cysteine, if the protein was reduced and alkylated prior to digestion) and possible variable modifications of amino acids side(e.g. methionine oxidation, deamidation, pyro-Glu formation); type of mass spectrometer (to provide information about the nature of the fragment ions). To perform the searches, the non-redundant NCBI protein database (NCBInr) was employed, which contains entries compiled from a variety of sources, such as GenBank (a genome sequence database from the National Institutes of Health), SWISS-Prot, PRF (Protein Research Foundation), PIR (International Protein Sequence Database), and PDB (Brookhaven Protein Databank) [87.].

Prior to database searching, LC-MS/MS data saved as an *.mgf file. These data were searched against the NCBInr protein data base by means of the Mascot MS/MS Ion Search engine, using a precursor tolerance of 0.2 Da and an MS/MS tolerance of 0.1 Da. Carbamidomethyl cysteine was defined as a fixed modification, whereas variable modifications included methionine and tryptophan oxidation, deamidation (Gln and/or Asn), and N-terminal formation of pyro-Glu and pyro- Gln. The sequences determined from the MS/MS data obtained for the identified peptides were validated manually.

b. BLAST

Basic Local Alignment Search Tool, or BLAST [160.], is an algorithm for comparing primary sequence information of proteins. A BLAST search

enables a researcher to compare a query sequence with a database of sequences, and identify library sequences that resemble the query. The peptides found by data base search and by de novo sequencing were introduced in BLAST to establish their possible position in the antibody sequence.

4. SUMMARY

In the last decade, mass spectrometry (MS) has emerged as a major analytical tool for the determination of protein structures and their biomolecular interactions. Of particular importance are "soft" ionization methods such as matrix assisted laser desorption ionization (MALDI) and electrospray ionization (ESI). MS provides unparalleled high sensitivity and mass determination accuracy for structure determination by means of specific fragmentation techniques. Furthermore, in combination with chromatographic and electrophoretic separation techniques, with proteolytic degradation and with bioaffinity methods, MS is well suitable for the analysis of complex biological samples and for structure determinations in biomedical applications.

The accumulation of extracellular plaques containing neurotoxic β-amyloid (Aβ) peptides in the brain is one of Alzheimer's disease (AD) hallmarks, the most common form of dementia in the aging population. At present, immunotherapy is considered a promising approach in preventing β-amyloid aggregation and accumulation in neuronal tissue. In recent years, it has been shown that naturally occurring Aβ-specific autoantibody is present in blood and cerebrospinal fluid of AD patients and healthy individuals, as well as in immunoglobulin preparations. Currently, Aβ-autoantibody is investigated as potential diagnostic and immunotherapeutic agent for AD. The elucidation of the structural and functional characteristics of Aβ-autoantibody could provide lead structures for AD therapy.

The first chapter of this thesis focused on the affinity-isolation of Aβ-autoantibody from immunoglobulin preparations. Affinity columns were prepared by immobilizing Cys-Aβ(1-40) and Cys-Aβ(12-40) on an

iodoacetyl matrix, followed by the isolation of Aβ-autoantibody and their quantification using a spectrophotometric protein assay. Depending on the type of analysis (structural determination or affinity characterization), different purification methods of isolated Aβ-autoantibody were employed.

In the second, main part of the thesis, the primary structures of polyclonal Aβ-autoantibody were determined. Due to the high variability in the amino acid sequences of the polypeptide chains, several analytical techniques were employed: (i.), chemical modification of Aβ-autoantibody through reduction of disulfide bridges and alkylation of cysteine residues; (ii.), electrophoretic separation of light and heavy chains; (iii.), electroblotting of light and heavy chains, followed by N-terminal Edman sequencing; (iv.), in gel proteolytic digestion using different endoproteases, with the aim of obtaining peptide fragments of different length; (v.), direct mass spectrometric analysis of the proteolytic mixtures. A second, complementary approach consisted of the following steps: (i.), reverse-phase HPLC separation of the proteolytic peptides; (ii.), analysis of HPLC fractions by MALDI-TOF and high resolution MALDI-FTICR mass spectrometry, Edman sequencing and tandem mass spectrometry; and (iii.), manual sequence alignment of Aβ-autoantibody. After separating the light and heavy chains by gel electrophoresis, Edman degradation provided one predominant N-terminal sequence for the heavy chain, and seven sequences for the light chain. In a second approach, in gel digestion with trypsin, LysC and chymotrypsin was performed and monitored by MALDI-TOF MS; the resulting proteolytic mixtures were then separated by analytical HPLC. The LC-MS/MS analysis of the HPLC fractions and the *de novo* sequence data analysis provided all detectable variations in the Aβ-autoantibody sequences for N-terminal, framework, CDRs and constant regions. Manual assembly of the Aβ-autoantibody sequences was carried out by overlapping the fragments and resulted in three complete sequences for the light chain (belonging to λ and κ classes) and in one complete sequence for the heavy chain.

Previous work our laboratory had shown that human Aβ-autoantibody recognizes an epitope located in the C-terminal domain of Aβ, Aβ (21-37). In order to identify the core epitope, affinity experiments (ELISA and affinity-mass spectrometry) were performed with different Aβ-peptides, and provided the shortest Aβ-fragment that binds to Aβ-autoantibody, Aβ (25-35), in agreement with previous epitope determinations. Furthermore, using online surface acoustic wave (SAW) biosensor-MS with overlapping Aβ-fragments, the core epitope recognized by Aβ-autoantibody could be assigned to the region Aβ(25-28)' (GSNK), which corresponds to the turn region of the Aβ-peptide. This result explains the binding of autoantibody to monomeric Aβ-peptide, but not to high molecular aggregates and plaques.

In the last chapter of the thesis, peptides comprising the CDR regions of both light and heavy chains of the Aβ-autoantibody were synthesized by solid phase peptide synthesis, purified by RP-HPLC and characterized by MS. The affinity of the synthetic CDR peptides towards Aβ was investigated by affinity-MS and online SAW-MS. It was found that synthetic peptides from CDR 1 and CDR2 from both the light and heavy chains bind to Aβ, in contrast to CDR3 containing peptides. These results were in agreement with a 3D structure modeling of the Aβ-autoantibody, which showed a limited surface exposure of the CDR3 regions. Furthermore, the binding constants K_D of the complexes formed between Aβ(1-40) and synthetic CDR-peptides were determined by SAW-affinity and found to be in the low micromolar range for CDR 1 and 2 peptides, in good agreement with the K_D of 840 nM for the complete antibody.

5. ZUSAMMENFASSUNG

In den letzten Jahren hat sich die die Massenspektrometrie (MS) zu einer zentralen analytischen Methode zur Aufklärung von Protein- Strukturen, und deren supramolekularen Interaktionen entwickelt, insbesondere bei Verwendung von „sanften“ MS- Ionisierungsmethoden wie Matrix-unterstützte Laserdesorption (MALDI-MS) und Elektrospray (ESI). ESI- und MALDI- Massenspektrometrie liefern hohe Empfindlichkeit, Massengenauigkeit, beieringem Substanzbedarf zur exakten Strukturbestimmung durch Fagmentierungsmethoden. Darüber hinaus wird die Massenspektrometrie in Kombination mit anderen Methoden, wie z.B. chromatographischen und elektrophoretischen Trennmethoden, proteolytischen Assays, , Bio-Affinitäts- Nachweis, spezifischen chemischen Modifizierungen von Aminosäuren sowie Bioinformatik-Verfahren mit großem Erfolg für komplexe Proben und Strukturmodifizierungen angewendet.

Die Alzheimersche Krankheit (AD) ist die meist verbreitete Neurodemenz der älteren Bevölkerung. Hauptmerkmal der AD ist die Bildung und Assoziation von extrazellulären Plaques im Gehirn, die neurotoxische β-Amyloid-Peptide (Aß) beinhalten. Immunotherapie wird als eine wirksame und vielversprechende neue Methode zur Vermeidung von Aß-Aggregatbildung und Akkumulierung im Nervengewebe, und zur Zerstörung der Aβ-Plaques angesehen. In den letzten Jahren wurde das Vorliegen von endogenen Aß- Autoantikörpern im Blut, CSF und in Immunoglobulin Präparaten nachgewiesen. Im ersten Abschnitt der vorliegenden Dissertation wird die Isolierung von Aβ-Autoantikörpern aus humanen Immunglobulinfraktionen beschrieben. Zur Antikörperisolierung wurden Cys-Aβ(1-40) und Cys-Aβ(1-40) in Affinitätsäulen auf einer Iodocetyl-matrix immobilisiert. Im Anschluss an die Affinitätsisolierung wurde die Quantifizierung der Aβ-Autoantikörper mittels BCA-

ProteinAssay. Für diese Untersuchungen, besonders zur zur Stukturaufklärung und Affinitäts-Charakterisierung, wurden verschiedene Probenpräperationsmethoden entwickelt und angewendet.

Der zweite und Hauptteil der Dissertation ist der Bestimmung der Primärstruktur der Aβ-Autoantikörper gewidmet. Aufgrund der hohen Variation der Polypeptidketten wurde eine kombinierte analytische Strategie eingesetzt, die chemische Modifizierungen durch Alkylierung von Cysteine-Resten, elektrophoretische Trennung von leichten und schweren Ketten,, N-terminale Partialdequenzierung der leichten und schweren Ketten durch Edman-Abbau, proteolytischen Abbau im Gel mit verschiedenen Endoproteasen, massenspektrometrische Charakterisierung der proteolytischen Gemische; HPLC-Trennung der proteolytischen Peptide, sowie die Analyse aller HPLC-Fraktionen durch MALDI-TOF-Massenspektrometrie, und Tandem-Massenspektrometrie umfasste. . Nach der Trennung von leichten und schweren Ketten durch Gelelektrophorese lieferte die Edman- Sequenzierung eine dominierende N-terminale Sequenz derschweren Kette, sowie 7 Sequenzen der leichten Kette. Zur “bottom-up” Strukturbestimmung wurde proteolytischer Abbau im Gel mit Trypsin, Lys C und Chemotrypsin, sowie anschliessende analytische HPLC-Trennung der proteolytischen Fragmente durchgeführt.

Die MALDI- ToF- MS ermöglichte die schnelle Analyse des proteolytischen Abbaus. Durch HPLC - Tandem -Massenspektrometrie - Analyse der HPLC-Fraktionen und de novo Datenanalyse - konnten die Aβ-Autoantikörper - Sequenzen aller Regionen (N-terminale Bereiche, Framework, CDR- und konstante Regionen) aufgeklärt werden. Die Aβ-Autoantikörper - Sequenzen wurden durch überlappende Sequenzfragmente ermittelt; hierdurch wurden drei vollständige und 33 partielle Sequenzen für die leichte Kette (λ und κ Klassen), sowie eine vollständige und 41 partielle Sequenzen für die schwere Kette (IgG1 und IgG2) erhalten.

Humane physiologische Aβ-Autoantikörper oder "Plaque-spezifische Antikörper " erkennen ein Epitop im C-terminalen Bereich vonAβ-. Durch SAW- Biosensor- Experimente konnte die Bindungskonstante K_D eines Aβ-Peptid – Aβ-Autoantikörper - Komplexes von ca. 800 nM bestimmt werden. Affinitäts-Experimente (ELISA, Affinitäts- Massenspektrometrie) verschiedener verkürzter Aβ-Peptide zeigten Aβ (25-35) als das kürzeste Fragment mit Affinität zum Aβ-Autoantikörper; dieses Ergebnis ist iin Übereinstimmung mit früheren Epitop- Bestimmungen, in denen das Epitop Aβ (21-37) identifiziert wurde. Die Epitop-Region wurde aus überlappenden Aβ-Fragmenten unter Verwendung der Affinitäts-Massenspektrometrie und Online-Biosensor-Massenspektrometrie identifiziert. Die Ergebnisse zeigten das „Core“-Epitop im BereichAß(25-28) (GSNK) in der „Turn-Region“ des Aβ- Peptids, das von zentraler Bedeutung fürdie Aggregation ist. Die Position des Epitops erkärtdie Bindung von Autoantikörpern an monomeres und oligomeres Aβ, , jedoch nichtan hochmolekulare Aggregate.

Im letzten Kapitel der Dissertation wurden Aβ-Autoantikörper- Peptide aus den CDR-Regionen der leichten und schweren Ketten durch Festphasenpeptidsynthese synthetisiert, mittelsHPLC gereinigt und durch Massenspektrometrie charakterisiert. Ihre Affinität zu Aβ wurde durch Affinitäts - Massenspektrometrie und Biosensor- MS, nachImmobilisierung von Aβ an Sepharose , untersucht. Die Ergebnisse zeigten, dass Peptide der leichten und schweren Ketten von CDR-1 und CDR-2 an Aβ binden, jedoch nicht von CDR-3, in Übereinstimmung mit Ergebnissen der 3D-Strukturmodellierung der Aβ-Autoantikörper, die nur geringe Oberflächenzugänglichkeit für CDR- 3 bsitzen. Die K_D-Werte der Aβ-CDR- Komplexe wurden durch SAW-Biosensor bestimmt, und befinden sich im unteren mikromolaren Bereich.

6. BIBLIOGRAPHY

1. Reports B: Mass Spectrometry 2013: A Focus on Sales Growth In Industry reports. Biopharm Reports; 2013:262.

2. Grayson MA: Measuring mass : from positive rays to proteins. Philadelphia: Chemical Heritage Press; 2002.

3. [http://www.nobelprize.org/nobel_prizes/lists/all/index.html]

4. Gross ML, Caprioli RM: Encyclopedia of mass spectrometry. 1st edition. Amsterdam ; Boston: Elsevier; 2003.

5. Encyclopedia of mass spectrometry : applications to biology: peptides and proteins. 1st edition. San Diego, CA: Elsevier; 2004.

6. Watson JT, Sparkman OD: Introduction to mass spectrometry : instrumentation, applications and strategies for data interpretation. 4th edition. Cwhichester, England ; Hoboken, NJ: John Wiley & Sons; 2007.

7. Fenn JB, Mann M, Meng CK, Wong SF, Whitehouse CM: Electrospray ionization for mass spectrometry of large biomolecules. Science 1989, 246(4926):64-71.

8. Gaskell S: Electrospray: Principles and practice (vol 32, pg 677, 1997). J Mass Spectrom 1997, 32(12):1378-1378.

9. Smith RD, Loo JA, Loo RRO, Busman M, Udseth HR: Principles and Practice of Electrospray Ionization - Mass-Spectrometry for Large Polypeptides and Proteins. Mass Spectrom Rev 1991, 10(5):359-451.

10. Koenig S: Biomacromolecular mass spectrometry research progress. New York: Nova Science Publishers; 2008.

11. Matthiesen R: Mass spectrometry data analysis in proteomics. New York: Springer; 2013.

12. Perdivara I, Deterding L, Moise A, Tomer KB, Przybylski M: Determination of primary structure and microheterogeneity of a beta-amyloid plaque-specific antibody using high-performance LC-tandem mass spectrometry. Anal Bioanal Chem 2008, 391(1):325-336.

13. Abbas AK, Lichtman AH, Pillai S: Cellular and molecular immunology. 7th edition. Philadelphia: Elsevier/Saunders; 2012.

14. Rodgers JR, Rich RR: Molecular biology and immunology: an introduction. J Allergy Clin Immunol 1991, 88(4):535-551.

15. Reineke U, Schutkowski M: Epitope mapping protocols. 2nd edition. New York: Humana Press; 2009.

16. Fiedler W, Borchers C, Macht M, Deininger SO, Przybylski M: Molecular characterization of a conformational epitope of hen egg white lysozyme by differential chemical modification of immune complexes and mass spectrometric peptide mapping. Bioconjug Chem 1998, 9(2):236-241.

17. Macht M, Fiedler W, Kurzinger K, Przybylski M: Mass spectrometric mapping of protein epitope structures of myocardial infarct markers myoglobin and troponin T. Biochemistry 1996, 35(49):15633-15639.

18. Dragusanu M, Petre BA, Slamnoiu S, Vlad C, Tu T, Przybylski M: On-line bioaffinity-electrospray mass spectrometry for simultaneous detection, identification, and quantification of protein-ligand interactions. J Am Soc Mass Spectrom 2010, 21(10):1643-1648.

19. Abrahamson M, Islam MQ, Szpirer J, Szpirer C, Levan G: The Human Cystatin-C Gene (Cst3), Mutated in Hereditary Cystatin-C Amyloid

Angiopathy, Is Located on Chromosome-20. Hum Genet 1989, 82(3):223-226.

20. Juszczyk P, Paraschiv G, Szymanska A, Kolodziejczyk AS, Rodziewicz-Motowidlo S, Grzonka Z, Przybylski M: Binding Epitopes and Interaction Structure of the Neuroprotective Protease Inhibitor Cystatin C with beta-Amyloid Revealed by Proteolytic Excision Mass Spectrometry and Molecular Docking Simulation. J Med Chem 2009, 52(8):2420-2428.

21. Przybylski M, Stefanescu R, Bacher M, Manea M, Moise A, Perdivara I, Marquardt A, Dodel RC: Molecular approaches for immuno-therapy and diagnosis of Alzheimer's disease based on epitope-specific anti-beta-amyloid antibodies. J Pept Sci 2006, 12:99-99.

22. Decker JM: Introduction to immunology. Malden, Mass.: Blackwell Science; 2000.

23. Warrington R, Watson W, Kim HL, Antonetti FR: An introduction to immunology and immunopathology. Allergy Asthma Clin Immunol 2011, 7 Suppl 1:S1.

24. Cunningham BA, Rutishauser U, Gall WE, Gottlieb PD, Waxdal MJ, Edelman GM: The covalent structure of a human gamma G-immunoglobulin. VII. Amino acid sequence of heavy-chain cyanogen bromide fragments H1-H4. Biochemistry 1970, 9(16):3161-3170.

25. Edelman GM: The covalent structure of a human gamma G-immunoglobulin. XI. Functional implications. Biochemistry 1970, 9(16):3197-3205.

26. Gall WE, Edelman GM: The covalent structure of a human gamma G-immunoglobulin. X. Intrachain disulfide bonds. Biochemistry 1970, 9(16):3188-3196.

27. Gottlieb PD, Cunningham BA, Rutishauser U, Edelman GM: The covalent structure of a human gamma G-immunoglobulin. VI. Amino acid sequence of the light chain. Biochemistry 1970, 9(16):3155-3161.

28. Hood LE, Potter M, McKean DJ: Immunoglobulin structure: amino terminal sequences of kappa chains from genetically similar mice (BALB/c). Science 1970, 170(3963):1207-1210.

29. Happell BM, Gaskin CJ, Hoey W, Nizette D, Veach K: The activities that nurses working in community mental health perform: a geographical comparison. Aust Health Rev 2013, 37(4):453-457.

30. Maurer K, Volk S, Gerbaldo H: Auguste D and Alzheimer's disease. Lancet 1997, 349(9064):1546-1549.

31. Shastry BS: Molecular and cell biological aspects of Alzheimer disease. J Hum Genet 2001, 46(11):609-618.

32. Morohashi Y, Tomita T, Iwatsubo T: [Molecular targeted therapy in Alzheimer disease]. Nihon Rinsho 2010, 68(10):1906-1910.

33. Bettens K, Sleegers K, Van Broeckhoven C: Current status on Alzheimer disease molecular genetics: from past, to present, to future. Hum Mol Genet 2010, 19(R1):R4-R11.

34. Octave JN: [Alzheimer disease: cellular and molecular aspects]. Bull Mem Acad R Med Belg 2005, 160(10-12):445-449; discussion 450-441.

35. Johnson HL, Gaskins SW, Seibert DC: Clinical skill and knowledge requirements of health care providers caring for children in disaster, humanitarian and civic assistance operations: an integrative review of the literature. Prehosp Disaster Med 2013, 28(1):61-68.

36. Rendell PG, Bailey PE, Henry JD, Phillips LH, Gaskin S, Kliegel M: Older adults have greater difficulty imagining future rather than atemporal experiences. Psychol Aging 2012, 27(4):1089-1098.

37. Glenner GG, Wong CW: Alzheimer's disease and Down's syndrome: sharing of a unique cerebrovascular amyloid fibril protein. Biochem Biophys Res Commun 1984, 122(3):1131-1135.

38. Glenner GG, Wong CW: Alzheimer's disease: initial report of the purification and characterization of a novel cerebrovascular amyloid protein. Biochem Biophys Res Commun 1984, 120(3):885-890.

39. Glenner GG, Wong CW, Quaranta V, Eanes ED: The amyloid deposits in Alzheimer's disease: their nature and pathogenesis. Appl Pathol 1984, 2(6):357-369.

40. Gaal P, Szigeti S, Panteli D, Gaskins M, van Ginneken E: Major challenges ahead for Hungarian healthcare. BMJ 2011, 343:d7657.

41. Savage MJ, Trusko SP, Howland DS, Pinsker LR, Mistretta S, Reaume AG, Greenberg BD, Siman R, Scott RW: Turnover of amyloid beta-protein in mouse brain and acute reduction of its level by phorbol ester. J Neurosci 1998, 18(5):1743-1752.

42. Pike CJ, Ramezan-Arab N, Cotman CW: Beta-amyloid neurotoxicity in vitro: evidence of oxidative stress but not protection by antioxidants. J Neurochem 1997, 69(4):1601-1611.

43. Pike CJ, Ramezan-Arab N, Miller S, Cotman CW: beta-Amyloid increases enzyme activity and protein levels of glutamine synthetase in cultured astrocytes. Exp Neurol 1996, 139(1):167-171.

44. Zhao WQ, De Felice FG, Fernandez S, Chen H, Lambert MP, Quon MJ, Krafft GA, Klein WL: Amyloid beta oligomers induce impairment of neuronal insulin receptors. FASEB J 2008, 22(1):246-260.

45. Hartley DM, Walsh DM, Ye CP, Diehl T, Vasquez S, Vassilev PM, Teplow DB, Selkoe DJ: Protofibrillar intermediates of amyloid beta-protein induce acute electrophysiological changes and progressive neurotoxicity in cortical neurons. J Neurosci 1999, 19(20):8876-8884.

46. Abel FL, Wilson SP, Zhao RR, Fennell WH: Cocaine depresses the canine myocardium. Circ Shock 1989, 28(4):309-319.

47. Gaskell CJ, Gaskell RM: Some other virus infections of cats. Vet Quart 1997, 19:S49-S50.

48. Stefanescu R: Molecular Identification of Antigen Recognition Structures in Immune Complexes for Immunotherapeutic Applications by Proteolytic and Mass Spectrometric Methods. Universität Konstanz, Chemistry; 2007.

49. Walker JR, Pacoma R, Watson J, Ou W, Alves J, Mason DE, Peters EC, Urbina HD, Welzel G, Althage A *et al*: Enhanced proteolytic clearance of plasma Abeta by peripherally administered neprilysin does not result in reduced levels of brain Abeta in mice. J Neurosci 2013, 33(6):2457-2464.

50. Boche D, Nicoll JA: The role of the immune system in clearance of Abeta from the brain. Brain Pathol 2008, 18(2):267-278.

51. Love S, Kehoe PG: Clearance of Abeta from the brain in Alzheimer's disease. Foreword. Brain Pathol 2008, 18(2):239.

52. Cloe AL, Orgel JP, Sachleben JR, Tycko R, Meredith SC: The Japanese mutant Abeta (DeltaE22-Abeta(1-39)) forms fibrils

instantaneously, with low-thioflavin T fluorescence: seeding of wild-type Abeta(1-40) into atypical fibrils by DeltaE22-Abeta(1-39). Biochemistry 2011, 50(12):2026-2039.

53. Sarell CJ, Syme CD, Rigby SE, Viles JH: Copper(II) binding to amyloid-beta fibrils of Alzheimer's disease reveals a picomolar affinity: stoichiometry and coordination geometry are independent of Abeta oligomeric form. Biochemistry 2009, 48(20):4388-4402.

54. Fandrich M, Meinhardt J, Grigorieff N: Structural polymorphism of Alzheimer Abeta and other amyloid fibrils. Prion 2009, 3(2):89-93.

55. Zhang A, Qi W, Good TA, Fernandez EJ: Structural differences between Abeta(1-40) intermediate oligomers and fibrils elucidated by proteolytic fragmentation and hydrogen/deuterium exchange. Biophysical Journal 2009, 96(3):1091-1104.

56. Liu YH, Giunta B, Zhou HD, Tan J, Wang YJ: Immunotherapy for Alzheimer disease: the challenge of adverse effects. Nat Rev Neurol 2012, 8(8):465-469.

57. Gouras GK: Immunotherapy for Alzheimer disease. MAbs 2009, 1(2):112-114.

58. Spires-Jones TL, Mielke ML, Rozkalne A, Meyer-Luehmann M, de Calignon A, Bacskai BJ, Schenk D, Hyman BT: Passive immunotherapy rapidly increases structural plasticity in a mouse model of Alzheimer disease. Neurobiol Dis 2009, 33(2):213-220.

59. Rosenberg RN: Immunotherapy for Alzheimer disease: the promise and the problem. Arch Neurol 2005, 62(10):1506-1507.

60. Ozerlat I: Alzheimer disease: CSF biomarkers could be used in Abeta immunotherapy trials for AD. Nat Rev Neurol 2012, 8(6):297.

61. Martin-Jones Z, Lasagna-Reeves C: Which is a better target for AD immunotherapy, A beta or tau? Alzheimer Dis Assoc Disord 2008, 22(2):111-112.

62. Geylis V, Steinitz M: Immunotherapy of Alzheimer's disease (AD): from murine models to anti-amyloid beta (Abeta) human monoclonal antibodies. Autoimmun Rev 2006, 5(1):33-39.

63. Raman EP, Takeda T, Barsegov V, Klimov DK: Mechanical unbinding of abeta peptides from amyloid fibrils. J Mol Biol 2007, 373(3):785-800.

64. Bodles AM, Guthrie DJ, Harriott P, Campbell P, Irvine GB: Toxicity of non-abeta component of Alzheimer's disease amyloid, and N-terminal fragments thereof, correlates to formation of beta-sheet structure and fibrils. European Journal of Biochemistry 2000, 267(8):2186-2194.

65. Shin RW, Ogino K, Kondo A, Saido TC, Trojanowski JQ, Kitamoto T, Tateishi J: Amyloid beta-protein (Abeta) 1-40 but not Abeta1-42 contributes to the experimental formation of Alzheimer disease amyloid fibrils in rat brain. J Neurosci 1997, 17(21):8187-8193.

66. Rodriguez-Rodriguez C, Rimola A, Rodriguez-Santiago L, Ugliengo P, Alvarez-Larena A, Gutierrez-de-Teran H, Sodupe M, Gonzalez-Duarte P: Crystal structure of thioflavin-T and its binding to amyloid fibrils: insights at the molecular level. Chem Commun 2010, 46(7):1156-1158.

67. Maftei M, Thurm F, Leirer VM, von Arnim CA, Elbert T, Przybylski M, Kolassa IT, Manea M: Antigen-bound and free beta-amyloid autoantibody in serum of healthy adults. PLoS One 2012, 7(9):e44516.

68. Yanagi K, Sakurai K, Yoshimura Y, Konuma T, Lee YH, Sugase K, Ikegami T, Naiki H, Goto Y: The monomer-seed interaction mechanism in

the formation of the beta2-microglobulin amyloid fibril clarified by solution NMR techniques. J Mol Biol 2012, 422(3):390-402.

69. Singh PK, Maji SK: Amyloid-like fibril formation by tachykinin neuropeptides and its relevance to amyloid beta-protein aggregation and toxicity. Cell Biochem Biophys 2012, 64(1):29-44.

70. Ma Q, Fan JB, Zhou Z, Zhou BR, Meng SR, Hu JY, Chen J, Liang Y: The contrasting effect of macromolecular crowding on amyloid fibril formation. PLoS One 2012, 7(4):e36288.

71. Suckau D, Kohl J, Karwath G, Schneider K, Casaretto M, Bitter-Suermann D, Przybylski M: Molecular epitope identification by limited proteolysis of an immobilized antigen-antibody complex and mass spectrometric peptide mapping. Proc Natl Acad Sci U S A 1990, 87(24):9848-9852.

72. Volpatti LR, Vendruscolo M, Dobson CM, Knowles TP: A clear view of polymorphism, twist, and chirality in amyloid fibril formation. ACS Nano 2013, 7(12):10443-10448.

73. Tsigelny IF, Sharikov Y, Kouznetsova VL, Greenberg JP, Wrasidlo W, Gonzalez T, Desplats P, Michael SE, Trejo-Morales M, Overk CR *et al*: Structural Diversity of Alzheimer's Disease Amyloid-beta Dimers and Their Role in Oligomerization and Fibril Formation. J Alzheimers Dis 2013.

74. Buchanan LE, Dunkelberger EB, Tran HQ, Cheng PN, Chiu CC, Cao P, Raleigh DP, de Pablo JJ, Nowick JS, Zanni MT: Mechanism of IAPP amyloid fibril formation involves an intermediate with a transient beta-sheet. Proc Natl Acad Sci U S A 2013, 110(48):19285-19290.

75. Shokri MM, Ahmadian S, Bemporad F, Khajeh K, Chiti F: Amyloid fibril formation by a normally folded protein in the absence of denaturants and agitation. Amyloid 2013, 20(4):226-232.

76. Zou Y, Li Y, Hao W, Hu X, Ma G: Parallel beta-sheet fibril and antiparallel beta-sheet oligomer: new insights into amyloid formation of hen egg white lysozyme under heat and acidic condition from FTIR spectroscopy. J Phys Chem B 2013, 117(15):4003-4013.

77. Streets AM, Sourigues Y, Kopito RR, Melki R, Quake SR: Simultaneous measurement of amyloid fibril formation by dynamic light scattering and fluorescence reveals complex aggregation kinetics. PLoS One 2013, 8(1):e54541.

78. Dovidchenko NV, Galzitskaya OV: Modeling amyloid fibril formation. Biochemistry (Mosc) 2011, 76(3):366-373.

79. Zerovnik E, Stoka V, Mirtic A, Guncar G, Grdadolnik J, Staniforth RA, Turk D, Turk V: Mechanisms of amyloid fibril formation--focus on domain-swapping. FEBS J 2011, 278(13):2263-2282.

80. Carulla N, Zhou M, Giralt E, Robinson CV, Dobson CM: Structure and intermolecular dynamics of aggregates populated during amyloid fibril formation studied by hydrogen/deuterium exchange. Acc Chem Res 2010, 43(8):1072-1079.

81. Merrifield RB: Solid-phase peptide synthesis. Adv Enzymol Relat Areas Mol Biol 1969, 32:221-296.

82. Merrifield RB, Stewart JM: Automated peptide synthesis. Nature 1965, 207(996):522-523.

83. Merrifield RB: Solid-Phase Peptide Syntheses. Endeavour 1965, 24:3-7.

84. Carpino LA, Han GY: 9-Fluorenylmethoxycarbonyl Amino-Protecting Group. J Org Chem 1972, 37(22):3404-&.

85. Manea M: Design, Structural and Immuno-.analytical Properties of Antigenic Polypeptides comprising a β-Amyloid-Plaque Specific Epitope. University of Konstanz., Chemistry; 2006.

86. Perdivara I: Structure Determination of Autoimmune Disease – Related Proteins by High Performance Liquid Chromatography – Mass Spectrometry. Universität Konstanz, Chemistry; 2009.

87. [http://www.matrixscience.com]

88. Mount DW: Using the Basic Local Alignment Search Tool (BLAST). CSH Protoc 2007, 2007:pdb top17.

89. Abhinandan KR, Martin AC: Analysis and improvements to Kabat and structurally correct numbering of antibody variable domains. Mol Immunol 2008, 45(14):3832-3839.

90. Hood LE: Wu and Kabat 1970: a transforming view of antibody diversity. J Immunol 2008, 180(11):7055-7056.

91. Johnson G, Wu TT: Kabat Database and its applications: future directions. Nucleic Acids Res 2001, 29(1):205-206.

92. Martin AC: Accessing the Kabat antibody sequence database by computer. Proteins 1996, 25(1):130-133.

93. Deret S, Maissiat C, Aucouturier P, Chomilier J: SUBIM: a program for analysing the Kabat database and determining the variability subgroup of a new immunoglobulin sequence. Comput Appl Biosci 1995, 11(4):435-439.

94. Jores R, Alzari PM, Meo T: Resolution of hypervariable regions in T-cell receptor beta chains by a modified Wu-Kabat index of amino acid diversity. Proc Natl Acad Sci U S A 1990, 87(23):9138-9142.

95. Liao J, Nickerson KG, Bystricky S, Robbins JB, Schneerson R, Szu SC, Kabat EA: Characterization of a human monoclonal immunoglobulin M (IgM) antibody (IgMBEN) specific for Vi capsular polysaccharide of Salmonella typhi. Infect Immun 1995, 63(11):4429-4432.

96. Desai R, Spatz L, Matsuda T, Ilyas AA, Berman JE, Alt FW, Kabat EA, Latov N: Molecular cloning of a human immunoglobulin heavy chain variable (VH) region with anti-myelin-associated glycoprotein activity. J Neuroimmunol 1990, 26(1):35-41.

97. Sikder SK, Kabat EA, Morrison SL: Alternative splicing patterns in an aberrantly rearranged immunoglobulin kappa-light-chain gene. Proc Natl Acad Sci U S A 1985, 82(12):4045-4049.

98. Kabat EA, Wu TT, Bilofsky H: Evidence supporting somatic assembly of the DNA segments (minigenes), coding for the framework, and complementarity-determining segments of immunoglobulin variable regions. J Exp Med 1979, 149(6):1299-1313.

99. Kabat EA, Wu TT, Bilofsky H: Variable region genes for the immunoglobulin framework are assembled from small segments of DNA--a hypothesis. Proc Natl Acad Sci U S A 1978, 75(5):2429-2433.

100. Kabat EA, Wu TT: Construction of a three-dimensional model of the polypeptide backbone of the variable region of kappa immunoglobulin light chains. Proc Natl Acad Sci U S A 1972, 69(4):960-964.

101. Wu TT, Kabat EA: An attempt to locate the non-helical and permissively helical sequences of proteins: application to the variable regions of immunoglobulin light and heavy chains. Proc Natl Acad Sci U S A 1971, 68(7):1501-1506.

102. Morea V, Tramontano A, Rustici M, Chothia C, Lesk AM: Conformations of the third hypervariable region in the VH domain of immunoglobulins. J Mol Biol 1998, 275(2):269-294.

103. Al-Lazikani B, Lesk AM, Chothia C: Standard conformations for the canonical structures of immunoglobulins. J Mol Biol 1997, 273(4):927-948.

104. Barre S, Greenberg AS, Flajnik MF, Chothia C: Structural conservation of hypervariable regions in immunoglobulins evolution. Nat Struct Biol 1994, 1(12):915-920.

105. Tramontano A, Chothia C, Lesk AM: Framework residue 71 is a major determinant of the position and conformation of the second hypervariable region in the VH domains of immunoglobulins. J Mol Biol 1990, 215(1):175-182.

106. Chothia C, Lesk AM: Canonical structures for the hypervariable regions of immunoglobulins. J Mol Biol 1987, 196(4):901-917.

107. Gaskin G, Turner AN, Ryan JJ, Rees AJ, Pusey CD: Significance of autoantibodies to purified proteinase 3 in systemic vasculitis. Adv Exp Med Biol 1993, 336:287-289.

108. Gaskin F, Kingsley BS, Fu SM: Autoantibodies to neurofibrillary tangles and brain tissue in Alzheimer's disease. Establishment of Epstein-Barr virus-transformed antibody-producing cell lines. J Exp Med 1987, 165(1):245-250.

109. Maftei M, Thurm F, Schnack C, Tumani H, Otto M, Elbert T, Kolassa IT, Przybylski M, Manea M, von Arnim CA: Increased levels of antigen-bound beta-amyloid autoantibodies in serum and cerebrospinal fluid of Alzheimer's disease patients. PLoS One 2013, 8(7):e68996.

110. Andra J, Bohling A, Gronewold TM, Schlecht U, Perpeet M, Gutsmann T: Surface acoustic wave biosensor as a tool to study the interaction of antimicrobial peptides with phospholipid and lipopolysaccharide model membranes. Langmuir 2008, 24(16):9148-9153.

111. Lee CH, Gopal J, Wu HF: Ionic solution and nanoparticle assisted MALDI-MS as bacterial biosensors for rapid analysis of yogurt. Biosens Bioelectron 2012, 31(1):77-83.

112. Klauke TN, Gronewold TM, Perpeet M, Plattes S, Petersen B: Measurement of porcine haptoglobin in meat juice using surface acoustic wave biosensor technology. Meat Sci 2013, 95(3):699-703.

113. Dragusanu M, Petre BA, Slamnoiu S, Vlad C, Tu TT, Przybylski M: On-Line Bioaffinity-Electrospray Mass Spectrometry for Simultaneous Detection, Identification, and Quantification of Protein-Ligand Interactions. J Am Soc Mass Spectr 2010, 21(10):1643-1648.

114. Vivekanandan S, Brender JR, Lee SY, Ramamoorthy A: A partially folded structure of amyloid-beta(1-40) in an aqueous environment. Biochem Biophys Res Commun 2011, 411(2):312-316.

115. Stefanescu R, Iacob RE, Damoc EN, Marquardt A, Amstalden E, Manea M, Perdivara I, Maftei M, Paraschiv G, Przybylski M: Mass spectrometric approaches for elucidation of antigen-anti body recognition structures in molecular immunology. Eur J Mass Spectrom 2007, 13(1):69-75.

116. Walker JM: The bicinchoninic acid (BCA) assay for protein quantitation. Methods Mol Biol 1994, 32:5-8.

117. [http://www.millipore.com]

118. Bjellqvist B, Ek K, Righetti PG, Gianazza E, Gorg A, Westermeier R, Postel W: Isoelectric focusing in immobilized pH gradients: principle, methodology and some applications. J Biochem Biophys Methods 1982, 6(4):317-339.

119. Laemmli UK, Molbert E, Showe M, Kellenberger E: Form-determining function of the genes required for the assembly of the head of bacteriophage T4. J Mol Biol 1970, 49(1):99-113.

120. http://www.thermoscientificbio.com/protein-electrophoresis/pageruler-unstained-protein-ladder/.

121. Damoc E, Youhnovski N, Crettaz D, Tissot JD, Przybylski M: High resolution proteome analysis of cryoglobulins using Fourier transform-ion cyclotron resonance mass spectrometry. Proteomics 2003, 3(8):1425-1433.

122. Komatsu S: Western blotting/Edman sequencing using PVDF membrane. Methods Mol Biol 2009, 536:163-171.

123. Manecke G, Gunzel G: [Peptide degradation according to Edman on a polyisothiocyanate]. Naturwissenschaften 1968, 55(2):84.

124. de Roeck-Holtzhauer Y, Petit F: [Review of substrates for proteases]. J Pharm Belg 1970, 25(6):497-520.

125. Inagami T, Murachi T: The Mechanism of the Specificity of Trypsin Catalysis. 3. Activation of the Catalytic Site of Trypsin by Alkylammonium Ions in the Hydrolysis of Acetylglycine Ethyl Ester. J Biol Chem 1964, 239:1395-1401.

126. Stults JT: Matrix-assisted laser desorption/ionization mass spectrometry (MALDI-MS). Curr Opin Struct Biol 1995, 5(5):691-698.

127. Benfenati E, Reginato R: A comparison of three methods of soft ionization mass spectrometry of crude phospholipid extracts. Biomed Mass Spectrom 1985, 12(11):643-651.

128. http://www.physik.uni-mainz.de/forschungsbericht/fb97/fb97.htm.

129. Kinsel GR, Grundwuermer JM, Grotemeyer J: High-resolution mass spectrometry of large molecules in a linear time-of-flight mass spectrometer. J Am Soc Mass Spectrom 1993, 4(1):2-10.

130. Wiley WC: Bendix Time-of-Flight Mass Spectrometer. Science 1956, 124(3226):817-820.

131. Ouyang Z, Wu G, Song Y, Li H, Plass WR, Cooks RG: Rectilinear ion trap: concepts, calculations, and analytical performance of a new mass analyzer. Anal Chem 2004, 76(16):4595-4605.

132. Biemann K: Sequencing of peptides by tandem mass spectrometry and high-energy collision-induced dissociation. Methods Enzymol 1990, 193:455-479.

133. [http://penyfan.ugent.be/labo/joelv/Esquire.html]

134. Sadagopan N, Watson JT: Mass spectrometric evidence for mechanisms of fragmentation of charge-derivatized peptides. J Am Soc Mass Spectrom 2001, 12(4):399-409.

135. Heeren RM, Kleinnijenhuis AJ, McDonnell LA, Mize TH: A mini-review of mass spectrometry using high-performance FTICR-MS methods. Anal Bioanal Chem 2004, 378(4):1048-1058.

136. Laskin J, Futrell JH: Collisional activation of peptide ions in FT-ICR mass spectrometry. Mass Spectrom Rev 2003, 22(3):158-181.

137. Laskin J, Futrell JH: Activation of large ions in FT-ICR mass spectrometry. Mass Spectrom Rev 2005, 24(2):135-167.

138. [http://openi.nlm.nih.gov]

139. [http://www.hec.utah.edu/anions/webversion/Webdocument.htm]

140. Shushan B: A review of clinical diagnostic applications of liquid chromatography-tandem mass spectrometry. Mass Spectrom Rev 2010, 29(6):930-944.

141. Nexo E: A new principle in biospecific affinity chromatography used for purification of cobalamin-binding proteins. Biochim Biophys Acta 1975, 379(1):189-192.

142. Marquardt WW, Johnson RB, Odenwald WF, Schlotthober BA: An indirect enzyme-linked immunosorbent assay (ELISA) for measuring antibodies in chickens infected with infectious bursal disease virus. Avian Dis 1980, 24(2):375-385.

143. McLaren ML, Lillywhite JE, Au AC: Indirect enzyme linked immunosorbent assay (ELISA): practical aspects of standardization and quality control. Med Lab Sci 1981, 38(3):245-251.

144. Henderson SC, Valentine SJ, Counterman AE, Clemmer DE: ESI/ion trap/ion mobility/time-of-flight mass spectrometry for rapid and sensitive analysis of biomolecular mixtures. Analytical Chemistry 1999, 71(2):291-301.

145. Macht M, Marquardt A, Deininger SO, Damoc E, Kohlmann M, Przybylski M: "Affinity-proteomics": direct protein identification from biological material using mass spectrometric epitope mapping. Anal Bioanal Chem 2004, 378(4):1102-1111.

146. Marchesini GR, Buijs J, Haasnoot W, Hooijerink D, Jansson O, Nielen MW: Nanoscale affinity chip interface for coupling inhibition SPR immunosensor screening with Nano-LC TOF MS. Analytical Chemistry 2008, 80(4):1159-1168.

147. Homola J: Surface plasmon resonance sensors for detection of chemical and biological species. Chem Rev 2008, 108(2):462-493.

148. [http://saw-instruments.com/]

149. Fomsgaard A, Dinesen B: ELISA for human IgG and IgM anti-lipopolysaccharide antibodies with indirect standardization. J Immunoassay 1987, 8(4):333-350.

150. Hannington G, Booth JC, Wiblin CN, Stern H: Indirect enzyme-linked immunosorbent assay (ELISA) for detection of IgG antibodies against Coxsackie B viruses. J Med Microbiol 1983, 16(4):459-465.

151. Perpeet M, Glass S, Gronewold T, Kiwitz A, Malave A, Stoyanov I, Tewes M, Quandt E: SAW sensor system for marker-free molecular interaction analysis. Anal Lett 2006, 39(8):1747-1757.

152. Gronewold TM, Baumgartner A, Weckmann A, Knekties J, Egler C: Selection process generating peptide aptamers and analysis of their binding to the TiO2 surface of a surface acoustic wave sensor. Acta Biomaterialia 2009, 5(2):794-800.

153. Gronewold TM: Surface acoustic wave sensors in the bioanalytical field: recent trends and challenges. Analytica Chimica Acta 2007, 603(2):119-128.

154. Gronewold TM, Schlecht U, Quandt E: Analysis of proteolytic degradation of a crude protein mixture using a surface acoustic wave sensor. Biosens Bioelectron 2007, 22(9-10):2360-2365.

155. [http://gpmaw.software.informer.com/]

156. [http://bruker-daltonics-dataanalysis.software.informer.com/]

157. http://www.bio-rad.com/en-us/product/pdquest-2-d-analysis-software.

158. [http://www.originlab.com/]

159. Pettersen EF, Goddard TD, Huang CC, Couch GS, Greenblatt DM, Meng EC, Ferrin TE: UCSF Chimera--a visualization system for exploratory research and analysis. J Comput Chem 2004, 25(13):1605-1612.

160. [http://blast.ncbi.nlm.nih.gov]

7. APPENDIX 1

Table 30. Aβ-autoantibody light chain peptides identified by HPLC separation and individual analysis of each fraction by LC-MS/MS

No.	Position	Sequence	Charge	$[M+H]^+_{calc}$ [a]	$[M+H]^+_{exp}$ [b]	Δm (Da)
1	001-011	**EVVLTQSPGTL**	2+	1143.6	1143.4	0.2
2	001-011	**EIVLTQSPATL**	2+	1171.6	1171.3	0.3
3	001-011	**EIVLTQSPATV**	2+	1157.6	1157.7	0.1
4	001-011	**EIVLTQSPASL**	2+	1157.6	1157.8	0.2
5	001-011	**EIVLTQSPGTL**	2+	1157.6	1157.3	0.3
6	001-011	**EIVLTKSPGTL**	2+	1157.6	1157.5	0.1
7	001-011	**ENVLTQSPGTL**	2+	1158.6	1158.9	0.3
8	001-011	**ETVLTQSPGTL**	2+	1145.6	1145.3	0.3
9	001-011	**DIVLTQSPGTL**	2+	1143.6	1144.0	0.4
10	001-011	**DIQLTQSPSSL**	2+	1188.6	1188.1	0.5
11	001-011	**DIQLTQSPSFL**	2+	1248.6	1248.2	0.4
12	001-011	**DIQMTQSPSTL + OX**	2+	1236.5	1236.7	0.2
13	001-011	**DIQMTQSPSSL + OX**	2+	1236.5	1236.6	0.1
14	001-011	**IIQMTQSPSSL**	2+	1204.6	1204.8	0.2
15	001-011	**PIQMTQSPSSL +OX**	2+	1204.6	1204.9	0.3
16	001-011	**NIQMTQSPSSL +OX**	2+	1221.5	1221.1	0.4
17	001-012	**DIVMTQSPSTL**	2+	1191.6	1191.5	0.1
18	002-014	**SELTQDPAVSVAL**	3+	1329.7	1330.4	0.7
19	005-013	**TVSPQTARI**	2+	972.5	973.1	0.6
20	005-015	**TVSSGGPRSPS**	2+	1031.5	1032.1	0.6
21	005-020	**TQPPSVSGAPGQRVT**	3+	1481.7	1481.6	0.1
22	005-020	**TQPPSVSAAPGQKVT**	3+	1467.7	1467.5	0.2
23	005-020	**TQPASVSGSPGQSLT**	3+	1416.7	1416.6	0.1
24	005-020	**TQPASVSGSPGQSIT**	3+	1416.6	1416.5	0.1
25	005-020	**TKPASVSGSPGQSIT**	3+	1416.7	1416.4	0.3

26	005-021	**TQPPSVSGAPGQRVTI**	3+	1594.8	1595.1	0.3
27	005-022	**TQPASVSSGSPGQSITI**	3+	1616.8	1616.4	0.4
28	009-023	**SLPVTPGEPASISC**	3+	1414.6	1414.4	0.2
29	009-023	**SLPVTPGQPASISC**	3+	1413.6	1413.0	0.6
30	011-023	**SASVGNRVTITC**	3+	1264.6	1264.2	0.4
31	011-023	**SASVGDRVTLTC**	3+	1265.6	1265.3	0.3
32	011-023	**SESPGQSVTITC**	3+	1265.6	1265.5	0.1
33	011-024	**SASVGRRVTITCG**	3+	1363.7	1363.8	0.1
34	011-021	**SVSPGESAAL**	2+	917.4	917.3	0.1
35	011-021	**SVSPGEGATL**	2+	917.4	917.5	0.1
36	011-021	**SLSPGEKVTL**	2+	1030.5	1030.4	0.1
37	011-021	**SLSPGERATL**	2+	1030.5	1030.3	0.2
38	011-021	**TVSPGEKVTL**	2+	1030.5	1030.6	0.1
39	011-021	**TVSPGQTARI**	2+	1029.5	1030.3	0.8
40	011-021	**SVTPGQPASISC**	2+	1103.5	1103.6	0.1
41	011-021	**AVTLGQPASISC**	2+	1203.5	1204.0	0.5
42	016-037	**GQPASISCRSSQ**	2+	1277.5	1277.3	0.2
43	019-024	**VTITCR**	2+	749.3	748.4	0.9
44	022-033	**SCRASQSVSSNY**	3+	1345.5	1345.4	0.1
45	022-033	**SCRASQSVSSIY**	3+	1344.6	1344.1	0.5
46	022-033	**SCRASQSVSSYL**	3+	1344.6	1344.2	0.4
47	022-033	**SCRASQSVSSSF**	3+	1302.5	1302.4	0.1
48	022-033	**SCRASQSVSSAY**	3+	1302.5	1302.5	0.0
49	022-033	**SCRASQSVSSNF**	3+	1329.5	1329.8	0.3
50	023-031	**CKSSQSVLY**	2+	1071.5	1071.9	0.4
51	031-039	**NYLAWYQQK**	2+	1213.6	1213.1	0.5
52	036-045	**YQQLPGTAPK**	2+	1102.6	1102.7	0.1
53	036-047	**YQQKPKGPPRLL**	3+	1424.8	1424.6	0.2
54	037-047	**QQLPGTAPKLL**	2+	1165.7	1165.6	0.1
55	042-050	**SQPKNPTVT**	2+	971.5	971.4	0.1

56	039-050	**HSGKAPKLMIYD**	3+	1359.7	1360.2	0.5
57	039-050	**QSGKAPKLMIYD**	3+	1350.7	1351.5	0.8
58	043-052	**SPQPLIYLGY**	2+	1150.6	1151.3	0.7
59	043-052	**APKLLIYGNY**	2+	1151.6	1151.9	0.3
60	046-050	**LLIYK**	2+	648.4	648.4	0.0
61	046-053	**LIIYDVTK**	2+	964.5	965.0	0.5
62	046-053	**LIIYEVSK**	2+	964.5	963.9	0.6
63	046-053	**LLIYDDNK**	2+	993.5	992.4	1.1
64	046-053	**LLIYDISK**	2+	964.5	963.9	0.6
65	046-053	**LLIYEVSK**	2+	964.5	963.9	0.6
66	046-053	**IIIYEVSK**	2+	964.5	965.0	0.5
67	046-053	**LMLTNYIK + Ox**	2+	1011.5	1012.1	0.6
68	046-053	**LMIYDVTK + Ox**	2+	998.5	998.0	0.5
69	046-054	**LLISDASNR**	2+	988.5	987.4	1.1
70	046-054	**LLIYGASAR**	2+	963.5	962.5	1.0
71	046-054	**LLIYAGSTR**	2+	993.5	992.5	1.0
72	046-054	**LLIYWASTR**	2+	1122.6	1121.7	0.9
73	046-054	**LIIYDVYKR**	2+	1182.6	1183.1	0.5
74	046-054	**LLMYDALKR + Ox**	2+	1138.6	1138.9	0.3
75	048-054	**IYDASTR**	2+	825.4	825.7	0.3
76	048-062	**IYGASSRATGIPDRF**	3+	1610.8	1610.5	0.3
77	048-062	**IYGASTRATGIPARF**	3+	1580.8	1581.3	0.5
78	050-062	**AVSSLQSGVPSRF**	3+	1334.7	1334.9	0.2
79	050-062	**AASSLQSGVPSRF**	3+	1306.6	1306.5	0.1
80	050-062	**SASVLQSGVPSRF**	2+	1334.7	1334.5	0.2
81	050-073	**AASDLQSGVPSRFSGSGSGTDTTL**	4+	2298.0	2298.8	0.8
82	055-061	**ATGIPAR**	2+	685.4	684.4	1.0
83	055-061	**ATDIPAR**	2+	743.4	743.4	0.0
84	055-061	**ATGIPDR**	2+	729.4	729.4	0.0

85	055-061	**APGIPDR**	2+	725.4	725.4	0.0
86	061-073	**SGSIDSSSISASL**	3+	1210.5	1210.9	0.4
87	061-073	**SGSIDSSSNSASL**	3+	1211.5	1211.8	0.3
88	061-076	**RFSGSKSGDTASLTIS**	3+	1613.8	1613.1	0.7
89	061-076	**SGSIDNSSNCASLTIS**	3+	1612.7	1613.4	0.3
90	062-070	**FSGSILGNK**	3+	922.5	921.6	0.9
91	062-070	**FSGSLLGGK**	2+	865.4	864.44	0.9
92	062-074	**FSGSGSGTDFTLK**	2+	1303.6	1303.6	0.0
93	062-079	**FSGSGSGTDFTLTISR**	3+	1632.7	1631.7	1.0
94	063-073	**SGSGSGTDFTL**	2+	1028.4	1028.9	0.5
95	065-072	**DSSLSGHV**	2+	801.3	801.5	0.2
96	065-074	**GGSNSGNTAT**	2+	865.3	865.6	0.3
97	065-075	**SGSNSGNTATL**	2+	1008.4	1008.7	0.3
98	065-075	**SGSNSGDTATL**	2+	1009.4	1009.1	0.3
99	065-075	**SGSNSGNATTL**	2+	1008.4	1008.1	0.3
100	065-075	**SGSKSGNTASL**	2+	1008.5	1008.2	0.3
101	065-075	**SGSKSGNTATL**	2+	1022.5	1021.0	1.5
102	065-075	**SGSQSGNTATL**	2+	1022.4	1022.9	0.5
103	065-075	**SGSTSGNTASL**	2+	981.4	981.3	0.1
104	065-075	**SGSDSGDTATL**	2+	1010.4	1010.6	0.2
105	065-075	**SGSSSGTVTTL**	2+	996.4	996.8	0.4
106	065-075	**SGSSSGTKATL**	2+	995.5	995.4	0.1
107	065-075	**SGSSSGTTVTL**	2+	996.4	996.6	0.2
108	065-075	**SGTTSGNTATL**	2+	1009.4	1009.5	0.1
109	066-075	**MSGNTASLTI**	2+	994.5	995.0	0.5
110	074-081	**TLTISRLQ**	2+	931.5	931.8	0.3
111	074-084	**TLTISRLKPED**	2+	1272.7	1272.2	0.5
112	074-085	**TLTISSLQPEDF**	2+	1350.6	1350.4	0.2
113	074-085	**TLTISSLKPEDF**	2+	1350.7	1350.5	0.2
114	074-085	**TLTVTSLQPEDF**	2+	1350.6	1350.4	0.2

115	074-085	**TLTISSLQSENF**	2+	1339.6	1339.5	0.1
116	074-085	**TLTISSLQTDDF**	2+	1340.6	1340.3	0.3
117	074-085	**TLTISSLQSEDF**	2+	1340.6	1340.3	0.3
118	074-085	**LTTISSLQSEDF**	2+	1340.6	1340.3	0.3
119	074-088	**TLTISRLQPEDFAVY**	3+	1752.9	1752.1	0.8
120	074-088	**TLTISRLKPEDFAVY**	3+	1752.9	1752.5	0.4
121	074-088	**TLTISRVEPEDFAVY**	3+	1739.8	1740.0	0.4
122	074-088	**TLTISSLQPEDTATY**	3+	1639.8	1639.9	0.1
123	074-088	**TLTISSLQPEDFGTY**	3+	1671.8	1672.1	0.3
124	074-088	**TLTISSLQPEDFATY**	3+	1685.8	1685.2	0.6
125	074-088	**TLTISSLQPEDFAIY**	3+	1697.8	1697.9	0.1
126	074-088	**TLTISSLQPETTATY**	3+	1625.8	1625.5	0.3
127	074-088	**TLTINKLEPEDFAVY**	3+	1752.9	1752.6	0.3
128	074-088	**TLTITNVQPDDFATY**	3+	1698.8	1698.6	0.2
129	074-088	**TLTLSSLQPDDFATY**	3+	1671.8	1671.4	0.4
130	074-088	**TLTVSNLQTEDFATY**	3+	1702.8	1703.1	0.3
131	074-088	**SLTISRLQPEDFAVY**	3+	1738.9	1739.1	0.2
132	074-089	**TLTISSLEPENFAVYY**	4+	1846.9	1847.2	0.3
133	074-089	**TLTISSLKPEDFAVYY**	4+	1846.9	1847.4	0.5
134	074-089	**TITISSLEPEDTAVYY**	4+	1801.8	1801.5	0.3
135	074-089	**TLTISRLQPDNFATYY**	4+	1902.9	1902.6	0.3
136	074-089	**TLTISSLQPDNFATYY**	3+	1833.9	1833.4	0.5
137	074-089	**TLTISSLQPEDFAVYY**	3+	1846.9	1847.4	0.5
138	074-089	**TLTISSLQPEDFATYY**	4+	1848.9	1848.7	0.2
139	074-089	**TLTISRLQPDDFATYY**	4+	1903.9	1903.6	0.3
140	074-089	**TLTISSLLEPDNFATY**	3+	1784.9	1784.5	0.4
141	076-088	**TISRLEPEDFAVY**	3+	1539.7	1539.6	0.1
142	076-088	**TLSRLEPEDFAVY**	3+	1539.7	1539.8	0.1
143	076-088	**TITRLEPEDFAVY**	3+	1553.7	1553.5	0.2
144	076-088	**TISSLQPDDCATY**	2+	1480.6	1480.7	0.1

145	076-089	**AISGLESEDEADYY**	2+	1561.6	1561.4	0.2
146	076-089	**AISGIESEDEADYY**	2+	1561.6	1561.7	0.1
147	076-089	**AISGLQSEDEADYY**	3+	1560.6	1560.8	0.2
148	076-089	**TVSGLQAEDEADYY**	2+	1560.6	1560.5	0.1
149	076-089	**TITGVQADDEADYY**	3+	1560.6	1560.4	0.2
150	076-089	**TISGLQAEDDADYY**	3+	1560.6	1560.3	0.3
151	076-089	**TISGLQAEDEADYY**	2+	1574.6	1574.8	0.2
152	076-089	**TITGVQAEDEADYY**	2+	1574.6	1574.7	0.1
153	076-089	**TITAVQAEDEADYY**	2+	1588.7	1588.8	0.1
154	076-089	**GITGLQTGDAADYY**	2+	1444.6	1444.4	0.2
155	076-089	**TISGLQAQDEADYF**	3+	1557.7	1557.6	0.1
156	076-089	**TISGLQAEDEADYF**	3+	1558.7	1558.6	0.1
157	078-088	**TSLRPEDSAVY**	2+	1236.6	1236.4	0.2
158	079-088	**RLEPQDFAVY**	2+	1237.6	1237.5	0.1
159	079-088	**RLEPEDFAVY**	2+	1238.6	1238.3	0.3
160	079-088	**RLKPEDFAVY**	2+	1237.6	1237.3	0.3
161	079-088	**SLQAKDVAVY**	2+	1093.6	1094.0	0.4
162	079-088	**SLQAEDVAVY**	2+	1094.5	1094.7	0.2
163	087-106	**DYYCSSYAGSNNLVFGGGTS**	4+	2118.8	2119.1	0.3
164	089-094	**YCQQSY**	2+	791.3	791.5	0.2
165	097-106	**TRVFGTGTKV**	2+	1065.6	1065.7	0.1
166	098-105	**LTELGQPK**	2+	885.5	885.4	0.1
167	098-105	**VTVLGQPK**	2+	841.5	840.6	0.9
168	098-105	**LTVLGQPK**	2+	855.5	854.4	1.1
169	098-105	**LTVNGQPK**	2+	856.5	855.6	0.9
170	099-105	**TFGQGTK**	2+	738.3	737.2	1.1
171	099-105	**VFGGGTK**	2+	665.3	664.2	1.1
172	099-108	**TFGPGTKVDL**	2+	1034.5	1034.4	0.1
173	099-109	**VFGTGTKATVL**	2+	1093.6	1093.5	0.1
174	099-108	**TFGPGTKVDI**	2+	1034.5	1034.7	0.2

175	103-111	**GQPKAAPST**	2+	856.4	856.7	0.3
176	103-111	**GQPKAAPVT**	2+	868.5	868.3	0.2
177	110-118	**RTVAAPSVF**	2+	947.5	947.6	0.1
178	110-128	**RTVAAPTVFIFPPSNEQLK**	4+	2115.1	2115.1	0.0
179	110-128	**RTVAVPSVFIFPPSDEQLK**	4+	2130.1	2128.7	1.4
180	110-128	**RTVAAPSVFIFPPSDEELK**	4+	2103.1	2102.1	1.0
181	110-128	**RTVAAPSVFIFPPSDEQLK**	4+	2102.1	2101.7	0.4
182	111-128	**TVAAPSVFIFPPSDEQLK**	4+	1946.0	1945.0	1.0
183	113-129	**ANPTVTLFPPSEELQANK**	4+	1956.0	1956.4	0.4
184	113-127	**AAPSVTLFPPRVWFNQ**	3+	1829.9	1830.2	0.3
185	113-129	**AAPSVTLFPPSSEELQANK**	4+	1986.0	1985.0	1.0
186	119-127	**IFPPSDEQL**	2+	1045.5	1045.6	0.1
187	119-130	**LFPPSSEELQAN**	2+	1331.6	1331.5	0.1
188	119-135	**IFPPSDEQLKSGTASVV**	3+	1774.9	1774.8	0.1
189	119-136	**IFPPSDEQLKSGTASVVC**	4+	1934.9	1934.7	0.2
190	119-137	**IFPPSNEQLKSGTASVVCL**	4+	2047.0	2047.4	0.4
191	119-137	**IFPPSDEQLKSGTASVVCL**	4+	2048.0	2048.6	0.6
192	119-137	**IFPPSNEELKSGTASVVCL**	4+	2048.0	2048.3	0.3
193	128-137	**KSGTASVVCL**	2+	1021.5	1021.8	0.3
194	129-144	**SGTASVVCLLDNFYPR**	3+	1798.8	1797.9	0.9
195	129-147	**SGTASVVCLLNNFHPREAK**	4+	2100.0	2100.8	0.8
196	136-150	**CLLNNFYPREAKVQW**	4+	1937.9	1937.7	0.2
197	136-150	**VLISNFYPGAVTVAW**	3+	1636.8	1637.1	0.3
198	136-150	**VLISDFYPGAVTVAW**	3+	1636.8	1636.9	0.1
199	137-150	**LISDFYPGAVTVAW**	3+	1538.8	1536.4	2.4
200	137-150	**LISNFYPGAVTVAW**	3+	1536.8	1536.7	0.1
201	138-150	**ISNFYPGAVTVAW**	3+	1424.7	1424.3	0.4
202	138-150	**ISDFYPGAVTVAW**	3+	1424.7	1424.5	0.2
203	139-144	**NNFYPR**	2+	810.3	810.6	0.3
204	139-146	**NNFYPREA**	2+	1010.4	1010.6	0.2

205	151-169	**KVDNALQSGNSQESVTEQD**	4+	2048.9	2049.3	0.4
206	151-172	**KVDNALQSGNSQESVTEQDSKD**	4+	2378.1	2378.8	0.7
207	151-172	**KVDNALQSGNSQESVTEQDEKD**	4+	2421.1	2421.4	0.3
208	151-175	**KVDNALQSGNSQESVTEQDSEDSTY**	4+	2731.1	2731.7	0.6
209	151-175	**KVDNALQSGNSQESVTEQDSKDSTY**	4+	2730.2	2731.0	0.8
210	152-171	**VDNALQSGNSQESVTEQDSK**	4+	2135.9	2135.1	0.8
211	156-163	**LQSGVPSR**	2+	843.4	842.4	1.0
212	156-174	**KADSSPVKAGVETTTPSKQ**	3+	1931.0	1931.8	0.8
213	157-163	**ADGSPVK**	2+	673.3	672.2	1.1
214	157-163	**ADSSPVK**	2+	703.3	702.2	1.1
215	158-175	**SGNSQESVTEQDSKDSTY**	3+	1961.8	1962.1	0.3
216	164-173	**AGVETTTPSK**	2+	990.5	989.7	0.8
217	172-185	**DSTYSLSSTLTLSK**	3+	1502.7	1501.8	0.9
218	172-185	**NSTYSLSSTLTLSK**	3+	1501.7	1502.5	0.8
219	172-185	**DSTYSLSSTLTISK**	3+	1502.7	1502.5	0.2
220	179-193	**YAASSYLSLTPEQWK**	3+	1743.8	1743.6	0.2
221	184-194	**SKADYEKHKVY**	2+	1367.7	1367.9	0.2
222	186-190	**ADYEK**	2+	625.3	625.2	0.1
223	193-309	**VYACEVTHQGLSSPVTK**	3+	1875.9	1875.0	0.9
224	193-309	**LYACEVTHQGLSSPVTK**	3+	1889.9	1889.8	0.1
225	195-203	**ACQVTHQGL**	2+	1013.4	1013.3	0.1
226	195-203	**ACEVTHQGL**	2+	1014.4	1014.5	0.1
227	195-209	**ACEVTHQGLSSPVTK**	3+	1613.7	1613.7	0.0
228	195-211	**ACEVTHQGLSSPVTKSF**	3+	1847.8	1847.4	0.4
229	197-211	**SYSCQVTHEGSTVEK**	3+	1711.7	1710.9	0.8
230	199-219	**SCQVTHEGSTVEKTVAPTQCS**	4+	2305.9	2305.7	0.2
231	199-219	**SCQVTHEGSTVEKTVAPTECS**	4+	2316.9	2318.4	1.5
232	199-219	**SCEVTHEGSTVEKTVAPTECS**	4+	2317.9	2318.2	0.3
233	199-219	**SCEVTHEGSTVQKTAVPTECS**	4+	2316.9	2316.8	0.1

234	201-211	**QGLSSPVTKSF**	2+	1150.6	1150.5	0.1
235	205-219	**EGSTVEKTVAPTECS**	3+	1594.7	1594.3	0.4
236	206-219	**WSTVEKTVAPTECS**	3+	1594.7	1594.1	0.6
237	210-213	**SFNR**	2+	523.2	522.8	0.4
238	212-219	**TVAPTECS**	2+	864.3	864.1	0.2

[a]GPMAW software 5.0 (Lighthouse Data, Denmark)

[b]mass spectrometric analysis by ESI ion trap mass spectrometry

8. APPENDIX 2

Table 31. Aβ-autoantibody heavy chain peptides identified by HPLC separation and individual analysis of each fraction by LC-MS/MS

No.	Position	Sequence	Charge	$[M+H]^+_{calc}$ [a]	$[M+H]^+_{exp}$ [b]	Δm (Da)
1	001-011	**pyroXVQLVQSQEVK**	2+	1267.6	1267.7	0.1
2	001-011	**EVQLVESGGGL**	2+	1087.5	1088.4	0.9
3	001-011	**EVQLVQSGGGL**	2+	1086.5	1086.6	0.1
4	001-011	**EVLLVESGGGL**	2+	1072.5	1072.4	0.1
5	001-011	**EVELVESGGGL**	2+	1088.5	1088.4	0.1
6	001-011	**QVQLVESGGAL**	2+	1100.5	1100.2	0.3
7	001-011	**QVQLVETGGGL**	2+	1100.5	1100.4	0.1
8	001-011	**QVQPQQSGPGL**	2+	1137.5	1137.6	0.1
9	001-011	**NVQLVESGGGL**	2+	1072.5	1072.4	0.1
10	001-011	**LIDLVESGGGL**	2+	1072.5	1072.4	0.1
11	001-011	**LIELVESGGGL**	2+	1086.5	1086.6	0.1
12	001-011	**LIMLVESGGGL**	2+	1088.5	1088.4	0.1
13	001-011	**PLQLVESGGGL**	2+	1069.5	1069.0	0.5
14	001-011	**PVQLQQSGGGL**	2+	1083.5	1083.2	0.3
15	001-013	**EVQLVQSGAEVK**	2+	1285.6	1285.4	0.2
16	001-013	**QVQLVQSGAEVK**	2+	1285.7	1285.9	0.2
17	001-013	**QLQLQQSGPGVK**	2+	1282.7	1282.1	0.6
18	001-013	**QVKLVQSGAEVK**	2+	1285.7	1285.5	0.2
19	001-013	**PLQLLQSGAEVK**	2+	1282.7	1282.8	0.1
20	001-013	**KVKLVQSGAEVK**	2+	1285.7	1285.6	0.1
21	001-014	**AGVQLVQSGAEVK**	2+	1285.7	1285.6	0.1
22	001-018	**EVQLVQSGAEVKKPGQSL**	3+	1897.0	1897.2	0.2
23	001-018	**EVQLVQSGAQVKKPGESL**	3+	1897.0	1897.2	0.2
24	001-018	**EVQLVPSGGGLVQPGGSL**	2+	1693.9	1694.2	0.3

25	001-018	**EVQLVESGGGLVQPGRSL**	3+	1824.9	1825.5	0.6
26	001-018	**EVQLVESGGGLVQPGGSL**	3+	1725.9	1726.5	0.6
27	001-018	**EVQLVESGGDLVQPGRSL**	3+	1883.9	1884.3	0.4
28	001-018	**EVQLVESGGGLIQPGGSL**	3+	1739.9	1740.3	0.4
29	001-018	**EVQLVESGGDLVKPGRSL**	3+	1883.0	1882.8	0.2
30	001-018	**EVQLVESGGDIVQPGRSL**	3+	1882.9	1882.8	0.1
31	001-018	**EVQLVESGGGLVQPGESL**	3+	1797.9	1798.5	0.6
32	001-018	**EVQLVESGGGLVQPEGSL**	3+	1797.9	1798.5	0.6
33	001-018	**EVQLVESGGGLVKPGESL**	3+	1797.9	1798.5	0.6
34	001-018	**EVQLVESGGGLVKPEGSL**	3+	1797.9	1798.5	0.6
35	001-018	**EVLLVESGGGVVQPGRSL**	3+	1796.7	1795.8	0.9
36	001-018	**EVQLVESGGGLVKPGGSL**	3+	1725.9	1726.5	0.6
37	001-018	**EVQLVESGGGLVQPRGSL**	3+	1824.9	1825.5	0.6
38	001-018	**EVQLVESGGGLVKPRGSL**	3+	1825.5	1825.5	0.0
39	001-018	**EVQLVESGGGLVEPGRSL**	3+	1825.9	1826.1	0.2
40	001-018	**EVKLVESGGGLVQPGRSL**	3+	1825.0	1825.5	0.5
41	001-018	**EVQLLESGGGLVQPGGSL**	3+	1739.9	1740.3	0.4
42	001-018	**PVQLQQSGGGLVQPGGSL**	2+	1721.9	1722.2	0.3
43	001-018	**WGQVVESGGGLVQPGRSL**	3+	1825.9	1825.5	0.4
44	001-018	**GVQLLESGGTLVQPGGSL**	3+	1711.9	1712.7	0.8
45	001-018	**PVQLQQSGGGLVQPGGSL**	2+	1721.9	1721.8	0.1
46	001-018	**PVQLVRSGGGLVQPGGSL**	2+	1720.9	1721.8	0.9
47	001-018	**QVQLPESGGGLVQPGGSL**	2+	1722.9	1721.8	1.1
48	001-018	**QVQLVQSGAEVKKPGQSL**	3+	1896.0	1897.2	1.2
49	001-018	**QVLLVESGGGVVQPGRSL**	3+	1795.0	1795.8	0.8
50	001-018	**QVKLVQAGGGVVQPGRSL**	3+	1794.0	1795.8	1.8
51	001-018	**QVQLVQAGGGVVQPGRSL**	3+	1793.0	1792.8	0.2
52	001-018	**IILVESGGDLVQPGGSL**	4+	1653.9	1654.8	0.9
53	001-018	**LVQLVESGGDVVPPGKSL**	3+	1794.0	1793.4	0.6
54	001-018	**LVQLVESGGDVVPPGESL**	3+	1794.9	1793.4	1.5

55	001-018	**LVQLVESGGGVVQPGRSL**	3+	1795.0	1794.6	0.4
56	001-018	**IVQLVESGGGVVQPGRSL**	3+	1795.0	1794.6	0.4
57	001-018	**DVHLVESGGGLVQPGGSL**	2+	1720.8	1721.8	1.0
58	001-018	**DVQLQQSGGGLVQPGGSL**	3+	1739.8	1740.3	0.5
59	001-018	**DVQLVESGGGLVQPGGSL**	3+	1711.8	1712.7	0.9
60	001-019	**EVQLVESGGGLVKPGGSLR**	3+	1882.0	1881.4	0.6
61	001-020	**EVQLVESGGGLVKPGGSLRL**	3+	1995.1	1995.9	0.8
62	001-020	**EVQLLESGGGLVQPGGSLRL**	3+	2009.1	2009.7	0.6
63	001-020	**EVQLVESGGGLVQPGGSLRL**	3+	1995.0	1996.2	1.2
64	001-020	**EVQLVESGGAVVQPGGSLRL**	3+	1995.0	1995.9	0.9
65	001-020	**EVQVVESGGGLVQPGGSLRL**	3+	1981.0	1981.8	0.8
66	001-020	**EVQVVESGGGLVKPGGSLRL**	3+	1981.1	1981.8	0.7
67	001-020	**DVQLVESGGGLVQPGGSLRL**	3+	1981.0	1981.8	0.8
68	001-020	**QVQLSESGGGLVQPGGSLRL**	3+	1982.0	1981.8	0.2
69	001-020	**IVQLVESGGGLVQPGGSLRL**	3+	1979.1	1978.5	0.6
70	002-018	**VQLVQSGGDLVQPGGSL**	4+	1653.8	1654.8	1.0
71	002-018	**VQLVKSGGDLVQPGGSL**	4+	1653.9	1654.8	0.9
72	005-018	**LDSGGGVVQPGGSL**	3+	1242.6	1242.9	0.3
73	005-018	**VKSGGGVVQPGGSL**	2+	1241.6	1241.8	0.2
74	005-018	**VESGGGVVQPGGSL**	2+	1242.6	1241.8	0.8
75	005-018	**VESGGGLVLPGRSL**	2+	1339.7	1340.0	0.3
76	005-018	**VQSGGGLVHPGGSL**	2+	1364.6	1364.3	0.3
77	005-018	**VQSGGGVVQPGGSL**	3+	1241.6	1241.4	0.2
78	005-030	**VESGGGLVQPGGSLRLSCAASGFNL**	4+	2433.2	2434.8	1.6
79	006-018	**ESGGGLVKPGGSL**	2+	1157.6	1157.4	0.2
80	006-018	**ESGGGIVQPGGSL**	2+	1157.6	1157.3	0.3
81	006-018	**DSGGALVQPGGSL**	2+	1157.5	1157.4	0.1
82	012-036	**VKPGGSLRLSCAASGFTFSDHYMSW + Ox**	4+	2778.2	2778.4	0.2
83	018-032	**LGLIKRSGRLMTSY**	3+	1594.9	1594.8	0.1

84	019-027	**RLSCAASGF**	2+	968.4	967.4	1.0
85	019-027	**RKSCAASGF**	2+	983.4	982.8	0.6
86	019-027	**KVSCKASGF**	2+	983.4	982.8	0.6
87	019-027	**RLSCKASGF**	2+	1025.5	1025.6	0.1
88	019-027	**RISCQASGF**	2+	1025.4	1025.6	0.2
89	019-032	**RLSCTASAFNLSDY**	3+	1604.7	1605.6	0.9
90	019-036	**RLCCAASGFTFRTYSMHW**	4+	2250.9	2251.2	0.3
91	019-036	**RLSCAASGFTLSSSAMSW**	4+	1918.8	1919.1	0.3
92	020-030	**LSCAASGFTFR**	3+	1215.0	1215.5	0.5
93	020-038	**VSCTASGFDFDYYFHWVR**	4+	2256.9	2256.5	0.4
94	020-037	**LSCAASGFTFSKYWMHWVR**	4+	2334.0	2333.7	0.3
95	020-037	**LSCAASGFTFTNYWMNWVR**	4+	2311.0	2310.8	0.2
96	020-037	**LSCAASGFTFNTCWMTWVR + Ox**	4+	2310.9	2310.9	0.0
97	020-037	**LSCAASGFTFSKYFMHWVR + Ox**	4+	2311.0	2310.7	0.3
98	020-037	**LSCAASGFTFSKYFMHFVR + Ox**	4+	2272.0	2271.7	0.3
99	020-042	**LSCAASGFGFGGQALSWVRQAPGK**	4+	2452.2	2451.6	0.6
100	021-036	**SCAASGFTLINYRHNW**	3+	1896.8	1896.5	0.3
101	021-036	**SCAASGFTFKDYGMHW**	4+	1864.7	1864.9	0.2
102	028-036	**IFSNFGMHW**	2+	1138.5	1138.6	0.1
103	028-036	**IFSNFGFHW**	2+	1154.5	1154.7	0.2
104	028-036	**IFSMNGMHW**	2+	1122.5	1122.8	0.3
105	030-045	**TSYDIDWVRQATGQGL**	3+	1809.8	1810.8	1.0
106	030-045	**STYGMSWVRQAAGKGL**	2+	1710.8	1710.8	0.0
107	030-047	**SSYEMNWVRQAPGKGLERF**	4+	2255.1	2256.0	0.9
108	032-050	**TFISWVRQAPGQGLEWMGW**	4+	2249.1	2250.0	0.9
109	033-047	**GMHWPRQAPGKGLEW + Ox**	2+	1764.8	1765.0	0.2
110	033-047	**AMHWIRQAWGKGLEW + Ox**	3+	1883.9	1885.8	1.9
111	033-047	**AMHWIRQATGKGLEW**	3+	1783.9	1784.7	0.8

112	033-047	**GMHWNRQAPGKGLEW**	2+	1765.8	1767.0	1.2
113	033-050	**YVHWVRQAPGQGLEWMGW + Ox**	3+	2216.1	2216.7	0.6
114	034-041	**GVSFTDYSW**	2+	1061.4	1061.4	0.0
115	034-045	**GVSWVRQGPGQGL**	2+	1340.7	1340.4	0.3
116	034-047	**WEWVRQPPGKGLEW**	2+	1767.9	1767.2	0.7
117	034-047	**WKWVRQPPGKGLEW**	2+	1766.9	1767.2	0.3
118	034-047	**WQWVRQPPGKGLEW**	2+	1766.9	1767.2	0.3
119	036-045	**SLSPGKRATL**	2+	1028.6	1028.6	0.0
120	036-045	**SLSPGQRATL**	2+	1028.5	1028.6	0.1
121	036-047	**SLSTSGVGVGWIRQTPGKALEW**	4+	2329.2	2328.8	0.4
122	037-045	**VRQAPGKGL**	2+	925.5	925.2	0.3
123	037-045	**ACQVTHQGL**	2+	1003.4	1003.4	0.0
124	037-045	**ACEVTHQGL**	2+	1004.4	1004.4	0.0
125	037-045	**VRKAPGKGL**	2+	924.5	924.2	0.3
126	037-047	**VRQAPGKGLKW**	3+	1239.7	1239.9	0.2
127	037-047	**VRQAPGKGLQW**	3+	1238.7	1239.9	1.2
128	037-047	**VRQAPGKGLEW**	3+	1240.6	1240.5	0.1
129	037-047	**VRQAPGQGIEW**	3+	1240.6	1240.5	0.1
130	037-047	**VRQAPGQGLKW**	3+	1239.7	1239.9	0.2
131	037-047	**VRQAPGQAVEW**	3+	1240.6	1240.5	0.1
132	037-047	**VRQAPGGKLEW**	3+	1240.6	1240.5	0.1
133	037-047	**VRQAPARGLEW**	2+	1282.7	1283.6	0.9
134	037-047	**VRKAPGKGLEW**	3+	1240.7	1239.9	0.8
135	037-047	**VQRAPGKGLEW**	3+	1240.6	1239.9	0.7
136	037-047	**IRQPPGMGLEW**	2+	1283.6	1283.6	0.0
137	037-050	**VRQAPGKGLEWVSL**	3+	1539.8	1539.9	0.1
138	037-050	**VRQAPGKGLEWLSY**	3+	1603.8	1603.8	0.0
139	037-050	**VRQAPGKGLEWISY**	3+	1603.8	1604.1	0.3
140	037-050	**FRQAPGKGLEWVGF**	3+	1591.8	1591.5	0.3
141	037-050	**IRQPPGKGLEWIGY**	3+	1613.8	1614.2	0.4

142	037-050	**IRKPPGQGLEWIGY**	3+	1613.8	1614.2	0.4
143	044-050	**GLVWVSR**	2+	816.4	815.7	0.7
144	044-050	**GLEWVGR**	2+	816.4	815.6	0.8
145	044-052	**GLEWLAVLK**	2+	1028.6	1028.0	0.6
146	044-052	**GLQWVALIK**	2+	1027.6	1028.0	0.4
147	044-052	**GLQWVANIK**	2+	1028.6	1028.0	0.6
148	044-052	**GLEWVALIK**	2+	1028.6	1028.0	0.6
149	044-052	**GLEWVAIIK**	2+	1028.6	1028.0	0.6
150	044-052	**GLEWIGLIK**	2+	1028.6	1028.0	0.6
151	044-052	**GLEWLGLIK**	2+	1028.6	1028.0	0.6
152	044-052	**GLQWVGQIK**	2+	1028.5	1028.0	0.5
153	044-053	**GLEWVAMISK**	2+	1133.6	1133.1	0.5
154	044-058	**ALEWLAVVYWNDYK**	4+	1769.9	1770.2	0.3
155	044-063	**GLEWASAIRGDGGFQYADAVK**	4+	2211.1	2211.5	0.4
156	046-056	**EWLAYMSSSGSY**	2+	1380.5	1380.1	0.4
157	046-059	**EYLSAISSDGETTY**	4+	1535.6	1535.2	0.4
158	046-059	**EWVSSISRSGDNTY**	3+	1600.7	1599.6	1.1
159	046-058	**EWVSVIGSAGDTYY**	2+	1546.7	1546.1	0.6
160	046-059	**EWVSTIVGSGDATF**	3+	1468.7	1467.9	0.8
161	046-061	**EWVGRIKSEADGGTTDY**	4+	1883.8	1884.8	1.0
162	046-063	**EWIGHVSGSGVAKYNPSL**	2+	1900.9	1900.6	0.3
163	046-063	**EWIGNVFSSGSTNYNPSL**	3+	1971.9	1972.8	0.9
164	048-059	**VANIKQDGGERY**	3+	1349.6	1350.3	0.7
165	048-059	**VANIKQDGSKKY**	3+	1350.7	1350.3	0.4
166	048-064	**MGRIFPLLGVAKYAQKF**	4+	1939.1	1939.4	0.3
167	048-064	**MGTIYGGDSDTRYNPSF**	2+	1880.8	1880.9	0.1
168	048-064	**MGGIIPLSETPNYAQKF**	2+	1865.9	1866.0	0.1
169	048-064	**MGWSSTDTGNTNHAQKF + Ox**	3+	1897.8	1897.5	0.3
170	050-055	**FTVSSGSAFGPTLFPL**	3+	1627.8	1627.6	0.2
171	051-071	**IYYSGSSNYNPSLKSRVTMSL +**	3+	2383.1	2383.8	0.7

		Ox				
172	052-060	**FNGDTYYNL**	2+	1106.4	1106.2	0.2
173	053-080	**NPSLKGRLTMSVDTSKNQLLL + Ox**	4+	2331.2	2332.4	1.2
174	057-064	**TNYNPSLK**	2+	936.4	936.4	0.0
175	066-072	**GRPTISR**	2+	786.4	786.4	0.0
176	066-076	**SRVDISLDTSK**	2+	1220.6	1220.5	0.1
177	065-076	**SRVTISVVASK**	2+	1146.6	1147.0	-0.4
178	065-076	**SRVTISLDASK**	2+	1176.6	1176.4	0.2
179	066-076	**SRLSISVDTSK**	2+	1192.6	1192.5	0.1
180	066-076	**SRLTLSLDTSK**	2+	1220.6	1220.3	0.3
181	066-076	**SRITISLDTSK**	2+	1220.6	1220.5	0.1
182	066-076	**SRVTISVDTSK**	2+	1192.6	1192.4	0.2
183	066-076	**TRVTISLDTSK**	2+	1220.6	1220.4	0.2
184	066-076	**NRATISVDTSK**	2+	1191.6	1191.5	0.1
185	066-077	**SRLTISLDTSKK**	3+	1348.7	1348.8	0.1
186	068-072	**FTVSR**	2+	608.3	608.1	0.2
187	068-072	**FTISR**	2+	622.3	622.3	0.0
188	068-074	**VTITADR**	2+	774.4	774.2	0.2
189	068-080	**FTISRDTSKNTLYL**	2+	1658.8	1659.0	0.2
190	069-079	**TISRDNAKNSLY**	2+	1381.7	1382.0	0.3
191	069-079	**TISRDNAKNSIY**	3+	1381.7	1382.2	0.5
192	070-079	**SVNTSKNQF**	2+	1024.5	1024.2	0.3
193	070-079	**NADTSQNQF**	2+	1024.4	1024.2	0.2
194	072-092	**RGRVTMTRNLSMSTAY**	4+	1843.9	1843.7	0.2
195	072-092	**QGRVTIITDESTSTAY**	3+	1741.8	1742.4	0.6
196	072-092	**QGRVTITANQSTSTAY**	3+	1697.8	1698.3	0.5
197	072-092	**KGRVTITADKSTSTAY**	3+	1698.9	1698.3	0.6
198	073-096	**NTLFMQMNSLRAEDTAVYYCVK**	4+	2654.2	2654.2	0.0
199	085-094	**ISSGGNIIYY**	2+	1086.5	1086.4	0.1

200	077-087	**NTLYLQMNSLR**	2+	1351.7	1351.6	0.1
201	079-094	**YLHMNSLRAEDMAIYY**	2+	1989.9	1990.1	0.2
202	079-094	**YLQMKSLRVEDTALYY**	4+	1993.0	1992.8	0.2
203	080-093	**LEMDSLRPEDTALY**	2+	1652.7	1653.0	0.3
204	081-090	**TTADTDFILL**	2+	1108.5	1108.4	0.1
205	081-090	**CVRVLTAASW**	2+	1162.5	1162.5	0.0
206	081-091	**CVKDATQLRYF**	2+	1400.6	1400.1	0.5
207	081-093	**DMNSLRADDTAVY**	2+	1470.6	1470.3	0.3
208	081-093	**QMDSLRGDDTAVY**	2+	1470.6	1470.9	0.3
209	081-093	**QMTSLRADDTAVY**	2+	1470.7	1470.8	0.1
210	082-093	**QMTSLKTEDTAVY**	3+	1486.7	1486.4	0.3
211	081-093	**QLNNLSGADTAIY**	3+	1378.6	1378.6	0.0
212	081-093	**LLTSVTAADTAVY**	2+	1324.7	1324.5	0.2
213	081-093	**TLISVTAADTAVY**	2+	1324.7	1324.1	0.6
214	081-093	**TIRGAQAADEADY**	2+	1380.6	1380.3	0.3
215	081-093	**ILTSVTAADTAVY**	2+	1324.7	1324.4	0.3
216	081-093	**NVNSVTAADSAIY**	2+	1324.6	1324.6	0.0
217	081-093	**NVTSVNAADTAVY**	2+	1324.6	1324.7	0.1
218	081-093	**NVNSVTAADTAVY**	2+	1324.6	1324.8	0.2
219	081-093	**NLKSATAADTAVY**	2+	1324.6	1324.3	0.3
220	081-093	**NLSSVNAADTAVY**	2+	1324.6	1324.4	0.2
221	081-094	**QMNSLTDDDTAVYY**	2+	1635.6	1635.7	-0.1
222	083-092	**TRNTSISTAY**	2+	1112.5	1111.8	0.7
223	083-093	**SSLRSNDTAVY**	2+	1212.5	1212.2	0.3
224	083-093	**SSVTAANTAVY**	2+	1083.5	1083.4	0.1
225	083-093	**SSVTAADTAVY**	2+	1084.5	1083.4	1.1
226	083-093	**SSVNAADTAVY**	2+	1097.5	1097.2	0.3
227	083-093	**NNLTSEDTAVY**	2+	1226.5	1226.4	0.1
228	083-093	**NSVTGEGTAVY**	2+	1097.5	1097.2	0.3
229	083-093	**NSVTPGDTAVY**	2+	1123.5	1123.4	0.1

230	083-093	**NSVIAADTAVY**	2+	1123.5	1123.4	0.1
231	083-093	**NSATAADTAVY**	2+	1083.4	1083.4	0.0
232	083-093	**NSLKTDDTAVY**	2+	1225.6	1226.4	0.8
233	083-093	**NSLKSDDTAVY**	2+	1212.5	1212.2	0.3
234	083-093	**NSLKSEDTAVY**	2+	1226.6	1226.4	0.2
235	083-093	**ITLTSEDTAVY**	2+	1212.6	1212.2	0.4
236	083-093	**ISLTAADTAVY**	2+	1124.6	1124.6	0.0
237	083-093	**RSVAAADTAVY**	2+	1124.6	1123.4	1.2
238	083-093	**RSVTAAATAVY**	2+	1109.6	1109.4	0.2
239	083-093	**RSVTAANTAVY**	2+	1152.6	1152.6	0.0
240	083-093	**TSLIVADTAVY**	2+	1152.6	1152.6	0.0
241	083-093	**TSVTAANTAVY**	2+	1097.5	1097.4	0.1
242	083-093	**TSVTAPDTAVY**	2+	1124.5	1124.6	0.1
243	083-093	**TSVTAANTAVY**	2+	1097.5	1097.2	0.3
244	083-093	**KSVTAADTAVY**	2+	1125.6	1125.2	0.4
245	083-093	**KSATAADTAVY**	2+	1097.5	1097.4	0.1
246	083-094	**SGLTSADTAVYF**	2+	1231.3	1231.4	0.1
247	083-094	**TSVSAADTAVYF**	2+	1231.6	1231.4	0.2
248	083-094	**SSVTAADTAVYF**	2+	1231.6	1231.4	0.2
249	083-098	**LSSVTAADTAVYYCAR**	3+	1747.8	1746.8	1.0
250	084-093	**MNPRNGDAVY + Ox**	2+	1136.5	1152.6	0.1
251	084-093	**GAIKDPTGVY**	2+	1020.5	1021.0	0.5
252	084-093	**SLRAKDTAVY**	2+	1123.6	1123.4	0.2
253	084-093	**SLRAEDTAVY**	2+	1124.5	1123.4	1.1
254	084-093	**SLEPEDTAVY**	2+	1123.5	1123.4	0.1
255	086-094	**QAEDEAVYY**	2+	1087.4	1086.2	1.2
256	086-094	**KVQDTAVYY**	2+	1086.5	1086.2	0.3
257	086-094	**EPEDTAVYY**	2+	1086.4	1086.4	0.0
258	086-094	**EPEDTAVYY**	2+	1086.5	1086.2	0.3
259	086-094	**RAENTAVYY**	2+	1086.5	1086.4	0.1

260	086-094	**RAQDTAVYY**	2+	1086.5	1086.4	0.1
261	086-094	**RAKDTAVYY**	2+	1086.5	1086.2	0.3
262	086-106	**TSEDTAVYYCATMKDGYNKVYYY**	2+	2805.1	2805.5	0.4
263	086-106	**RSEDTAVYYCARVMVRGVISLDY**	4+	2724.3	2725.2	0.9
264	086-099	**RVEDTGMYYCARDF+ Ox**	3+	1798.7	1799.0	0.3
265	086-099	**SPEDTAMYFCARDL**	4+	1675.7	1675.6	0.1
266	086-100	**QVRGVTLYYQSLDVW**	3+	1826.9	1826.1	0.8
267	086-108	**TSDDAAVYYCAVDSGAKAGNYY**	2+	2360.9	2361.0	0.1
268	087-105	**SYSTAYLQWSSLKASDTAM**	3+	2109.9	2110.0	0.1
269	092-104	**IYYSGSTKYNSSL**	3+	1482.7	1482.5	0.2
270	092-104	**IYYSGTTNYNSSL**	3+	1482.7	1482.4	0.3
271	092-104	**IYYTGSTNYNSSL**	3+	1482.7	1482.5	0.2
272	093-099	**YYVDSVK**	2+	872.4	872.3	0.1
273	094-107	**YCARGEYYGSGSL**	3+	1482.6	1482.5	0.1
274	094-109	**YCARGRKSYFDVGGYY**	2+	1961.8	1961.9	0.1
275	094-110	**YCARDESEYSSSSLDL**	4+	1881.7	1881.6	0.1
276	095-104	**CARGAARLDY**	2+	1151.5	1151.4	0.1
277	095-105	**CARGLVERRTW**	2+	1403.7	1403.9	0.2
278	095-105	**CARVGYYGSGY**	3+	1253.5	1253.4	0.1
279	095-105	**CARSDFSGMDV**	2+	1244.4	1244.6	0.2
280	095-106	**CARVGYYGSGVY**	2+	1315.6	1314.0	1.6
281	095-106	**CARVHRGGSYYL**	3+	1338.6	1338.9	0.3
282	095-107	**CARHRPTYGVYYY**	3+	1706.7	1706.1	0.6
283	095-109	**CARGAGMVQGVITTL**	2+	1533.7	1534.0	0.3
284	095-111	**CARVRSGGGSSFPSDAF**	4+	1757.7	1758.4	0.7
285	095-112	**CARDFVVVVGGTQWDMNY + Ox**	4+	2132.9	2132.8	0.1
286	096-107	**DSSGYSAYYYYY**	2+	1500.9	1500.4	0.5
287	098-107	**QGLLKPSETL**	2+	1085.6	1085.8	0.2
288	098-108	**GAGLLKPSETL**	2+	1085.6	1085.4	0.2
289	098-108	**FGEVILRAGWF**	3+	1294.7	1294.2	0.5

290	098-110	**QFFSGALATGSVK**	2+	1311.7	1311.6	0.1
291	098-110	**QFFSGSPATGSVK**	2+	1311.7	1311.6	0.1
292	101-112	**NDAYGGGIDYWG**	3+	1286.5	1286.1	0.4
293	101-122	**FYYYYGMDVWGQGTTVTVSSG + Ox**	4+	2397.0	2398.0	1.0
294	102-121	**DGPYAYDIWGQGTMVAVSL**	4+	2059.9	2060.3	0.4
295	104-116	**GGWFDPWGQGTL**	2+	1320.6	1321.0	0.4
296	105-116	**NWFDPWGQGTL**	2+	1320.6	1321.0	0.4
297	106-116	**WFDPWGQGTL**	2+	1206.5	1206.6	0.1
298	107-116	**ELDYWGTGTL**	2+	1154.5	1154.6	0.1
299	107-116	**LDNWGQGTL**	2+	1003.4	1003.0	0.4
300	107-116	**IDNWGQGTL**	2+	1003.4	1003.0	0.4
301	107-116	**LNDWGQGTL**	2+	1003.5	1003.0	0.5
302	108-116	**DYWGQGTL**	2+	939.9	939.0	0.9
303	108-116	**DYWGKGTL**	2+	939.4	939.0	0.4
304	108-116	**DFWGQGTL**	2+	923.4	923.2	0.2
305	108-116	**YDWGQGTL**	2+	939.4	939.2	0.2
306	108-128	**DLWGQGTLVSVSSASTKAHP**	4+	2041.0	2041.6	0.6
307	108-128	**GGGTEVTVLGQPKAAPSVTL**	4+	1882.0	1882.8	0.8
308	108-121	**YSPSFQGQVMSVDK+OX**	3+	1572.7	1572.9	0.2
309	109-114	**SFPLLLTLL**	2+	1016.6	1016.2	0.4
310	112-122	**GQGTLVTVSSA**	2+	1018.5	1018.2	0.3
311	112-124	**GQGTLVTVSSAST**	2+	1206.6	1206.4	0.2
312	112-125	**GQGTLVTVSSASTK**	2+	1334.7	1334.6	0.1
313	112-125	**GQGTLVTVSSASTQ**	2+	1334.6	1334.6	0.0
315	112-121	**GQGAPVTVTS**	2+	915.4	914.8	0.6
316	112-122	**GPGTMVTVSSA**	2+	1006.5	1006.2	0.3
317	112-124	**GQGTTVTVSSAST**	2+	1195.5	1194.4	1.1
318	112-132	**GLGTLVTVSSASTKGPSVFPL**	3+	2018.1	2018.7	0.6
319	112-132	**GQGQTITVSSASTKGPSVFPL**	3+	2062.0	2061.6	0.4

320	112-132	**GQGSRVTVSSASTKGPSVFPL**	3+	2062.0	2061.6	0.4
321	112-132	**GQGTLVTVSSASTKGPSVFPL**	3+	2033.0	2033.4	0.4
322	112-132	**GQGTNVTVSSASTKGPSVFPL**	3+	2034.0	2033.4	0.6
323	113-129	**CLTCTVSGGSIGSSSY**	3+	1635.6	1637.4	1.8
324	113-132	**SLTCTVSGGSISSGSYYWSW**	4+	2184.9	2184.4	0.5
325	114-125	**GTTVIVSSASTK**	2+	1150.6	1149.5	1.1
326	115-126	**GTWTVSSASTK**	2+	1124.5	1125.5	1.0
327	115-127	**TVLHQDWLNGKEY**	3+	1602.8	1603.8	1.0
328	117-132	**VIVSSASTKGPSVFPL**	3+	1588.9	1589.4	0.5
329	117-132	**IVVSSASTKGPSVFPL**	3+	1588.9	1589.4	0.5
330	117-132	**FTVSSGSAFGPTLFPL**	3+	1627.8	1627.9	0.1
331	117-132	**VTVSSASTKGPSVFPL**	3+	1576.8	1577.1	0.3
332	117-132	**VTVSVASTKGPSVFPL**	3+	1588.8	1589.4	0.6
333	118-127	**HQDWLIGKEY**	2+	1288.6	1288.0	0.6
334	126-135	**GPSVFPLAPC**	2+	1044.5	1043.4	1.1
335	126-137	**GPSVFPLAPSSK**	2+	1186.6	1185.6	1.0
336	133-146	**AHFSKSTSGGTAAL**	2+	1334.7	1334.6	0.1
337	138-151	**STSESTAALGCLVK**	2+	1423.6	1422.8	0.8
338	138-151	**STSGGTAALGCLVK**	2+	1322.6	1321.6	1.0
339	138-151	**STSGGTAALACLVK**	2+	1335.6	1335.4	0.2
340	141-157	**SGTAARRGPFTNTMDVW + Ox**	2+	1882.9	1884.0	1.1
341	146-156	**SKSTSGGTAAL**	2+	978.5	978.4	0.1
342	147-162	**GCLVKDYFPEPVTVSW**	3+	1911.9	1911.4	0.5
343	147-162	**GCQVKDYFPEPVTVSW**	3+	1911.8	1911.3	0.5
344	149-159	**TCPPCPAPELL**	2+	1254.6	1254.6	0.0
345	149-164	**TLPPSRDELTKNQVSL**	3+	1797.9	1798.2	0.3
346	150-163	**VKDYFPEPVTVSW**	2+	1566.7	1567.0	0.3
347	150-163	**VKDYFPQPVTVSW**	2+	1565.8	1567.0	1.2
348	154-162	**FPEPVTVSW**	2+	1061.5	1061.2	0.3
349	163-178	**NSGALTSGVHTFPAVL**	2+	1570.8	1571.0	0.2

350	168-178	**TSGVHTFPAVL**	2+	1128.6	1128.6	0.0
351	168-184	**TSGVHTFPAVLESSGLY**	3+	1764.8	1764.6	0.2
352	185-198	**SLSSVVTVPSSSL**	2+	1262.6	1262.6	0.0
353	185-198	**SLSSVVTVPSSNF**	3+	1262.6	1262.6	0.0
354	185-203	**SLSSVVTVTSSNFGTQTY**	3+	1877.9	1878.9	1.0
355	185-203	**SLSSVVTVPSSSLGTQTY**	3+	1812.9	1813.2	0.3
356	185-203	**SLSSVVTVPSSNFGTQTY**	3+	1873.9	1874.4	0.5
357	185-203	**SLSSVVTVPSSSLGTKTY**	3+	1812.9	1813.2	0.3
358	187-203	**SSVVTVPSSSLGTQTY**	2+	1612.8	1611.8	1.0
359	187-203	**SSVVTVPSSSLGTKTY**	2+	1612.8	1611.8	1.0
361	194-203	**SSSWYVGDGF**	2+	1104.4	1104.4	0.0
362	197-208	**WYVDGVEVHNAK**	2+	1415.7	1415.7	0.0
363	187-198	**SSVVTVPSSSL**	2+	1062.5	1061.4	1.1
364	187-202	**SSVVTVPSSSLGTQTY**	2+	1612.8	1611.8	1.0
365	187-202	**SSVVTVPSSSLGTKTY**	2+	1612.8	1611.8	1.0
366	203-213	**ICNVNHKPSNT**	3+	1283.6	1283.4	0.2
367	219-230	**TPLGDTTHTCPR**	2+	1354.6	1354.6	0.0
368	226-252	**CCVECPPCPAPPVAGPSVFLFPPKPK**	4+	2908.3	2907.1	1.2
369	227-245	**GPPCPSCPAPEFLGGPSVF**	3+	1972.8	1973.7	0.9
370	229-245	**TCPPCPAPELLGGPSVF**	3+	1798.8	1799.4	0.6
371	246-254	**LFPPKPKDT**	3+	1042.5	1042.7	0.2
372	246-255	**LFPPKPKDTL**	2+	1155.6	1155.7	0.1
373	251-163	**NTLYLQMISLK+OX**	2+	1339.7	1339.6	0.1
374	251-163	**NTLYLQMISLK**	2+	1323.7	1323.4	0.3
375	251-163	**NTLYLQMDGLK**	2+	1285.6	1286.0	0.4
376	251-163	**SIAYLQMISLK+OX**	2+	1282.7	1282.5	0.2
377	253-259	**DLTMISR**	2+	835.4	835.6	0.2
378	253-278	**DTLMISRTPEVTCVVVDVSHEEPEVK**	4+	2969.4	2970.0	0.6
379	255-267	**FTISRDTSKNTLYL**	4+	1658.8	1659.1	0.3

380	256-266	**TISRDNAKNSIY**	3+	1381.7	1381.8	0.1
381	256-273	**MISRDNSKSTVTLQMNSL + Ox**	4+	2041.0	2041.6	0.6
382	256-279	**MISRTPEVTCVVVDVSHEDPMVQF**	4+	2775.3	2776.4	1.1
383	266-279	**VVVDVSHEDPEVQF**	3+	1598.7	1599.3	0.6
384	279-292	**FNWYVDGVEVHNAK**	3+	1676.8	1677.8	1.0
385	279-292	**FNWYVDGVQVHNAK**	3+	1676.8	1677.8	1.0
386	294-311	**TVTKDASRNQVVLTMTNL**	4+	1991.0	1991.4	0.4
387	295-306	**AISSDTSRNRVVL**	2+	1417.7	1417.8	0.1
388	305-317	**RVVSVLTVLHQDW**	3+	1551.8	1551.9	0.1
389	305-323	**RVVSVLTVVHQDWLNGKEY**	4+	2242.2	2242.4	0.2
390	306-321	**VVSVLTVLHQDWLDGK**	3+	1808.9	1809.3	0.4
391	306-321	**VVSVLTVLHQDWLIGK**	3+	1807.0	1806.9	0.1
392	306-321	**VVSVLTVLHQDWLVGK**	3+	1793.0	1793.5	-0.5
393	306-321	**VVSVLTVVHQDWLNGK**	3+	1793.9	1793.1	0.8
394	306-321	**VVSVLTVLHQDWLKGK**	3+	1822.0	1822.7	0.7
395	306-321	**VVSVLTVLHQDWLQGK**	3+	1822.0	1822.6	0.6
396	306-321	**VVSVLTVLHQDWLEGK**	3+	1822.2	1822.4	0.2
397	311-317	**TVVHQDW**	2+	883.2	883.2	0.0
398	311-317	**ISFAMNW**	2+	868.4	868.2	0.2
399	311-317	**SLFAMNW**	2+	868.4	868.2	0.2
400	311-317	**SLGSGYNW**	2+	883.4	883.2	0.2
401	311-323	**TVVHQDWLNGKEY**	3+	1588.8	1589.1	0.3
402	327-334	**ALPAPIEK**	2+	837.5	837.4	0.1
403	327-334	**GLPAPIEK**	2+	823.4	823.5	0.1
404	329-334	**PAPIEK**	2+	653.4	653.4	0.0
405	341-360	**GQPREPQVYTLPPSREEMTK**	4+	2342.1	2342.5	0.4
406	341-360	**GQPREPQVYTLPPSREELTK**	4+	2325.2	2325.6	0.4
407	345-355	**EPQVYTLPPSR**	2+	1285.6	1285.5	0.1
408	345-360	**EPQVYTLPPSRDELTK**	4+	1871.9	1871.7	0.2

409	260-278	**TPEVTCVVVDVSHEDPEVK**	4+	2139.0	2138.3	0.7
410	361-366	**NQLSLK**	2+	701.4	701.4	0.0
411	361-370	**NQVSLTCLVK**	2+	1161.6	1160.4	1.2
412	361-381	**NQFSLQLISMTPEDTAVYFCR**	4+	2520.1	2521.1	1.0
413	368-376	**FSDSVKGRF**	2+	1041.5	1041.8	0.3
414	368-376	**YANSVKGRF**	2+	1041.5	1041.8	0.3
415	368-376	**YANSVQGRF**	2+	1041.5	1041.8	0.3
416	370-376	**TCLVKGF**	2+	824.4	824.2	0.2
417	370-385	**TCLVKGFYPSDIAVEW**	3+	1884.9	1885.5	0.6
418	370-395	**TCLVKGFYPSDIAVEWESDDGEPENY**	4+	3020.3	3022.0	1.7
419	373-385	**VKGFYPSDIAVEW**	2+	1510.7	1510.8	0.1
420	375-395	**GFYPSDIAVEWESNGQPENYK**	4+	2430.1	2431.5	1.4
421	375-395	**GFYPSDIAVEWESNGQPEDYK**	4+	2431.0	2431.5	0.5
422	375-395	**GFYPSDIAVEWESNGQPQNYK**	4+	2429.1	2431.5	2.4
423	377-385	**YPSDIAVEW**	2+	1079.4	1079.4	0.0
424	386-395	**ESNGEPQDNY**	2+	1152.4	1152.6	0.2
425	386-395	**ESNGQPENNY**	2+	1151.4	1152.6	1.2
426	397-408	**KTTPPVLDSDGSF**	2+	1363.6	1363.8	0.2
427	397-409	**KTTPPVLDSDGSFF**	2+	1510.7	1510.8	0.1
428	397-410	**KTTPPVLDSVGSFFL**	3+	1607.8	1608.3	0.5
429	398-413	**TTPPMLDSDGSFFLYSK**	3+	1905.9	1906.8	0.9
430	410-414	**LTVDK**	2+	575.3	574.2	1.1
431	410-416	**LTVDKSR**	2+	817.4	817.3	0.1
432	417-435	**WQQGNVFSC**	2+	1125.4	1124.6	0.8
433	417-439	**WQEGNVFSCSVMHEALHNHYTQK**		2802.2	2801.4	0.8
434	428-436	**SCSVMHEAL**	2+	1033.4	1033.1	0.3
435	428-440	**SCSVMHEALHNHY**	3+	1586.6	1586.1	0.5

[a]GPMAW software 5.0 (Lighthouse Data, Denmark)

[b]mass spectrometric analysis by ESI ion trap mass spectrometry

9. APPENDIX 3

Abbreviations

aa	Amino acid
ACN	Acetonitrile
Ab	Antibody
APS	Ammoniumperoxodisulfat
BCA	Bicinchoninic acid assay
BSA	Bovine serum albumine
CID	Ccllision-induced dissociation
CD	Circular dichroism
CDR	Complementary determining region
Da	Dalton
DHB	Dihydroxybenzoic acid
DMF	Dimethylformamide
DTT	Dithiothreitol
EDC	N-(3- dimethylaminopropyl)-N-ethylcarbodiimide
ELISA	Enzyme linked immunosorbent assay
ESI-MS	Electrospray ionization- Mass spectrometry
FTICR	Fourier transform-ion cyclotron resonance
Fmoc	9-Fluorenylmethoxycarbonyl
HCCA	4-Hydroxy-α-cynamic acid
HPLC	High performance liquid chromatography
h	Hours
IAA	iodoacetamide
IgG	γ-Immunglobulins
MALDI-MS	Matrix-assisted laser desorption-/ionization-mass spectrometry
min	Minute
m/z	Mass over charge ratio
MS	Mass spectrometry

NHS	N-hydroxysuccinimide
NMM	N-Methyl-morpholine
PBS	Phosphate buffered saline
pH	Negative logarithm of H3O+-iones concentration
ppm	Parts per million
PyBOP	Benzotriazol-1-yloxy-tris-pyrrolidinophosphonium-PF6
RP	Reversed phase
Rt	Retention time
SDS-PAGE	Sodiumdodecylsulfat-Polyacrylamid-Gel electrophoresis
T	Tesla
TCA	Trichloroacetic acid
TEMED	N,N,N',N'-Tetramethylethylendiamine
TFA	Trifluoroacetic acid
TFE	Trifluoroethanol
TIC	Total ion chromatogram
TIPS	Triisopropylsilane
ToF	Time of flight
Tris	Tris-(hydroxymethyl-) aminomethane
Tween	Polyoxyethylen Sorbitan Monolaurat
UV	Ultraviolet
V	Volt
VH	Antibody heavy chain variable region
VL	Antibody light chain variable region
Δm	Mass difference
°C	Grad Celsius

10. APPENDIX 4

Table 32. Amino acids abbreviations:

Name	One letter code	Three letters code	Mass increment
Alanin	A	Ala	71.08
Arginin	R	Arg	156.19
Asparagin	N	Asn	114.10
Aspartic acid	D	Asp	115.09
Cysteine	C	Cys	103.14
Glutamin	Q	Gln	128.13
Glutamic acid	E	Glu	129.12
Glycin	G	Gly	57.05
Histidin	H	His	137.14
Isoleucin	I	Ile	113.16
Leucin	L	Leu	113.16
Lysin	K	Lys	128.17
Methionin	M	Met	131.20
Phenylalanin	F	Phe	147.18
Prolin	P	Pro	97.12
Serin	S	Ser	S 87.08
Threonin	T	Thr	101.11
Tryptophan	W	Trp	186.21
Tyrosin	Y	Tyr	163.18
Valin	V	Val	99.13